

**DEVELOPMENT OF AN ANTI CORROSION COATING
USING ORGANIC RESINS HYBRID SYSTEM**

RAMIS RAO A/L SUBRAMANIAN

**FACULTY OF SCIENCE
UNIVERSITY OF MALAYA
KUALA LUMPUR**

2016

**DEVELOPMENT OF AN ANTI CORROSION
COATING USING ORGANIC RESINS HYBRID SYSTEM**

RAMIS RAO A/L SUBRAMANIAN

**THESIS SUBMITTED IN FULFILMENT OF THE
REQUIREMENTS FOR THE DEGREE OF
DOCTOR OF PHILOSOPHY**

**DEPARTMENT OF PHYSICS
FACULTY OF SCIENCE
UNIVERSITY OF MALAYA
KUALA LUMPUR**

2016

UNIVERSITY OF MALAYA
ORIGINAL LITERARY WORK DECLARATION

Name of Candidate: RAMIS RAO A/L SUBRAMANIAN

Registration/Matric No: SHC090031

Name of Degree: DOCTOR OF PHILOSOPHY

Title of Project Paper/Research Report/Dissertation/Thesis (“this Work”):

**DEVELOPMENT OF AN ANTI CORROSION COATING
USING ORGANIC RESINS HYBRID SYSTEM**

Field of Study: MATERIALS SCIENCE

I do solemnly and sincerely declare that:

- (1) I am the sole author/writer of this Work;
- (2) This Work is original;
- (3) Any use of any work in which copyright exists was done by way of fair dealing and for permitted purposes and any excerpt or extract from, or reference to or reproduction of any copyright work has been disclosed expressly and sufficiently and the title of the Work and its authorship have been acknowledged in this Work;
- (4) I do not have any actual knowledge nor do I ought reasonably to know that the making of this work constitutes an infringement of any copyright work;
- (5) I hereby assign all and every rights in the copyright to this Work to the University of Malaya (“UM”), who henceforth shall be owner of the copyright in this Work and that any reproduction or use in any form or by any means whatsoever is prohibited without the written consent of UM having been first had and obtained;
- (6) I am fully aware that if in the course of making this Work I have infringed any copyright whether intentionally or otherwise, I may be subject to legal action or any other action as may be determined by UM.

Candidate’s Signature

Date:

Subscribed and solemnly declared before,

Witness’s Signature

Date:

Name: Prof. Dr. Ramesh T. Subramaniam

Designation: Professor and Supervisor

ABSTRACT

The objective of this study is to develop anti-corrosion coating using organic resins hybrid system. The hybrid systems were prepared by blending acrylic polyol resin with epoxy polyol resin in various weight ratios using polyisocyanate resin as hardener. A series of acrylic(A) - epoxy(E) resin blends with the ratio of 10A:90E, 20A:80E, 30A:70E, 40A:60E, 50A:50E, 60A:40E, 70A:30E, 80A:20E and 90A:10E have been prepared and applied on the pre-treated cold rolled mild steel panels. In this investigation, no specific hardener was used to cure epoxy resin. The dry film thickness was maintained within the range 40 μm to 80 μm . The panels were allowed to cure under ambient air condition for one week prior to testing. The physical, mechanical, thermal, structural, electrochemical and corrosion resistance properties were investigated to obtain the best formulation. From these studies, the hybrid binder system with 90A:10E ratio shows excellent properties. This best performing binder system was chosen for the formulation of paint using various inorganic pigments such as Titanium Dioxide (TiO_2), Silitin Z 86, Aktisil AM and Aktisil PF 777. This study will demonstrate interesting correlations between viscosity, dry film thickness, adhesion, impact resistance, accelerated UV weathering, acid resistance studies, DSC, EDAX, EIS, FTIR, SEM and TGA to identify the critical pigment volume concentration (CPVC). These studies conclusively confirm that Paint 3, consisting Aktisil AM as pigment at CPVC 20 % provided the best overall anti-corrosion improvement.

ABSTRAK

Penyaduran anti pengaratan dengan menggunakan sistem hibrid resin organik telah disediakan secara pengadunan antara resin akrilik polioliol dan resin epoksi polioliol dalam pelbagai nisbah kandungan berat menggunakan poli-isosainat sebagai agen pengeras. Serangkaian formulasi campuran resin akrilik(A) - epoksi(E) dengan nisbah 10A:90E, 20A:80E, 30A:70E, 40A:60E, 50A:50E, 60A:40E, 70A:30E, 80A:20E dan 90A:10E telah disediakan. Formulasi campuran ini disadurkan pada plat panel besi terawat. Kajian ini tidak menggunakan sebarang agen pengeras spesifik untuk resin epoksi. Ketebalan filem saduran dikekalkan dalam julat 40 μm hingga 80 μm . Panel-panel ini dikeringkan dalam keadaan suhu bilik selama seminggu sebelum dikaji selidik. Untuk memperoleh nisbah formulasi terbaik, pelbagai kaedah digunakan iaitu kajian secara fizikal, mekanikal, termal, struktur, elektrokimia dan anti pengaratan dijalankan. Daripada kaji selidik ini, sistem pengadunan hibrid dengan nisbah 90A:10E menunjukkan pencirian yang terbaik. Nisbah terbaik ini digunakan untuk formulasi cat bercampur dengan pigmen bukan organik khususnya. Prestasi cat bercampur dengan pigmen Titanium Dioksida (TiO_2), Silitin Z 86, Aktisil AM dan Aktisil PF 777 akan ditunjukkan dan dinilai. Perbandingan ciri-ciri antara cat berpigmen dijalankan secara menyeluruh dalam penelitian perlindungan dari proses pengaratan. Kajian ini juga akan menunjukkan kesinambungan antara kelikatan, kelekatan, ketebalan filem penyaduran, hentakan, kesan pecutan persekitaran UV, ujian asid, DSC, EDAX, EIS, FTIR, SEM dan TGA untuk mengenalpasti kepekatan isipadu pigmen kritikal (CPVC). Kajian ini secara menyeluruh mengesahkan bahawa cat P3, Aktisil AM sebagai pigmen yang memberi kesan terbaik untuk peningkatan pencirian anti pengaratan pada CPVC 20 %.

ACKNOWLEDGEMENTS

First and foremost, my most sincere and profound appreciation goes to my supervisors, Professor Dr. Abdul Kariem Arof and Professor Dr. Ramesh T. Subramaniam for their instrumental role in assisting me to complete this thesis. Their valuable guidance, patience and understanding were the essential factor in the progress of my study. A special word of thanks dedicated to Dr. B. Vengadaesvaran and Dr. K. Ramesh and for their valuable time and professional advices. Thank you, my respected laboratory mates for helping to build the good rapport and conducive environment for carrying out research together: Dr. Zul and Dr. Ghassan, Mr.Nordin, Mr.Ismail, Mr.Din, Mr Josh, Vignesh, Ammar, Arun, Vinod, Umaira and others who indirectly contributed to this work.

A note of gratitude to all staff of Physics Dept. Laboratory and Workshop (UM), NANOCEN (UM) and Engineering Dept. (UM), UM Fellowship scheme and IPPP grants for the vital financial aid provided towards the completion of my thesis. Thankful to Bayer (Malaysia) Sdn. Bhd, World Wide Resins & Chemicals (Malaysia) Sdn. Bhd and Hoffmann Mineral (Germany) for the assistance in providing Acrylic Polyol Resin, Epoxy Resin, Pigments and respected industry ideas which greatly contributed core elements to work and learn in the accomplishment of my thesis.

My heartfelt appreciation also goes to my wife Sri Paramesh Warthini and my both daughters, Yoamsiny and Moharsshana who have been my strength and motivator in chasing and reaching my goals. Not forgetting my parents, in laws and family members support throughout. My final acknowledgement goes out to the ONE who has no finality. HE has answered my prayers in many ways and blessed me with the faculties that have enabled me to achieve the impossibilities. Thank you for not giving up on me.

TABLE OF CONTENTS

Abstract	iii
Abstrak	iv
Acknowledgements	v
Table of Contents	vi
List of Figures	xi
List of Tables.....	xxi
List of Symbols and Abbreviations.....	xxiii
CHAPTER 1: INTRODUCTION.....	1
1.1 Background.....	1
1.2 Objectives of the Present Investigation	4
1.3 Scope of the Thesis.....	6
CHAPTER 2: LITERATURE REVIEW.....	9
2.1 Introduction.....	9
2.1.1 Types of Corrosion and its Mechanism.....	9
2.2 Why Steel?.....	12
2.3 Mild Steel.....	12
2.4 How do we stop Steel from Corroding?	13
2.5 Types of Corrosion	17
2.5.1 General or Uniform Corrosion	17
2.5.2 Pitting Corrosion	18
2.5.3 Stress Corrosion Cracking.....	19
2.5.4 Fatigue Corrosion	20
2.5.5 Intergranular Corrosion	22

2.5.6	Filiform Corrosion.....	23
2.5.7	Crevice Corrosion.....	24
2.5.8	Galvanic or Bi-Metallic Corrosion.....	25
2.5.9	Fretting Corrosion	27
2.5.10	Erosion Corrosion.....	28
2.5.11	High Temperature Corrosion.....	29
2.6	Coating.....	30
2.6.1	Why Hybrid Organic Coatings?	32
2.7	Paint Composition	33
2.7.1	Factors in selection of Paint or Coating System.....	35
2.8	Binder	36
2.8.1	Acrylic Polyol Resin	37
2.8.2	Epoxy Resin	39
2.9	Solvent	42
2.9.1	Xylene	44
2.10	Pigment.....	45
2.11	Pigment Volume Concentration	46
2.11.1	Titanium Dioxide	47
2.11.2	Hoffmann Mineral.....	49
2.12	Polyisocyanate	51
CHAPTER 3: EXPERIMENTAL MATERIALS AND METHODOLOGY		53
3.1	Introduction.....	53
3.2	Materials	53
3.2.1	Preparation of Hybrid Coating and Paint System.....	55
3.3	Characterization.....	59
3.3.1	Viscosity Measurement	59

3.3.2	Drying Time	60
3.3.3	Dry Film Thickness	61
3.3.4	Glossiness	61
3.3.5	Adhesion (Cross-Hatch Method).....	63
3.3.6	Impact Resistance	65
3.3.7	Accelerated UV Weathering Test.....	66
3.3.8	Fourier Transform Infrared Spectroscopy	68
3.3.8.1	Generic Coating Identification	69
3.3.8.2	Fingerprinting by FTIR	70
3.3.8.3	Crosslinking between Hybrid System	71
3.3.9	Scanning Electron Microscope and Energy Dispersive Analysis of X-ray	74
3.3.10	Thermogravimetric Analysis	76
3.3.11	Differential Scanning Calorimetry	78
3.3.12	Acid Immersion Test	80
3.3.13	Electrochemical Impedance Spectroscopy	83

CHAPTER 4: RESULTS AND DISCUSSION ON BINDER SYSTEM 91

4.1	Introduction.....	91
4.2	Viscosity	91
4.3	Drying Time.....	93
4.4	Dry Film Thickness	95
4.5	Adhesion (Cross-Hatch Method).....	96
4.6	Impact Resistance	98
4.7	Fourier Transform Infrared Spectroscopy	101
4.8	Thermogravimetric Analysis	103
4.9	Differential Scanning Calorimetry	108

4.10 Electrochemical Impedance Spectroscopy	113
4.11 Summary.....	118

CHAPTER 5: RESULTS AND DISCUSSION ON PAINT SYSTEM

PHYSICAL AND MECHANICAL	120
5.1 Introduction.....	120
5.2 Dry Film Thickness	120
5.3 Adhesion (Cross-Hatch Method).....	123
5.4 Glossiness and Accelerated UV Weathering Test	129
5.5 Summary.....	140

CHAPTER 6: RESULTS AND DISCUSSION ON PAINT SYSTEM

THERMAL AND STRUCTURAL.....	141
6.1 Introduction.....	141
6.2 Thermogravimetric Analysis	141
6.3 Differential Scanning Calorimetry	153
6.4 Fourier Transform Infrared Spectroscopy	166
6.5 Scanning Electron Microscope and Energy Dispersive Analysis of X-ray.....	170
6.6 Summary.....	177

CHAPTER 7: RESULTS AND DISCUSSION ON PAINT SYSTEM

CORROSION AND ELECTROCHEMICAL	179
7.1 Introduction.....	179
7.2 Acid Immersion Test	179
7.2.1 Paint System with TiO ₂ – P1	180
7.2.2 Paint System with Silitin Z 86 – P2	183
7.2.3 Paint System with Aktisil AM – P3	186

7.2.4	Paint System with Aktisil PF 777 – P4	189
7.3	Electrochemical Impedance Spectroscopy	192
7.3.1	Paint System with TiO ₂ – P1	192
7.3.2	Paint System with Silitin Z 86 – P2	197
7.3.3	Paint System with Aktisil AM – P3	201
7.3.4	Paint System with Aktisil PF 777 – P4	205
7.4	Summary.....	209

CHAPTER 8: RESULTS AND DISCUSSION ON PAINT SYSTEM

	CRITICAL PIGMENT VOLUME CONCENTRATION.....	210
8.1	Introduction.....	210
8.2	Critical Pigment Volume Concentration	211
8.3	Summary.....	215

CHAPTER 9: DISCUSSION

CHAPTER 10: CONCLUSION AND SUGGESTIONS

	References	238
	List of Publications and Papers Presented	251

LIST OF FIGURES

Figure 2.1: Absorption of O ₂	10
Figure 2.2: Corrosion Mechanism.....	11
Figure 2.3: Composition and Properties of Mild Steel	13
Figure 2.4: Corrosion (A + B + C) Triangle	13
Figure 2.5: Uniform Corrosion	17
Figure 2.6: Pitting Corrosion	18
Figure 2.7: Stress Corrosion Cracking.....	19
Figure 2.8: Corrosion Fatigue	20
Figure 2.9: Corrosion Fatigue	21
Figure 2.10: Intergranular Corrosion	22
Figure 2.11: Filiform Corrosion.....	24
Figure 2.12: Crevice Corrosion.....	25
Figure 2.13: Galvanic Corrosion.....	26
Figure 2.14: Fretting Corrosion	27
Figure 2.15: Erosion Corrosion.....	28
Figure 2.16: High Temperature Corrosion.....	29
Figure 2.17: a) Coated Metal Surface b) Un-Coated Metal Surface.....	30
Figure 2.18: Metal Substrate coated with Multilayer and Hybrid Coating.....	32
Figure 2.19: Typical Paint Compositions.....	34
Figure 2.20: Typical Paint Formulations (Percentage by Volume)	34
Figure 2.21: General Structure of Acrylic Polyol Resin.....	37
Figure 2.22: General Structure of Epoxy Resin	40
Figure 2.23: General Structure of Xylene Isomers	44

Figure 2.24: Crystal Structure of TiO ₂ a) Rutile b) Anatase.....	48
Figure 3.1: Elcometer Rotary Viscometer (RV1-L)	59
Figure 3.2: a) Elcometer 456 Thickness Gauge b) Sensor Tip	61
Figure 3.3: Novo-Gloss Lite Gloss Meter.....	62
Figure 3.4: a) Sheen 750 b) Dino-Lite	63
Figure 3.5: a) Tubular Impact Tester b) Pinhole Detector	65
Figure 3.6: a) Accelerated Weathering Tester, QUV b) Scheme of QUV.....	67
Figure 3.7a: FTIR spectrum of epoxy coating	70
Figure 3.7b: FTIR spectra of aliphatic polyurethane coating (Manufacturer A).....	70
Figure 3.7c: FTIR spectra of aliphatic polyurethane coating (Manufacturer B).....	71
Figure 3.8a: FTIR transmission spectrum of acrylic blended with epoxy resin (Magnification of the course from 650 to 900 cm ⁻¹).....	72
Figure 3.8b: FTIR transmission spectrum of acrylic blended with epoxy resin (Magnification of the course from 1100 to 1900 cm ⁻¹).....	72
Figure 3.8c: FTIR transmission spectrum of acrylic blended with epoxy resin (Magnification of the course from 500 to 4000 cm ⁻¹).....	73
Figure 3.9: FTIR Spectrometer (ATR-Nicolet iS10).....	73
Figure 3.10: SEM-EDAX Spectrometer (XL30)	75
Figure 3.11: TGA Instrument (Q500)	77
Figure 3.12: DSC Instrument (Q200S RCS90).....	79
Figure 3.13: a) Cross Scribed Panel b) Coated Panel	81
Figure 3.14: Acid Immersion Test	82
Figure 3.15: The three electrodes cell used for EIS studies.....	84
Figure 3.16: EIS Instrument with Faraday Cage.....	84
Figure 3.17: Electrical Equivalent Circuits	
Model (a) Before corrosion start Model (b) After corrosion start	86

Figure 3.18: Bode plot	
Model (a) Before corrosion start Model (b) After corrosion start	87
Figure 3.19: Nyquist plot (a) capacitive behavior (b) one semi-circle	
(c) two semi circles (d) 45° to real axis	87
Figure 3.20: The schematic value for good, fair and poor of coating resistances.....	90
Figure 4.1: Viscosity Variation of nAnE Binder System.....	93
Figure 4.2: Thickness Variation of nAnE Binder System.....	95
Figure 4.3: Adhesion Variation of nAnE Binder System	96
Figure 4.4: Cross Cut Images of nAnE Binder System	97
Figure 4.5: Impact Resistance Variation of nAnE Binder System.....	98
Figure 4.6: Intrusion Impact Images of nAnE Binder System.....	99
Figure 4.7: Extrusion Impact Images of nAnE Binder System.....	100
Figure 4.8a: FTIR transmission spectrum of acrylic blended with epoxy resin (Magnification of the course from 650 to 900 cm ⁻¹).....	101
Figure 4.8b: FTIR transmission spectrum of acrylic blended with epoxy resin (Magnification of the course from 1100 to 1900 cm ⁻¹).....	102
Figure 4.8c: FTIR transmission spectrum of acrylic blended with epoxy resin (Magnification of the course from 500 to 4000 cm ⁻¹).....	102
Figure 4.9a: TGA Thermogram of 20A80E.....	104
Figure 4.9b: TGA Thermogram of 30A70E	104
Figure 4.9c: TGA Thermogram of 40A60E.....	105
Figure 4.9d: TGA Thermogram of 50A50E	105
Figure 4.9e: TGA Thermogram of 60A40E.....	105
Figure 4.9f: TGA Thermogram of 70A30E	106

Figure 4.9g: TGA Thermogram of 80A20E	106
Figure 4.9h: TGA Thermogram of 90A10E	106
Figure 4.9i: TGA Thermogram of 100A.....	107
Figure 4.10: Percentage of residue left after degradation	107
Figure 4.11a: DSC Thermogram of 20A80E	108
Figure 4.11b: DSC Thermogram of 30A70E.....	108
Figure 4.11c: DSC Thermogram of 40A60E	109
Figure 4.11d: DSC Thermogram of 50A50E.....	109
Figure 4.11e: DSC Thermogram of 60A40E	109
Figure 4.11f: DSC Thermogram of 70A30E	110
Figure 4.11g: DSC Thermogram of 80A20E.....	110
Figure 4.11h: DSC Thermogram of 90A10E.....	110
Figure 4.11i: DSC Thermogram of 100A	111
Figure 4.12: Glass Transition Temperature of nAnE Binder System	111
Figure 4.13: Electrical Equivalent Circuit Model	113
Figure 4.14: Pore Resistance (R_p) vs Time of immersion.....	114
Figure 4.15: Coating Capacitance (C_c) vs Time of immersion	115
Figure 4.16: Dielectric Constant (ϵ) vs Time of immersion	116
Figure 4.17: Volume Fraction of Water (ϕ_w) vs Time of immersion.....	117
Figure 5.1: Thickness Variation of P1 paint system (TiO_2).....	121
Figure 5.2: Thickness Variation of P2 paint system (Silitin Z 86)	121
Figure 5.3: Thickness Variation of P3 paint system (Aktisil AM)	122
Figure 5.4: Thickness Variation of P4 paint system (Aktisil PF 777)	122
Figure 5.5: Cross Cut Images of P1 paint system	125

Figure 5.6: Cross Cut Images of P2 paint system	126
Figure 5.7: Cross Cut Images of P3 paint system	127
Figure 5.8: Cross Cut Images of P4 paint system	128
Figure 5.9: Image of P110 paint system a) 0 h and b) 720 h after exposure to accelerated UV weathering test.....	130
Figure 5.10: Image of P120 paint system a) 0 h and b) 720 h after exposure to accelerated UV weathering test.....	130
Figure 5.11: Image of P130 paint system a) 0 h and b) 720 h after exposure to accelerated UV weathering test.....	130
Figure 5.12: Image of P140 paint system a) 0 h and b) 720 h after exposure to accelerated UV weathering test.....	131
Figure 5.13: Image of P150 paint system a) 0 h and b) 720 h after exposure to accelerated UV weathering test.....	131
Figure 5.14: Glossiness test results of P1 paint system at 0 h and 720 h after exposure to accelerated UV weathering test.....	131
Figure 5.15: Image of P210 paint system a) 0 h and b) 720 h after exposure to accelerated UV weathering test.....	132
Figure 5.16: Image of P220 paint system a) 0 h and b) 720 h after exposure to accelerated UV weathering test.....	133
Figure 5.17: Image of P230 paint system a) 0 h and b) 720 h after exposure to accelerated UV weathering test.....	133
Figure 5.18: Image of P240 paint system a) 0 h and b) 720 h after exposure to accelerated UV weathering test.....	133

Figure 5.19: Image of P250 paint system a) 0 h and b) 720 h after exposure to accelerated UV weathering test.....	134
Figure 5.20: Glossiness test results of P2 paint system at 0 h and 720 h after exposure to accelerated UV weathering test.....	134
Figure 5.21: Image of P310 paint system a) 0 h and b) 720 h after exposure to accelerated UV weathering test.....	135
Figure 5.22: Image of P320 paint system a) 0 h and b) 720 h after exposure to accelerated UV weathering test.....	135
Figure 5.23: Image of P330 paint system a) 0 h and b) 720 h after exposure to accelerated UV weathering test.....	135
Figure 5.24: Image of P340 paint system a) 0 h and b) 720 h after exposure to accelerated UV weathering test.....	136
Figure 5.25: Image of P350 paint system a) 0 h and b) 720 h after exposure to accelerated UV weathering test.....	136
Figure 5.26: Glossiness test results of P3 paint system at 0 h and 720 h after exposure to accelerated UV weathering test.....	136
Figure 5.27: Image of P410 paint system a) 0 h and b) 720 h after exposure to accelerated UV weathering test.....	137
Figure 5.28: Image of P420 paint system a) 0 h and b) 720 h after exposure to accelerated UV weathering test.....	138
Figure 5.29: Image of P430 paint system a) 0 h and b) 720 h after exposure to accelerated UV weathering test.....	138
Figure 5.30: Image of P440 paint system a) 0 h and b) 720 h after exposure to accelerated UV weathering test.....	138

Figure 5.31: Image of P450 paint system a) 0 h and b) 720 h after exposure to accelerated UV weathering test.....	139
Figure 5.32: Glossiness test results of P4 paint system at 0 h and 720 h after exposure to accelerated UV weathering test.....	139
Figure 6.1a: TGA Thermogram of P110 paint system.....	143
Figure 6.1b: TGA Thermogram of P120 paint system	143
Figure 6.1c: TGA Thermogram of P130 paint system.....	143
Figure 6.1d: TGA Thermogram of P140 paint system	144
Figure 6.1e: TGA Thermogram of P150 paint system.....	144
Figure 6.2a: TGA Thermogram of P210 paint system.....	146
Figure 6.2b: TGA Thermogram of P220 paint system	146
Figure 6.2c: TGA Thermogram of P230 paint system.....	146
Figure 6.2d: TGA Thermogram of P240 paint system	147
Figure 6.2e: TGA Thermogram of P250 paint system.....	147
Figure 6.3a: TGA Thermogram of P310 paint system.....	149
Figure 6.3b: TGA Thermogram of P320 paint system	149
Figure 6.3c: TGA Thermogram of P330 paint system.....	149
Figure 6.3d: TGA Thermogram of P340 paint system	150
Figure 6.3e: TGA Thermogram of P350 paint system.....	150
Figure 6.4a: TGA Thermogram of P410 paint system.....	151
Figure 6.4b: TGA Thermogram of P420 paint system	151
Figure 6.4c: TGA Thermogram of P430 paint system.....	152
Figure 6.4d: TGA Thermogram of P440 paint system	152
Figure 6.4e: TGA Thermogram of P450 paint system.....	152

Figure 6.5: The influence of TiO ₂ pigment on T _g value of P1 paint system.....	154
Figure 6.6a: DSC Thermogram of P110 paint system	155
Figure 6.6b: DSC Thermogram of P120 paint system.....	155
Figure 6.6c: DSC Thermogram of P130 paint system	156
Figure 6.6d: DSC Thermogram of P140 paint system.....	156
Figure 6.6e: DSC Thermogram of P150 paint system	156
Figure 6.7: The influence of Silitin Z 86 pigment on T _g value of P2 paint system	157
Figure 6.8a: DSC Thermogram of P210 paint system	158
Figure 6.8b: DSC Thermogram of P220 paint system.....	158
Figure 6.8c: DSC Thermogram of P230 paint system	158
Figure 6.8d: DSC Thermogram of P240 paint system.....	159
Figure 6.8e: DSC Thermogram of P250 paint system	159
Figure 6.9: The influence of Aktisil AM pigment on T _g value of P3 paint system	160
Figure 6.10a: DSC Thermogram of P310 paint system	161
Figure 6.10b: DSC Thermogram of P320 paint system.....	161
Figure 6.10c: DSC Thermogram of P330 paint system	161
Figure 6.10d: DSC Thermogram of P340 paint system.....	162
Figure 6.10e: DSC Thermogram of P350 paint system	162
Figure 6.11: The influence of Aktisil PF 777 pigment on T _g value of P4 paint system.....	163
Figure 6.12a: DSC Thermogram of P410 paint system	164
Figure 6.12b: DSC Thermogram of P420 paint system.....	164
Figure 6.12c: DSC Thermogram of P430 paint system	164
Figure 6.12d: DSC Thermogram of P440 paint system.....	165
Figure 6.12e: DSC Thermogram of P450 paint system	165

Figure 6.13: FTIR transmission spectrum of binder system and all P1 paint system...	167
Figure 6.14: FTIR transmission spectrum of binder system and all P2 paint system...	168
Figure 6.15: FTIR transmission spectrum of binder system and all P3 paint system...	169
Figure 6.16: FTIR transmission spectrum of binder system and all P4 paint system...	169
Figure 6.17: SEM micrograph and the corresponding EDAX results of P1 paint system	171
Figure 6.18: SEM micrograph and the corresponding EDAX results of P2 paint system	173
Figure 6.19: SEM micrograph and the corresponding EDAX results of P3 paint system	175
Figure 6.20: SEM micrograph and the corresponding EDAX results of P4 paint system	176
Figure 7.1: Acid resistance response for P1 system after a) 0, b) 4, c) 8, d) 15, e) 22 and f) 40 days of immersion in H ₂ SO ₄ 10 % solution	181
Figure 7.2: Acid resistance response for P2 system after a) 0, b) 4, c) 8, d) 15, e) 22 and f) 40 days of immersion in H ₂ SO ₄ 10 % solution	184
Figure 7.3: Acid resistance response for P3 system after a) 0, b) 4, c) 8, d) 15, e) 22 and f) 40 days of immersion in H ₂ SO ₄ 10 % solution	187
Figure 7.4: Acid resistance response for P4 system after a) 0, b) 4, c) 8, d) 15, e) 22 and f) 40 days of immersion in H ₂ SO ₄ 10 % solution	190
Figure 7.5: Coating Resistance (R _c) vs Time of immersion of P1 paint system.....	193
Figure 7.6: Coating Capacitance (C _c) vs Time of immersion of P1 paint system	194
Figure 7.7: Dielectric Constant (ε) vs Time of immersion of P1 paint system.....	195
Figure 7.8: Volume Fraction of Water (φ _w) vs Time of immersion of P1 paint system	195
Figure 7.9: Coating Resistance (R _c) vs Time of immersion of P2 paint system.....	197
Figure 7.10: Coating Capacitance (C _c) vs Time of immersion of P2 paint system	198
Figure 7.11: Dielectric Constant (ε) vs Time of immersion of P2 paint system.....	199

Figure 7.12: Volume Fraction of Water (ϕ_w) vs Time of immersion of P2 paint system	199
Figure 7.13: Coating Resistance (R_c) vs Time of immersion of P3 paint system	202
Figure 7.14: Coating Capacitance (C_c) vs Time of immersion of P3 paint system	202
Figure 7.15: Dielectric Constant (ϵ) vs Time of immersion of P3 paint system	203
Figure 7.16: Volume Fraction of Water (ϕ_w) vs Time of immersion of P3 paint system	203
Figure 7.17: Coating Resistance (R_c) vs Time of immersion of P4 paint system	206
Figure 7.18: Coating Capacitance (C_c) vs Time of immersion of P4 paint system	206
Figure 7.19: Dielectric Constant (ϵ) vs Time of immersion of P4 paint system	207
Figure 7.20: Volume Fraction of Water (ϕ_w) vs Time of immersion of P4 paint system	207
Figure 8.1: a) Coating Resistance, R_c b) Diffusion coefficient, D	212
Figure 8.2: Coating Resistance, R_c vs PVC % of AE binder and paint system	212
Figure 8.3: Paint Diffusion Coefficient Rate, D vs PVC % of paint system	214

LIST OF TABLES

Table 2.1: Stress Corrosion Cracking Causing Metals and Environments	20
Table 2.2: Galvanic Metal Series	26
Table 2.3: Paint Formulation (Fineness of grind < 20 μm)	50
Table 3.1: Properties of Acrylic Polyol Resin	53
Table 3.2: Properties of Epoxy Resin	54
Table 3.3: Properties of Polyisocyanate Resin	54
Table 3.4: Properties of Xylene	54
Table 3.5: Blending Formulation of Acrylic-Epoxy Resin.....	56
Table 3.6: Paint Formulation with Pigment (Fineness of grind < 20 μm).....	57
Table 3.7: Formulation Analysis.....	58
Table 3.8: Classification of Adhesion Results	64
Table 3.9: Functional Groups and Vibration Bands	69
Table 4.1: Viscosity Results of nAnE Binder System	92
Table 4.2: Drying Time of nAnE Binder System	94
Table 6.1: The residue values of P1 paint system.....	145
Table 6.2: The residue values of P2 paint system.....	145
Table 6.3: The residue values of P3 paint system.....	148
Table 6.4: The residue values of P4 paint system.....	151
Table 6.5: The glass transition temperature of acrylic system, acrylic-epoxy binder system and P1 paint system.....	154
Table 6.6: The glass transition temperature of acrylic system, acrylic-epoxy binder system and P2 paint system.....	157

Table 6.7: The glass transition temperature of acrylic system, acrylic-epoxy binder system and P3 paint system.....	160
Table 6.8: The glass transition temperature of acrylic system, acrylic-epoxy binder system and P4 paint system.....	163
Table 7.1: Coating Resistance and Coating Capacitance values after 1, 15 and 30 days of immersion in 3.5 % NaCl of P1 paint system.....	196
Table 7.2: Dielectric Constant and Water uptake values after 1, 15 and 30 days of immersion in 3.5 % NaCl of P1 paint system	196
Table 7.3: Coating Resistance and Coating Capacitance values after 1, 15 and 30 days of immersion in 3.5 % NaCl of P2 paint system.....	200
Table 7.4: Dielectric Constant and Water uptake values after 1, 15 and 30 days of immersion in 3.5 % NaCl of P2 paint system	200
Table 7.5: Coating Resistance and Coating Capacitance values after 1, 15 and 30 days of immersion in 3.5 % NaCl of P3 paint system.....	204
Table 7.6: Dielectric Constant and Water uptake values after 1, 15 and 30 days of immersion in 3.5 % NaCl of P3 paint system	204
Table 7.7: Coating Resistance and Coating Capacitance values after 1, 15 and 30 days of immersion in 3.5 % NaCl of P4 paint system.....	208
Table 7.8: Dielectric Constant and Water uptake values after 1, 15 and 30 days of immersion in 3.5 % NaCl of P4 paint system	208
Table 7.9: Acid Resistance Test and EIS Performance Comparison	209
Table 8.1: Paint Coating Resistance values at 30 days of immersion in 3.5 % NaCl...	213
Table 8.2: Paint Diffusion Rate values at 30 days of immersion in 3.5 % NaCl.....	214

LIST OF SYMBOLS AND ABBREVIATIONS

P1	:	Paint 1 – TiO ₂
P2	:	Paint 2 – Silitin Z 86
P3	:	Paint 3 – Aktisil AM
P4	:	Paint 4 – Aktisil PF 777
A100	:	pure 100 % acrylic resin
P100	:	pure 100 % AE (90A10E)
A	:	surface area of the exposed coating
d	:	coating thickness
t	:	time
C ₀	:	coating capacitance at t is zero
C _c	:	coating capacitance
C _{dl}	:	double layer capacitance
C _s	:	coating capacitance saturation
C _t	:	coating capacitance after time (t) of immersion
D	:	diffusion coefficient
R _c	:	coating resistance
R _{ct}	:	charge-transfer resistance
R _p	:	pore resistance
R _{po}	:	polarization resistance
R _s	:	electrolyte resistance
R _u	:	uncompensated resistance
ε	:	dielectric constant
ε _a	:	dielectric constant of air phase
ε ₀	:	dielectric constant of free space
ε _s	:	dielectric constant of solid

ϵ_w	:	dielectric constant of water
T_g	:	glass transition temperature
ϕ_w	:	volume fraction of water
wt%	:	weight percentage
AC	:	Alternating Current
AE	:	Acrylic-Epoxy hybrid binder system
AU	:	Acrylic Urethane
ASTM	:	American Society for Testing and Materials
ATR	:	Attenuated Total Reflectance
BTEX	:	Benzene, Toluene, Ethyl benzene and Xylene
CE	:	Counter Electrode
CPVC	:	Critical Pigment Volume Concentration
DC	:	Direct Current
DETA	:	Diethylenetriamine
DFT	:	Dry Film Thickness
DGEBA	:	Diglycidyl Ether of Bisphenol-A
DSC	:	Differential Scanning Calorimetry
DTGS	:	Deuterated Triglycine Sulfate
EDAX	:	Energy Dispersive Analysis of X-Ray
EIS	:	Electrochemical Impedance Spectroscopy
EM	:	Electromagnetic
ENM	:	Electrochemical Noise Method
FTIR	:	Fourier Transform Infrared Spectroscopy
GU	:	Gloss Unit
HBP	:	Hyper Branched Polyester
IR	:	Infra-Red

MPA/X	:	Methoxy Propyl Acetate / Xylene
NSE	:	Neuburg Siliceous Earth
OEM	:	Original Equipment Manufacturer
PTE	:	Platinum Electrode
PVC	:	Pigment Volume Concentration
RE	:	Reference Electrode
SCE	:	Saturated Calomel Electrode
SEM	:	Scanning Electron Microscope
SRB	:	Sulfate Reducing Bacteria
TGA	:	Thermogravimetric Analysis
UV	:	Ultra Violet
VOC	:	Volatile Organic Compound
WE	:	Working Electrode

CHAPTER 1: INTRODUCTION

1.1 Background

Coating is a covering that is applied to the surface of an object. Dating from prehistory, coatings developed slowly to meet every day needs. Coatings were used by many in human civilization such as Mayan, Olmec, Inca, Aztec, Egyptians, Greeks, Romans, Hindus, and Chinese to name few. Archaeologist reportedly found pigments and paint crushing equipment believed to be between 350000 and 400000 years old. Coating is one of the ancient techniques that have been used in communication and decorative values prevail well past the Renaissance. The protective functions of coatings developed after Industrial Revolutions of human kind. Today, coating has become a subject of scientific investigation and are applied everywhere for various functions.

Steel is the major metal used worldwide and is susceptible to deterioration due to environmental corrosion. Coatings can be described by their functions may consist of organic, inorganic or both materials. Because of their low cost, versatility and aesthetic attributes, organic coatings are the natural choice for corrosion protection. Many paints and high performance coatings have been developed as a need to protect the surface of metal based equipment from environmental destruction. Extensive researches were made in protective coating applications. These applications consist of converted coating into high-technology protective layer to preserve and protect the surface of valuables from environmental damages and natural deterioration.

Corrosion can be defined as the destruction or deterioration of a metalloid material. To prevent corrosion, anti-corrosion coating for raw materials worth billions of dollars were spent into architecture coatings such as Original Equipment Manufacturer (OEM) coating, specialized coating and miscellaneous paint products. In

this study, developed hybrid protective coatings were used as an anti-corrosion coating for mild steel panel at ambient conditions.

Corrosion can be caused by oxidation process as well as by severe attacks from a wide variety of chemical compounds, including un-combusted fumes from automobiles, adverse weather conditions and pollution. It is an electrochemical process whereby a material reacts with its exposed environment. It results in the damages of properties which cause economic losses, structural failure, affecting safety and raising environmental concerns. Although corrosion is not a problem with a 100 % cure, the use of current technology can moderate its damaging effects.

About one-third of the total output of metal is eliminated from technical consumption because of corrosion. It is estimated that up to 7-8 % of a industrialized nations annual income is lost due to corrosion (Sangaj & Malshe, 2004). The severity of the problem has become acute with the beginning of development, fast growing industrialization, huge infrastructures required for the same and consequent polluted environment to which vulnerable metals are exposed.

In a widely-cited corrosion cost study by the National Association of Corrosion Engineers (NACE) and the direct cost of corrosion in the U.S. was estimated equal to \$276 Billion dollars in 1998 (NACE, 2013). In that case, the total cost of corrosion is \$993 Billion in March 2013 and estimated to exceed \$1 Trillion dollars by June 2013. However, this estimate is incomplete and closer examination of the NACE data indicates that total corrosion cost in the U.S. may exceed \$1.5 Trillion dollars annually (NACE, 2013) and with the same correlation, it is estimated about \$2 Trillion dollars in year 2015. Major corrosion control measures will save our world's resources while in the process recovering Trillions of U.S. dollars presently being lost.

Coating manufacturers can no longer rely on their current coating products to be sold or receives good response from customers. However it is still compatible to use in these days. Eventually these products will be phased out sooner or later with the invention of new ideas or materials. As the development of the protective coating industry moves into the 21st century, the need to develop high-performance and cost effective coating is essential. Coating materials with superior physical, mechanical, thermal, structural and electrochemical properties to suit the stringent environmental conditions is pressing. This has shifted the manufacturers to emphasize onto laboratory research for new coating materials, particularly in accelerated anti-corrosive coatings.

Corrosion control can be achieved with proper material selection, environmental modifications, alloying, anodizing, cathodic protection and protective coating. Coatings may possibly be organic (polymer), inorganic (ceramics or glass) or metallic (electroplating or galvanizing metals) and hybrid coatings (Rau et al., 2011; Xing et al., 2011). Although corrosion control techniques are much diversified, in principle coating prevents contact between the corrosion agent and the material surface (Bierwagen, 1996).

Paints are most commonly used as a coating material. There is variety of commercially available paints. Paints are mixtures of organic polymers with pigments of different colours. Basically they contain organic substance as binders and inorganic materials as pigments. The fundamental physical and mechanical properties of the paint materials have to be studied. Recent researches have been done using hybrid coatings with a blend of resins such as silicone, acrylic, epoxy, polyester and polyurethane resin to obtain the optimum properties. From the reports, it is known that these hybrid coatings have some important properties such as corrosion resistance, impact resistance, flexibility, chemical and permeation of moisture, adhesion and cohesion of the coating on the metal substrate can be analyzed and improved (Raps et al., 2009). Corrosion

prevention compounds are materials that can both prevent new corrosion sites from forming as well as suppress corrosion that has initiated (Gui & Kelly, 2006).

The large family of epoxy resin represents some of the highest performance resins available at present. Epoxies outperform most resins in terms of mechanical properties and resistance to environmental degradation. Epoxy chemistry also lends itself to a vast range of modifications as reported (Rau et al., 2011). Epoxy resins are widely used as marine coatings due to their outstanding properties, but are not cost effective. Amine-cured epoxy resin formulations are widely used in ambient temperature cured coatings (Rau et al., 2011). If polymerization occurs during conditions in cool ambient temperatures or high humidity, such coatings can develop a surface oiliness, exudates, or whitish spots variously referred to as “amine-blush,” “sweating,” or “bloom”. While acrylic polyol resin is a cost effective thermoplastic resin and is used for exterior or interior coating systems. The developed acrylic-epoxy hybrid coating system can cure under ambient conditions without causing any blushing. The present investigation illustrates some characteristics of acrylic-epoxy resin that may serve the above purpose.

1.2 Objectives of the Present Investigation

General Research Objectives

- ✓ To develop anti-corrosion coatings
- ✓ To investigate the properties of the prepared organic resin blend system
- ✓ To choose the best performing binder system for paint formulation, using suitable pigments
- ✓ To analyze paint properties

Details of Present Research Objectives

Specifications in this investigation have been carried out to complete the following objectives:

- ✓ To develop new hybrid system using acrylic-epoxy resin for corrosion protection
- ✓ To study the physical, mechanical, thermal, structural, electrochemical and corrosion resistance properties.
- ✓ To study the physical and mechanical properties correlation such as viscosity, dry film thickness, adhesion and impact resistance of the developed systems.
- ✓ To study the thermal properties like glass transition temperature and thermal degradation of the coating system, by using differential scanning calorimetry and thermogravimetric analysis respectively.
- ✓ To study the structural and surface morphology using Fourier transform infrared spectroscopy, scanning electron microscopy and energy dispersive of X-ray analysis.
- ✓ To study the electrochemical properties in terms of corrosion protection by electrochemical impedance spectroscopy, accelerated UV weathering test and acid immersion studies.
- ✓ To identify the critical pigment volume concentration.
- ✓ To identify the best performing hybrid system and to formulate paint systems using inorganic pigments.

1.3 Scope of the Thesis

The objective of this study is to develop anti-corrosion hybrid coating system using a mixture of commercially available organic resins and pigments. The study is divided into two parts. The first part deals with identifying the best blending ratio between resin components of the hybrid system. In this development, Acrylic Polyol resin (A) was blended with Epoxy resin (E) and Polyisocyanate resin was used as a curing agent. Hybrid coating system also exhibits a unique performance-to-cost ratio because it can produce hard and flame resistant films as reported (Xing et al., 2011).

In the second part of study, it deals with the formulated paint systems incorporated with pigments in the best blending ratio will be analyzed. Four types of inorganic pigments were used to formulate paint systems namely P1, P2, P3 and P4. The effect of the ratio of the pigment volume concentration (PVC) to the critical pigment volume concentration (CPVC) on the corrosion resistance properties of paint system has been investigated (Gowri & Balakrishnan, 1994). The study will be established on the variation of the composition of the pigments that has been used to prepare primer coat and finish coat or top coat on mild steel panel.

Before the actual work is carried out, an extensive review of the types of corrosion, corrosion control, paint systems, organic resins, pigments and its application on treated mild steel panel, etc. was carried and presented in Chapter 2. Apart from this, works that have been done in this field are also presented.

Chapter 3 presents the experimental materials and methodology of sample preparation, development of the hybrid binder systems, paint formulation and formulae employed (Rodriguez et al., 2004) in characterization of the coating and paint systems. In this study, two organic resins (A and E), and four pigment based paint systems (P1, P2, P3 and P4) have been used for the development of anti-corrosion hybrid coating.

The analytical methods involve the viscosity measurement, drying time, glossiness measurement, dry film thickness (DFT), cross hatch method, impact resistance, accelerated UV weathering test, thermogravimetric analysis (TGA), differential scanning calorimetry (DSC), Fourier transform infrared spectroscopy (FTIR), scanning electron microscopy (SEM), energy dispersive of X-ray analysis (EDAX), acid immersion and electrochemical impedance spectroscopy (EIS).

In Chapter 4, the results of the hybrid binder system developed by Acrylic Polyol resin (A) with Epoxy resin (E) and Polyisocyanate resin (NCO) was used as a curing agent have been analyzed in terms of physical, mechanical, thermal, structural and electrochemical properties. Experimental results with various blending ratio hybrid system (AE) that been developed explored extensively in this chapter.

Chapter 5 presents the results from physical, mechanical and accelerated UV weathering studies of four paint systems formulated using the best performing Acrylic-Epoxy blending ratio. Titanium Dioxide (TiO_2) (Clerici et al., 2009; Kardar et al., 2014) and Hoffmann Minerals-Neuburg Siliceous Earth (NSE) (Essen, 2005) have been served as the inorganic pigments.

Chapter 6 focusses on the thermal and structural properties on the various Acrylic-Epoxy paint systems. The durability and flexibility of the paint systems were identified using TGA, DSC, FTIR, SEM and EDAX.

Chapter 7 presents results of acid immersion and EIS studies. From EIS the coating resistance, coating capacitance, dielectric constant and volume fraction of water of the four paint systems were determined.

In Chapter 8 a simple analysis to determine the CPVC percentage was carried out using coating resistance and diffusion rate relation comparisons. The effect of the PVC content ratio to the CPVC on the corrosion resistance properties of paint system has been analyzed (Ferreira et al., 2001).

Chapter 9 focuses on the discussion of the overall results with correlation in greater depth brought together and analyzed to understand the properties of the paint system.

Chapter 10 draws a conclusion for the analysis and results obtained; further provides suggestions for future research in corrosion protection using hybrid paints.

University of Malaya

CHAPTER 2: LITERATURE REVIEW

2.1 Introduction

What is Corrosion?

- ✓ It is the process of degradation or deterioration.
- ✓ Decay of metallic materials by reaction with its environment.
- ✓ If it is Iron, then it is called Rusting.
- ✓ If any two different metals are in contact with each other, the more reactive metal will corrode in preference to the less reactive metal.

2.1.1 Types of Corrosion and its Mechanism

❖ Dry or Chemical Corrosion

- This type of corrosion occurs by direct chemical attack of atmospheric gases like Oxygen (O_2) on the metal (M) surface to form Metal Oxide (MO_n) layer.
- $2M + nO_2 \rightarrow 2MO_n$ (Metal Oxide)

Nature of Metal Oxide layer:

- **Stable:** It acts as a barrier between metal and O_2 , prevents further corrosion.
- **Unstable:** It decomposes back to metal and O_2 . Argentum (Ag), Aurum (Au) and Platinum (Pt) are protected by this manner.
$$2M + nO_2 \rightleftharpoons 2MO_n$$
- **Volatile:** Layer volatilizes and metal exposed for further corrosion.

- **Porous:** Corrosion occurs through pores and continues until the entire metal gets corroded.
- Corrosion is also caused by some other gases like Halogens (F₂, Cl₂, and Br₂), Hydrogen Sulphide (H₂S) and Sulfur Dioxide (SO₂) etc. This type of corrosion depends on chemical attraction between metal and gas.

❖ Wet or Electrochemical Corrosion

- This type of corrosion occurs when a liquid medium is involved. One part behaves as anode and undergoes oxidation. The other part acts as cathode and undergoes reduction.
- Liquid medium involved acts as electrolyte. It is further of two types:
 - (a) Evolution of Hydrogen (H₂) type corrosion
 - (b) Absorption of Oxygen (O₂) type corrosion

Evolution of H₂ type corrosion

- It occurs in the acidic environment.
- At anode : $M \rightarrow M^{n+} + ne^{-}$ (Oxidation)
- At cathode : $2H^{+} + 2e^{-} \rightarrow H_2$ (Reduction)

Absorption of O₂ type corrosion

- Rusting of Iron as shown in Figure 2.1.

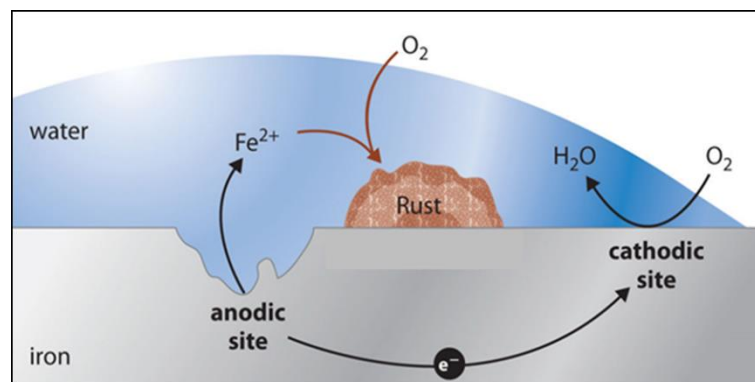


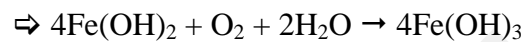
Figure 2.1: Absorption of O₂ (Photo sourced from www.assignmenthelp.net)

If the layer of Iron develops some cracks, this damaged surface acts as anode while the other intact metal behaves as cathode. Presence of moisture acts as an electrolyte.

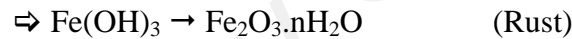
The reactions occurring are:

- $\text{Fe} \rightarrow \text{Fe}^{2+} + 2\text{e}^-$ (Oxidation)
- $\text{O}_2 (\text{g}) + \text{H}_2\text{O} + 4\text{e}^- \rightarrow 4\text{OH}^-$ (Reduction)
- ⇒ $\text{Fe}^{2+} + 2\text{OH}^- \rightarrow \text{Fe}(\text{OH})_2$ (Redox Reaction)

In the presence of excess oxygen, $\text{Fe}(\text{OH})_2$ oxidizes to $\text{Fe}(\text{OH})_3$ as:



This Ferric Hydroxide ($\text{Fe}(\text{OH})_3$) formed decomposes to Hydrated Ferric Oxide ($\text{Fe}_2\text{O}_3 \cdot n\text{H}_2\text{O}$) as summarized in Figure 2.2.



The formation of rust depends more on the condition of the surrounding environment. This may cause a total failure of the structure, which can lead to a high economical loss and human fatality (Davis, 2000).

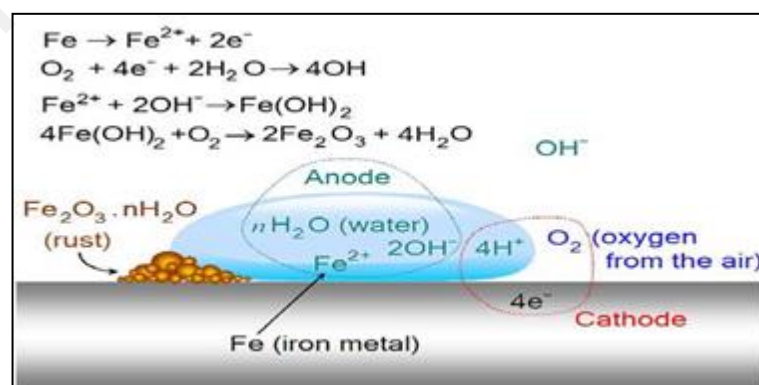


Figure 2.2: Corrosion Mechanism

(Photo sourced from www.duluxprotectivecoatings.com.au)

2.2 Why Steel?

Steel is an excellent choice of building material due to its high flexural and compressive strength. It allows the design of much taller multi-storey buildings and structures with wider spans because of its high strength to mass ratio. It is also lighter to transport, quick to erect and is versatile in design. Steel has unique properties which makes it a leading contributor to sustainable construction and for a long-term environmental performance of buildings of all descriptions. At the end of a building's life, the recovered steel can either be reused or recycled into new steel products. This ensures cost effectiveness and reducing raw material dependence.

2.3 Mild Steel

Steel is derived from Iron. Iron ore or known as Hematite requires great thermal energy (around 1500 °C) to reduce into its metallic form of Iron. The Iron is then alloyed with Carbon and metals such as Nickel or Tungsten to produce steel. Steels are described as Mild, Medium or High-Carbon steel, according to the percentage content of Carbon. Mild steel is an Iron alloy that contains less than 0.25 % Carbon as shown in Figure 2.3.

Mild steel is very reactive and will readily revert back into Iron Oxide (rust) in the presence of water, oxygen and ions. The readiness of steel to oxidize on the exterior exposure means that it must be adequately protected from the environmental elements. New mild steel surfaces should be inspected for mill scale, rust, sharp edges, laminations, welding flux, forming or machine oils, salts, chemical contamination or mortar splashes on them, all of which must be removed properly (Dulux, 2009).

COMPOSITION AND PROPERTIES OF MILD STEEL

- ✦ Also known as **Low-Carbon Steel**.
- ✦ **Composition:-**
 - Ferum: 99.70%wt - 99.98%wt
 - Carbon: 0.02%wt – 0.25%wt
- ✦ **General properties:**
 - Density: 7800 – 7900 kgm⁻³
- ✦ **Mechanical properties:**

Modulus of Elasticity	200 – 250 GPa
Yield Strength	250 – 395 MPa
Tensile Strength	345 – 580 MPa
Elongation	26% – 47%
Hardness	107.5 – 172.5 HV



Figure 2.3: Composition and Properties of Mild Steel
(Photo sourced from www.duluxprotectivecoatings.com.au)

2.4 How do we stop Steel from Corroding?

For corrosion to occur, an anode, a cathode and electrolyte are essential as shown in the corrosion triangle below (Figure 2.4). For any reasons the linkage within this triangle is broken, corrosion can be controlled and probably prevented.

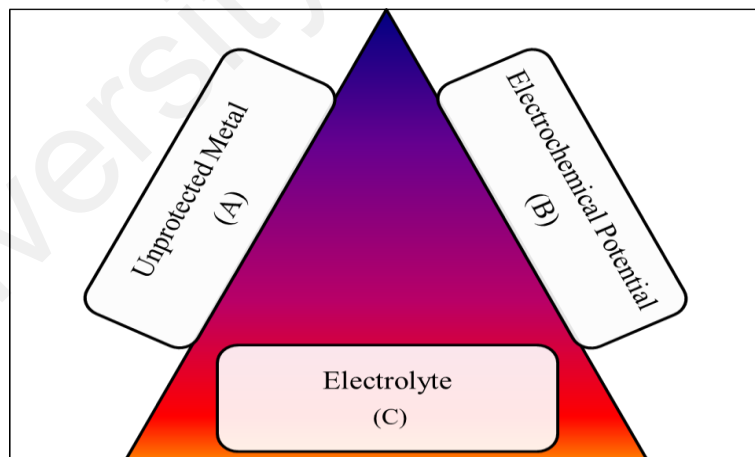


Figure 2.4: Corrosion (A + B + C) Triangle

There are four basic methods that can be used to control and protect steel from corrosion (Jones, 1995).

1. Selecting corrosion resistant materials:

- Apart from the factors of cost, availability and others, corrosion resistance must be considered as a part of overall material selection process. Analysis from previous applications experience and corrosion testing data are used for material selection in specific locations of our system. Down to the basics, a metal less willing to oxidize in our conditions is the material we are looking for. A metal with higher standard electric potential for oxidation of hydrogen is preferred generally from the electromotive series.

2. Corrosion inhibitors:

- They aid in modifying the environment around our system so as to prevent or slow corrosion down. Inhibitors retard corrosion by increasing polarization of anode and cathode and by increasing the electric resistance due to formation of a deposit on the surface of metal. Examples of corrosion control using inhibitors include, modifying structures to provide desired drainage, using inhibitors in power plants or engine cooling systems.

3. Cathodic protection:

- The basic of this method depends in lowering the difference between potential of anode and cathode by supplying an electric current from an external source. Structures buried and in contact with water like pipelines and underground storage tanks are protected effectively using this method. Thus the natural electrochemical cell action is hampered by the

use of cathodic protection method. There are 2 different ways in which current can be delivered:

- **Sacrificial Anode:** This way the active metal is sacrificed by corroding itself and protecting the surface where we want to control corrosion. In this process, corrosion of an active metal like Zinc (Zn), will produce standard electric potential. In order to quantify the use of this method, natural corrosion potential is used in the selection of which the metal to be sacrificed.
- **Impressed current:** In this method, we supply direct electric current from any other external source (sometimes even using a rectifier to convert AC to DC). An inert anode material is used in the process to complete the circuit.

4. Protective coatings:

- This method of corrosion control is the most widely used techniques around the world today. When protective coatings used with other methods of corrosion control explained previously, it becomes very effective. There are 3 basic mechanisms which makes the coatings to enhance corrosion control:
 - **Barrier protection:** Moisture and other electrolytes become impermeable to the coating, thus a barrier is formed between surfaces which are susceptible to corrosion and the corrosion causing factors in the environment. Thus it slows down or stops the process of oxygen to approach the metal surface.
 - **Cathodic protection of steel:** In some protective coatings there is present of high Zinc (Zn) particles (or any other active metal)

loading. These particles are in electric contact with each other as well as with the underlying metal. Therefore, cathodic protection is created by the protective film.

- **Inhibitive pigments:** Protective coatings also function as inhibitors due to some pigments present in the coating. These pigments inhibit the corrosion at the interface of metal and coating.

5. Some other methods:

- **Stable oxide layer forming metals:** Due to formation of a stable oxide layer on the surface, further corrosion is prevented. Thus at first stage, metal which forms stable oxide layer must be selected and oxidation resistance of some metals (generally alloys) has to be improved by adding alloying elements like Chromium (Cr), Silicon (Si), Aluminium (Al) etc. These elements on reaction with oxygen tend to form a stable oxide layer which acts as a protective coating for metal when it is exposed to their service environments.

As seen from the corrosion triangle explained in Figure 2.4, if efforts are made wherever possible to keep metals dry and away from moist conditions, most forms of corrosion can be stopped. To protect steel against corrosion, surface preparation and coating application would be the most cost effective methods. Correct execution of the surface preparation steps is the most important method because maximum performance of the coating system can only be achieved on a uniformly clean and well-profiled surface (Davis, 2000). The coating system then needs to be maintained periodically.

2.5 Types of Corrosion

There are various corrosion mechanisms available. They differ in the nature, size, and effects.

2.5.1 General or Uniform Corrosion

General or Uniform Corrosion is the most common form of corrosion that occurs due to chemical attacks. The metal appears dull, then becomes thinner and finally fails. Figure 2.5b is a sectional schematic of uniform corrosion on steel. Uniform corrosion can be prevented by using thicker metals, paints or metallic coating. Usage of corrosion inhibitors or modifying the environment would be an addition help. For uniform corrosion, the corrosive environment must have same access to all parts of the metal surface as shown in Figure 2.5a and Figure 2.5c. Metals such as steel that do not form passive layer show uniform corrosion.



Figure 2.5: Uniform Corrosion

(Photo sourced from www.corrosion-doctors.com)

2.5.2 Pitting Corrosion

Pitting corrosion is a localized form of corrosive attack that produces holes or small pits on a metal surface. These holes could be big or small and many in which it will form a rough surface as shown in Figure 2.6a. The remaining surface of the metal remains unaffected. The unaffected area of the passive surface layer will retain its original shine. Pitting is often found in situations where resistance against general corrosion is conferred by passive surface coatings. Localized pitting attack normally happens when these passive coating have broken. Figure 2.6b is a sectional schematic of pitting corrosion on stainless steel.

The main constituents of common salt such as Halides and microbial activity such as Sulfate Reducing Bacteria (SRB) (Xu et al., 2012) encourage pitting as shown in Figure 2.6c. This portion will become of a negative pole because of non-noble potential and the surrounding passive layer becomes the positive pole, where a battery is formed. The corrosion advances rapidly, when positive pole area is far larger than the negative pole area.

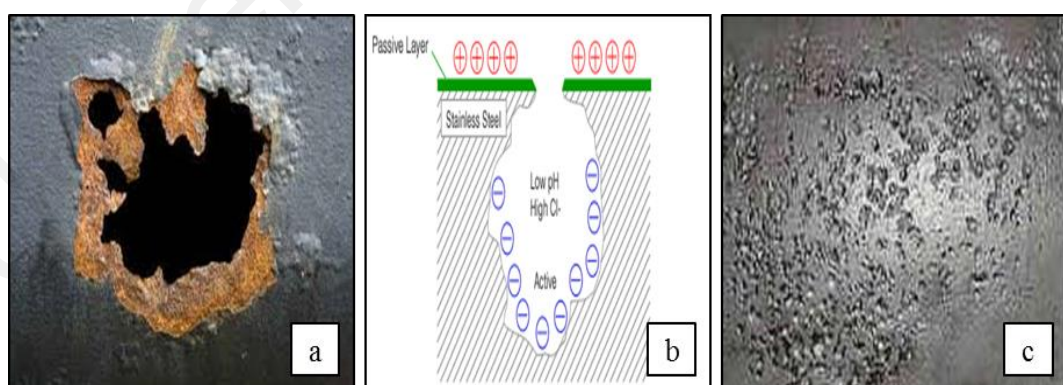


Figure 2.6: Pitting Corrosion

(Photo sourced from www.corrosion-doctors.com)

2.5.3 Stress Corrosion Cracking

This type of corrosion is observed in fabricated objects which are subjected to various mechanical operations. This stress corrosion cracking happens due to the simultaneous influence of static tensile stresses. Figure 2.7b is a sectional schematic of stress corrosion on metals. The stresses can be from internal cause such as cold work, welding and heat treatment or external forces caused by mechanical stresses set up by assembly practices referring to bending, hammering and annealing. The cracking occur perpendicular to the applied stresses as shown in Figure 2.7a and Figure 2.7c.

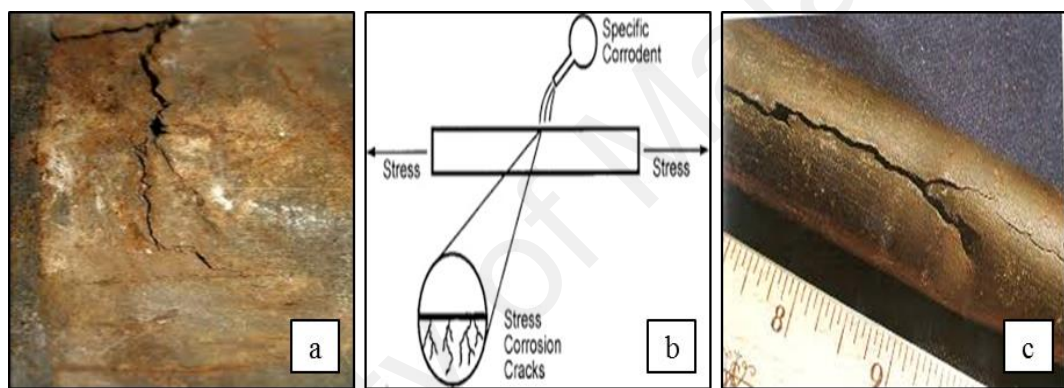


Figure 2.7: Stress Corrosion Cracking

(Photo sourced from www.corrosion-doctors.com)

Stress corrosion cracking occurs in some specific combination of metals and environments, as shown in Table 2.1. The corrosion occurs only when the specific corrosion environment exists along presence of tensile stress. It can be said that this type of corrosion occurs in limited environments.

Table 2.1: Stress Corrosion Cracking Causing Metals and Environments

Metal	Causative Material	Environment Example
Carbon Steel	NO_3^-	High Temperature NaNO_3 Solution
	OH^-	High Temperature / Concentrated NaOH Solution
High Tensile Steel	H_2S	H_2S Solution
Austenitic Stainless Steel	Cl^-	High Temperature Sea Water
	OH^-	High Temperature / Concentrated NaOH Solution
	Polythionic Acid	Exposed to hygrophytic environment after sulfurating
	High Temp. Water	Plumbing for boiling water type nuclear reactors
Brass	NH_3	Atmosphere containing NH_3
	Amines	Amine Solution
High Strength Aluminium Alloy	Cl^-	Sea Water
High Strength Titanium Alloy	Cl^-	Sea Water, High Temperature NaCl

2.5.4 Fatigue Corrosion

Fatigue corrosion is a special case of stress corrosion caused by the combined effects of cyclic stress in a corrosive environment. For example, a wire will break if it is repeatedly bent and straightened. This is because the metal is fatigues and resulted in a fracture due to stress build-up by repeated bending as illustrated in Figure 2.8.

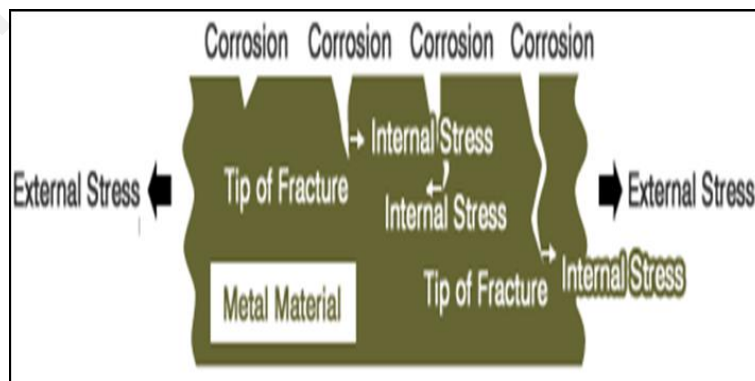


Figure 2.8: Corrosion Fatigue

(Photo sourced from www.misumi-techcentral.com)

There are many objects that are exposed to repeated stress in this real world. Railway tracks are subjected to stress every time a train passes, and marine structures such as bridges receive large cyclic stresses when it is hit by waves. Pressure bulkheads of large aircrafts are subjected to stresses caused by air pressure differentials during the take-off. The metal fatigue occurs in atmosphere, in water and in vacuum. Fatigue crack propagates through the metal as illustrated in Figure 2.9b. The cyclic stressing will extensively affect the fractured crack until it brittles as shown in Figure 2.9a. When the stress corrosion phenomenon happens, it will only occur if the stresses or corrosion exist simultaneously.

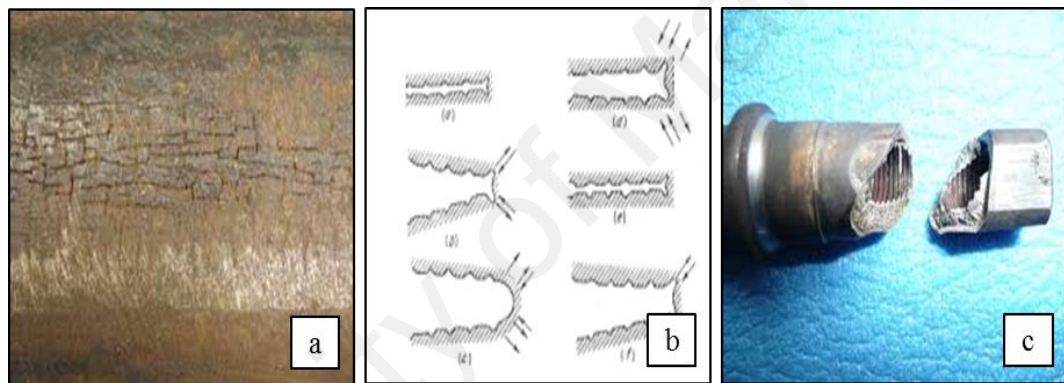


Figure 2.9: Corrosion Fatigue

(Photo sourced from www.corrosion-doctors.com)

When applied stresses are below Fatigue Limits, the metals do not fracture even if it is repeatedly exposed to the stresses. This fact establishes important indices for designs on machines and equipment that are exposed to repeated stresses. However, metals can fracture when it is exposed to repeated stresses. This can happen at even less than the Fatigue Limit if a corrosive environment is combined. At the same time, fractures can occur with less repetition cycles at the same stress levels.

This means the Fatigue Limit disappears. In other words, metal will fracture as shown in Figure 2.9c, regardless of repeated stress levels, and if enough repeated stresses are applied. This is called "Fatigue Corrosion" (Gangloff, 2005). Control of fatigue can be achieved by lowering the cyclic stress or by corrosion controller. The brittle fracture surface shows roughened appearance as shown in Figure 2.9.

2.5.5 Intergranular Corrosion

Intergranular corrosion is an attack on the grain boundaries of a metal or an alloy. Grain Boundary is the contacting surface of the crystals. Within each crystal, the atoms are in an orderly alignment. However the alignments of the atoms in adjacent crystals are different as shown in Figure 2.10a. The atoms within the grain boundary areas must integrate with atoms of both crystals in dissimilar alignments. Therefore, they are in mixed orientations. This means that the energy levels are in high state. This high energy state of grain boundaries is evident from microscopic observations of corrosive solution etched specimen. As shown in Figure 2.10c, where the grain boundaries are dissolved and the crystals becoming clearly visible (Ziegler et al., 2005).

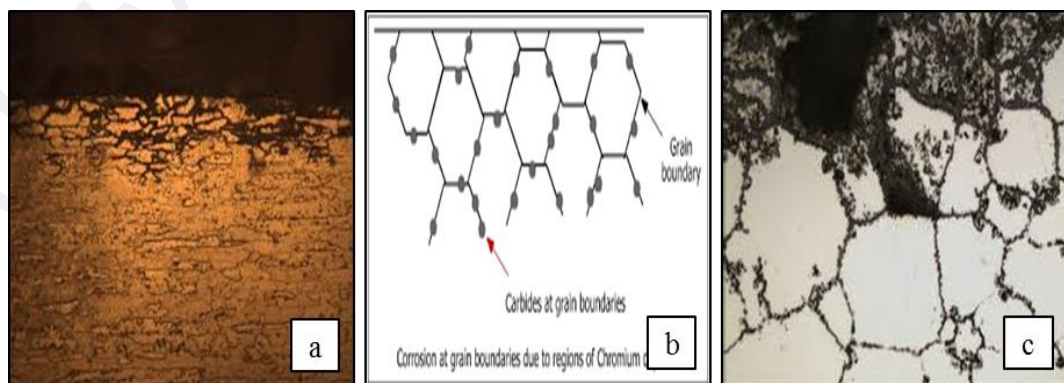


Figure 2.10: Intergranular Corrosion

(Photo sourced from www.corrosion-doctors.com)

Intergranular corrosion remains on the surface and does not advance further. But if it is heated under a certain conditions the crystal grain boundaries will forego chemical composition changes and some selective corrosion will occur. Figure 2.10b is a sectional schematic of Chromium Carbides form at grain boundary areas. In a carbide form, Chromium does not contribute in creation of passive layer. Therefore, exposed steel surface will be lacking the passive layer along the grain boundaries. When the steel is in this state, then it is exposed to corrosive environments and corrosion along the grain boundaries will progress.

2.5.6 Filiform Corrosion

Filiform Corrosion is a type of corrosion that is commonly known as "filamentary" or underfilm corrosion. It is normally linked to Magnesium (Mg), Aluminium (Al) and Iron alloys that utilize an organic form of coating (McMurray et al., 2010). This corrosion also can be visually recognized without using a microscope.

The mechanism for corrosion allows water and oxygen to migrate under painted surfaces as shown in Figure 2.11a. The dissolved oxygen has its highest concentration at the back of the head. When the oxygen is reduced in the tail region, the metal ion dissolute and the formation proceeds to the head (Schneider et al., 2007).

This type of corrosion has a tendency of taking place in conditions with a high level of humidity. Figure 2.11b is a sectional schematic of filiform corrosion on a coated metal substrate. Anions that contain Halides have been associated with filiform corrosion (McMurray et al., 2010). In places where the corrosion has taken place, there is a thread-like filament appearance that forms under the coating layer as shown in the Figure 2.11c. A number of approaches have been known to reduce the effect of filiform

corrosion. One of them is the application of a number of layers of protective coating and reduced relative humidity.

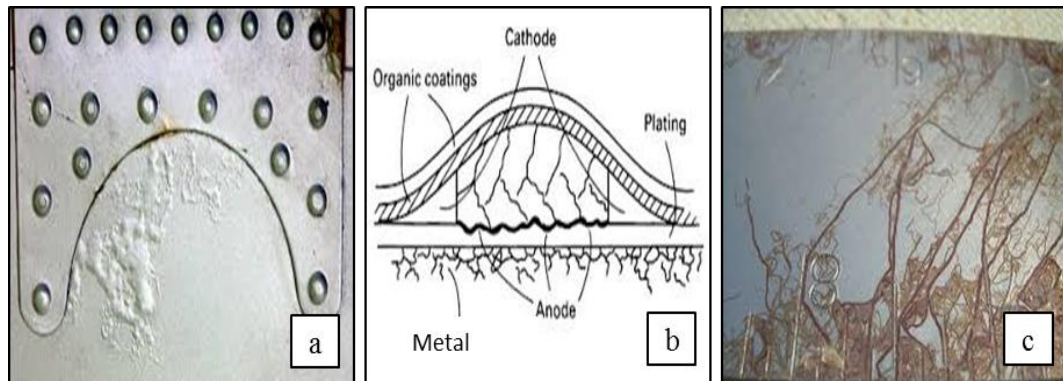


Figure 2.11: Filiform Corrosion

(Photo sourced from www.corrosion-doctors.com)

2.5.7 Crevice Corrosion

A crevice is a narrow gap between two pieces of metal or strongly adhered material like plastic. Crevice or contact corrosion is the corrosion occurred at the region of two joined metal contact due to its geometry of the structures like riveted plates, welded fabrications or threaded joints as shown in Figure 2.12a and Figure 2.12b. Contact between metal with non-metallic solids, e.g. plastics, rubber, glass and deposits of sand, dirt or permeable corrosion products on the metal surface.

Crevice corrosion is a type of localized corrosion that can be found within crevices or at secured surfaces where a stagnant solution is present. Many metals and alloys are susceptible to crevice corrosion, but in stainless steels, crevices are the first and most common place for corrosive attack to begin (Wika, 2012). It is one of the most frequently encountered forms of localized corrosion and at the same time one of the most harmful ones. This is because it happens in the alloys that normally exhibit perfect corrosion resistance such as stainless steels. It also occurs in areas that are not

immediately visible (Rashidi et al., 2007). Therefore crevice corrosion may lead to a sudden failure of the metal during its usage.

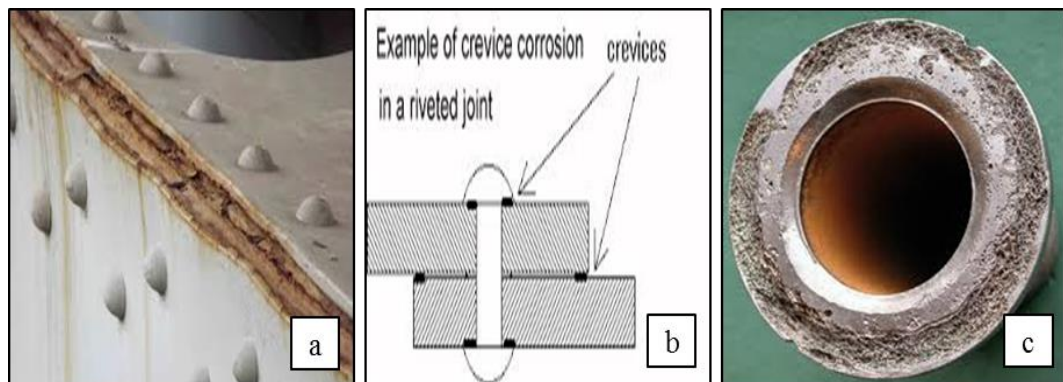


Figure 2.12: Crevice Corrosion

(Photo sourced from www.corrosion-doctors.com)

The simplest method for preventing crevice corrosion is reducing crevices in the design of the structure. When it is not possible to get rid of crevices, improving drainage and sealing the edges or keep the crevices as open as possible. This will help to prevent the entrance of moisture and it will be the best protective action. It may occur at washers, under barnacles, at sand grains, under applied protective films or coatings, and at pockets formed by threaded joints as shown in the Figure 2.12c.

2.5.8 Galvanic or Bi-Metallic Corrosion

Galvanic corrosion takes place between two different metals which are joined together in the presence of an electrolyte. As seen in Figure 2.13, a galvanic couple formation makes one of the metals in the couple becomes the anode and corrodes faster than it would all by itself. While the other becomes the cathode and corrodes slower than it would alone (Perez-Quiroz et al., 2014). The most severe attack occurs at the joint between the metal couples as shown in Figure 2.13b.

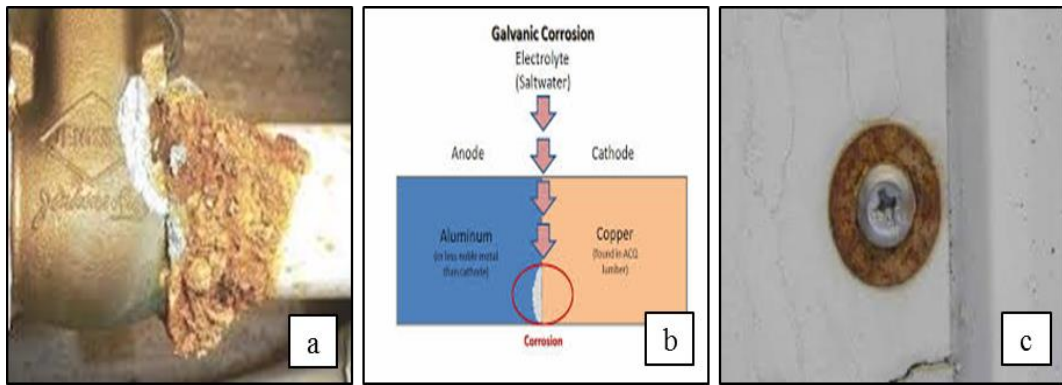


Figure 2.13: Galvanic Corrosion

(Photo sourced from www.corrosion-doctors.com)

Further away from the bi-metallic joint as shown in Figure 2.13a, the degree of accelerated attack is reduced. Each metal has its own potential that differs from each other when placed in an electrolyte. A series can be built up of all the metals relative to each other. According to the potential values as shown in Table 2.2, metals at the top of the table are more anodic than those at the bottom. When it is in an electrical contact in the electrolyte, it will corrode in preference to the metal which is listed at the bottom of the table. The further apart the metals, the faster corrosion rate will take place.

Table 2.2: Galvanic Metal Series

ANODIC / CORRODED END	LESS NOBLE
Zinc	
Aluminum	
Galvanized Steel	
Cadmium	
Mild steel – wrought iron	
Cast iron	
Stainless steel, types 304 & 316, active*	
Lead-tin solder	
Lead	
Brass, Bronze	
Copper	
Stainless steel, types 304 & 316, passive*	
CATHODIC / PROTECTED END	MORE NOBLE
<div style="display: flex; align-items: center; justify-content: center;"> <div style="writing-mode: vertical-rl; transform: rotate(180deg);">Flow of electrons</div> </div>	
*active stainless is stainless that hasn't been chemically treated	

2.5.9 Fretting Corrosion

Fretting corrosion is the rapid corrosion that occurs at the interface between contacting surfaces. The contacting interface; Body 1 and Body 2 must be under load as schematic Figure 2.14b or relative motion must occur and should be sufficient enough to produce deformation on the surface as shown in Figure 2.14a and Figure 2.14c. This type of corrosion is most common in bearing surfaces in machinery, such as connecting rods, splined shafts, and bearing supports which often causes a fatigue failure.

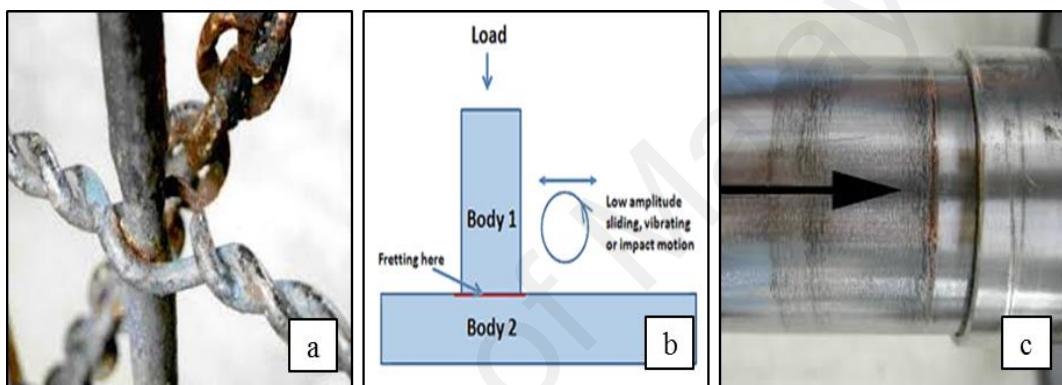


Figure 2.14: Fretting Corrosion

(Photo sourced from www.samtec.com)

Problems generated by fretting corrosion are very expensive to fix. There is no standard test method to identify fretting corrosion. Mechanical design plays a very important role than material selection when facing these kind of corrosion (Scopelliti, 2013). While it cannot be eliminated completely, it can be decrease by reducing relative movement between materials or increase the hardness by using materials that are not susceptible to fretting corrosion. Simple and cost effective methods will be by using contact lubricant and seal to absorb vibrations.

2.5.10 Erosion Corrosion

Erosion corrosion refers to the combined action involving erosion and corrosion in the presence of a moving corrosive fluid or a metal component, moving through the fluid leading to accelerated loss of protective layers on the metal surfaces. Erosion corrosion can also be intensified by faulty workmanship which could have wrongly directed the flow of fluids.(El Rayes et al., 2013).

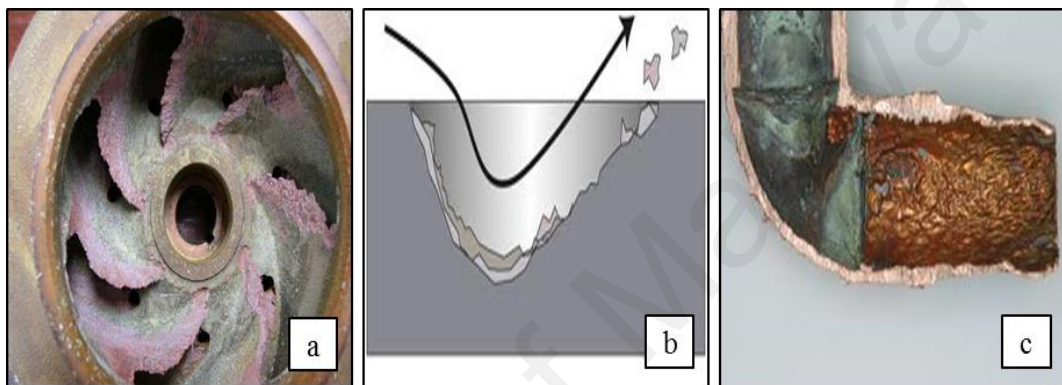


Figure 2.15: Erosion Corrosion

(Photo sourced from www.corrosion-doctors.com)

It is attributed to entrained air bubbles, suspended matter and particulates under a flow rate of sufficient velocity. Erosion is similar to impingement attack and it is primarily found at elbows and tees, or in those areas where the water sharply changes direction as shown in Figure 2.15a and Figure 2.15c. Softer metals such as Copper (Cu) and Brass are inherently more susceptible to erosion corrosion than steel. Figure 2.15b is a sectional schematic of cavitation that caused by high speed water bubbles leading to pits on the metal surface. Erosion can be controlled by design and material selection.

2.5.11 High Temperature Corrosion

High temperature corrosion is defined as the oxidation of metal at elevated temperatures and does not require the presence of a liquid electrolyte. This non-galvanic form of corrosion can occur when a metal is subject to a high temperature atmosphere containing oxygen, sulphur or other compounds that is capable of oxidizing the concerned metal. For example, materials used in aerospace, power generation station and in car engines have to resist sustained periods at high temperature in which they may be exposed to an atmosphere containing potentially high corrosive products of combustion. As shown in Figure 2.16a and 2.16c, this type of damage is called “dry corrosion” or “scaling” that generally occurs at the exhaust manifold.

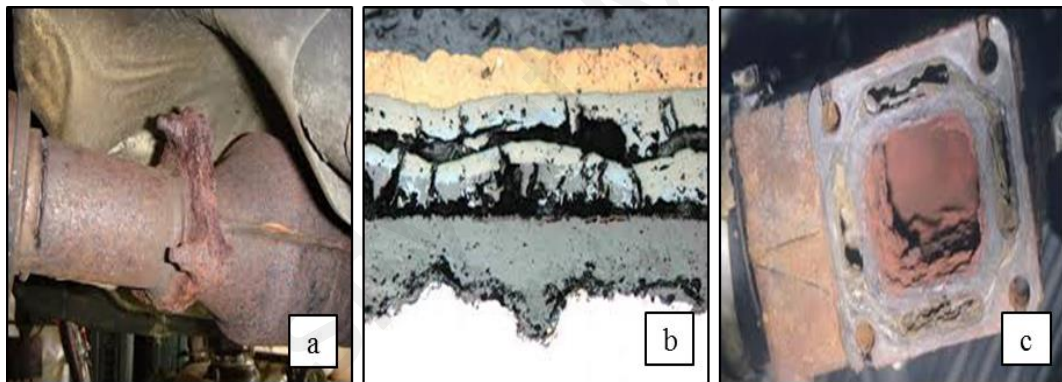


Figure 2.16: High Temperature Corrosion

(Photo sourced from www.corrosion-doctors.com)

Oxidation is the most important high temperature corrosion reaction. The formation of oxides on stainless steels, for example it can provide a protective layer preventing further atmospheric attack, allowing for a material to be used for sustained periods at both room and high temperature in hostile conditions (Lang, 2012). The corrosion mechanism is indicated by the most abundant corrosion deposits observed on the metal after corrosion, i.e. oxidation by metal oxides, sulfidation by metal sulphides, sulfidation or oxidation by mixtures of sulphides and oxides, carburization by metal carbides, and chlorination by metal chlorides (Marcus, 2011).

2.6 Coating

Coating is a technique of corrosion prevention that can be described by application of an external layer of film onto a metal substrate as shown in Figure 2.17. Formation of metal oxidation on the un-coated metal surface is shown in Figure 2.17b. The coatings are applied on the metal surface for the primary protection and to prevent contact of the environment with surfaces (Rau et al., 2012). The manufacturing processes of the layer need to be improved against corrosion requires the coatings to possess flexibility, resistance against impact, chemical resistance to the environment, resistance to permeation of moisture, good adhesion and cohesion (Wicks Jr et al., 2007). Coatings may be organic (polymer), inorganic (ceramics or glass) or metallic (electroplating or galvanizing metals). Paints are most commonly used as a coating material. Basically they contain organic substance as binders and inorganic materials as pigments. However some paints contain corrosion inhibiting substance which enable them to reduce corrosion on the steel substrate and can produce galvanic action (Rau et al., 2012).

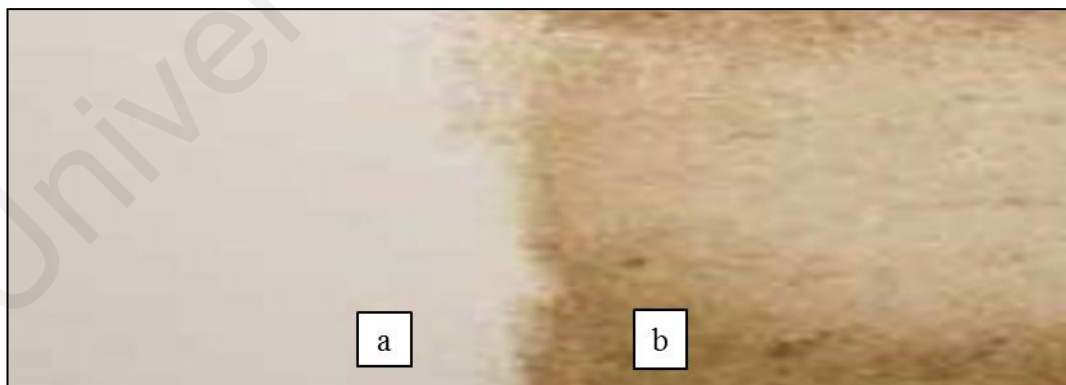


Figure 2.17: a) Coated Metal Surface b) Un-Coated Metal Surface

These coatings may vary in their appearance (clear, pigmented, metallic, or glossy) and by their function (corrosion protective, abrasion protective, decorative or photosensitive). Coatings can be divided into 3 groups: Organic, Inorganic and Hybrid coatings.

- **Organic Coating:** This is most widely used corrosion prevention method due to low cost factor. Paints, lacquers and varnishes are the examples of organic coatings. Acrylics, polyurethanes, epoxies, alkyds and polyesters are the most common organic resins used to develop organic coatings.
- **Inorganic Coating:** This coating consists of metallic and ceramics particles that can provide a good corrosion barrier. Electroplating, cladding, flame spraying and vapor deposition are few examples of metallic coating that can provide resistance to heat and radiation, biological inertness and electrical conductivity. Silicon (Si) based coating are most important inorganic element after oxygen that has been used commonly in organic coatings. Even though it has high thermal resistance property, but it is known for its brittleness due to highly functional inorganic chains. Replacement in some of the elements with organic functional groups gives improvements in flexibility and other mechanical properties.
- **Hybrid Coating:** Modern protective coating that may consist of organic-organic resin or organic-inorganic resin that combined for general coating properties enhancement. These coatings forms single layer coating compared to multilayer coatings that is used widely.

2.6.1 Why Hybrid Organic Coatings?

The major organic resins are often classified by its curing mechanism. The two basic types of cured coatings are nonconvertible and convertible (NACE, 2013). Convertible coatings, on the other hand, cure primarily by a polymerization process in which the resin undergoes an irreversible chemical change. Most convertible can be cured by polymerization.

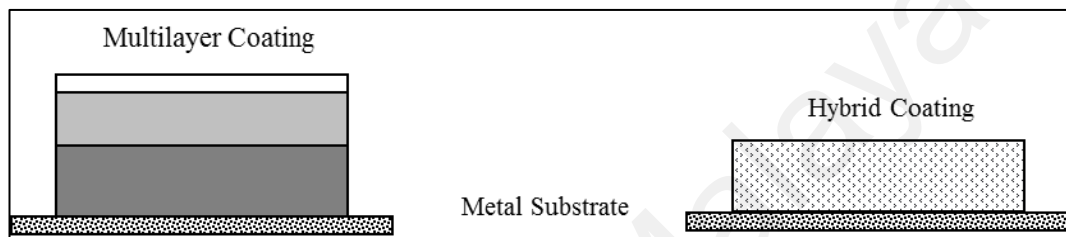


Figure 2.18: Metal Substrate coated with Multilayer and Hybrid Coating

Polymerization occurs when two or more resin molecules combines chemically to form a single, more complex molecules – single layer hybrid coating as shown in Figure 2.18. The resin molecule may be monomer (single unit) or they may be shorter chain polymers, which react to form longer chain polymer (NACE, 2013). These polymerized coating would be the most cost effective way of corrosion prevention for materials not inherently corrosion resistant.

Paints and coatings are generally applied at low additional cost to the least expensive structural materials. Minimizing the additional cost is an integral part of ensuring the economic viability of painting and coating as a corrosion control solution. Therefore paints and coatings generally do not last as long as the operating lifetime of the material to be protected, the ability to maintain the coating systems is vital (Revie, 2008).

Surface preparation, selection of primer coat and top coat would be considered as top priority when organic coating application. Improper preparation could lead to

failure of coating systems. When a coating system is applied on a well prepared metal substrate, it will spread and solidify in the crevices and voids. Such formation is called the mechanical bonding of the coat which will further improve the coating adhesion.

Using hybrid organic coating will prevent multilayers of application on substrate. Indirectly prevents impurities such as dust and air bubbles trapped within the coating. A forced drying time may results in a higher area of strata to cure first. This will lead to solvent trapped inside multilayer coating which will cause lower abrasion resistance and weaker adherence to the substrate. Therefore, modern protective coating that comprise hybrid coating mixture would improve overall coating performances.

2.7 Paint Composition

These coatings or paints contain 3 major components which are the Binder, Solvent and Pigments as shown in Figure 2.19. For example, many coatings consist of inorganic pigment particles dispersed in an organic matrix (the binder). Coating in this study emphasizes of organic coatings to those materials that can be traced historically back to paints. What is the difference between a coating and paint? Not much - the terms are often used interchangeable.

Paint can be thought of as a pigmented liquid, which protects and beautifies surfaces. Various raw materials are utilized to make this pigmented liquid. These two basic categories make up two portions of paint. The vehicle is the liquid portion of the paint (binder and solvent) and the pigment is the solid portion of the paint.

Paints have been manufactured since prehistoric times. Today paints are used for coloring and protecting many surfaces. Each of these different applications requires a different nature of paint. Hence, these differences of composition will be the focus of this study. Figure 2.19 shows a typical paint essential composition. The binder is the

film forming portion of a paint to adhere together all components as well to affix the paint systems with the substrate. The solvent is used to thin or disperse the binder and enables easier application of the paint layer. Pigments are used as source of color and help to control corrosion.

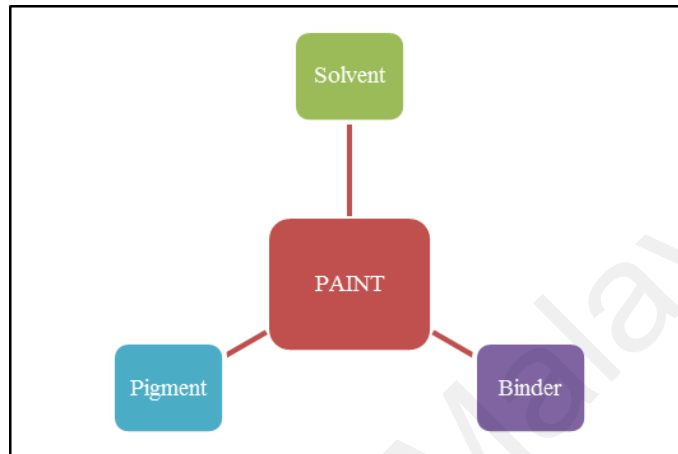


Figure 2.19: Typical Paint Compositions

Paint is a term used to describe a number of substances that consist of a pigment suspended in a liquid or paste medium such as oil or water. By using a brush, a roller or even a spray gun, paint is applied in a thin coat to various surfaces.

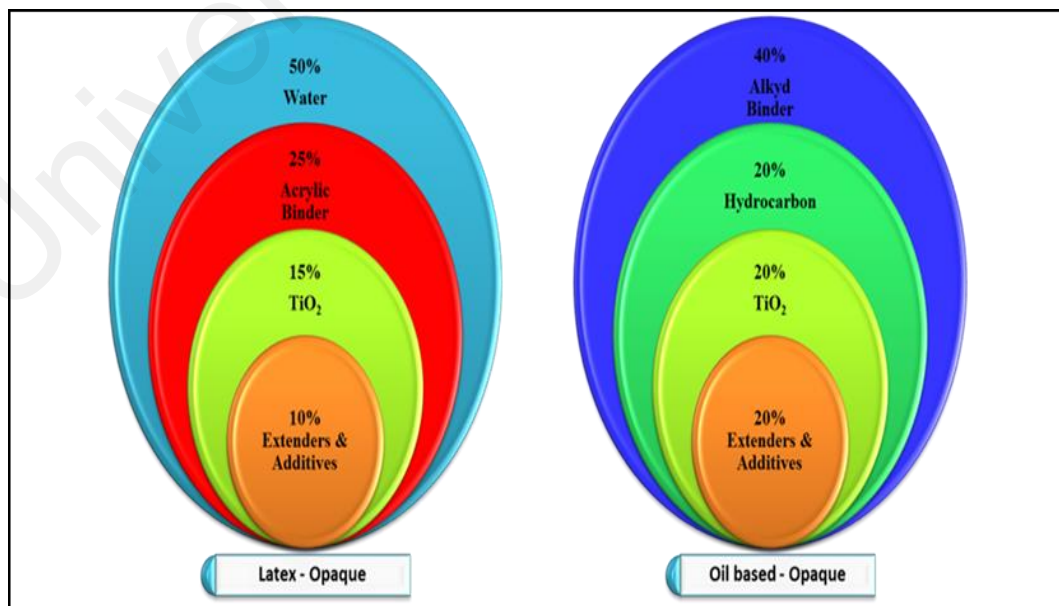


Figure 2.20: Typical Paint Formulations (Percentage by Volume)

The main paint ingredients include binders, solvents, pigments, extenders, additives and antimicrobials (Wicks Jr et al., 2007). Figure 2.20 depicts the formulation of a typical water-based opaque latex Acrylic topcoat and a typical opaque oil-based Alkyd topcoat.

2.7.1 Factors in selection of Paint or Coating System

When a system is chosen, several alternatives may appear to be officially acceptable, and it is necessary to identify relevant factors affecting corrosion control and costing. The most important factors are:

- high project cost, prestige or failure consequences may warrant the choice of high performance materials
- track record of the selected system for the environmental and operating conditions expected
- ease access to substrate work surface quality of applicator and contractor
- compliance with legislative and environmental requirements
- maintenance conditions and compatibility with existing materials
- life expectancy of coating to first maintenance
- type of substrate to be coated and delivery logistics

2.8 Binder

The binder is the film forming portion of a paint to adhere together all components as well to affix the paint systems with the substrate. It plays a vital role in determining the adhesion properties of the system. A wide range of binders is used in anticorrosive coatings, and indeed it may be assumed that any binder that is relatively inert and durable has applications in this area. Resins (liquid plastics, i.e. epoxies, acrylics, polyesters, polyurethane and vinyl esters) are commonly used in many applications.

Organic resins used as binder are divided into thermosetting and thermoplastic polymers. Thermosets are uncured, irreversible polymers the present in liquid form at room temperature. Most of them are regularly used as adhesives and have the chemical bond formation that sticks the coating to the substrate (Petzow, 1999). Thermosets also practically the strongest and most durable coating system compared to thermoplastics polymers due to polymer cross-linking and have higher resistance to heat (Forsgren, 2006). Examples of thermosets are epoxy, polyester and urethane.

On the other hand, thermoplastics are polymers that can be reformed into shape and have no reinforcement providing strength. Although they lack of adhesion property, their resistant to impact is comparable to thermosets (Forsgren, 2006). Examples of thermoplastics are acrylic, polycarbonate and vinyl.

2.8.1 Acrylic Polyol Resin

Almost every acrylic polyol in the market today breaks down to free-radical polymerization where an initiator, most commonly a compound with an azo link ($R-N \equiv N-R'$) or a peroxy link ($R-O-O-R'$) (Forsgren, 2006). The word 'polyol' refers to multiple hydroxyl functionality groups in its structure.

Acrylics are made by dissolving polymers made of acrylic acid and methacrylic acids. General mixtures result for acrylic polyol structure as shown in Figure 2.21. Hydroxyl group residue in the monomers plays an important role in incorporating additional functional groups as well as improving the properties of the final resin products. These are available in the forms of solids, solutions in organic and inorganic solvents and in water, emulsions and dispersions.

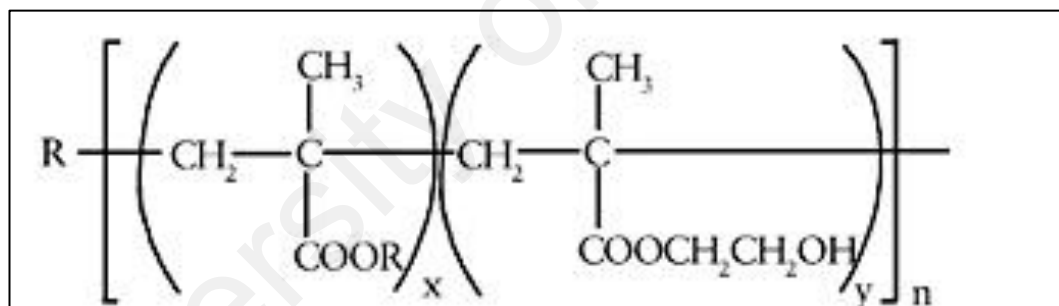


Figure 2.21: General Structure of Acrylic Polyol Resin

Acrylic resins have excellent durability. It is transparent or non-yellowing. It has resistance to hydrolysis and inertness to aliphatic solvents, cleaners and polishes. Both thermoplastic and thermosetting acrylic resins are being used industrially and in automotive industry. Acrylic resins can be cross linked with melamine formaldehyde and polyisocyanate resins (Wicks Jr et al., 2007). For them to perfectly cross-link, one of the species needs to have at least two reactive sites while the other has at least three reactive sites per molecule or chain (Forsgren, 2006).

The acrylic component can be formulated to give correct flexibility, weathering properties and gloss necessary for a car finish, particularly of the metallic type. They have high gloss and gloss retention and higher stability to hydrolysis. Aqueous acrylic coatings are being increasingly used for wood coatings, or corrosion protection coatings. These paints are not often baked, instead mechanical properties improved by cross linking at room temperature. Sometimes the acrylic resins cured by elevated temperature without the addition of external hardeners. Methyl methacrylate possesses higher weather resistance and gloss retention. They are compatible with other organic polymers like polyurethane, polyester, epoxy, and silicone etc.

Acrylic resin and polyurethane resin has been blended to produce hybrid emulsions. The emulsion hybrid provides advantages of acrylic resin such as economical product, with good hardness, gloss, weather ability and chemical resistance and the advantageous of polyurethane such as excellent adhesion and toughness (Aznar et al., 2006; Jiang et al., 2011; Peruzzo et al., 2011).

Mechanical and electrochemical properties of acrylic increased when 10-20 wt% of epoxy was added into the blending system. However, this improvement declined greatly when the percentage of epoxy increased (Rau et al., 2013). A study has shown that the stiffness and the barrier properties of acrylic coating can be improved by adding solid phenyl silicone. From the experimental analyses, the blend with 30 wt% of silicone resin and 70 wt% acrylic resin showed good adhesion and impact resistance properties on mild steel substrate (Vengadaesvaran et al., 2009).

A suitable protective coating to concrete reinforcing bar (rebar) is found to improve the durability of such structures under aggressive exposures. The performance of a few polymeric coatings based on different resins such as acrylic polyol-aromatic isocyanate, polyester polyol-aromatic isocyanate, acrylic resin and epoxy-silicone-

polyamide containing ordinary Portland cement or fly ash as extenders and Titanium Dioxide and Zinc Phosphate as main pigments on rebar in concrete has been evaluated using mechanical strength tests and accelerated corrosion tests to be well as effective and durable coatings (Selvaraj et al., 2009).

2.8.2 Epoxy Resin

The term 'epoxy' refers to a chemical group consisting of an oxygen atom bonded to two carbon atoms that are already bonded in some way. The simplest epoxy is a three-member ring structure known by the term 'alpha-epoxy' or '1,2-epoxy'. The large family of epoxy resin represents some of the highest performance resins of those available at this time. Epoxies generally out-perform most other resin types in terms of mechanical properties and resistance to environmental degradation. The epoxy molecule also contains two ring groups at its center which are able to absorb both mechanical and thermal stresses better than other linear groups.

Epoxy chemistry also lends itself to a vast range of modifications (Rau et al., 2011). As a laminating resin their increased adhesive properties and resistance to water degradation make these resins ideal for use in marine applications such as boat building. Epoxy resins are formed from a long chain molecular structure similar to vinyl ester with reactive sites at either end. In the epoxy resin, however, these reactive sites are formed by epoxy groups instead of ester groups. The absence of ester groups means that the epoxy resin has particularly good water resistance.

Diglycidyl ether of bisphenol-A (DGEBA) is a typical commercial epoxy resin and is synthesized by reacting bisphenol-A with epichlorohydrin in presence of a basic catalyst as shown in Figure 2.22. The properties of the DGEBA resins depend on the value of n , which is the number of repeating units commonly known as degree of

polymerization. The number of repeating units depends on the stoichiometry of synthesis reaction. Typically, n ranges from 0 to 25 in many commercial products (Wicks Jr et al., 2007).

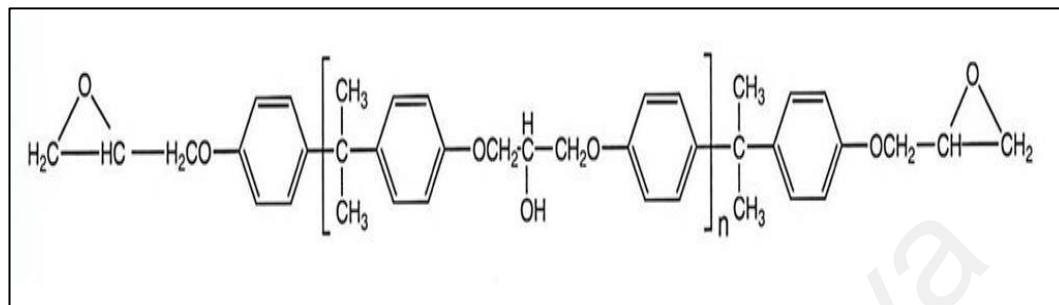


Figure 2.22: General Structure of Epoxy Resin
(Diglycidyl Ether of Bisphenol A, DGEBA)

The curing process is a chemical reaction in which the epoxide groups in epoxy resin reacts with a curing agent (hardener) to form a highly crosslinked three-dimensional network. In order to convert epoxy resins into a hard, infusible, and rigid material, it is necessary to cure the resin with hardener. Epoxy resins cure quickly and easily at practically any temperature from 5-150 °C depending on the choice of curing agent. A wide variety of curing agent for epoxy resins is available depending on the process and properties required. The commonly used curing agents for epoxies include amines, polyamides, phenolic resins, anhydrides and polyisocyanates. One of the most advantageous properties of epoxies is their low shrinkage during cure, which minimizes fabric ‘print-through’, and internal stresses (Rau et al., 2009).

Major investigation of epoxies mixture reveals that this combination would give major improvements from aerospace industry up to marine application (Bierwagen et al., 1996). Bierwagen et.al, investigated epoxy-polyamide-coating system for marine and pipeline coatings. From this study epoxy-polyamide provides good corrosion protections when it was characterized by using electrochemical noise method (ENM).

Electrochemical methods used mainly to evaluate corrosion resistance on epoxy-based coatings. This method is very important to evaluate corrosion resistance for protective paints (Behzadnasab et al., 2011; Ramesh & Vasudevan, 2012).

Electrochemical impedance spectroscopy (EIS) studies have been carried out to characterize the corrosion properties of polyester-epoxy coating systems. The results showed that sample contained 90 wt% of polyester (90P10E) obtained the excellent corrosion performance from the beginning until the end of exposure time. Moreover, the water uptake and dielectric constant were the lowest at the end of exposure which were indicating that the sample has good corrosion protection capabilities (Ramesh et al., 2013).

Epoxy-functionalized Hyper Branched Polyester (HBP) was synthesized and used as toughening additive in epoxy based UV-curable formulations. The addition of the HBP-epoxy induced an increase of epoxy group conversion, probably through both an activated monomer mechanism, involving the residual hydroxyl groups, and a copolymerization reaction, involving the epoxy functionalities present on the surface of the HBP. Phase separation was reached during UV-Curing, which assured to maintain the good thermomechanical properties of the cured epoxy matrix improving the impact resistance (Foix et al., 2012).

The properties of epoxy resins can be effectively modified regularly by an addition of reactive silanes, polysiloxanes, silsesquioxanes, silica, montmorillonite, and other fillers. These modifications with reactive silanes, silicon containing monomers and polymers, and silica based fillers, enabling improvement of their mechanical properties, thermal and flame resistance as well as providing corrosion and antimicrobial protection (Chrusciel & Lesniak, 2015).

2.9 Solvent

In general, solvents are liquids that are used to dissolve other components. In the paint industry, solvents are liquids or mixtures of liquids that dissolve resin and carry pigments and other paint components. In the case of water borne paints, the solvent is water, but the resin (or latex) is emulsified in the water, not dissolved in it. Small amounts of other solvents are also added to water based paints. There are three major uses of solvent in the paint industry:

- As a cleaning agent to remove oily deposits from a substrate in preparation for painting, to clean up equipment, to remove paint splatter and spillages after paint application.
- As an integral part of a paint formulation.
- As a paint thinner, to be post-added to paint to adjust application properties.

The purpose of solvents in a paint formulation is to carry the paint from the container to the substrate in a form that allows the paint to be sprayed, brushed or rolled uniformly. Solvents also assist in achieving the gloss level and dry film thickness required to offer the performance properties as stated on the product data sheet. Without a solvent that extends drying time, paint dries too quickly during application, and becomes too thick and stringy to allow a good finish. Solvents can be chosen to improve the balance between application properties of paint, such as viscosity, flow out, dry time, spreading rate and wet edge. For example, fast dry time is desirable when spraying to reduce turnaround time, but can be a hindrance when brushing or rolling due to reduced wet edge and the appearance of excessive brush-marks. When the viscosity of the coating increases rapidly, this leads to a limited window of workability. Small

molecule alkylene glycols such as ethylene and propylene glycol are routinely incorporated in aqueous coatings as humectants, but are limited in utility since they are considered to be volatile organic compounds (McCreight et al., 2011). A solvent that maintains maximum dispersion and mobility of the polymers during film formation promotes a homogenous dense structure. The opposite is true when the resin is precipitated out of the solvent. The attraction between the polymer molecules is not just limited to film formed from solution, but it is the underlying basis of all films, and is the force that holds the molecules together. In order to obtain a smooth and homogenous resin film, it is usually necessary to use a combination of solvents (Dulux, 2014).

Commonly solvent are petroleum-based chemicals which dissolve the pigment and binding agent for application. Most enamel-based paints use a mild petroleum-based solvent with an alkyd vehicle, and have a long drying and curing time. Conversely, lacquer-based paints require stronger solvents to speed the drying time. The most widely used aromatic hydrocarbons solvents in paint are benzene, toluene, mixed xylenes, ethylbenzene (BTEX), and high flash aromatic naphthas; aliphatic hydrocarbons include hexanes and heptane (Sigma, 2014).

2.9.1 Xylene

Xylene is a colourless mixture of chemically related hydrocarbons that often finds use as a solvent for paints. This is an advantage in situations where there is need to dissolve a compound but then evaporate the solvent. Xylene can be obtained naturally. Xylene exists in three isomeric forms as shown in Figure 2.23. They are ortho-xylene (1,2-dimethylbenzene), meta-xylene (1,3-dimethylbenzene) and para-xylene (1,4-dimethylbenzene).

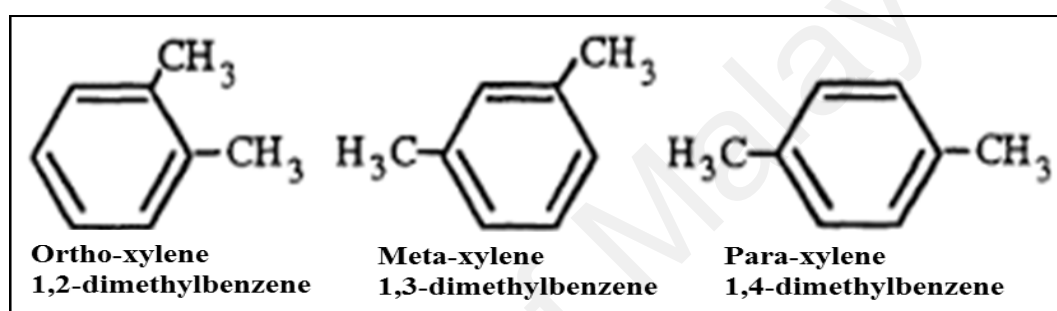


Figure 2.23: General Structure of Xylene Isomers

Of the three isomers, the para-xylene is the most industrially sought after since it can be easily oxidized and in liquid form at room temperature. Its melting range would be of -48 °C to 13 °C and boiling temperature varies from 138 °C to 144 °C. Having since low boiling points, Xylene is volatile which means it evaporates readily and precaution steps must be applied all time. When exposed to xylene in certain short or long periods, one can experience effects on the Nervous System. Exposure of 100-200 ppm will cause nausea and headache. Exposure of 200-500 ppm, a person would feel "high" dizziness, weakness, irritability, vomiting, slowed reaction time. High exposure of 800-10000 ppm will lead to giddiness, confusion, clumsiness, slurred speech, loss of balance, ringing in the ears. When the exposure is above 10000 ppm, it may cause sleepiness, loss of consciousness and even death (DHS, 2008).

2.10 Pigment

The pigment is the solid portion of the paint. Pigments are used not only to give the paint its color, opacity and finish, but also serve to protect the surface underneath from corrosion and weathering as well as helping to hold the paint together. Pigments are finely grind, insoluble and dispersed solid particles. Pigments can be either natural or synthetic and inorganic or organic. Both inorganic and organic substances are used generally, with the inorganic ones being in general cheaper but with less clear colors (Freitag & Stoye, 2008; Kalendova et al., 2008). Special pigments that are composed of tiny metallic solid particles less than 1 μm in diameter, a size that enables them to refract light (light has wavelengths between 0.4 μm and 0.7 μm) (Ahmed & Abdel-Fatah, 2012). These pigments can be used to give metallic finishes in automotive industry, to be hard wearing and for road markings where hard wearing involved.

They also can function as fillers, reinforcements and property modifiers. For the pigment to be effective it has to be evenly dispersed throughout the solvent and in contact with the solvent. Surrounding pigment particles is a layer of moist air and in some cases, other gases. To bring the pigment into contact with the solvent this layer has to be displaced and this displacement is known as wetting. If a pigment is not properly wetted in paint, it may result in color streakiness in the finished paints. Thus solvents and pigments must be chosen that result in a well wetted pigment. Wetting and dispersing agents are used to improve the wetting properties of the resin or solvent system. These pigments must be compatible with binders used in the paint system. Inorganic pigments are also widely used as they do not bleed, are heat and light stable. In addition they are used for some specialized pigments (such as anti-corrosion pigments), and for black and white pigments, as it is not possible to get pure black or white organic pigments. One such white pigment, Titanium Dioxide, is widely agreed to be the single most important pigment in use today. It is the strongest known pigment in

terms of both opacity and tinting power which, coupled with its pure white tint and its fine particle size, means that it can be used as an opacifier to prepare films with a high hiding power and reduced pigment content (Diebold, 2014). This has resulted in paints with much improved elasticity and hence improved durability.

However natural and organic pigments are inactive, highly colored synthetic compounds that are pure, brighter and rich in color compared to inorganic ones. Eventually, they tend to fade away easier under sunlight, lower chemical resistant and lower heat stability (Hao et al., 2013; Kalendova et al., 2008).

2.11 Pigment Volume Concentration

The volume percentage of pigment in a dry paint has been defined as pigment volume concentration (PVC). The term PVC should never be used to specify the volume of pigment in a wet paint film. As the PVC increased in a series of coating made with the same pigments and binders, the density, adhesion, mechanical strength, increases to a maximum. When PVC equals critical pigment volume concentrations (CPVC), the overall performance of coating system is usually at its best at this point. The values of CPVC are a characteristic of a particular system varies from one system to another (Kalendova et al., 2008; Sorensen et al., 2009a). Hence the formulation of paint should not exceed CPVC.

$$\%(\text{PVC}) = \frac{\text{Volume of pigment}}{\text{Volume of pigment} + \text{Volume of binder}} \times 100\%$$

The CPVC is an important parameter to each coating system containing one kind or more pigments. Liu et al., has reported that there is many experimental methods were used as reference method of CPVC, such as calculation of oil absorption values, internal

stress measurement, hiding power, mercury porosimetry and gas permeation. Among these methods, the Scanning Electron Microscope (SEM) observation and Electrochemical Impedance Spectroscopy (EIS) measurement were regarded as the most reproducible methods to distinguish the undercritical from overcritical coatings (Liu et al., 2012).

Various methods can be used to determine this percentage with one of them is via EIS method. EIS is a suitable method to determine the critical pigment volume concentration (CPVC) of coatings, especially for inorganic pigments based organic coatings (Liu et al., 2010).

2.11.1 Titanium Dioxide

Titanium Dioxide (TiO_2), also known as Titanium (IV) Oxide or Titania, is the most significant inorganic white pigment in coating industry. This is due to its low cost, more stable and safer to use compared to other white pigments such as white leads. When used as a pigment, it is called titanium white, Pigment White 6 (PW6) with Colour Index International System code of CI 77891. Approximately 4.6 million tons of TiO_2 pigments are used annually worldwide, and this number is expected to increase as utilization continues to rise (Winkler, 2013). Titanium Dioxide has high refractive index ranging from 2.5 to 2.7 and very high melting and boiling points (Dupont, 2007). It is insoluble in both water and organic solvents, while offers maximum opacity capability.

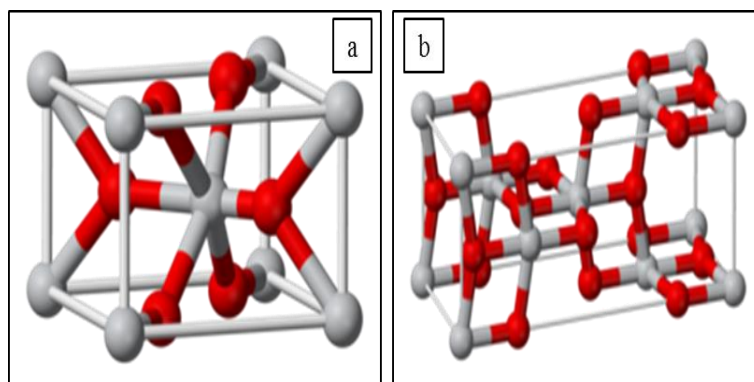


Figure 2.24: Crystal Structure of TiO_2 , a) Rutile b) Anatase

(Photo sourced from www.corrosion-doctors.com)

Largely TiO_2 is available in the form of 2 naturally occurring crystals; Rutile and Anatase; that differ in the arrangements of oxygen and titanium ions within the crystals as shown in Figure 2.24. Rutile is more preferable because it has scattering advantage of 18 %, longer life expectancy, more stable and durable than Anatase (Diebold, 2014; Ferreira et al., 2001). It has a wide range of applications, from paint to sunscreen and food coloring. A study conducted to investigate the extent to which the color change and yellowing of epoxy caused due to weathering of an aliphatic amine namely, Diethylenetriamine (DETA) cured Diglycidyl-ether of bisphenol-A (DGEBA) based epoxy system, when exposed to accelerated weathering conditions, could be lowered by means of a ultraviolet (UV)-blocking additive, namely nano Zinc oxide (ZnO). A Titanium Dioxide (TiO_2) based white coating with DGEBA epoxy and DETA was formulated and applied on mild steel panels for the weathering study (Rajgopalan & Khanna, 2013).

The effect of nanoparticle dispersion on surface morphological changes and degradation process in polymeric coatings during exposure to ultraviolet radiation were investigated using three types of nano-Titanium Dioxide (nano- TiO_2) were selected and dispersed into Acrylic Urethane (AU) coating to generate degrees of nanoparticle dispersion states (Kardar et al., 2014; Pang et al., 2014; Xing et al., 2011).

The incorporation of nano-sized inorganic pigment particles into organic coatings may offer the potential for improving many of their properties, including corrosion resistance, at relatively low loadings. Titanium Dioxide with a crystallite size of 5-10 nm was added to a waterborne organic primer and the corrosion resistance of the modified coatings was measured by neutral salt spray corrosion testing and electrochemical impedance spectroscopy (EIS), with non-pigmented film tested for comparison. 3 wt% TiO₂ appeared to produce an optimum improvement in the corrosion resistance (Lewis et al., 2012).

2.11.2 Hoffmann Mineral

Functional fillers, along with the selected binder system and anti-corrosion pigments play an important role by contributing to the protection of metals with organic coatings. The multitude of the fillers offered and the different surface treatments methods offer starting points to develop ever better performing formulation. Often, fillers as pigments have to meet very special requirements. In such cases not only good dispersion characteristics are of importance, but also mechanical and dynamic properties of the final products. Improved electrical insulation resistance, better aging and fluid resistance in many materials and improved anti-corrosion properties have a crucial role to play in many areas.

While in the earlier times conventional formulations with high solvent content were used. At present days, developments are preferably direct towards aqueous or solvent free systems. Such studies are being pushed by intense efforts to limit the emission of volatile organic compounds (VOC). The use of hybrid system with high solid coatings represents an appropriate step in this direction with minimum usage of solvent systems due to protective application.

The objective of the present study would be using Acrylic-Epoxy anti-corrosion formulation in comparison with commercially available TiO₂ and special fillers from Hoffmann Minerals-Neuburg Siliceous Earth (NSE) (Essen, 2005) has been served as the pigments.

Four paint systems were formulated using the best performing blending ratio of hybrid systems as shown in Table 3.

Table 2.3: Paint Formulation (Fineness of grind < 20 µm)

Paint	Pigment	Source
P1	TiO ₂	General
P2	Sillitin Z 86	Hoffmann Mineral
P3	Aktisil AM	Hoffmann Mineral
P4	Aktisil PF 777	Hoffmann Mineral

This special filler is made by treating the surface of Neuburg Siliceous Earth with chemical agents, especially silanes. The reaction by-products (e.g. alcohol) formed during the manufacture is largely removed right away during the process. The coupling reaction fixes the silane to the surface of the filler. Any undesirable side-effects that can occur during mixing by direct addition of the silane are virtually eliminated (Essen, 2005).

These fillers with inert polar group forms linkage with common resin like epoxy, acrylic, polyurethane, alkyd and polyester. These hybrid systems can be applied for improvements in high performance industrial paints, wood and foil coatings, anti-corrosion coatings, automobile industry, thickening and rheology control, and sealing

and embedding purposes. It stands out for its excellent dispersion properties, moderate yield point and pseudo plasticity with a high abrasion resistance.

In non-pigmented, it achieves good transparency with a slight yellow tinge.

Special fillers from Hoffmann Minerals:

- Sillitin Z 86 – $\text{SiO}_2\text{-Al}_2[(\text{OH})_4\text{Si}_2\text{O}_5]$ is a natural combination of corpuscular, crypto-crystalline and amorphous silica and lamellar kaolinite. These two elements mixture of silica kaolinite together form a loose structure which offers particular advantages in term of application possibilities (Z86, 2008).
- Aktisil AM – $\text{SiO}_2\text{-Al}_2[(\text{OH})_4\text{Si}_2\text{O}_5]$ is an activated Sillitin Z 86, produced by modifying the surface with amino functional silane. These amino groups may react with appropriate functional groups of the binder or build strong interaction in the form of hydrogen bridge linkage (AM, 2008).
- Aktisil PF 777 – $\text{SiO}_2\text{-Al}_2[(\text{OH})_4\text{Si}_2\text{O}_5]$ is an activated Sillitin Z 86, produced by modifying the surface with alkyl silane. The non-polar alkyl groups of the coating agent impart the desired hydrophobic properties to the filler surface to improve optimum wetting (PF, 2008).

2.12 Polyisocyanate

Isocyanates are essential components required for crosslinking for hybrid coating. These are di-or polyfunctional isocyanates containing two or more ($-\text{NCO}$) groups per molecule. The isocyanate group bears cumulated double bond sequence as ($\text{R}-\text{N} \equiv \text{C}-\text{O}$), wherein the reactivity of isocyanate is governed by the positive character of the carbon atom, which is susceptible to attack by nucleophiles, and oxygen and nitrogen by electrophiles (Dusek et al., 2000). These isocyanate groups is extremely

reactive and will cross-link with any type of functional groups having an unstable hydrogen atom (Hirose et al., 2000). Partially blocked polyisocyanate will yield thermosetting binders when blended and reacted with excess amounts of hydroxyl groups. Isocyanates can be aliphatic or aromatic type.

Aromatic isocyanates react faster, but have less usage for coating properties. A mixture of aliphatic isocyanates with acrylic polyol hybrid system will produce improved coating. Acrylic polyol resin with 2.9 % of OH value and Bisphenol-A Epoxy resin were used in the binder formulations using Bayer Aliphatic Polyisocyanate (NCO) Desmodur N75 MPA/X as a cross-linking agent. NCO was used as the last component added into the coating mixture for all stages of this study. The amount of NCO used is based on acrylic resin wt%. The scope of this study is to find the best performing hybrid system. These resins have been taken in different compositions from 20-80 wt% and vice versa. The mixtures were thoroughly blended and were applied on the pre-treated mild steel panels (Rau et al., 2009).

Although these resins are chemically inert in their fully reacted form, the risks of asthmatic symptoms arise on human exposure even in smaller concentrations due to the volatility associated with isocyanates. On exposure to flames, hazards of ignition are feared. Isocyanates may also be sensitive on our skin. Some isocyanates may also be anticipated as carcinogens. Thus, persons working with isocyanates must be equipped with proper protection devices such as gloves, masks, respirators, goggles, and others, as precautionary measures (DHS, 2008).

$$\text{Amount of NCO} = \frac{\% \text{ OH} \times 2.47}{\% \text{ NCO}} \times 100 \text{ g}$$

CHAPTER 3: EXPERIMENTAL MATERIALS AND METHODOLOGY

3.1 Introduction

This chapter explains the method of preparation of the samples and different analytical methods to evaluate the properties of the coatings developed. Various techniques will be used to study the physical, mechanical, structural, thermal, electrochemical and corrosion resistance properties of the prepared resins and paint systems. The purpose of this study is to develop hybrid coating systems using acrylic polyol and epoxy resins for corrosion protection.

3.2 Materials

The following chemicals were used for the resin preparation of the hybrid paint system.

- Acrylic Polyol resin with 2.9 % OH value (Bayer - Desmophen A365 BA/X), designated as (A) and obtained from Bayer MaterialScience AG, D-51368 Leverkusen, Germany.

Table 3.1: Properties of Acrylic Polyol Resin

Non-volatiles (Solid content wt%)	65 % \pm 1 %
Acid value	7.5 \pm 2.5 mg KOH/g
Hydroxyl content	2.9 \pm 0.4 %
Viscosity at 23 °C	3000 \pm 500 mPa.s
Density	1.04 gcm ⁻³
Solvent	Butyl Acetate / Xylene

- Epoxy resin (NPSN-901X75 Bisphenol-A - World Wide Resin), designated as (E) and obtained from World Wide Resin A.C.R Tech. Co. LTD, Taipei, Taiwan.

Table 3.2: Properties of Epoxy Resin

Non-volatiles (Solid content wt%)	75 % \pm 1 %
Molecular weight	450 ~ 500 g
Viscosity at 25 °C	8000 ~ 15000 mPa.s
Density	1.10 gcm ⁻³
Solvent	Xylene

- Aliphatic Polyisocyanate resin (NCO) (Bayer - Desmodur N75 MPA/X), obtained from Bayer MaterialScience AG, D-51368 Leverkusen, Germany.

Table 3.3: Properties of Polyisocyanate Resin

Non-volatiles (Solid content wt%)	75 % \pm 1 %
NCO content	16.5 \pm 0.3 %
Viscosity at 23 °C	250 \pm 75 mPa.s
Density	1.07 gcm ⁻³
Solvent	Methoxypropylacetate / Xylene

- Xylene (AC S Reagent), obtained from Sigma-Aldrich, 3050 Spruce Street, Saint Louis, MO 63103, USA.

Table 3.4: Properties of Xylene

\geq 98.5 % xylenes + ethylbenzene basis	
Vapour density	3.7 (vs air)
Vapour pressure	18 mmHg (37.7 °C)
Density	0.86 gcm ⁻³ at 25 °C

3.2.1 Preparation of Hybrid Coating and Paint System

This investigation is divided into two main parts, which is:

- **Part 1: Preparation of acrylic-epoxy hybrid systems**

In this development, acrylic polyol resin (A) will be blended with epoxy resin (E) using polyisocyanate resin (NCO) as hardener. The proportion of polyisocyanate resin with acrylic resin was maintained at a weight ratio of 3(polyisocyanate) to 7(acrylic polyol resin) as specified in the data sheet for acrylic polyol resin. Generally the epoxy resin is prepared by dissolving a known amount of commercial grade xylene as solvent and suitable hardener. The above resins mixture and the suitable solvent are added to round bottom flask and refluxed to dissolve the resin and stirred by a magnetic stirrer. By using the same preparation method, the acrylic-polyisocyanate-epoxy resins will be blended with different blending ratios and tabulated as shown in Table 3.5.

In this investigation no specific hardener were used to cure epoxy resin. The results have shown that amine hardener causes blushing, which occurs only under ambient conditions, has significant effect on the surface morphology and microstructure of the epoxy (Gu et al., 2005). As expected the blending system consisting of 90 wt% epoxy resin in 10 wt% acrylic resin (10A90E) was not cured permanently as shown in Table 3.5. These mixtures were let to settle for few minutes before applying on the panels to avoid the formation of bubbles.

Table 3.5: Blending Formulation of Acrylic-Epoxy Resin

Acrylic (wt%)	10	20	30	40	50	60	70	80	90	100
Epoxy (wt%)	90	80	70	60	50	40	30	20	10	0
Sample nAnE	Not Cured	20A80E	30A70E	40A60E	50A50A	60A40E	70A30E	80A20E	90A10E	100A

The prepared blend systems (nAnE) were applied by brushing method on the cold rolled mild steel panels (Q panels) sized 0.5 mm thick x 50 mm wide x 75 mm long. These steel panels were obtained from steel industries (GT Stainless, Melaka, Malaysia) and degreased by using an organic solvent ethanol first. Secondly, the surfaces of the panels were sand-blasted with 60 grit Aluminium Oxide media at 414 kPa pressure. This sand blasting techniques is one of the most important techniques in surface cleaning of steel to eliminate rust from the steel structure. This method would leave the panels with uniform rough surface which will increase the adhesion of the coating with the substrate (Forsgren, 2006; Soresen et al., 2009b).

The thickness of the coatings have been maintained between 40 to 80 μm and determined using a digital Elcometer 456 (Elcometer Instruments Ltd, Manchester, UK) coating thickness gauge model. The coatings were cured under ambient condition of $(29 \pm 1) ^\circ\text{C}$ and relative humidity of 80 % prior to one week according to ASTM D1640. The key properties of these hybrid systems were analyzed and investigated for the best performing hybrid ratios.

- **Part 2: Preparation of paint systems**

From the analytical methods, the best performing binder compositions will be chosen for the formulation of heavy duty anti-corrosion protection paint using different functional filler inorganic pigments such as TiO_2 and Hoffmann Minerals-Neuburg Siliceous Earth (NSE).

Four paint systems were formulated using the best performing blending ratio of hybrid system as shown in Table 3.6.

Table 3.6: Paint Formulation with Pigment (Fineness of grind < 20 μm)

Paint	Pigment
P1	TiO_2
P2	Sillitin Z 86 $\text{SiO}_2\text{-Al}_2[(\text{OH})_4\text{Si}_2\text{O}_5]$
P3	Aktisil AM $\text{SiO}_2\text{-Al}_2[(\text{OH})_4\text{Si}_2\text{O}_5]$ Amino Silane
P4	Aktisil PF 777 $\text{SiO}_2\text{-Al}_2[(\text{OH})_4\text{Si}_2\text{O}_5]$ Alkyl Silane

Investigation on the effect of the addition of various inorganic pigments, namely Titanium Dioxide (P1 system), Silitin Z 86 (P2 system), Aktisil AM (P3 system) and Aktisil PF 777 (P4 system), in enhancing properties of the hybrid acrylic-epoxy

polymeric matrix were studied. These prepared paint system will be coated on the mild steel panels. Various techniques will be used to study the physical, mechanical, thermal, electrochemical and corrosion resistance properties of the prepared paint systems.

This work reveals the blending complexity is very important for the selective resins. Therefore the complexity is beneficial for the practical performance which is by controlling the different hybrid systems with organic, inorganic and functional fillers. This may give the key roles of the best and cost effective anti-corrosion coatings. The investigation will be included at different Pigment Volume Concentration (PVC), the variation of the composition of the pigments has been used to prepare the developed paints. The essential properties of these developed anti-corrosion coatings will be analyzed by the given established techniques in Table 3.7.

Table 3.7: Formulation Analysis

Physical Properties	Mechanical Properties	Structural Analysis	Thermal Analysis	Electrochemical Analysis
Rheological Viscosity Drying Time Thickness Glossiness	Adhesion Impact Resistance UV Weathering	FTIR SEM EDAX	TGA DSC	Acid Immersion EIS

3.3 Characterization

In this study, two organic resins (A and E), and four pigment based paint system (P1, P2, P3 and P4) have been used for the development of anti-corrosion hybrid coatings. The analytical methods involve the viscosity measurement, drying time, glossiness measurement, dry film thickness (DFT), cross hatch method, impact resistance, accelerated UV weathering test, Fourier transform infrared spectroscopy (FTIR), scanning electron microscopy (SEM), energy dispersive of X-ray analysis (EDAX), thermogravimetric analysis (TGA), differential scanning calorimetry (DSC), acid immersion and electrochemical impedance spectroscopy (EIS).

3.3.1 Viscosity Measurement

Rheology is the science of flow and deformation of materials. Rheological properties crucially affect the application and performance of coatings. Viscosity is a measure of resistance to flow and is defined as the shear stress divided by the shear rate (Wicks Jr et al., 2007). When shear flow is driven by gravity, kinematics viscosity is measured.



Figure 3.1: Elcometer Rotary Viscometer (RV1-L)

Almost all low molecular weight liquids, solutions of resins in good solvents and dispersions exhibits Newtonian flow where else, solutions of resins in poorer solvents in which there are clusters of resin molecules usually exhibits non-Newtonian flow (Wicks Jr et al., 2007). In good solvents the viscosity increases with the square root of the molecular weight of the resins and viscosity almost always decreases as the temperature of the system increases (Puteh et al., 2009). The Elcometer Rotary Viscometer (RV1-L) as shown in Figure 3.1 was used in accordance with ASTM D2196. A spindle type L4 is rotated at fixed speed in the coating to be tested. The data were processed using Viscosity Master Software and average viscosities at fixed temperature ranging (29 ± 1) °C were recorded.

3.3.2 Drying Time

A paint or coating is considered cured upon touching finger marks were not visible on the coated substrate. Recognized stages of drying were described in ASTM 154-52. In general, drying tests can be divided into few stages (dust free stage, tack free stage, through free stage, full hardness and recoat time). Time is measured for each stage. However the definition varies from one test to another. Testing laboratories and many paint companies, have instruments that automatically and continuously apply sand, or lint, or some sort of indenting devices to the surface (Wicks Jr et al., 2007). The ability of the devices to stick to the drying surface at certain intervals and the depth of the indenting devices indicates of drying (Talbert, 2007). Touching and observing finger marks was used to determine the curing time of the panels at ambient conditions (Freitag & Stoye, 2008).

3.3.3 Dry Film Thickness

Many methods can be used to measure dry film thickness (DFT). A digital Coating Thickness Gauge model Elcometer 456 as shown in Figure 3.2 was used in accordance with the Ferrous (F) ASTM D1186. Total range is 0 μm to 1500 μm with accuracy of 0.1 % to 3 % measured by the gauge. At least 50 readings taken from different panel within same sample coating and the average thickness were recorded.

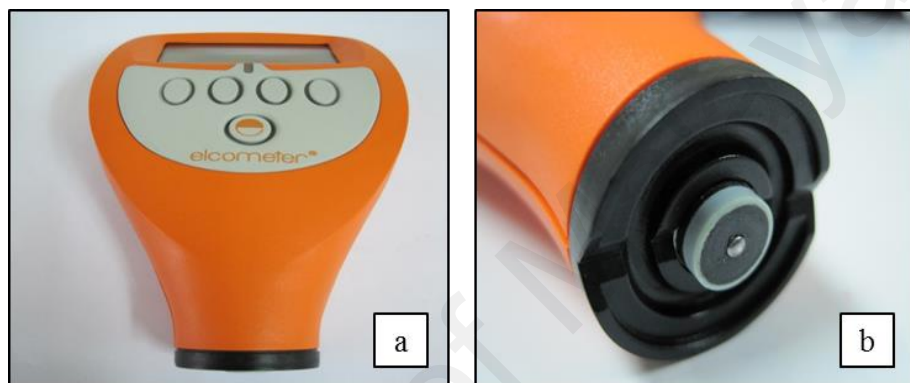


Figure 3.2: a) Elcometer 456 Thickness Gauge b) Sensor Tip

3.3.4 Glossiness

Glossiness is a very important feature of coating and it is also a term to express the capacity of surfaces to reflect directed light. Glossiness; when a beam of light is incident on an air-film interface, a percentage of the light is refracted into the body of the film and the remaining percentage is reflected. Many factors like the reflection characteristics of the material, the surface texture, the illuminating and viewing geometry would affect glossiness of a coated substrate (Malshe & Waghoo, 2004). This degree of gloss, which is varied according to how the paint exhibit specular reflection, is divided into the categories full gloss, semi-gloss and flat. For an ideal flat surface, the light is scattered and reflected equally in all directions (Dashtizadeh et al., 2011).

Accordance to ASTM D2457 specifies values of 20° and 60°. The 20° geometry is intended to be used on high gloss coating surfaces such as automotive paint finish, polished metals and plastics. The 60° geometry is used on coating films one universal gloss measurement angle for all applications (Leloup et al., 2010).

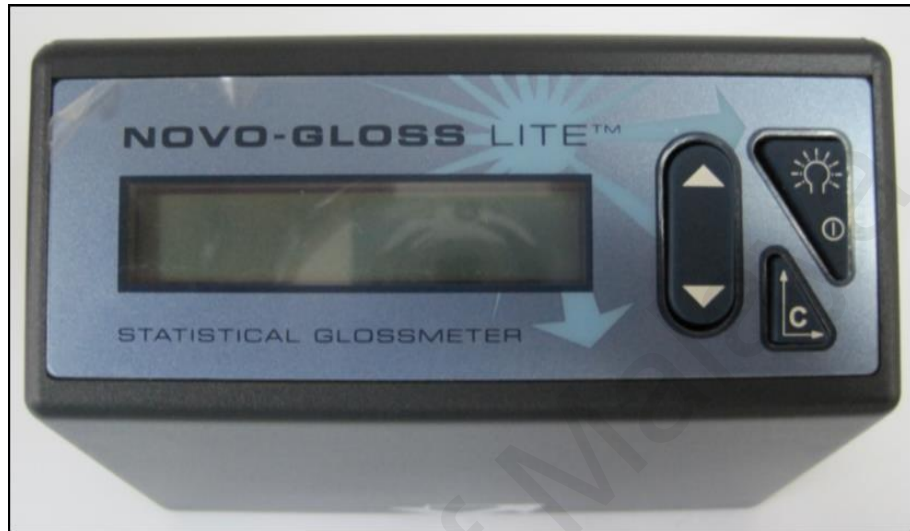


Figure 3.3: Novo-Gloss Lite Gloss Meter

A digital Novo-Gloss Lite instrument as shown in Figure 3.3 has data resolution of 0.1 gloss unit (GU), repeatability accuracy of 0.1 % and reproducibility of 0.5 %. At least 20 readings taken from different panel within same sample coating and the average glossiness were recorded for both angle of 20° and 60°. In this investigation, paint glossiness for P1, P2, P3 and P4 before and after exposure to accelerated UV weathering were studied. Both at 0 hour and at 720 hours were recorded.

3.3.5 Adhesion (Cross-Hatch Method)

The adhesion of the coating is generally considered to be good indicator of its longevity and measured by using Cross-Hatch method. A Sheen 750, cross-hatch cutter was used in this study as shown in Figure 3.4a. This has been well designed according to the international standards to assess the adhesion properties of coating.

The test method specifies suitable cutting tools with either single or multiple cutting edges. The tool was held with forefinger along the handle, fingertip over and above the cutting edge. The cutter was then carefully and firmly drawn under pressure over the section of coating to be tested to form, by two cross cuts, a square or diamond shaped lattice. The sample area was given a stiff brushing (Ramesh et al., 2007). After this the pattern inscribed was examined in order to define the classification of test results.

All the tests were carried out following ASTM D3359 standards. This test method specifies a procedure for assessing the resistance of the coating system to separation from substrates when a right angle lattice pattern is cut into the coating, penetrating through the substrate. The crossed samples were checked for damages using a digital polarized microscope (Dino-Lite, AM413ZT) as shown in Figure 3.4b. These were compared with the standard damage schemes.

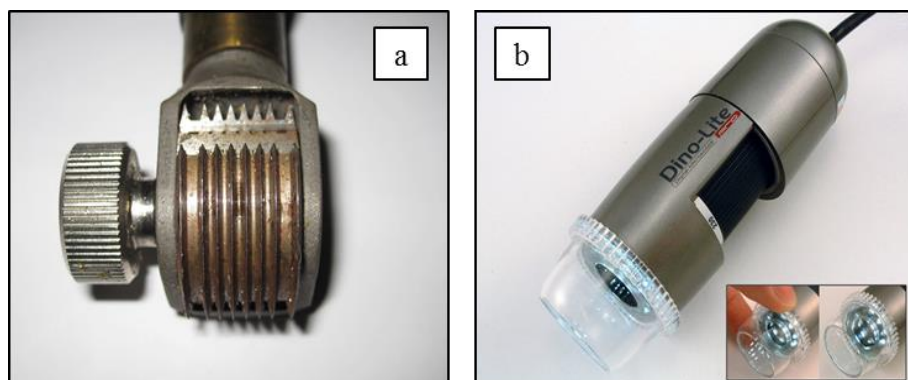
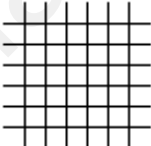
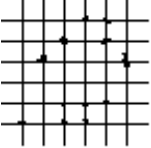
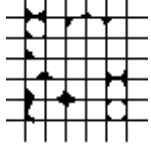
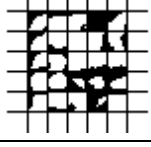
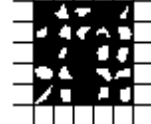


Figure 3.4: a) Sheen 750 b) Dino-Lite

Under the ASTM D3359 procedure there are two methods to assess the adhesion of a coating film; Method A and Method B. Method A is primarily intended for use at job sites while method B is more suitable for the use in the laboratory (Blustein et al., 2006). In this work method B is used to establish whether the adhesion of a coating to substrate has achieved an adequate level. The tested samples were checked for the damage as shown in Table 3.8.

Table 3.8: Classification of Adhesion Results (ASTM D3359-B)

Classification and Description	Surface of cross cut area from which flaking has occurred. (Has example for six parallel cuts)
The cuts are completely smooth with none of the squares of the coating in lattice detached.	 5B
Small flakes of the coating are detached at the intersections with less than 5% of the area is affected.	 4B
Small flakes of the coating are detached along edges and at the intersections of cuts for about 5 to 15% of the lattice.	 3B
The coating has flaked along the edges and on parts of the squares. The area affected 15 to 35% of the lattice.	 2B
The coating has flaked along the edges of cuts in large affected areas about 35% to 65% of the lattice.	 B
Flaking and detachment worse than that graded as in one (1).	Greater than 65%

3.3.6 Impact Resistance

The surface coatings, especially automobile paintings, must be hard enough to withstand the attack from any substance. When the surface is attacked by the external impacts, there may be a chance to expose the metal surface to the corrosive medium. The penetration of the electrolyte will delaminate the coating and will affect the whole area. The coatings must have good impact resistance.

ASTM D2794 standard was followed to carry out the experiments. An indenter of 1 kg weight was raised to a set height and released. In this work, a Tubular Impact Tester 806/25 as shown in Figure 3.5a was used for impact resistance test. The tester consisted of a graduated vertical tube mounted into a solid base. The tube acted as a guide for an impacting weight. The height of the drop of the weight was changed. By using the locking collar exactly the same force of impact was produced for each test. The test panel was placed on the die, and clipped into place with the indenter tool resting on the panel. The weight was raised to a set height and released. The height is increased by some intervals until coating failed. By calculating the impact energy (height x mass) samples were classified.

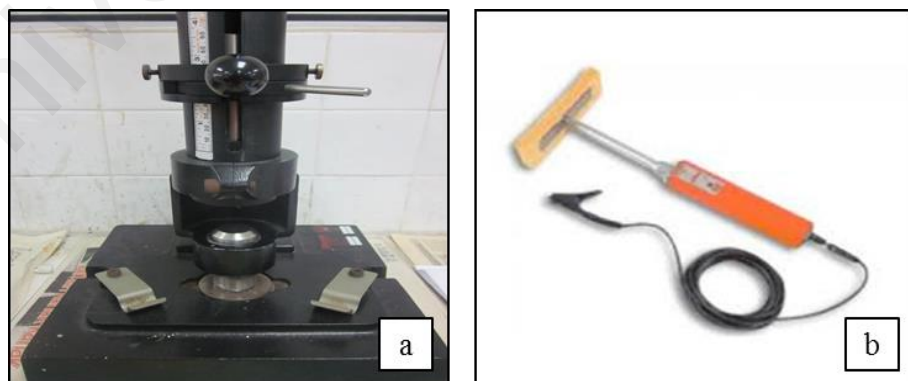


Figure 3.5: a) Tubular Impact Tester b) Pinhole Detector

The panels were checked for cracks using Dino-Lite and pinhole detector (Elcometer 270/4) as shown in Figure 3.5b. By calculating the impact energy (height x mass) due to gravity, samples were classified. The impact resistance is explained in terms of impact energy (Radhakrishnan et al., 2009). When the intender hits the surface, the pressure distribution becomes uneven and local stress concentrations all over the contact area are encountered. This may lead to damage with a significant decrease in the coating performance (Kalendova et al., 2008).

3.3.7 Accelerated UV Weathering Test

This test simulates weather situations and the effects of rust, blistering and discolouration. The most common chemical processes leading to the degradation of coating are photo initiated oxidation and hydrolysis resulting from exposure to sunlight, air and water as shown in Figure 3.6b. Accelerated tests are intended to provide quick answers on weathering effects by establishing general trends. The results can be accelerated in two ways.

- One is by continuous exposure to the weathering condition rather than waiting for the intermittent effects of direct exposure. For example, rain is an occasional occurrence and sunlight intensity varies during the day. Each of these occurrences can be approximately duplicated by the use of specialized equipment and applied to the coating in an orderly cyclic arrangement.
- The other method is to increase the intensity of the exposure condition above that normally found in nature. Generally the rate of degradation is not proportional to the intensity of the exposure condition and in many instances the breakdown of the coating will occur at a vastly increased rate.

It is often observed that alternating wet and dry conditions (cyclic) in weathering test causes faster blistering than continuous exposure to high humidity (Kardar et al., 2014). Rust is filled in the blisters that are formed as a result of corrosion under the coating film (McMurray et al., 2010). The cyclic test simulates more closely for natural outdoor exposures than those obtained only after salt spray test. It has been found that the combination of the UV-condensation cycle with wet and dry condition gives a more realistic simulation (Rajgopalan & Khanna, 2013). Weathering exposure is able to induce changes in the chemical composition of the paint that drives the changes in the mechanical properties. The main changes in mechanical properties of coating films during weathering processes are stress, glass transition temperature, fracture energy, dry adhesion, the appearance of cracks and weight loss (Kardar et al., 2014).

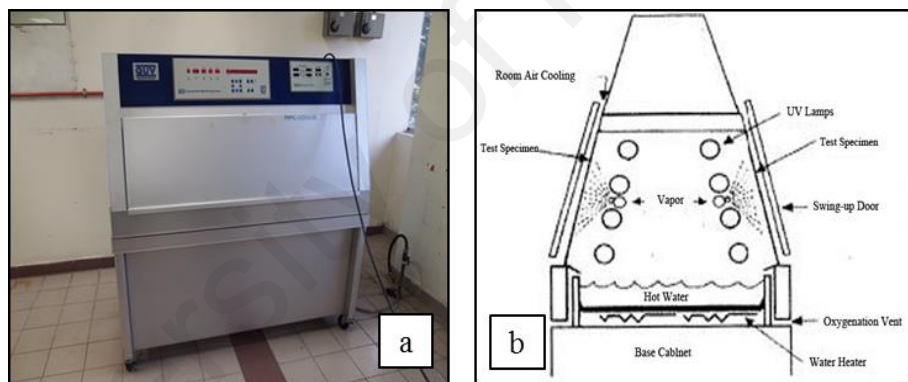


Figure 3.6: a) Accelerated Weathering Tester, QUV b) Scheme of QUV

(Photo sourced from www.liyi-test.com)

ASTM D4587 standard with cycle No.4 for general metal coating was followed to carry out the experiments. The cycle used was 8 hours UV exposure at (60.0 ± 2.5) °C followed by 4 hours condensation at (50.0 ± 2.5) °C at dark period repeatedly (D4587, 2011). In this investigation, paint glossiness for P1, P2, P3 and P4 before and after exposure to accelerated UV weathering test was studied, both at 0 hour and at 720 hours was recorded.

3.3.8 Fourier Transform Infrared Spectroscopy

Fourier Transform Infrared Spectroscopy (FTIR) is well established coating analytical technique for functional group analysis and to study the hydrogen bonding structures and phase separation behavior in polymers. Since mid-infrared spectral changes in band intensity and frequency shifts are known, the presence and strength of functional groups and hydrogen bonds can be specified. It is well known that the total energy of a particular bond or functional group in a macromolecule arises from the contribution of translational, rotational, vibrational, and electronic energies (Sharmin et al., 2004). Therefore, an interaction with radiation of the electromagnetic (EM) spectrum will result in different energy transitions of the bond or functional group involved in the macromolecule (Socrates, 2004).

An IR absorption profile is unique to a specific molecular vibration frequency. Therefore, identification of functional groups is a major application of IR spectrometry. The modes of vibrations are stretching (distance between two atoms increases or decreases) and bending (position of the atom changes relative to the original bond axis) (Ramesh et al., 2013).

Organic functional groups differ from one another both in the strength of the bonds and in the masses on the atoms involved are shown in Table 3.9. For example, the O-H and C=O functional groups contain atoms of different masses connected by bonds of different strengths. According to the rotational kinetic energy equation it is expected that the O-H and C=O groups to absorb IR radiation at different positions in the spectrum which is between 3400 and 3200 cm^{-1} for O-H group and 1700 cm^{-1} for C=O group. The infrared spectrum can be divided into three regions for organic molecules. The transitions between 4000-1300 cm^{-1} are primarily due to specific functional groups and bond types. Those between 1300 and 909 cm^{-1} , the finger print region are primarily

due to more complex interactions in the molecules; and those between 909 and 605 cm^{-1} are usually associated with the presence of benzene rings in the molecule (Ramesh et al., 2013).

Table 3.9: Functional Groups and Vibration Bands

(Table sourced from www.compoundchem)

Peak Value (cm^{-1})	Functional Group
3300 - 3600	O - H stretching
3000 - 3100	Aromatic C - H stretching
2800 - 3000	C - H stretching
2280	NCO
1720 - 1760	C=O
1640 - 1685	C=C stretching
1518 - 1581	N - H stretching
1400 - 1500	C - H bending
1250	C - N
1060 - 1330	C - O stretching
990	C - H
800 - 1300	C - C
730	C - H bending
705 - 744	Aromatic out of plane
690 - 700	C - H out of plane deformation

3.3.8.1 Generic Coating Identification

Coatings with different compositions have a unique FTIR spectrum. An unknown coating contains a group of bands that is specific for the generic type identification. These groups of bands are used in generic identification on protective coating by RAE Engineering and Inspection Ltd (Zhu et al., 2010). For example, a bisphenol epoxy as shown in Figure 3.7a, can be readily differentiated from an aliphatic polyurethane (used in outdoor painting applications), Figure 3.7b. Both spectra have a sharp band at about 1725 cm^{-1} , due to the carbonyl group, C=O, that they both contain. However, the epoxy also has a group of bands related to its aromatic content (eg. bands at 3000 to 3100, 1590, 1490 and 830 cm^{-1}). The aliphatic polyurethane has a tight cluster of bands at 2800 to 3000 cm^{-1} due to its aliphatic groups, but no aromatic bands.

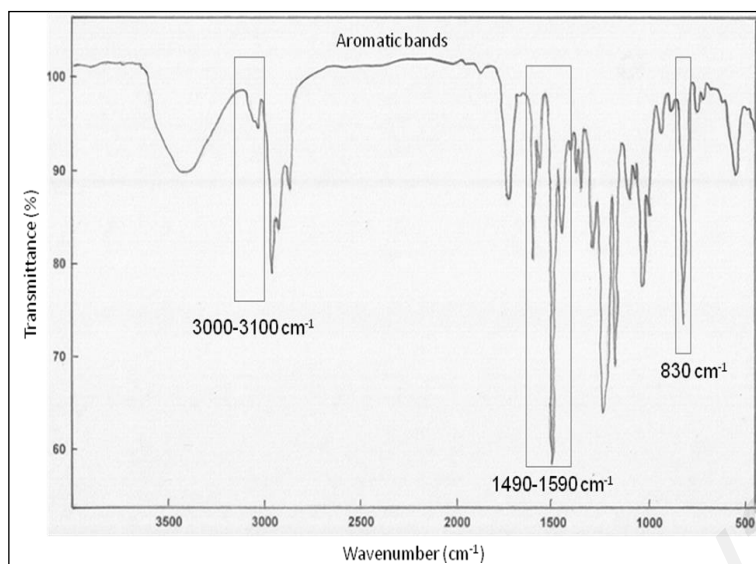


Figure 3.7a: FTIR spectrum of epoxy coating

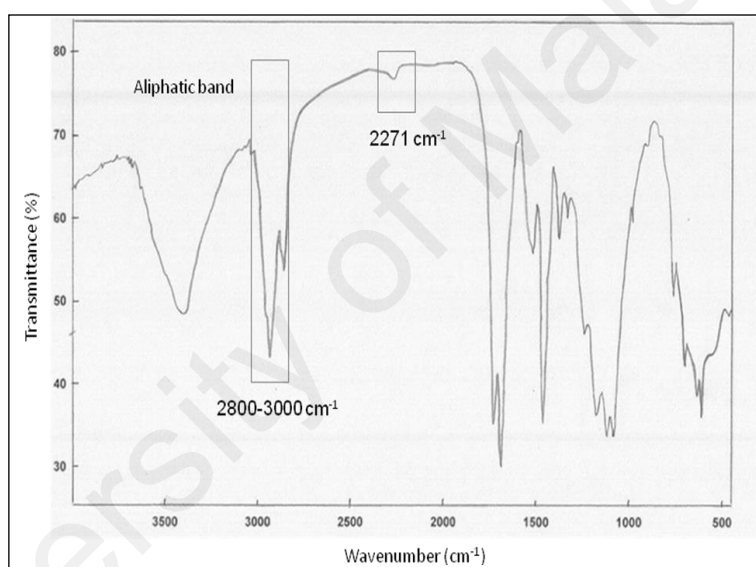


Figure 3.7b: FTIR spectra of aliphatic polyurethane coating (Manufacturer A)

3.3.8.2 Fingerprinting by FTIR

In addition to the main bands used in generic identification, each spectrum contains a complex combination of minor bands, fine structure, and minor frequency shifts of some bands. The result is a fingerprint spectrum, for each coating is studied by RAE Engineering and Inspection Ltd (Zhu et al., 2010). This attribute can be used to determine, for example, that a particular coating is manufacturer A's polyurethane (and not manufacturer B's polyurethane) with a C≡N vibrations present at 2271 cm⁻¹. Spectra

for this type of analysis are shown in Figure 3.7b and Figure 3.7c. Comparison with a spectrum obtained for a control sample known to be manufacturer A's polyurethane confirmed the identification, as the pattern of bands was virtually identical between the two samples (Lacnjevac et al., 2010).

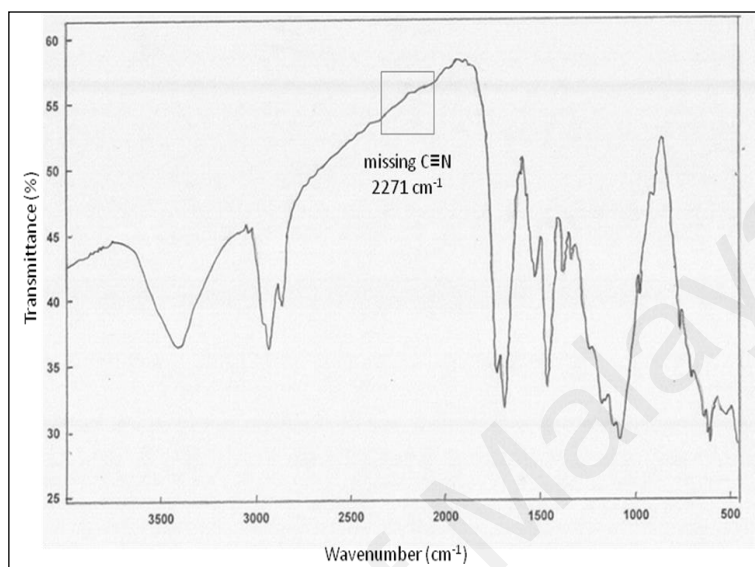


Figure 3.7c: FTIR spectra of aliphatic polyurethane coating (Manufacturer B)

3.3.8.3 Crosslinking between Hybrid System

Crosslinking between acrylic (A), epoxy (E) resin and polyisocyanate as hardener were shown in Figure 3.8. The existence of stretching asymmetrical C-C band and contraction of the C-O band confirms some crosslinking (Rau et al., 2011). This band was not observed in the pure acrylic sample, but observed in all samples containing epoxy resin, as shown in Figure 3.8a. In 100 wt% A, the C-N band is observed at 1258 cm^{-1} . As the epoxy concentration increases in the acrylic matrix, a prominent band shift observed at 1249 cm^{-1} related to the asymmetrical -C-O-C- stretching of aryl alkyl ether of DGEBA-epoxy is observed, as shown in Figure 3.8b. It is also reported a sharp peak in the spectrum of epoxy resins at 1183 cm^{-1} and attributed it to ether linkages. The band corresponding to C-O which was observed at 1174 cm^{-1} shows a shift to 1183 cm^{-1} , further confirming the formation of polymer network

between acrylic-epoxy hybrid systems. The identical peak for the NCO group has been reported as 2280 cm^{-1} (Rau et al., 2011). From the spectra analysis, NCO band at 2280 cm^{-1} is not observed in Figure 3.8c. The NH stretching band is expected to appear in the range of $1518\text{-}1581\text{ cm}^{-1}$ as confirmed as shown in Figure 3.7b. This indicates that the crosslinking between acrylic and polyisocyanate resin has occurred.

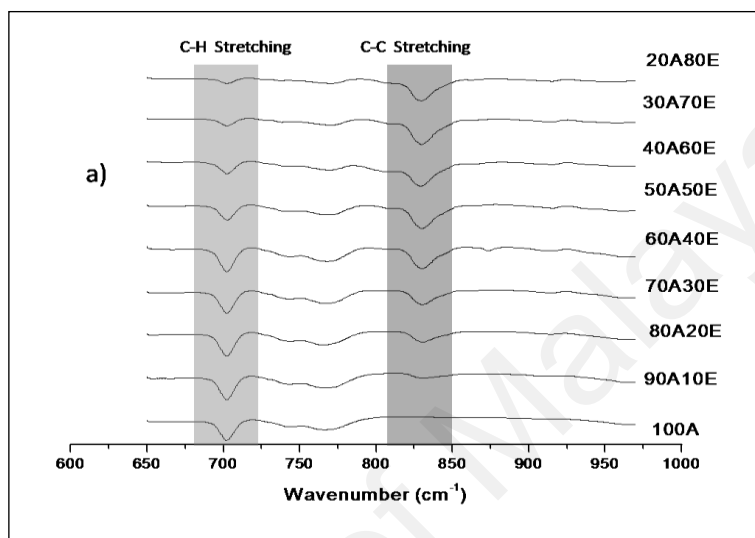


Figure 3.8a: FTIR transmission spectrum of acrylic blended with epoxy resin (Magnification of the course from $650\text{ to }900\text{ cm}^{-1}$)

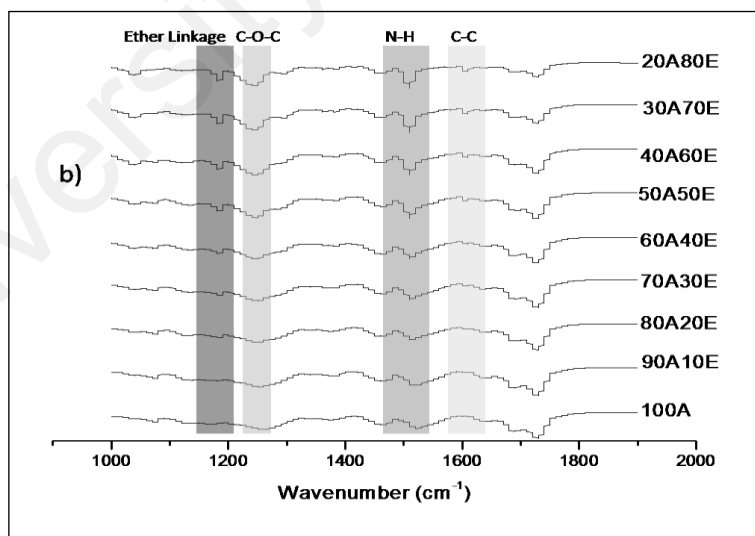


Figure 3.8b: FTIR transmission spectrum of acrylic blended with epoxy resin (Magnification of the course from $1100\text{ to }1900\text{ cm}^{-1}$)

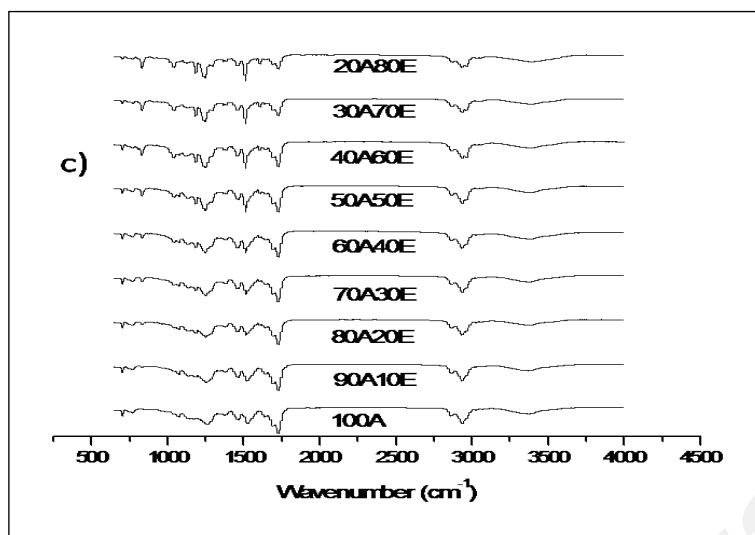


Figure 3.8c: FTIR transmission spectrum of acrylic blended with epoxy resin (Magnification of the course from 500 to 4000 cm^{-1})

In this study, FTIR has been used to locate the functional groups of two organic resins (A and E), and four pigment based paint system (P1, P2, P3 and P4). Testing for Chemical Properties of Polymers FTIR Analysis (ASTM E1252) was used as guide. FTIR spectrum was recorded in the transmittance mode using an Attenuated Total Reflectance (ATR-Nicolet iS10) spectrophotometer with OMNIC spectra software from Thermo Scientific as seen in Figure 3.9. Deuterated Triglycine Sulfate Potassium Bromide (DTGS KBr) method with velocity 0.6329 ms^{-1} was used for the measurements. For all spectra recorded, a 32 scan data accumulation in a range 400-4000 cm^{-1} was carried out at a resolution of 4.0 cm^{-1} .



Figure 3.9: FTIR Spectrometer (ATR-Nicolet iS10)

3.3.9 Scanning Electron Microscope and Energy Dispersive Analysis of X-ray

The interpretation of data from scanning electron microscopy (SEM) combined with energy dispersive analysis of X-rays (EDAX) is dependent on the size of the excitation volume and the magnitude of organic materials compositions. SEM-EDAX routinely used to obtain general morphological information of the coating surface and identification of chemical composition. High resolution images of surface topography, with excellent depth of field are produced using a highly focused scanning electron beam. The compositional and morphological data are then combined for exploratory data analysis. EDAX is a widely used technique to investigate the chemical components in a material under SEM. This method detects the X-rays produced as the result of the electron beam interactions with the sample. Mapping of the distribution of the different chemical elements constituting the specimen can be obtained. X-ray data is processed to obtain the percentage of each measured element present in the individual particles. Hence, qualitative elemental information could be obtained.

The examination of SEM-EDAX images can yield information (Mathivanan & Arof, 1998) of the following material properties:

- **Topography** - The surface features of an object or "how it looks", its texture; direct relation between these features and materials properties (hardness, reflectivity and etc.)
- **Morphology** - The shape and size of the particles making up the object; direct relation between these structures and materials properties (ductility, strength, reactivity and etc.)
- **Composition** - The elements and compounds that the object is composed of and the relative amounts of them; direct relationship between composition and materials properties (melting point, reactivity, hardness and etc.)

- **Crystallographic Information** - How the atoms are arranged in the object; direct relation between these arrangements and materials properties (conductivity, electrical properties, strength and etc.)

This analysis can help to identify the uniformness of the coating, composition of pigment, as well as characterization of the defect itself (Ahmed & Selim, 2010). Evaluation of these pigments was undertaken using ASTM international standard testing methods (Chawla, 2013). The pigments were then incorporated in solvent based acrylic-epoxy paint formulations using polyisocyanate curing agent. The physical and mechanical properties of dry films and their corrosion properties were tested using accelerated laboratory tests. In this study, the SEM-EDAX analysis has been used in studying the degradation and dispersion of pigments in formulated paint. Apart from that, characterization of pigments using SEM-EDAX analysis technique was used to assure the presence of TiO_2 (Ferreira et al., 2001). The formulated paints have been applied on cold rolled mild steel panel by brushing technique at ambient condition. Spectrometer as seen in Figure 3.10 was used to do complete analysis of SEM-EDAX, model Philips XL 30 EDAX Spectrometer.



Figure 3.10: SEM-EDAX Spectrometer (XL 30)

3.3.10 Thermogravimetric Analysis

Thermogravimetric Analysis (TGA) is a technique to provide thermal analysis which examines the mass change of a sample with heating under controlled atmosphere condition. These conditions may be in the presence of hydrogen, nitrogen or synthetic air with constant heat rate. A mass loss indicates that a degradation of the measured substance takes place. The reaction with oxygen from the synthetic air for example could lead to an increase of mass. It is used to characterize the decomposition and thermal stability of material under a variety of conditions and to examine the kinetics of the physic-chemical processes occurring in the sample (Ramesh et al., 2013). The advantages in using TGA include the following:

- Considerably fewer data is required. The temperature dependence of the volatilization rate may be determined over various temperature ranges from the results of a single experiment, whereas several separate experiments are required for each temperature range when isothermal methods are used.
- The continuous recording of weight loss versus temperature ensures that no features of the pyrolysis kinetics are overlooked.
- A single sample is used for the entire TGA trace, hence avoiding a possible source of variation in the estimation of kinetic parameters.

For example, to assess the thermal stability of a sample, one would like to know the temperature at which 10 % weight loss occurs, or at what rate evaporation or sublimation takes place. TGA is an important tool to investigate the thermal stability and thermal degradation of the polymer blends (Huang et al., 2009). TGA can be used to study the thermal stability and the degradation temperature on heat resistance coatings (Vengadaesvaran et al., 2013).



Figure 3.11: TGA Instrument (Q500)

In this study a TA Instruments Model Q500 thermal gravimetric analyzer (Instrument serial number: Q500-1448) was used for the measurements as shown in Figure 3.11. The results were evaluated with TA Universal Analysis Version 4.5A software package. Standard Test Method for Compositional Analysis by Thermogravimetry (ASTM E1131) was used as guide. The measurements were carried out from 30 °C to 800 °C at a rate of heating equal to 20 °C/min under nitrogen gas flow rate of 60 ml/min and balance nitrogen gas flow rate of 40 mL/min. Samples with a mass range between 1 mg to 2 mg were used for TGA measurement.

3.3.11 Differential Scanning Calorimetry

Differential Scanning Calorimetry (DSC) is used to study the thermal performance of thermosetting and thermoplastic polymers by determining the glass-transition temperature (T_g) of the samples according to ASTM. DSC also performs precise temperature measurements. DSC is a powerful tool for the characterization of polymer coatings given its high sensitivity and ease of use. Glass transition temperature (T_g) provides very important information in coating industries. The T_g is widely accepted as a predominant factor in determining the physical and mechanical properties of polymer. T_g is defined as the temperature where the polymer changed from a hard, often brittle glass-like material into soft, rubber-like properties. It is useful as a guideline for low temperature flexibility and ambient temperature hard and soft points. T_g for thermoplastic copolymers and the plasticized system can be affected by the molecular interaction between components. The level of cross-linking in thermoset affects the magnitude of accompanying physical changes and the temperature range of the T_g (Sharmin et al., 2004).

In this study, T_g taken into account, because it is an important factor to evaluate the physical properties and mechanical strength of the polymer materials. From the changes in T_g , the cross-linking between the polymer molecules can be explained (Rau et al., 2011). The cross-linking increases with the increase in the T_g values (Rau et al., 2009). The T_g values of the polymers can be highly affected during the polymerization between those of different molecular weights (Weldon, 2009).

A TA Instruments Model Q200S with Refrigerated Cooling System (RCS90) as shown in Figure 3.12 was used in the experiments accordance to Differential Scanning Calorimetry (DSC) of Polymers (ASTM D3418). The system was automated with a sample robot. The purge gas was Nitrogen flowing at 50 ml/min. The results were

evaluated with TA Universal Analysis Version 4.5A software package. Samples of about 5-10 mg were measured in hermetically sealed 40 μ l Aluminium crucibles in a self-generated atmosphere. The self-generated atmosphere was obtained by piercing a 50 μ m hole in the Aluminium lid of a sealed crucible. The DSC temperature program ran dynamically under Nitrogen condition with a flow rate of 50 ml/min.

The samples were measured with the following temperature program:

- ✓ Heating the sample from $-20\text{ }^{\circ}\text{C}$ to $120\text{ }^{\circ}\text{C}$ at $10\text{ }^{\circ}\text{C}/\text{min}$ (to eliminate or equalize the thermal history of all the samples)
- ✓ Cooling from $120\text{ }^{\circ}\text{C}$ to $-20\text{ }^{\circ}\text{C}$ at $10\text{ }^{\circ}\text{C}/\text{min}$
- ✓ Heating from $-20\text{ }^{\circ}\text{C}$ to $500\text{ }^{\circ}\text{C}$ at $10\text{ }^{\circ}\text{C}/\text{min}$ will be the actual measurement.



Figure 3.12: DSC Instrument (Q200S RCS90)

3.3.12 Acid Immersion Test

Sulphuric acid and many other acid solutions are generally used in industrial scale for many purposes, such as acid pickling, acid descaling, industrial acid cleaning, and oil well acidizing (Bahrami et al., 2010; Hosseini et al., 2010). On the other hand, the aggressive nature of the acidic mediums leads to the necessity to find a method to protect the exposed surfaces of the metals. One of the easiest and most economical method to overcome corrosive effects of the acid solutions, and other corrosive mediums, is to change the properties of the metal surface by the application of various coating materials i.e., organic coatings.

However, there is more than one mechanism of the corrosion protection given by the coating systems. Inhibiting the metal corrosion by the addition of corrosion inhibitors consider one of the available protection methods that were investigated by many researchers. Q.B. Zhang and Y.X. Hua., (2009) and M.J. Bahrami et al., (2010) report that inhibitors are commonly utilized to reduce the corrosive attack on the metallic surface. This inhibiting behaviour was attributed by F.Bentiss et al., (2002) due to the adsorption of molecules and ions on the metal surface upon the beginning of the corrosion reaction.

Preventing the penetration of the corrosive agents and limiting the diffusion of the oxygen and water molecules toward the interface between the metal and coating film could be considered as the second mechanism of the corrosion protection that given by the application of coatings. This barrier behaviour of the coating film could give the metal parts the durability to resist the corrosion and gain longer time in service with maintaining the good functional properties.

The 2009 work of X. Shi et al., described the vital role of the introducing different types of inorganic pigments, in nano-scale, within epoxy polymeric matrix. X.

Shi et al. and many other researchers attributed the influence of the pigments in enhancing the anti-corrosion performance and the barrier properties due to reducing the porosity and the diffusion pathways, which in turn enforce the corroding agents to travel a longer tortuous path to reach the surface of the substrate (Matin et al., 2015; Nematollahi et al., 2010; Shi et al., 2009).

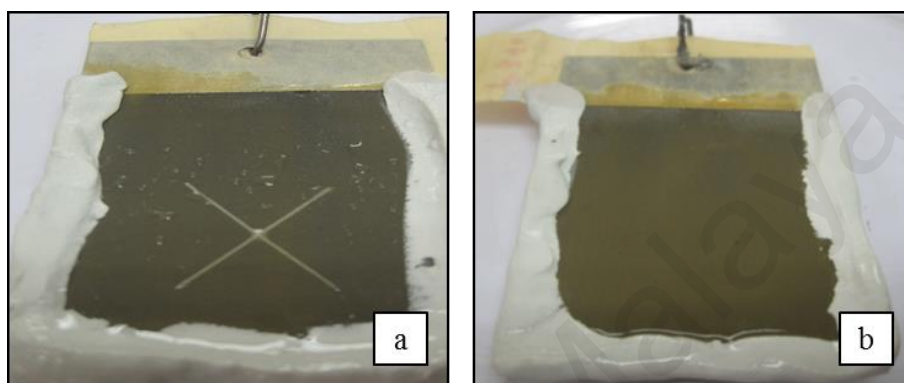


Figure 3.13: a) Cross Scribed Panel b) Coated Panel

The acid immersion test is considered as a powerful tool to investigate the anti-corrosion performance of the coating systems. The basic principle of this test is based on the visual observation of the immersed cross-scribed coated panel as in Figure 3.13a and non-scribed coated panel as shown in Figure 3.13b. Visual observation is conducted after different periods of immersion in the diluted acidic medium and studies the effects of the exposure conditions on different spots of the immersed area of the panels.

As sulphuric acid is classified as a highly corrosive mineral acid, so it was so useful to determine the response of the treated metal surfaces to such solution and determine the role of the added inorganic pigments in enhancing the barrier properties and overcome the penetrating of the corrosive agents toward the coated metal interface.

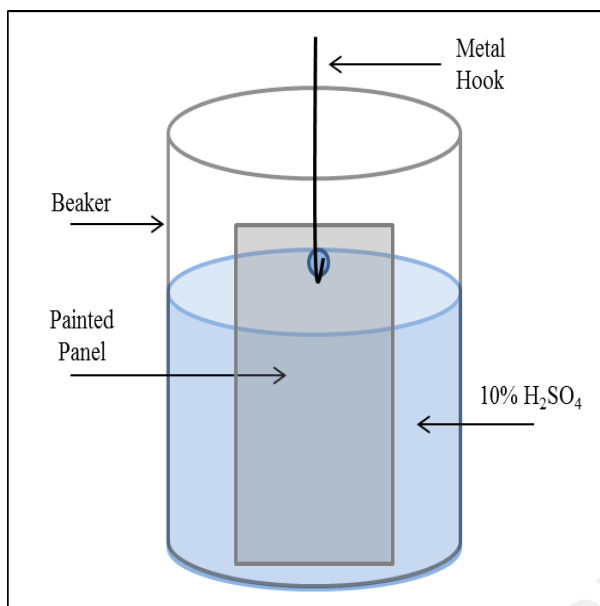


Figure 3.14: Acid Immersion Test

In this study, acid immersion test samples with protected edges as seen in Figure 3.13 was used to investigate the effect of the addition of various inorganic pigments, namely Titanium Dioxide (P1 system), Silitin Z86 (P2 system), Aktisil AM (P3 system) and Aktisil PF777 (P4 system), in enhancing the chemical resistance of the hybrid acrylic-epoxy polymeric matrix. This test was carried out in order to evaluate the chemical resistance of the developed paint systems. The painted metal panels were cross-scribed on the one surface only prior the immersion in diluted sulphuric acid. The experimental procedure was accordance with ISO 2812-1. Evaluation is based on color change, blistering and gloss retention. Values are set in accordance with technical requirements. The response of all developed paint systems was recorded after 0, 4, 8, 15, 22 and 40 days of immersion in 10 % H₂SO₄ solution as shown in Figure 3.14.

3.3.13 Electrochemical Impedance Spectroscopy

There are many powerful techniques that have been used in turn of investigating the electrochemical properties of the organic coatings. In this work, electrochemical impedance spectroscopy (EIS) was used to determine the anti-corrosion properties and to evaluate the barrier performance of all developed coating systems (binder and paint systems).

In the last few decades, EIS method has become a unique technique that used in research activities as well as in industrial applications. Evaluating the corrosion protection performance and the barrier behavior are some of the advantages that could be given are utilizing EIS technique. The vital role of EIS lies on the ability of EIS to give rapid and trusted results over different periods of immersion which in turn leads to gain a full understanding about the tested systems, determine the degradation mechanisms, evaluate the quality of the coating systems and study the corrosive effects of particular environment or condition.

In the present work, EIS has been employed in order to evaluate the anti-corrosion performance and the barrier performance of the developed hybrid binder and paint systems (P1, P2, P3 and P4). All experimental activities were carried out by using the three electrodes cell that illustrated in the schematic diagram in Figure 3.15. The poly(vinyl chloride) tube used bound to a coated panel with an Araldite[®] adhesive. The uncoated part of the samples represented the working electrode while the area exposed to the artificial seawater (3.5 % NaCl) was managed to be equal to 3 cm². Saturated calomel electrode (SCE) (AS 002056 RE-2B, BAS Inc, JAPAN) was used as a reference electrode, and a platinum electrode (PTE) (OD: 6.0 mm, ID: 1.6 mm, BAS Inc, JAPAN) served as a counter electrode. The frequency range of 0.1 Hz to 300 kHz was used in order to perform the EIS tests in artificial seawater (3.5 % NaCl) medium at

ambient condition and the signal amplitude was at 10 mV. The samples of all prepared coating systems were subjected to the EIS studies up to 30 days of immersion and readings were recorded from time to time in order to determine the exact degradation time of each individual system and its reasons.

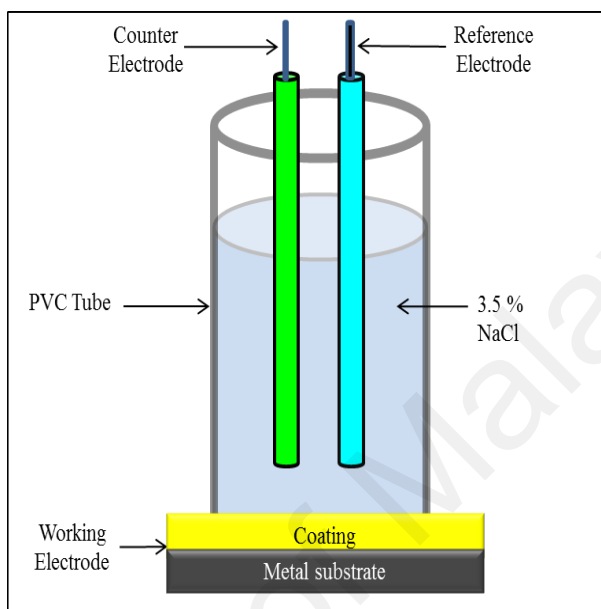


Figure 3.15: The three electrodes cell used for EIS studies

Gamry PC14G300 potentiostat (Gamry Instruments, Warminster, PA, USA) was used to perform EIS experiments. Furthermore, to reduce the surrounding noise, faraday cage was utilized. The whole set is shown in Figure 3.16. It is worth to mention that Echem Analyst Version 6.03 analyzer was utilized for the results evaluation.



Figure 3.16: EIS Instrument with Faraday Cage

Parameters such as coating resistance (R_c), coating capacitance (C_c), dielectric constant (ϵ) and the volume fraction of water (ϕ_w) were used in order to obtain detailed studies about the acrylic- epoxy hybrid binder which has been reinforced with various types of inorganic pigments, and investigate the effect of each type of the added pigments in enhancing the overall anti-corrosion performance and improve the barrier performance of the polymeric matrix.

The 1995 work of Amirudin and Thierry well documented the EIS fundamental principle where they explained the reason behind the necessary to study the degradation of the coating systems over a wide range of frequency which was attributed by them due to the fact that the coating resistance and capacitance are frequency dependent. Therefore the employment of EIS is recommended where the impedance of the coated can be studied as a function of the frequency of an applied a.c. wave (Amirudin & Thierry, 1995).

One of the most important concepts that must be considered during analyzing the data, which extracted from EIS technique, is the electrical equivalent circuit. Recently, many researchers have used simple equivalent circuits such as the one depicted in Figure 3.17 in order to describe the electrochemical behaviour. It is worth to be mention that the model of the equivalent circuit that provide a good fitting for EIS data could differ during the immersion time. In Figure 3.17 the model (a), which consists of electrolyte resistance (R_s), coating resistance (R_c) and coating capacitance (C_c), represents the superior anti-corrosion performance where there is no sign for any corrosion initiation or electrolyte penetrating. Heidarian et al., (2010) have reported that this model is representing a superior barrier performance of the coating system. Whereas model (b) indicates a non-barrier behavior and gives a sign on that the corrosion process is started already.

Double-layer capacitance (C_{dl}) and the charge-transfer resistance (R_{ct}) are also observed in model (b). In this context, new components in the model (b) such C_{dl} which represents the distribution of ionic charges around the affected areas of the metallic substrate while the new R_{ct} is inversely proportional to the corrosion rate (Heidarian et al., 2010).

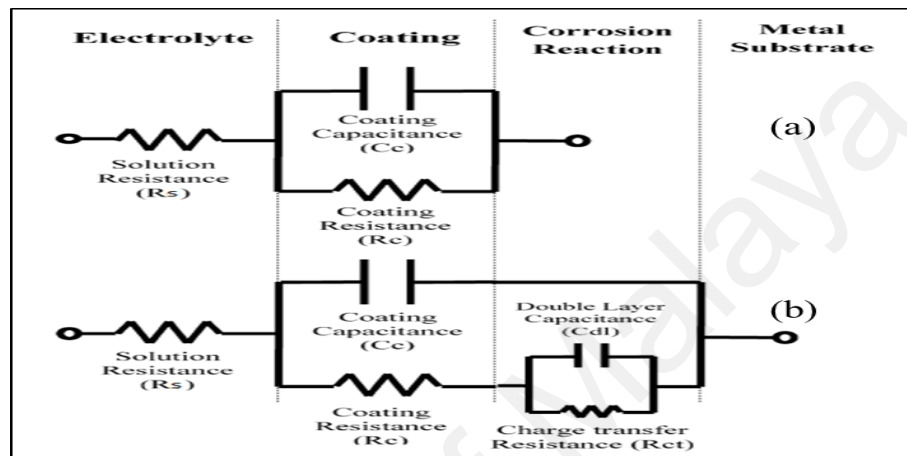


Figure 3.17: Electrical Equivalent Circuits

Model (a) Before corrosion start **Model (b)** After corrosion start

The above mentioned models of the equivalent circuits and so many different models also have been using frequently in the last decades in order to achieve the numerical fitting of impedance plots, Bode and Nyquist plots, over different periods of immersion times. Heidarian et al., 2010 and Nematollahi et al., 2010 have described the linkage mechanism between Bode and Nyquist plots as resulting from the EIS instrument and the equivalent circuits depicted in Figure 3.17.

Model (a) of the equivalent circuit usually utilize to fit the intact coating systems with superior barrier performance which perform Bode plot as the one illustrated in Figure 3.18 (a) with a straight line with a slope of -1 and Nyquist plot as shown in Figure 3.19 (a) with a capacitive arc. The arc in Nyquist plot may become a semi-circle as the electrolyte start penetrate the coating Figure 3.19 (b).

As the days of the immersion progress, one can observe significant changes in the Body plot with the appearance of a second time constant, which is a clear evidence of the corrosion initiation on the metal - coating interface, (Figure 3.18 b) and two semicircles in Nyquist plot (Figure 3.19 c and d) which in turn could be corresponded to the exist of two capacitive time constants. At this stage of the corrosion reaction, the model 3.17 (b) of the equivalent circuit is considered the most suitable one for fitting the EIS data (Heidarian et al., 2010; Nematollahi et al., 2010).

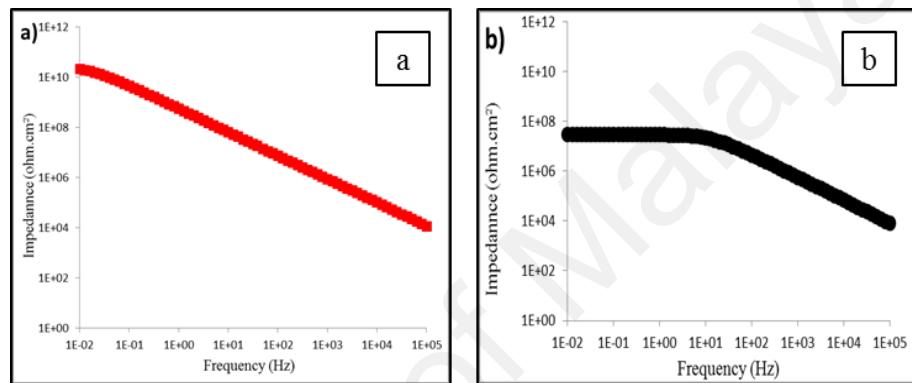


Figure 3.18: Bode plot

Model (a) Before corrosion start **Model (b)** After corrosion start

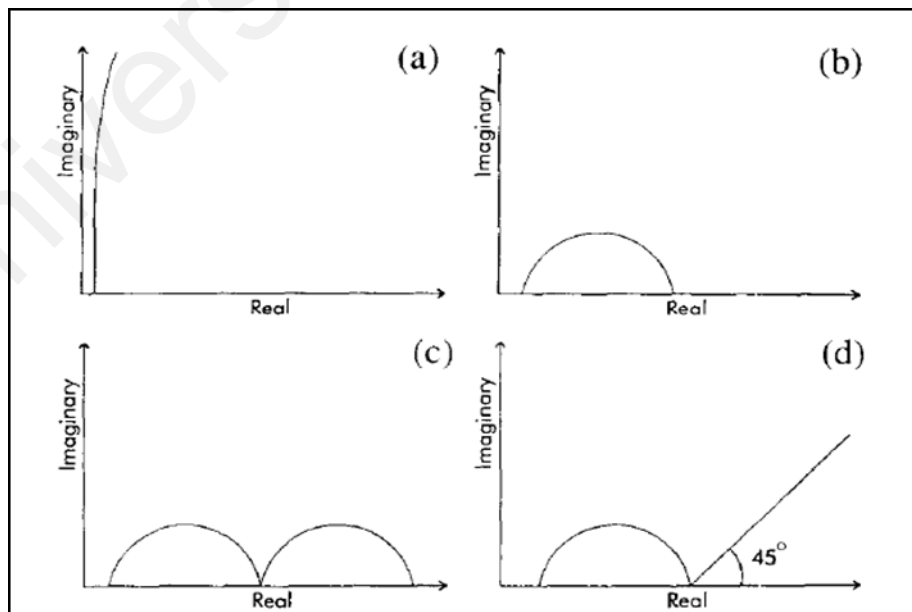


Figure 3.19: Nyquist plot

(a) capacitive behavior **(b)** one semi-circle **(c)** two semi-circles **(d)** 45° to real axis

In this study, all the illustrated results were obtained from the resulting Bode and Nyquist plots after been fitted by the suitable electrical equivalent circuit. Coating resistance (R_c) as one of the most important characters, was used mainly to determine the corrosion protection capability of the developed coating systems, was interpreted by Amirudin and Thierry, (1995) as the resistance of the coating that generally results from the penetrating of the electrolyte solution.

Besides, coating capacitance (C_c) which is given by Equation 3.1:

$$C_c = \frac{(\epsilon \cdot \epsilon_0 \cdot A)}{d} \quad (\text{Equation 3.1})$$

where:

C_c : capacitance of the coating (F).

ϵ : dielectric constant

ϵ_0 : dielectric constant of free space (8.85×10^{-12} F/m)

A : surface area of the exposed coating (m^2)

d : coating thickness (m)

The value of the dielectric constant (ϵ) can correspondingly be determined from the resulting EIS data. In addition, the C_c values could be utilized to study the tendency of the polymeric coating films to absorb water by the employment of the Brasher and Kingsbury equation (Amirudin & Thierry, 1995; Castela & Simoes, 2003) as shown in Equation 3.2:

$$\phi_w = \frac{\log \left(\frac{C_t}{C_0} \right)}{\log \epsilon_w} \quad (\text{Equation 3.2})$$

where:

ϕ_w : volume fraction of water

C_0 : coating capacitance at t is zero

C_t : coating capacitance after time (t) of immersion

ϵ_w : water dielectric constant ($\epsilon_w = 80$)

EIS give an accurate measurement using Equation 3.3, to determine diffusion coefficient of water because of the separation of interfacial and diffusion process on the frequency scale for CPVC measurements (Bierwagen et al., 2008; Hinderliter et al., 2006). Actually, the critical pigment volume concentration (CPVC) is a transition point with respect to moisture transport. Most additives seriously enlarge solubility and equilibrium absorption values of water in the coating, thereby increasing permeability.

$$\sqrt{\left(\frac{4Dt}{d^2\pi}\right)} = \frac{\log\left(\frac{C_t}{C_o}\right)}{\log\left(\frac{C_s}{C_o}\right)} \quad (\text{Equation 3.3})$$

where:

- D : diffusion coefficient
- d : coating thickness (m)
- t : time (s)
- C_o : coating capacitance at t is zero
- C_t : coating capacitance at t
- C_s : coating capacitance saturation

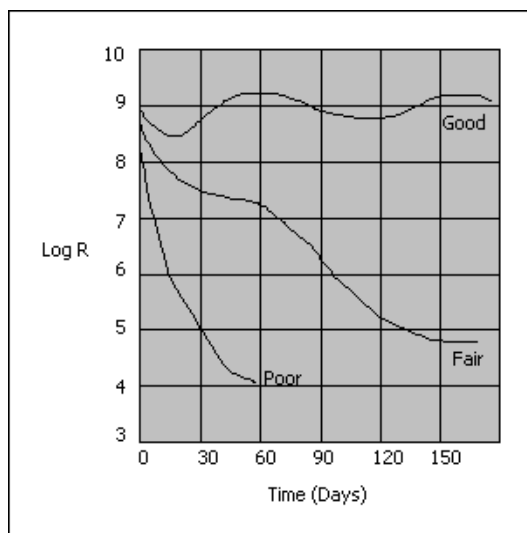


Figure 3.20: The schematic value for good, fair and poor of coating resistances

The coating resistance (R_c) values of all prepared paint systems with different PVC, up to 30 days of immersion in 3.5 % NaCl solution, were recorded and plotted against the time of immersion in order to investigate the effective role of pigments in enhancing the anticorrosion behavior. The performance of all prepared samples was divided according to the R_c value, after 30 immersion days, into three categories, good, fair and poor coating as shown in Figure 3.20. The classification procedures were based on the fact that R_c values above $10^9 \Omega\text{cm}^{-2}$ represent that the coating is very intact and has been described as good coating. Whereas, R_c values in the range between $10^9 - 10^8 \Omega\text{cm}^{-2}$ could be related to the diffusion barrier of electrolyte via coating pores. Coatings with R_c in this range were reported as fair coatings. However, $R_c < 10^6 \Omega\text{cm}^{-2}$ represents that the coating is undergoing a large area of delamination where blister formation and corrosion starts (Bierwagen et al., 2000; Loveday et al., 2004).

CHAPTER 4: RESULTS AND DISCUSSION ON BINDER SYSTEM

4.1 Introduction

This chapter focused on the results obtained from the first part of the investigation. Two type of resins, Acrylic Polyol resin (A) and Epoxy resin (E) were blended together with Polyisocyanate resin as a curing agent to obtain hybrid coating system. Experimental results with various blending ratio hybrid systems (AE) have been developed and explored extensively in this chapter.

Each sample of AE hybrid binder system were applied using decorative brush on mild steel panels were cured under ambient condition of $(29 \pm 1) ^\circ\text{C}$ and relative humidity of 80 % prior to one week according to ASTM D1640. The key properties in terms physical, mechanical, structural, thermal and electrochemical of these hybrid binder systems were analyzed and investigated for the best performing hybrid ratios.

4.2 Viscosity

In view of the increasing use of modern coating systems, their rheological characterization is becoming more important to guarantee constant product quality in terms of pot life and application preference (Dulux, 2010). Mean viscosity increase rate per minute was measured as a way to characterize pot life of a coating system. Higher average viscosity figures indicate a shortened open time or better curing time (Wicks Jr et al., 2007). Crucially affect the application and performance of the coating. In the experiment, the viscosity measurement has been taken as a measure of resistance to flow and as the shear stress divided by shear rate (Ocampo et al., 2005). When shear flow is driven by gravity, kinematics viscosity is measured. If the shear rate is high then the viscosity is low and vice versa.

A spindle is rotated at fixed speed in the coating system. A spindle fitted with a disc or a cylinder is rotated in the sample to be tested. A spring is connected between the spindle and the motor shaft which rotates at a fixed speed. The angle of deviation between the spindle and the motor shaft is measured electronically and converted to torque. The data were processed using Viscosity Master Software and average viscosities at fixed temperature ranging (29 ± 1) °C were tabulated below. Table 4.1 shows the experimental results for the average viscosity rates for the blending systems.

Table 4.1: Viscosity Results of nAnE Binder System

Sample	Acrylic (wt%)	Epoxy (wt%)	Average Viscosity (mPa.s)	Average Temperature (°C)
20A80E	20	80	1699.05	29.17
30A70E	30	70	1952.53	29.25
40A60E	40	60	2723.94	29.40
50A50E	50	50	2234.56	29.53
60A40E	60	40	4568.96	28.83
70A30E	70	30	4506.33	29.51
80A20E	80	20	4802.61	29.50
90A10E	90	10	3914.53	29.52
100A	100	0	2771.67	29.61

From the results as shown in Table 4.1, it is observed that the temperatures were almost constant during all the measurements and pure acrylic resin (100 wt%) has lower viscosity compared to values given in data sheet. Hence, this spindle rotations are opposed by resistance and causes the temperature to increase, indirectly viscosity decreases (Wicks Jr et al., 2007). In Figure 4.1, viscosity bar charts are presented with different blending ratios. Viscosities for 20-50 wt% of acrylic resin (A) are lower due to higher percentage of epoxy resin and less chemical reaction between the resins. This is caused by poor ratio in blending system. Conversely hybrid systems with 60-90 wt% of A have a higher viscosity with shear thickening compared to 100 wt% A. The coating developed to be highly protective, tend to have higher viscosities. To achieve good

application characteristics, good paints have to be non-Newtonian liquids, which are highly shears rate dependent (Ocampo et al., 2005). The coating system must flow well over the substrate will have a good intermolecular contact between the interfaces of the substrate (Rau et al., 2011). It is possible that the available hydroxyl group in acrylic resin to form bonding in order to increase network density, thereby increasing viscosity of the blending systems as reported by Ocampo et al., 2005 and Rau et al., 2011.

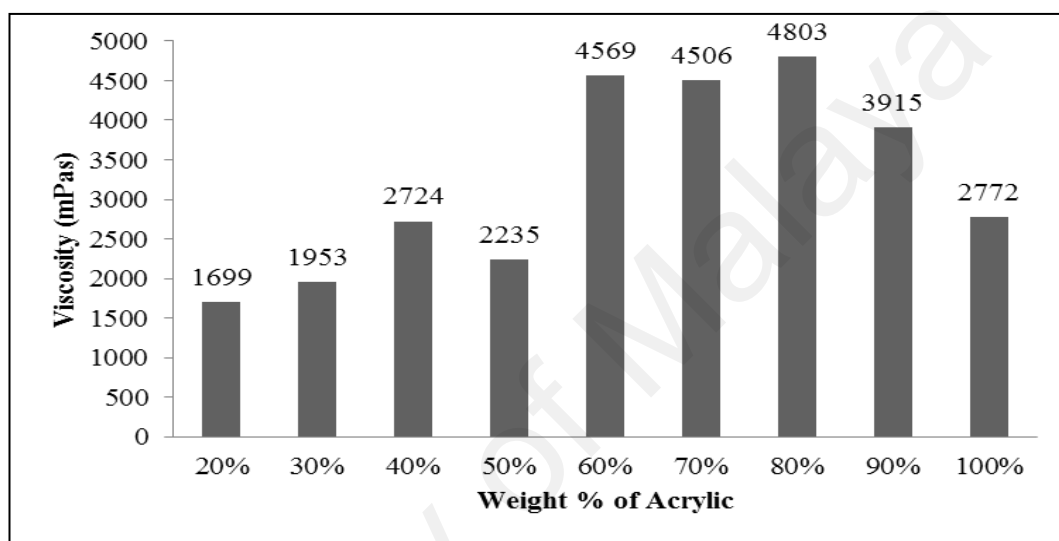


Figure 4.1: Viscosity Variation of nAnE Binder System

4.3 Drying Time

In general, drying tests can be divided into few stages (dust free stage, tack free stage, through free stage, full hardness and recoat time). A paint or coating is considered cured if upon touching finger marks were not visible on the coated substrate after curing the mild steel panels at ambient condition. Touching and observing finger marks was used in this study to determine the average drying time. Time is measured to the nearest hour after application on mild steel panels. The coating system cures at ambient condition due to solvent evaporation which brings the molecules of the resins into close contact so that there will be a mutual chemical attraction draws them together (Ocampo et al., 2005). Film properties are influenced by the molecular arrangement or structure

within the film. Xylene as solvent for this coating system helps in maintaining maximum dispersion and mobility of the polymers during the formation promotes a homogenous dense structure.

From the Table 4.2, it is observed that the average drying time was decreasing when blending percentage of epoxy resin decreases. As expected, the binder system consisting of 10 wt% acrylic resin and 90 wt% epoxy resin (10A90E) was not cured permanently. Polyisocyanate resin was the only hardener used and epoxy resin was prepared by dissolving a known amount of commercial grade xylene as solvent. From the results, high viscosity of the coating system consisting 80A20E and 90A10E takes about 3 hours to cure. This denotes that high viscosity system has lower solvent content. Therefore, amounts of solvent which evaporate during the film formation are also low and having lower curing time. As the percentage of epoxy resin increases above 40 wt%, the coating system takes an average of 30 hours to cure completely. This is due to the absent of polyamide resin as a curing hardener (Rau et al., 2013).

Table 4.2: Drying Time of nAnE Binder System

Sample	Acrylic (wt %)	Epoxy (wt %)	Average Drying Time (hours)
10A90E	10	90	Not Cured
20A80E	20	80	72
30A70E	30	70	24
40A60E	40	60	10
50A50E	50	50	10
60A40E	60	40	5
70A30E	70	30	6
80A20E	80	20	3
90A10E	90	10	3
100A	100	0	3

4.4 Dry Film Thickness

A digital Coating Thickness Gauge model Elcometer 456 was used in accordance with the Ferrous (F) ASTM D1186. Total range is 0 μm to 1500 μm with accuracy of 0.1 % to 3 % measured by the gauge. At least 50 readings taken from different panels within same sample coating and the average thickness were calculated and recorded. The hybrid mixtures were thoroughly blended and were applied on the pre-treated mild steel panels. The coating system must flow well over the panels to have a good intermolecular contact. The panels were allowed to dry for 1 week before carried out the characteristic analysis.

From Figure 4.2, the dry film thickness of the coatings was found to be in the average range of 40-80 μm . From the results, good film thickness observed in the coating system consisting 80A20E and 90A10E that expected to improve mechanical and electrochemical properties. As the percentage of epoxy resin increases above 50 wt%, the coating system gives lower values of thickness and may have lower adhesive strength and flexibility towards impact test (Selvaraj et al., 2009).

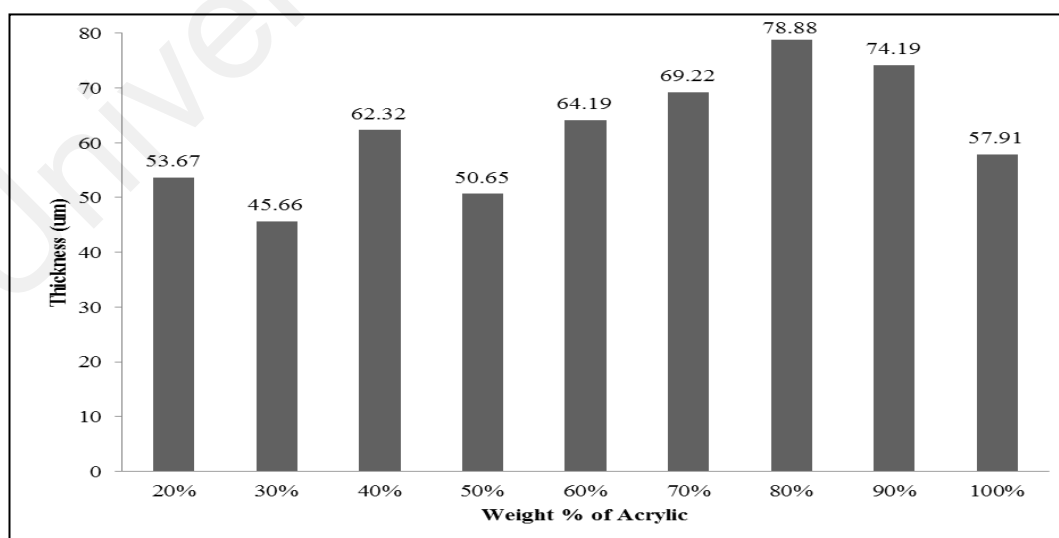


Figure 4.2: Thickness Variation of nAnE Binder System

4.5 Adhesion (Cross-Hatch Method)

The adhesion of the coating is generally considered to be good indicator of its longevity and measured by using Cross-Hatch method. This test method specifies a procedure for assessing the resistance of the coating system separation from substrates when a right angle lattice pattern is cut into the coating, penetrating through the substrate. The crossed samples were checked for damages using a digital polarized microscope, Dino-Lite. These images were compared with the standard damage schemes following ASTM D3359 method B. Wet adhesion is an important factor in ability of the coating to resist corrosion of the substrate. The coating system must flow well over the substrate to have a good intermolecular contact between the surfaces of the substrate and forms coating thickness in the range of 40-80 μm .

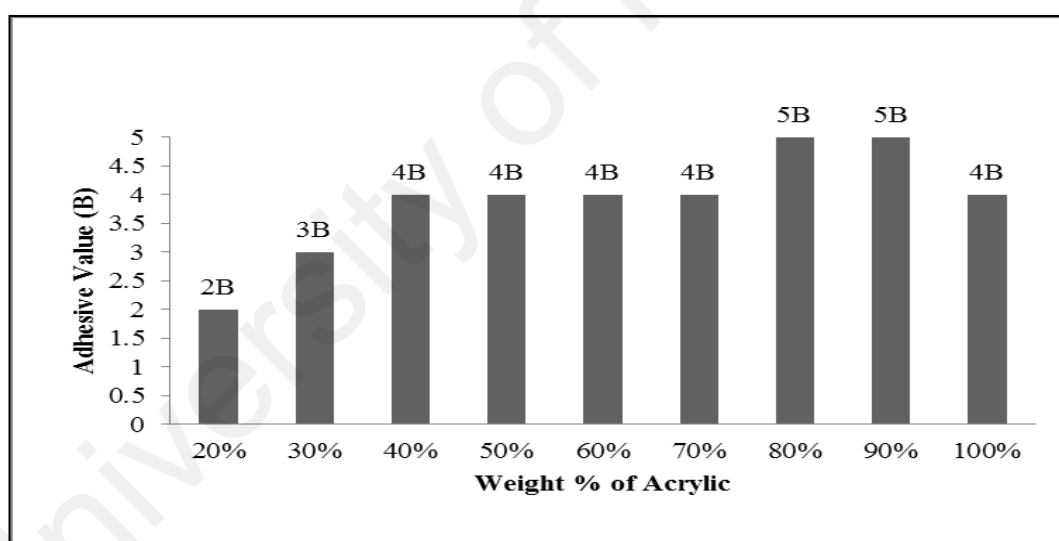


Figure 4.3: Adhesion Variation of nAnE Binder System

Figure 4.3 represents the degree of adhesion for the various AE blends. It is observed that coatings 80A20E and 90A10E have good adhesion to the substrate compared to the coating 100A, pure acrylic polyol resin (Rau et al., 2012). The epoxy resin contributes additional carboxylic and hydroxyl functional groups that together with the functional groups in the acrylic polyol resin form hydrogen bonding with the

oxides and hydroxides on the metal substrate. This increases crosslinking and network density resulting in improved adhesion to the substrate (Ramesh et al., 2008).

For other compositions 40-70 wt% A, the degree of adhesiveness is slightly lower (4B). Coating with 3B adhesiveness for sample 30A70E and 2B for 20A80E, can be easily peeled off from the substrate as shown in the Figure 4.4. It may be inferred that increasing above 20 wt% epoxy resin in the acrylic matrix, the cross link density produces strain in the coating membrane and lowers the resistance to scratch and introduces brittleness (Sharmin et al., 2004).



Figure 4.4: Cross Cut Images of nAnE Binder System

4.6 Impact Resistance

Impact resistance is one of the important mechanical properties of surface coatings. ASTM D2794 standard was followed to carry out the experiments. The intender weight was raised to a set height and released onto the panels. The height was increased by some intervals until the coating failed. Each impact with different height was tested with new panels. The coatings were observed from images taken using digital polarized microscope and checked for cracks using pinhole detector. The impact resistance is explained in terms of impact energy and sufficiently strong to withstand external attacks (Radhakrishnan et al., 2009). From the falling weight method, the ability to withstand impact has been studied. Initial increase in the concentration of acrylic resin (A) in the polymers improves the film property and made the coating harder and brittle. Further increase in the concentration above 50 wt% A provides superior impact resistance behaviour which indicates that the coating has formed a strong adhesive bonding over the substrate as shown in Figure 4.5.

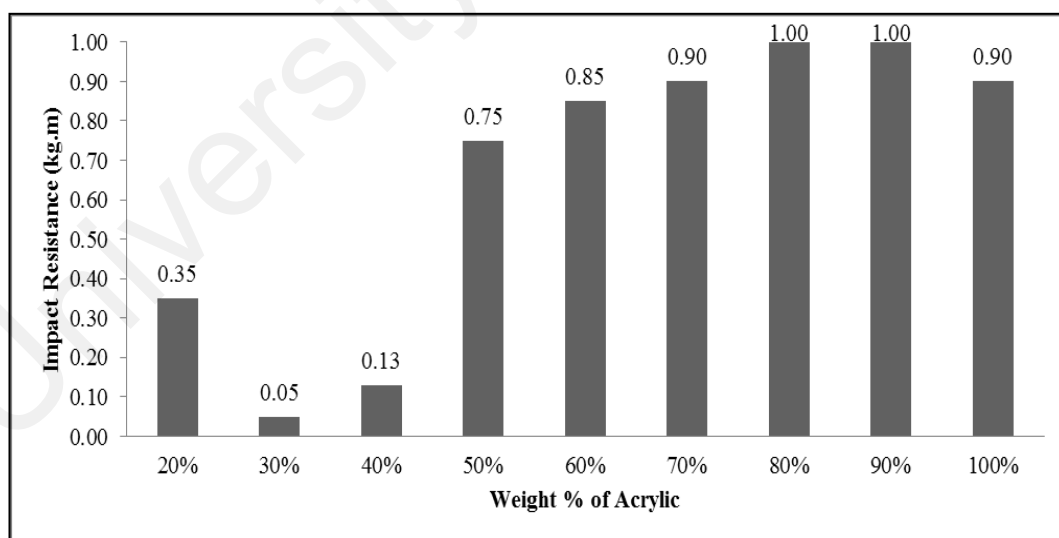


Figure 4.5: Impact Resistance Variation of nAnE Binder System

Increase in the concentration of epoxy above 30 wt% in the acrylic matrix leads to moderate and poor impact resistance. These materials also exhibit low adhesive properties. As a result of poor adhesion, the coating-substrate interface can be filled

with air. When the indenter strikes the coating, a shock wave is generated that induces stress to the coating causing the molecules in the coating membrane to vibrate (Rau et al., 2011). As the stress wave propagates into the coating, a reaction force from beneath the coating forces the resin coating to detach from the substrate and gives rise to delamination. These vibrations will generate cracks that propagate along the surface of the coating. The intensity of the crack depends on coating flexibility, which is composition dependent. Epoxy resin in high concentration increases inner tension which can weaken cohesive forces between the molecules in the blend (Kader et al., 2002). The maximum impact energy obtained using 10-20 wt% E as seen in Figure 4.5.

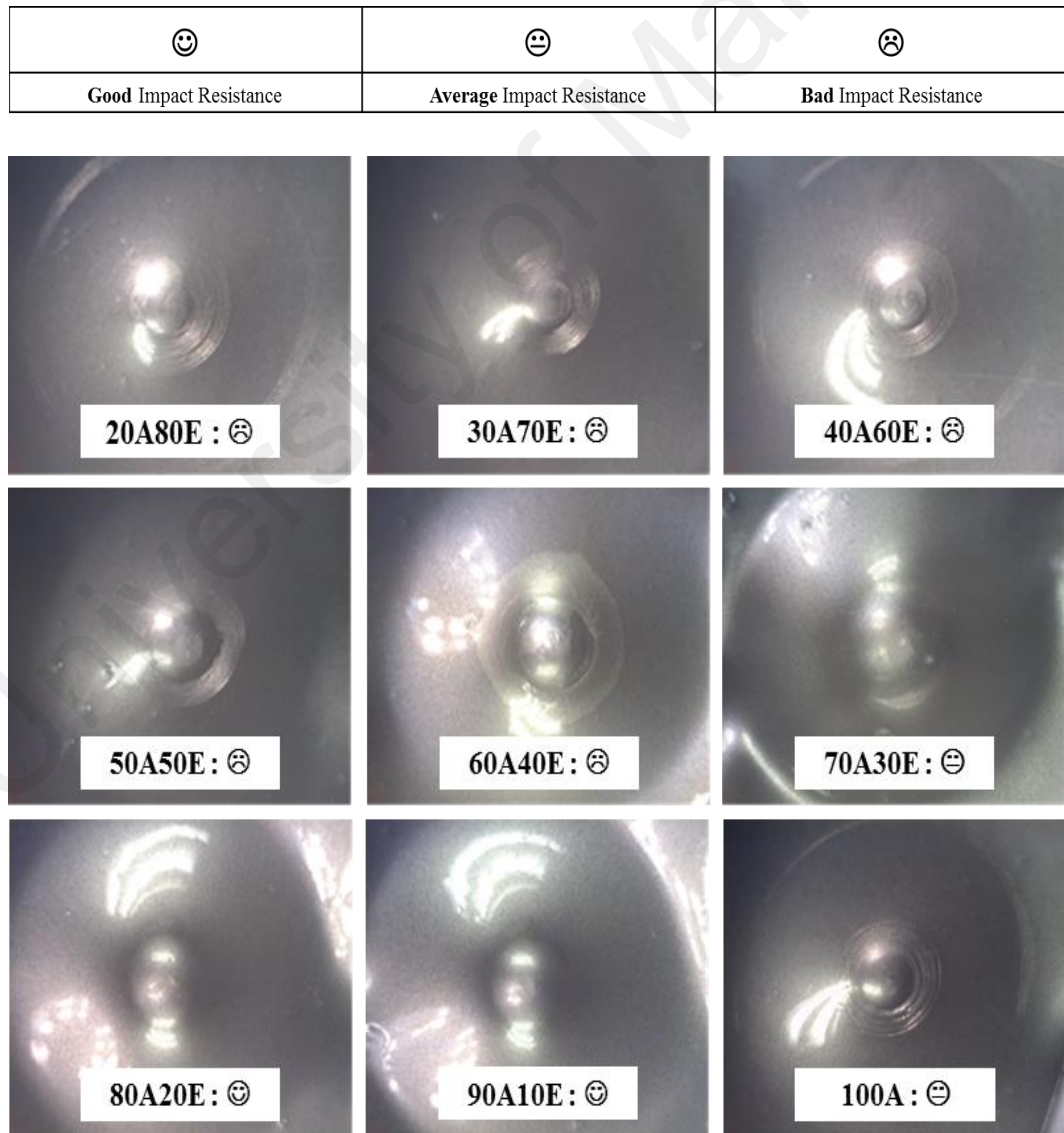


Figure 4.6: Intrusion Impact Images of nAnE Binder System

The coating were observed from images taken using digital polarized microscope and counter checked with pinhole detector. Images of intrusion and extrusion impact flexibility on the hybrid system were presented in Figure 4.6 and Figure 4.7. From the cross hatch and impact test, it is observed that the coating 80A20E and 90A10E have excellent attraction between molecules as well as with the substrate.

☺	☹	☹
Good Impact Resistance	Average Impact Resistance	Bad Impact Resistance



Figure 4.7: Extrusion Impact Images of nAnE Binder System

4.7 Fourier Transform Infrared Spectroscopy

In this study, FTIR has been used to locate the positions of functional groups in AE hybrid systems. Crosslinking between acrylic, epoxy resin and polyisocyanate as hardener were identified here. Figure 4.8 depicts the FTIR spectra for the acrylic-epoxy blends from 650 to 900 cm^{-1} , 1100 to 1900 cm^{-1} and from 500 to 4000 cm^{-1} . Evidence confirming crosslinking between A and E is the existence of stretching asymmetrical C-C band and contraction of the C-O band (Rau et al., 2011). This band was not observed in the pure acrylic sample (100A), but observed in all samples containing epoxy resin, as shown in Figure 4.8a.

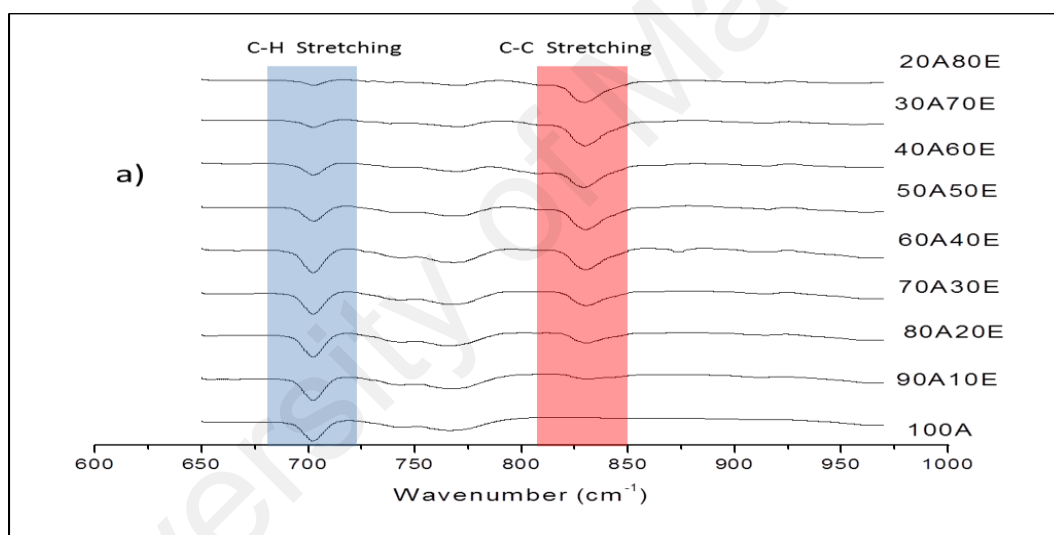


Figure 4.8a: FTIR transmission spectrum of acrylic blended with epoxy resin (Magnification of the course from 650 to 900 cm^{-1})

In 100 wt% A, the C-N band is observed at 1258 cm^{-1} . As the epoxy concentration increases in the acrylic matrix, a prominent band shift observed at 1249 cm^{-1} related to the asymmetrical -C-O-C- stretching of aryl alkyl ether of DGEBA-epoxy (Sharmin et al., 2004) is observed, as shown in Figure 4.8b. Sharmin et al. also reported a sharp peak in the spectrum of epoxy resins at 1182 cm^{-1} and attributed it to ether linkages. The band corresponding to C-O which was observed at 1174 cm^{-1} shows a shift to 1182 cm^{-1} , further confirming the formation of polymer network between AE

hybrid systems. Polyisocyanate was used as a hardener. The identical peak for the NCO group has been reported as 2280 cm^{-1} (Rau et al., 2011). From the spectra analysis, NCO band at 2280 cm^{-1} is not observed in Figure 4.8c. As such, The NH stretching band is expected to appear in the range of $1518\text{-}1581\text{ cm}^{-1}$ as confirmed as shown in Figure 4.8b. This indicates that the crosslinking between acrylic and polyisocyanate resin has occurred.

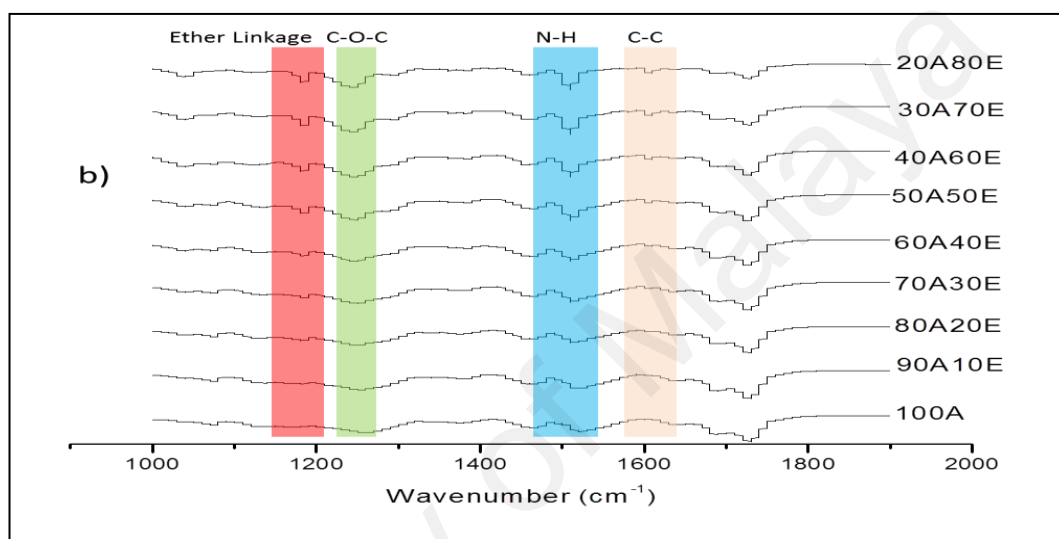


Figure 4.8b: FTIR transmission spectrum of acrylic blended with epoxy resin (Magnification of the course from $1100\text{ to }1900\text{ cm}^{-1}$)

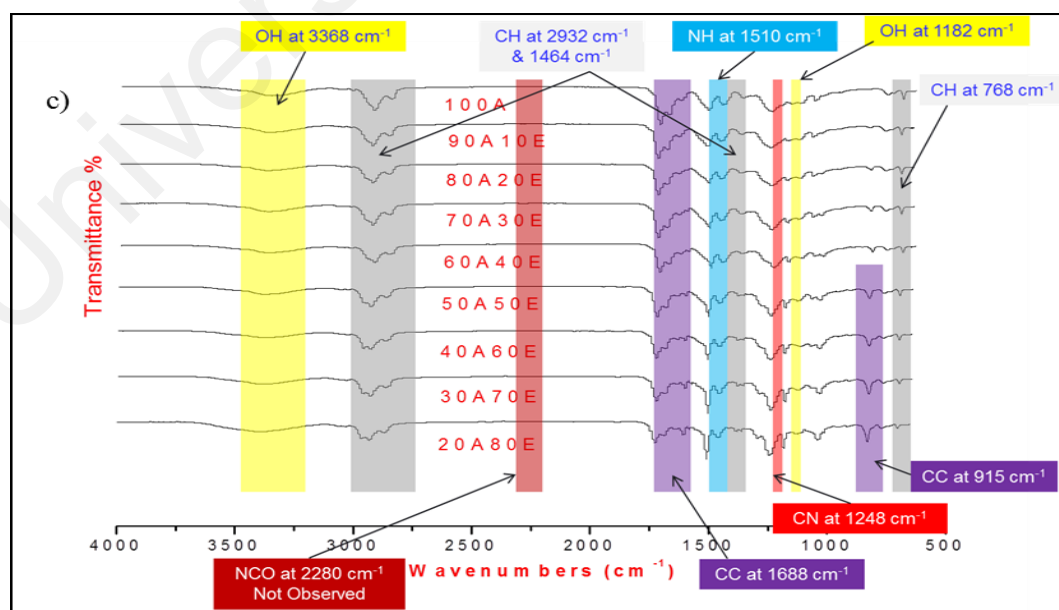


Figure 4.8c: FTIR transmission spectrum of acrylic blended with epoxy resin (Magnification of the course from $500\text{ to }4000\text{ cm}^{-1}$)

4.8 Thermogravimetric Analysis

Thermogravimetric analysis (TGA) is an analytical technique used to determine a material's thermal stability and its fraction of volatile components by monitoring the weight change that occurs as a sample is heated. TGA is an important tool to investigate the thermal stability and thermal degradation of the polymer blends (Huang et al., 2009). From the thermogravimetric analysis graphs, there are different stages available. These are obtained due to the various stages of degradation of the xylene, polyisocyanate, acrylic resin and epoxy resin in the hybrid system. Every stage reduction is related to the degradation of an individual or group of compounds present in the system.

According to data sheet, boiling point of Xylene is 135-145 °C, polyisocyanate is 280 °C, epoxy resin is 300 °C and acrylic resin is 370 °C. Figures 4.9 show the TGA thermograms of AE hybrid system and Figure 4.10 show the percentage of the residue left at the end of the degradation for all sample ratios. These thermograms reveal that the blends have thermal degradation patterns of four steps. The first step weight loss occurs at temperature range 90-120 °C, which is due to loss of solvent and moisture in resins. The second stage of loss is due to the degradation of polyisocyanate started degrading after this stage that ended around 320 °C.

A further slight weight loss at about 275-320 °C can be explained by the degradation of the secondary hydroxyl group of the propyl chain in epoxy resin. The major weight loss occurs in the range 365-420 °C, which corresponds to the loss of bisphenol-A group (Rau et al., 2013). The third step of the degradation takes place at a temperature before 380 °C and this can be attributed to epoxy degradation. Finally the point of inflexion at 320 °C until 380 °C, the decrease in mass occurs at a slower rate. This could be due to the smaller loss in acrylic resin percentage and above 380-450 °C,

the loss in mass again occurs at a faster rate and at 450 °C the mass remain almost constant until 480 °C. Figure 4.9 illustrates the TGA thermograms for all AE sample used in this study.

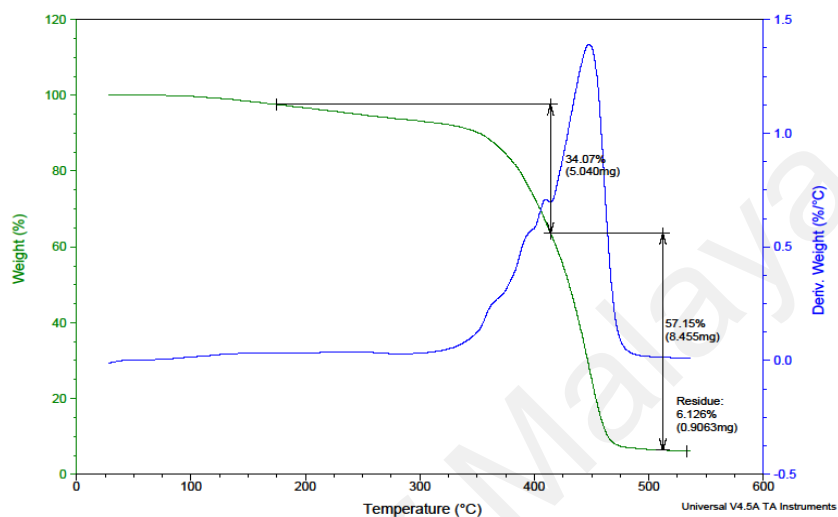


Figure 4.9a: TGA Thermogram of 20A80E

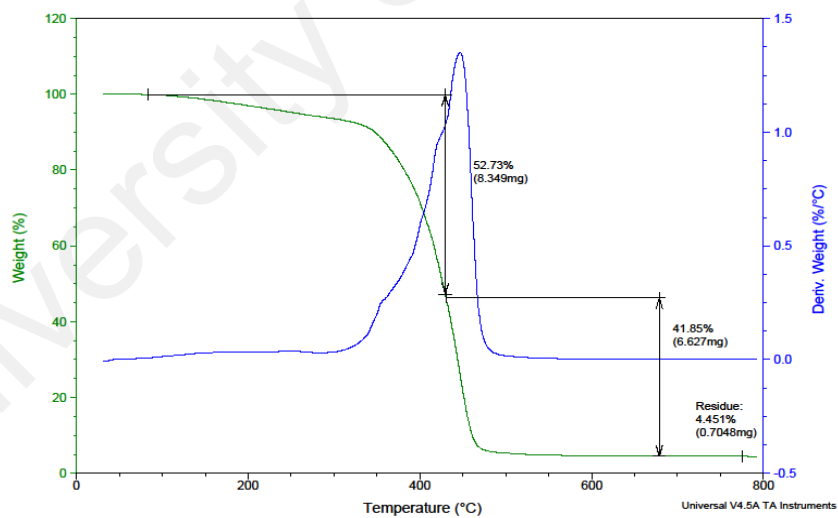


Figure 4.9b: TGA Thermogram of 30A70E

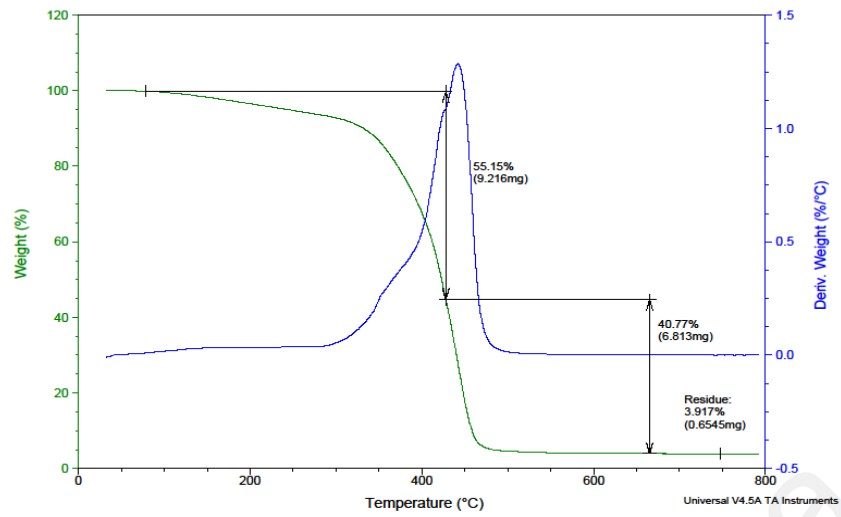


Figure 4.9c: TGA Thermogram of 40A60E

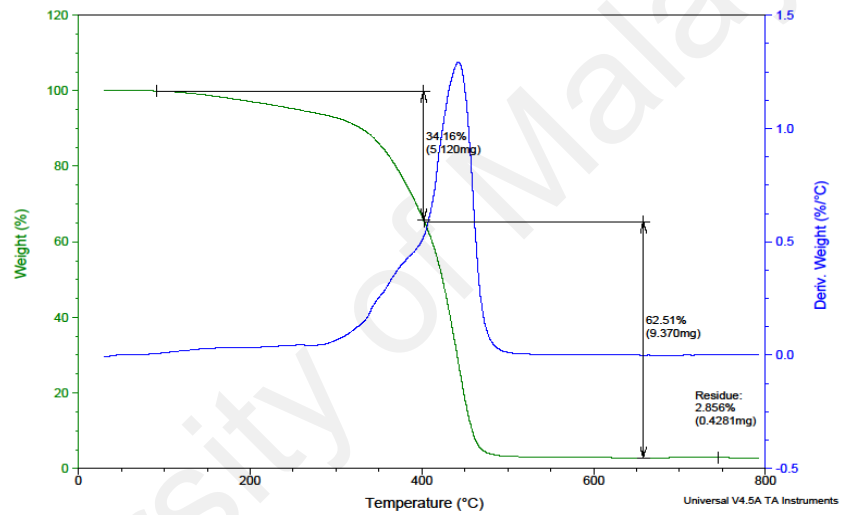


Figure 4.9d: TGA Thermogram of 50A50E

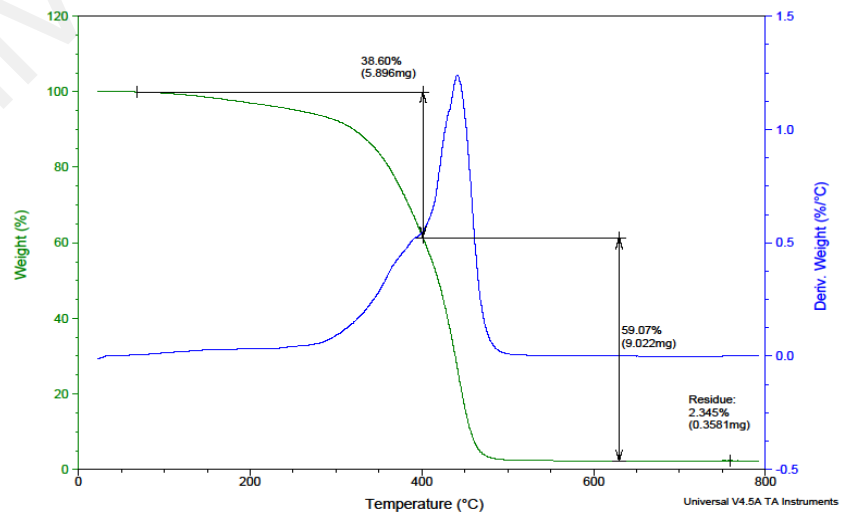


Figure 4.9e: TGA Thermogram of 60A40E

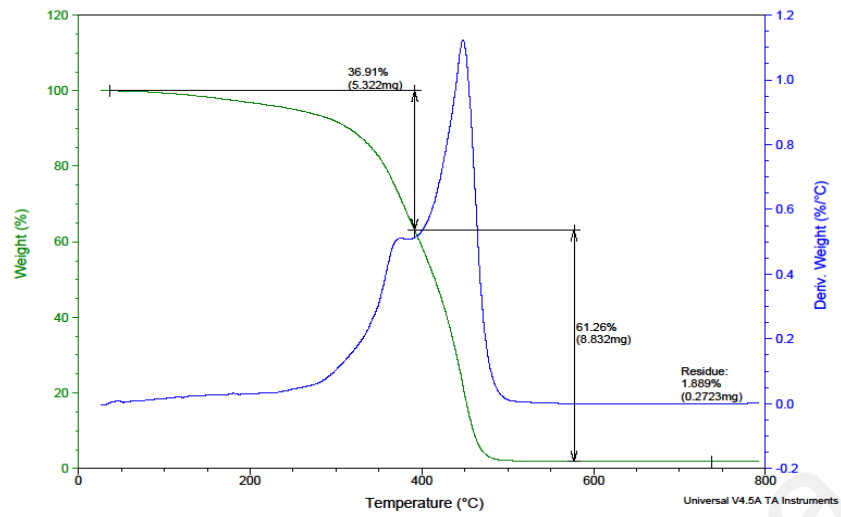


Figure 4.9f: TGA Thermogram of 70A30E

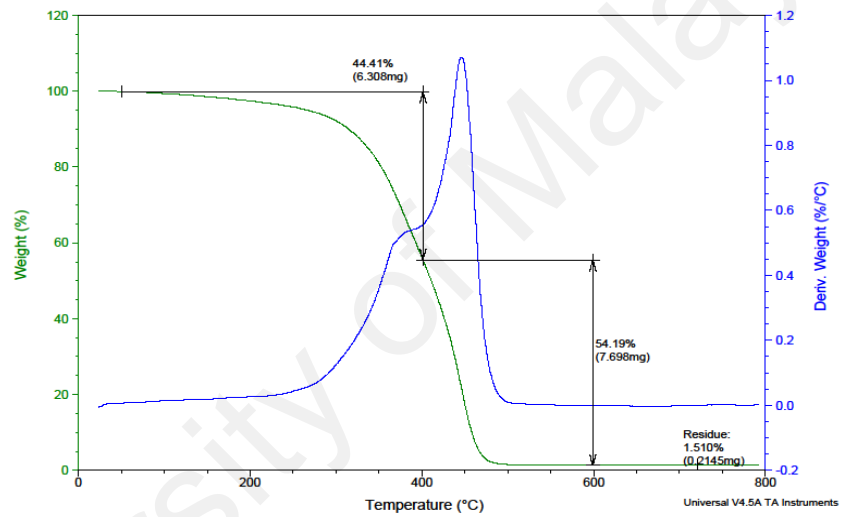


Figure 4.9g: TGA Thermogram of 80A20E

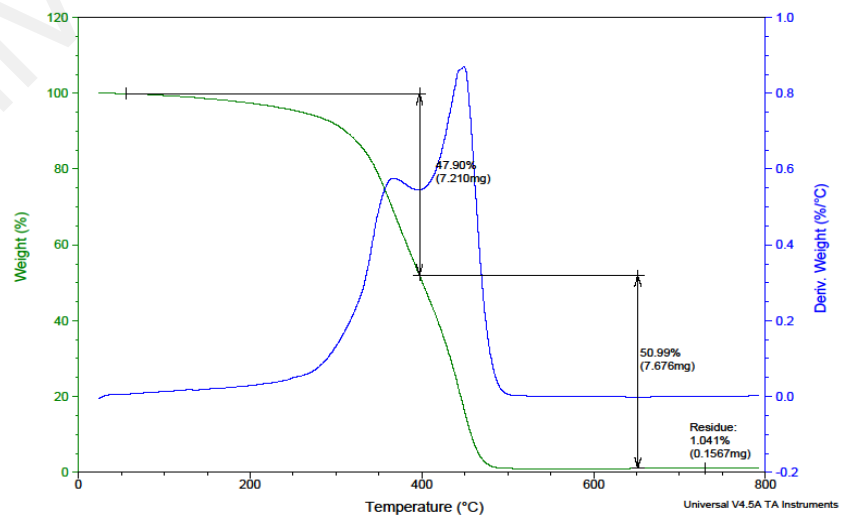


Figure 4.9h: TGA Thermogram of 90A10E

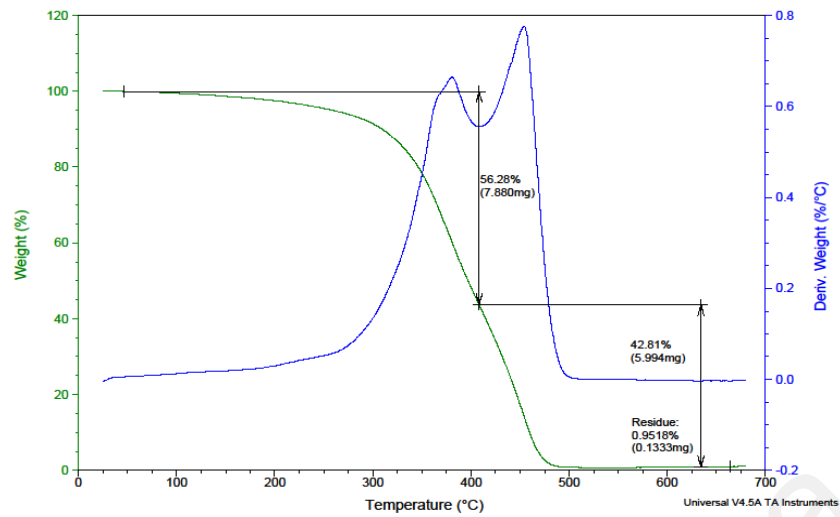


Figure 4.9i: TGA Thermogram of 100A

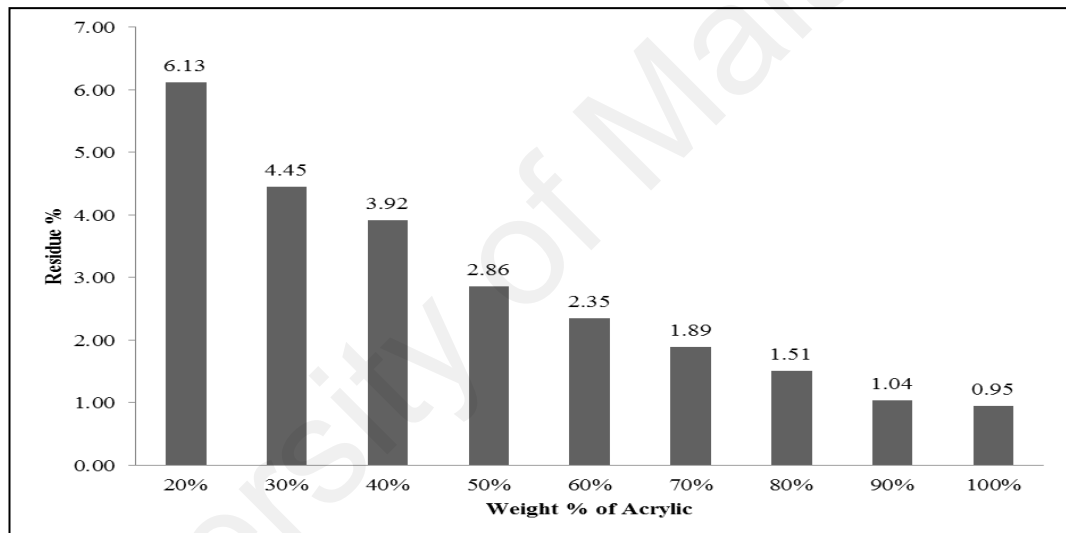


Figure 4.10: Percentage of residue left after degradation

From Figure 4.10, the final percentage of residue of all binder systems can be seen. It is understood that the higher the amount of E in the mixture, the higher the percentage of residue left at the end of the combustion. This is due to the properties of the epoxy resin itself that can withstand high heat (Yew & Ramli Sulong, 2011). The weight loss curves show clearly that the rate of degradation of acrylic resin is largely reduced following epoxy resin combination and furthermore the beginning of polymer decomposition improves as a greater amount of mixture component is incorporated into the epoxy network (Cardiano et al., 2003).

4.9 Differential Scanning Calorimetry

Differential Scanning Calorimetry (DSC) is used to study the thermal behavior of thermosetting and thermoplastic polymers by determining the glass-transition temperature (T_g) of the samples according to ASTM D7426. DSC is a powerful tool for the characterization of polymer coatings given its high sensitivity and ease of use. T_g provides very important information in coating industries. Figure 4.11 shows the DSC thermograms with the T_g values and Figure 4.12 show the summary of T_g values of AE hybrid system for all samples.

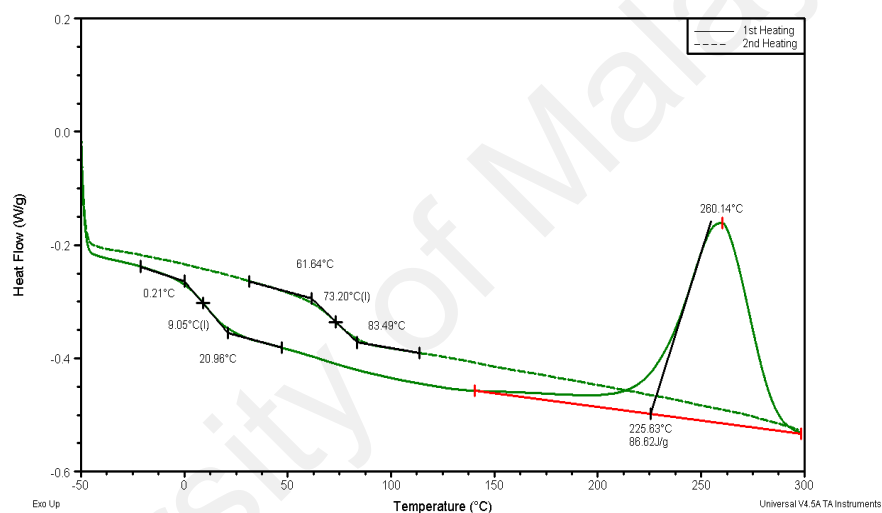


Figure 4.11a: DSC Thermogram of 20A80E

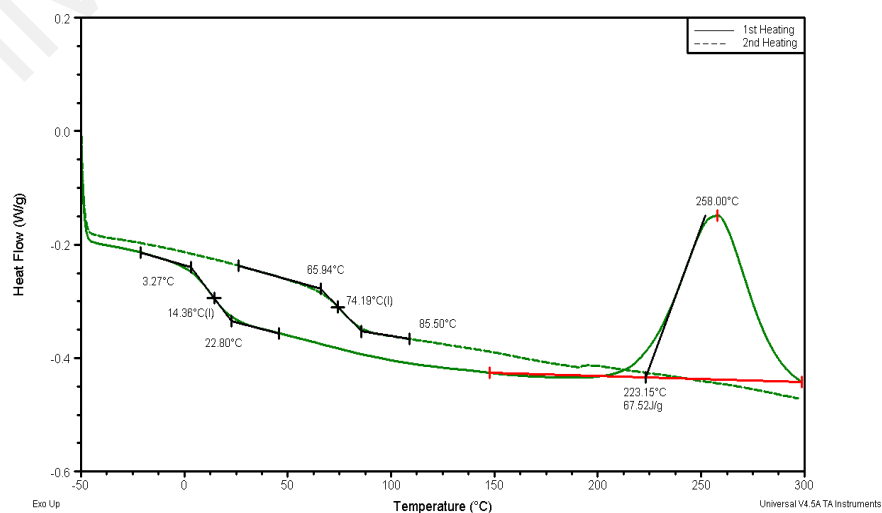


Figure 4.11b: DSC Thermogram of 30A70E

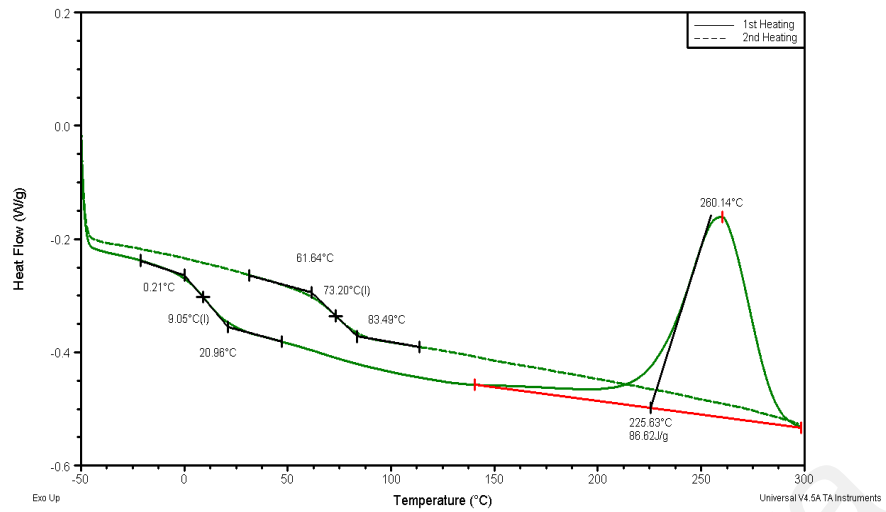


Figure 4.11c: DSC Thermogram of 40A60E

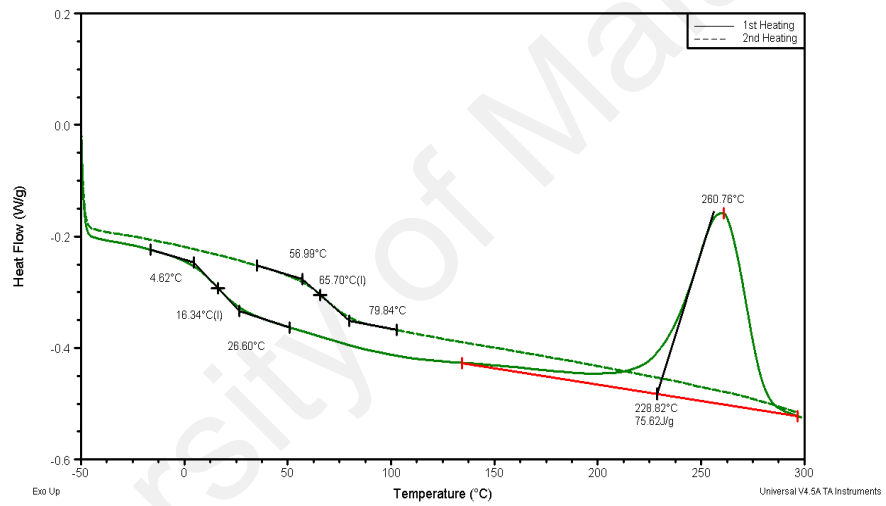


Figure 4.11d: DSC Thermogram of 50A50E

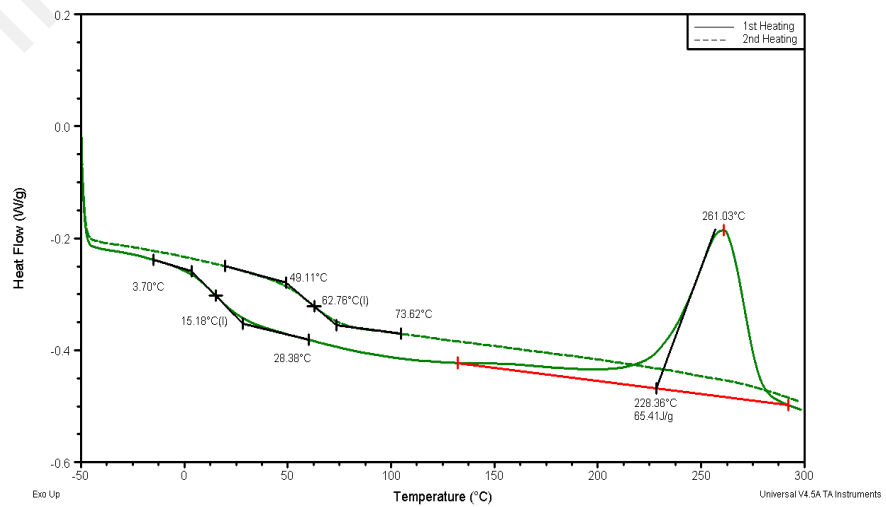


Figure 4.11e: DSC Thermogram of 60A40E

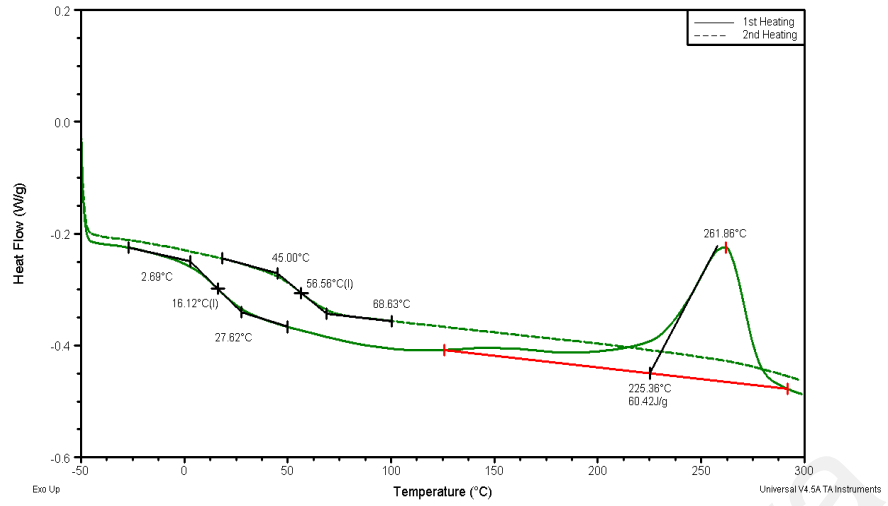


Figure 4.11f: DSC Thermogram of 70A30E

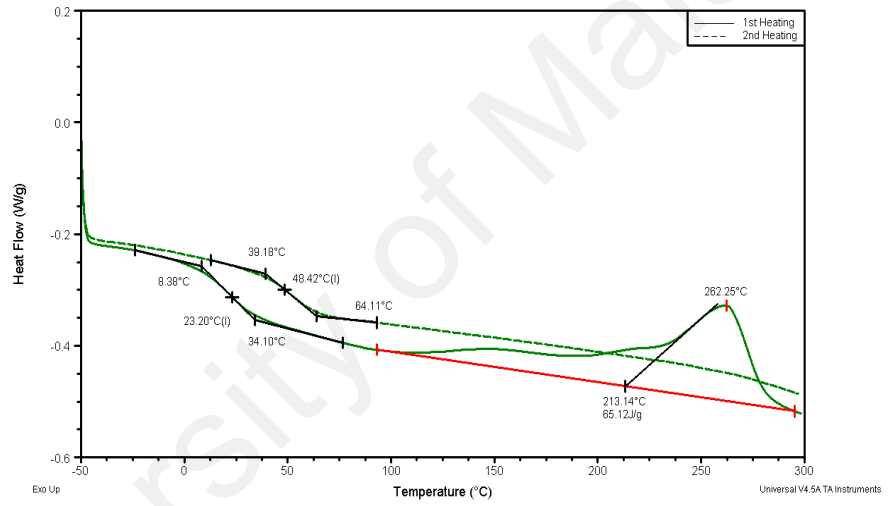


Figure 4.11g: DSC Thermogram of 80A20E

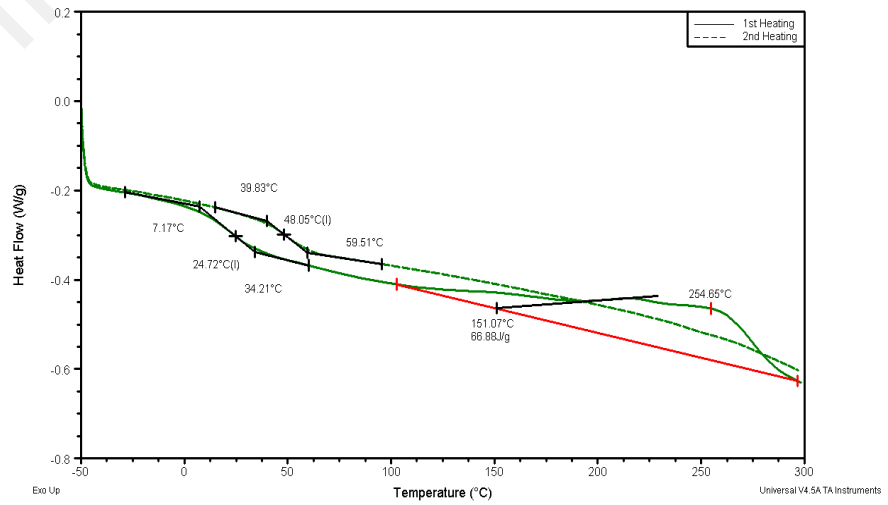


Figure 4.11h: DSC Thermogram of 90A10E

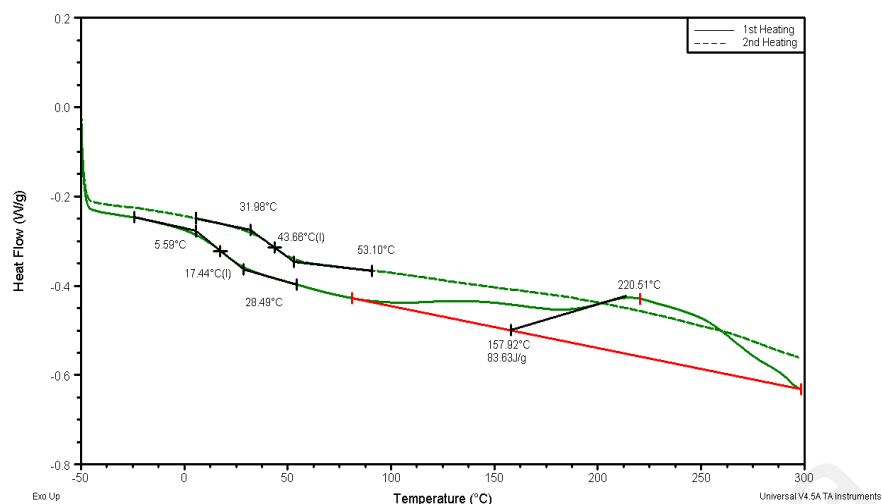


Figure 4.11i: DSC Thermogram of 100A

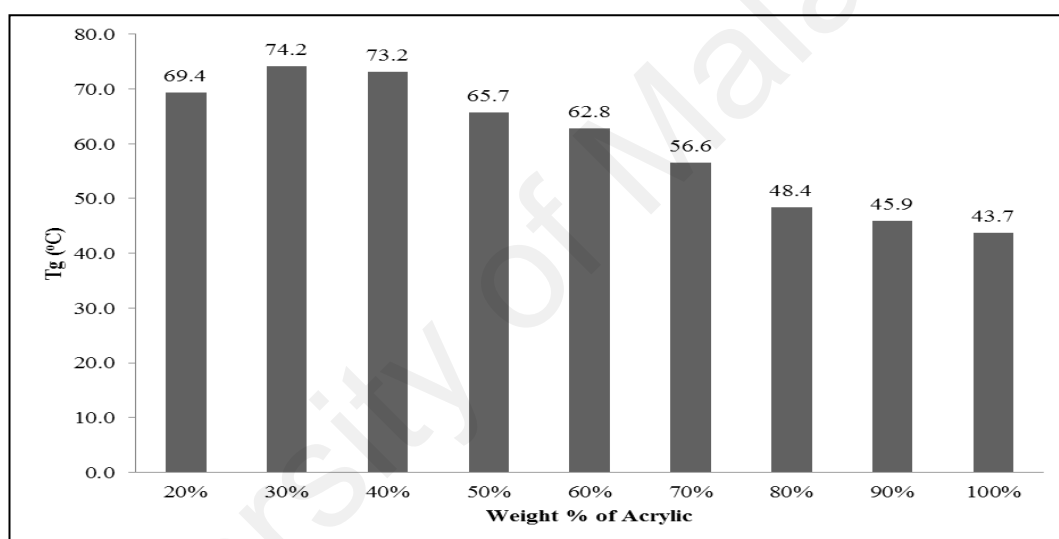


Figure 4.12: Glass Transition Temperature of nAnE Binder System

Glass transition temperature (T_g) is the main characteristic transformation temperature of the amorphous phase. T_g of the hybrid system shows an decreasing trend. This behavior perhaps can be explained by relating that the homogenous cross-linking increases as the epoxy concentration increases in the acrylic matrix. The cross-linking network might be highly achieved by the addition of the hardener, aliphatic polyisocyanate resin (Ramesh et al., 2006). The decrease in T_g has improved mechanical properties up to 20 wt% E in AE matrix. Adhesion property also showed a good result for this composition. All samples with E content higher than 30 wt% in the blending

ratios did not show better property in the mechanical testing studies and adhesion test as well. It was observed that the coatings were becoming brittle as the E content exceeds 30 wt%. A brittle coating leads to higher inner tension and thus lowers the cohesive strength (Rau et al., 2011). Therefore it can be concluded here that the increasing T_g for samples with epoxy content greater than 30 wt% causes a reduction in the mechanical properties and adhesion power of the coating (Rau et al., 2013). An optimal cross-linking density is desired for best performing coating properties. In this study incorporation of 10 wt% and 20 wt% of E in the developed hybrid systems gave the best performance. Coating with composition 80A20E and 90A10E have like characteristics. These both coating samples are sufficiently flexible, satisfactory strong adhesion and best in withstanding impact test.

4.10 Electrochemical Impedance Spectroscopy

In this study, EIS was used to determine the anti-corrosion properties and to evaluate the barrier performance of all developed hybrid binder system. Impedance data obtained from Bode plots and equivalent circuit model shown in Figure 4.13 describes the behavior of AE coated panels. In this model R_u is the uncompensated resistance of the electrolyte between the working electrode and reference electrode, C_c is the coating capacitance of the coating, R_p is the pore resistance due to the penetration of electrolyte into the micro pores of the coating, C_{dl} is the double layer capacitance at the delaminated coating/metal interface and R_{po} is the polarization resistance of the metal substrate electrode.

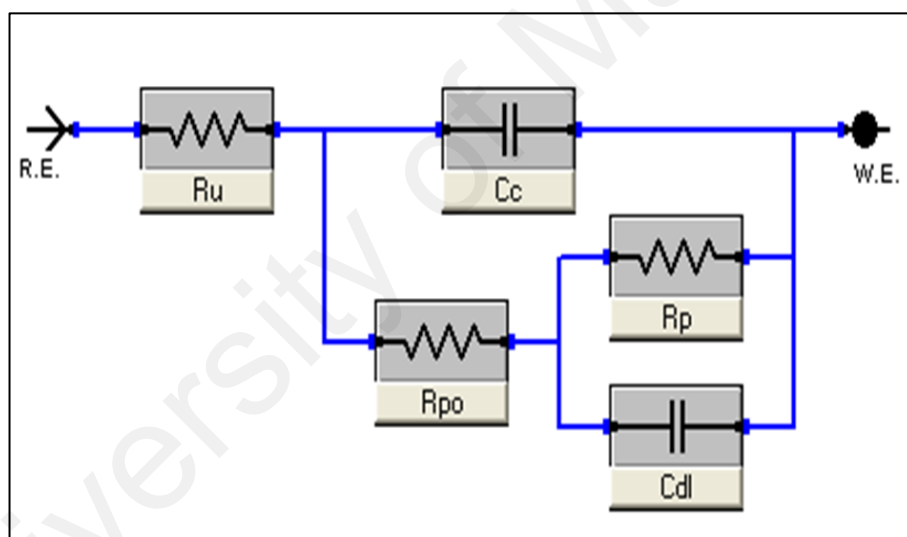


Figure 4.13: Electrical Equivalent Circuit Model

The value of R_p , C_c and C_{dl} were fitted by Echem Analyst Version 6.03 software based on the electrochemical circuit in Figure 4.13. The variations of R_p with immersion time of 30 days for different ratios of AE blend is shown in Figure 4.14. The sample with 10 wt% E in 90 wt% A (90A10E) shows that the R_p values of the pore resistant is in the order of $10^9 \Omega\text{cm}^{-2}$ up to 30 days of immersion. The high resistance values indicate that the coating is very intact. Higher R_p values above $10^8 \Omega\text{cm}^{-2}$ relate to diffusion barrier of electrolyte via the pore. R_p is the ionic resistance of the coating

which is inversely proportional to the area of delamination (Deflorian & Rossi, 2006). When the R_p value decreases below $10^6 \Omega\text{cm}^{-2}$, coating is undergoing large area of delaminating where blister formation and corrosion starts (Bierwagen et al., 2000; Loveday et al., 2004) which can be observed in all the other samples as shown in Figure 4.14.

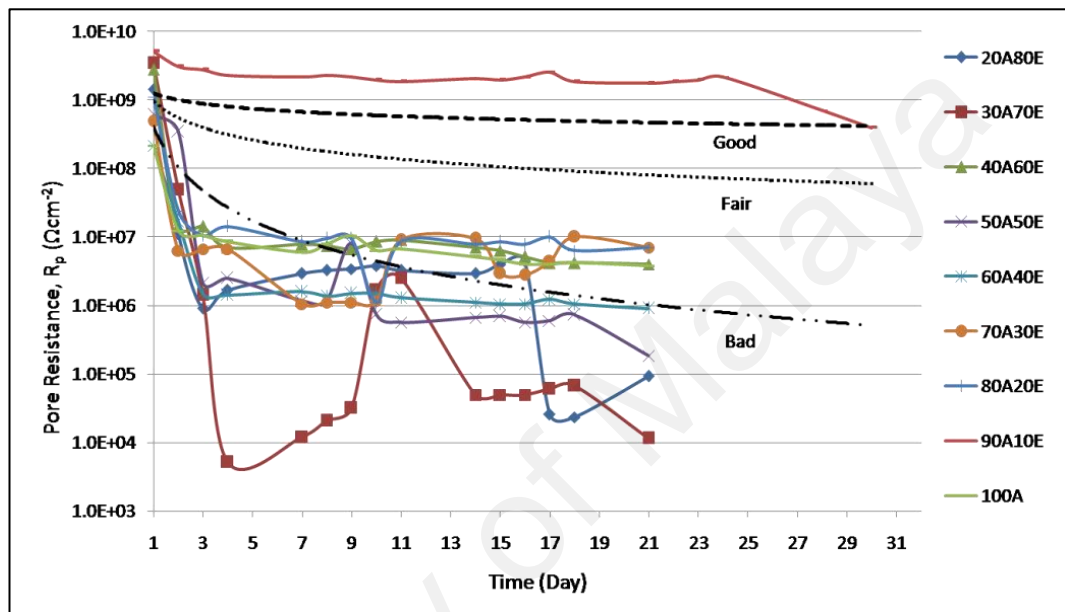


Figure 4.14: Pore Resistance (R_p) vs Time of immersion

The uptake of electrolyte (3.5 % NaCl solution) in organic coatings can be determined directly from capacitance measurements. The evaluation of C_c is shown in Figure 4.15. The ion diffusion processes through the coatings can be divided into 3 phases. In Phase I, upon immersion of coating in electrolyte, ions penetration begins which leads to a rapid increase in the coating capacitance. In Phase II, the coating is saturated with ions leading to a plateau where the capacitance remains constant. In Phase III, there is further accumulation of electrolyte at the coating-metal interface indicating adhesion loss and possible onset of corrosion (Rau et al., 2012).

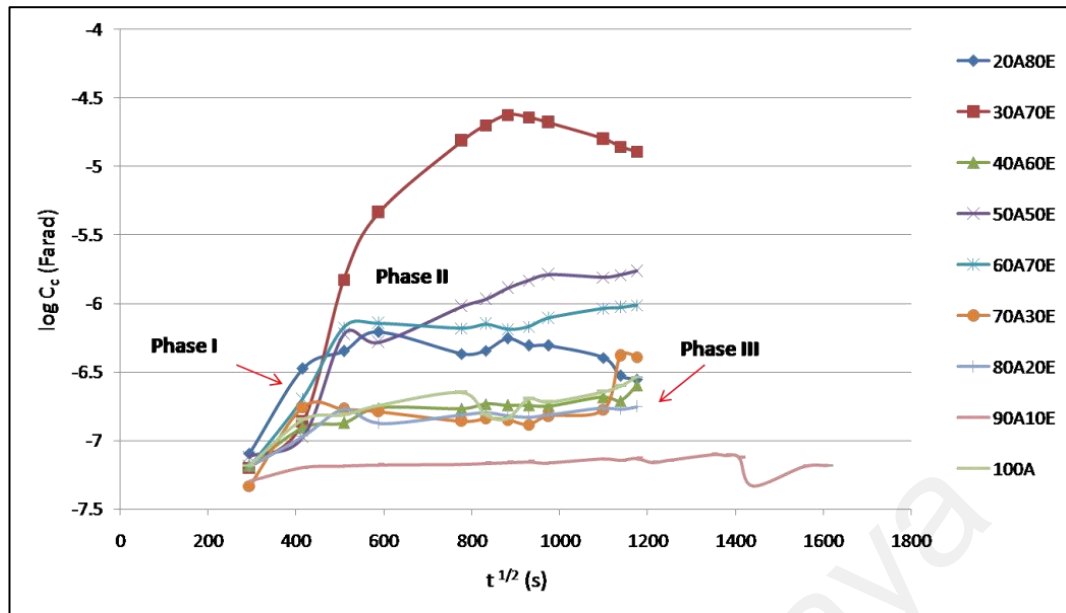


Figure 4.15: Coating Capacitance (C_c) vs Time of immersion

Intact coating adhesion to metal substrate possesses high R_p value and low C_c value (Baukh et al., 2012). All the other AE hybrid system shows the phase transitions (Phase I, Phase II and Phase III) as mentioned above except sample 90A10E. From Figure 4.15, it is observed that, only sample 90A10E shows a very low coating capacitance and is almost constant for 30 days of immersion time in the 3.5 % NaCl electrolyte. This result supports the destructive adhesion cross hatch cut test. The continuous increase in C_c is attributed to a gradual increase in sodium and chloride ions at the coating metal interface. This lead to swelling of the coating and loss of its ideal dielectric behaviour (Amirudin & Thierry, 1995).

Using data from C_c plots, the coating is treated as parallel plate capacitor and then its capacitance is related with the relative dielectric constant (ϵ) using Equation 3.1

$$C_c = \frac{(\epsilon \cdot \epsilon_0 \cdot A)}{d}$$

where ϵ_0 is the dielectric constant of free space (8.85×10^{-12} F/m), A (m^2) the surface area of the coating and d (m) is the coating thickness. Since the relative dielectric constant of polymers is typically in the range of 3-8, and for pure water is 80 at 25 °C,

then the uptake of electrolyte will lead to an increase of the dielectric constant and a higher coating capacitance (Castela & Simoes, 2003).

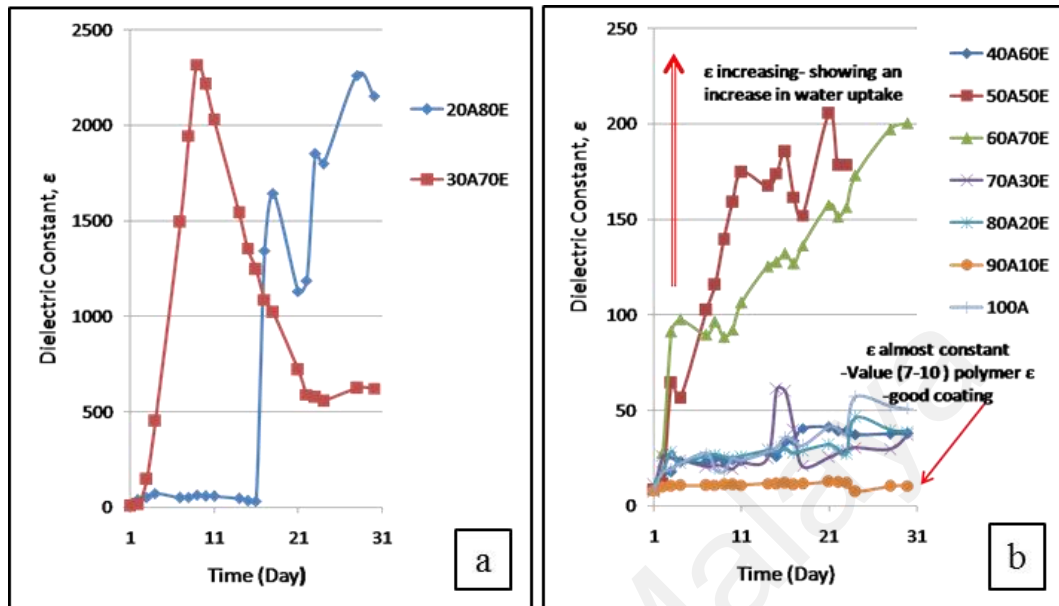


Figure 4.16: Dielectric Constant (ϵ) vs Time of immersion

According to Castela and Simoes, the dielectric constant of solid water and air tri-phase coating is given by Equation 4.1:

$$\epsilon = \epsilon_s \cdot \epsilon_w \cdot \epsilon_a \quad (\text{Equation 4.1})$$

where ϵ_s is the solid dielectric constant, ($\epsilon_w \approx 80$) is the water dielectric constant and ($\epsilon_a \approx 1$) is the air-phase dielectric constant respectively (Castela & Simoes, 2003). Dielectric constant, ϵ values are plotted in Figures 4.16. It is observed that the 90A10E sample shows a small increase in dielectric constant but within the range of an inert coating system (8-10). This implies that the 90A10E sample exhibits small porosity and possesses good barrier properties. Other samples show dielectric constant values higher than 10 as shown in Figure 4.16, indicating the presence of pores and voids which may lead to electrolyte uptake and transport of sodium and chloride ions at the coating-metal interface.

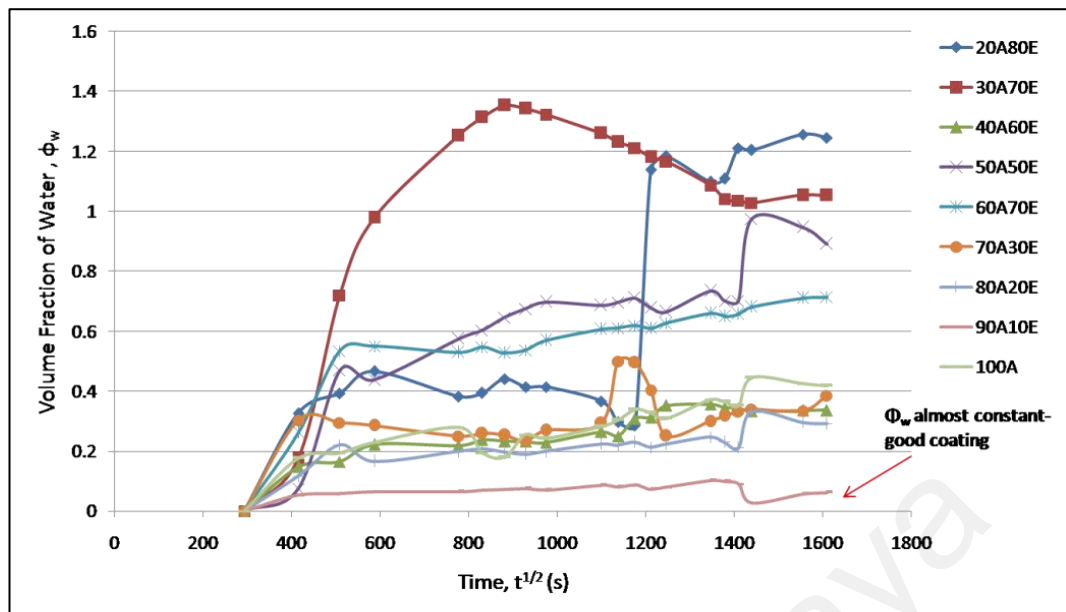


Figure 4.17: Volume Fraction of Water (ϕ_w) vs Time of immersion

Volume fraction of water, ϕ_w , is calculated from the equation given by Equation 3.2:

$$\phi_w = \frac{\log\left(\frac{C_t}{C_0}\right)}{\log \varepsilon_w}$$

where C_t is the capacitance at instant t and C_0 is usually obtained by extrapolating the coating capacitance to $t = 0$ as reported by Castela and Simoes. When ϕ_w increases, ε increases, resulting in higher capacitance. ϕ_w for AE hybrid coating is presented in Figure 4.17. Only sample 90A10E has a low water absorption at the saturation stage. Also, as seen in Figure 4.14, the 90A10E sample becomes saturated leading to a plateau where the capacitance remains constant, indicating better barrier properties. As a consequence, the observed changes in the capacitance are linearly related to the water uptake. However, after the saturation of the coating has been reached, coating capacitance continues to increase slowly. This phenomena may be due to different electrolyte uptake rate or is due to disbanding of the hybrid coating which depends on hydroxide ion generation at the coating and metal interface (Popov et al., 1993).

4.11 Summary

Coating formulation involves a combination of performance and cost. Applications for excellent resistance to extreme environments require resins that are more costly, such as epoxies and polyurethanes. Most decorative finishes contain lower cost acrylic resin that is perfectly suitable for general settings. Different resins can be combined into a hybrid mixture designed to deliver specific performance capabilities.

In this first part of study, a hybrid system which forms compatible blends with epoxy resin was developed. The developed hybrid systems can be used as a flexibilizer and toughener for acrylic polyol resin. The properties of the developed hybrid coating systems (AE) have been methodically investigated using different analytical methods covering physical, mechanical, structural, thermal and electrochemical performances in order to satisfy corrosion protection.

This study demonstrates an interesting correlation between viscosity, adhesion, impact resistance and FTIR, TGA, DSC and EIS. The blending system with 10 wt% and 20 wt% epoxy resin exhibits good physical and mechanical properties. High viscosity of the coating system consisting 80A20E and 90A10E provides a uniform dry film thickness and takes about 3 hours to cure. Blending ratio of 40 wt% A represents minimum degree of adhesion for the various AE blends. It is observed that coatings 80A20E and 90A10E have the best adhesion onto the mild steel panels. These two sample ratios also performed well in impact resistant test conforming to have excellent attraction between molecules as well as with the interface. FTIR revealed cross linking between the components of the binders and has the maximum thermal stability. Thermal studies confirms that the T_g of these binders range between 35-75 °C making coating samples are sufficiently flexible, satisfactory strong adhesion and best in withstanding

impact test. Both 80A20E and 90A10E have similar characteristics in terms of physical, mechanical and thermal performances.

Electrochemical studies provide detailed anti-corrosion properties of all samples. EIS reveals the properties of the coating adhesion in terms of pore resistance (R_p), coating capacitance (C_c), dielectric constant (ϵ) and volume fraction of water (ϕ_w). The sample with 10 wt% E in 90 wt% A (90A10E) shows that the R_p value of the pore resistant is in the order of $10^9 \Omega\text{cm}^{-2}$ and a very low C_c ($<10^{-7}$ Farad) that is almost constant for 30 days of immersion time in the 3.5 % NaCl electrolyte. A small increase in ϵ , but within the range of an inert coating system (8-10) and ϕ_w with low water absorption at the saturation stage indicates that the 90A10E sample exhibits small porosity and possesses good barrier properties. In this study incorporation of 10 wt% of epoxy resin in acrylic polyol resin in the developed hybrid systems gave the best performing binders for the development of the paint systems.

CHAPTER 5: RESULTS AND DISCUSSION ON PAINT SYSTEM

PHYSICAL AND MECHANICAL

5.1 Introduction

In the second part study for the development of anti-corrosion coating using organic resins hybrid system study, blending ratio of 90A10E was used as the base binder for the development of all paint system. This chapter presents the results from physical and mechanical studies of the Acrylic-Epoxy of the four paint systems formulated using the best performing blending ratio consisting of 10 wt% E in 10 wt% A (90A10E).

Studies continued to investigate the influence of the different inorganic pigments used, namely Titanium Dioxide, TiO_2 (P1 system), Silitin Z 86 (P2 system), Aktisil AM (P3 system) and Aktisil PF 777 (P4 system) on the physical and mechanical properties of the polymeric matrix over the pre-treated cold rolled mild steel panels. The effect of the pigment volume concentration (PVC) ratio to the critical pigment volume concentration (CPVC) on the corrosion resistance properties of paint system has been investigated in four paint systems namely P1, P2, P3 and P4. The study will be established on the variation of the composition of the pigments has been used to prepare single hybrid paint coat on mild steel panel.

5.2 Dry Film Thickness

A digital Coating Thickness Gauge model Elcometer 456 was used in accordance with the Ferrous (F) ASTM D1186. At least 50 readings taken within same paint system sample and the average thickness were calculated. The hybrid paint system mixtures were thoroughly blended using a paint mixer. Mixing the 90A10E base

without hardener and additives of inorganic pigment to achieve a complete dispersion in the paint container for the right thickness for improvement in mechanical properties (Rodriguez et al., 2004) and were applied on the pre-treated mild steel panels. The coating system must flow well over the panels to have a good intermolecular contact. This achieved by adding known amount of xylene as solvent in the mixture. The panels were allowed to dry for 1 week before carried out the characteristic analysis.

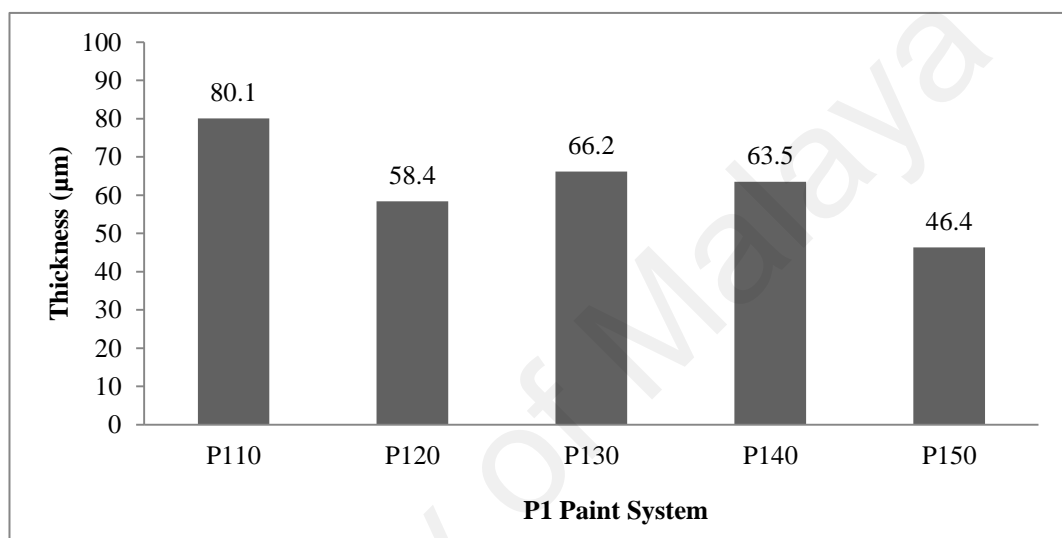


Figure 5.1: Thickness Variation of P1 paint system (TiO₂)

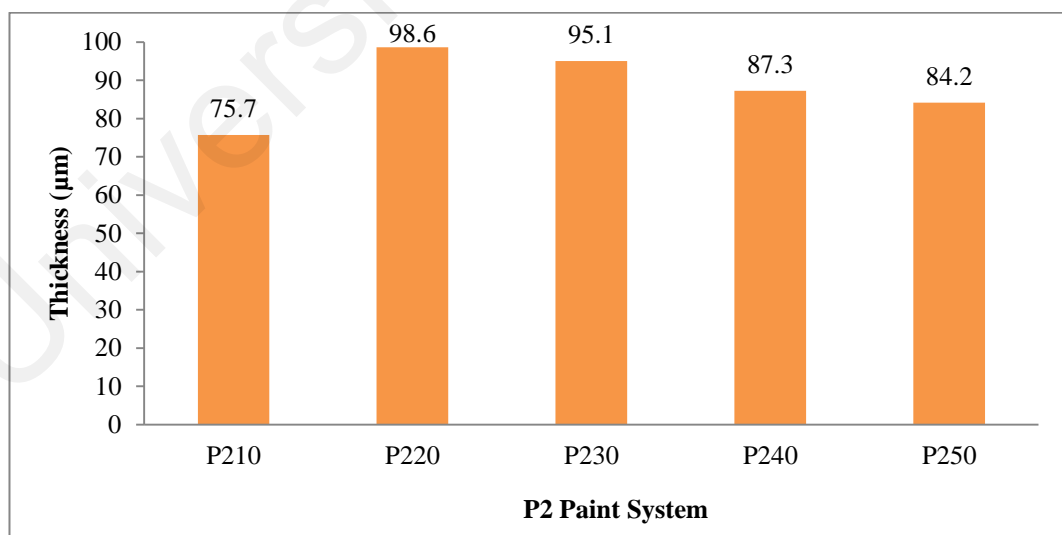


Figure 5.2: Thickness Variation of P2 paint system (Silitin Z 86)

From Figure 5.1 to Figure 5.4, the dry film thickness of the all paint systems was found to be in the average range of 40-80 µm. From the 90A10E binder system results,

good film thickness observed in the coating system (Rau et al., 2013). It was clearly observed from the P1, P2 and P3 paint system plots with all pigment volume concentration (PVC) percentages, that these paint system had good dry film thickness. Meanwhile, film thickness is decreasing for P4 system with higher PVC content. Lower coating thickness will have disadvantages in mechanical, electrochemical and corrosion studies (Hu et al., 2012). These results will contribute an early prediction on adhesion, acid resistance and EIS investigations. Its worth to mention that all paint system with PVC below 40 % would observe better performance. However, the P4 samples with $PVC \geq 40\%$ would fail in accelerated investigations.

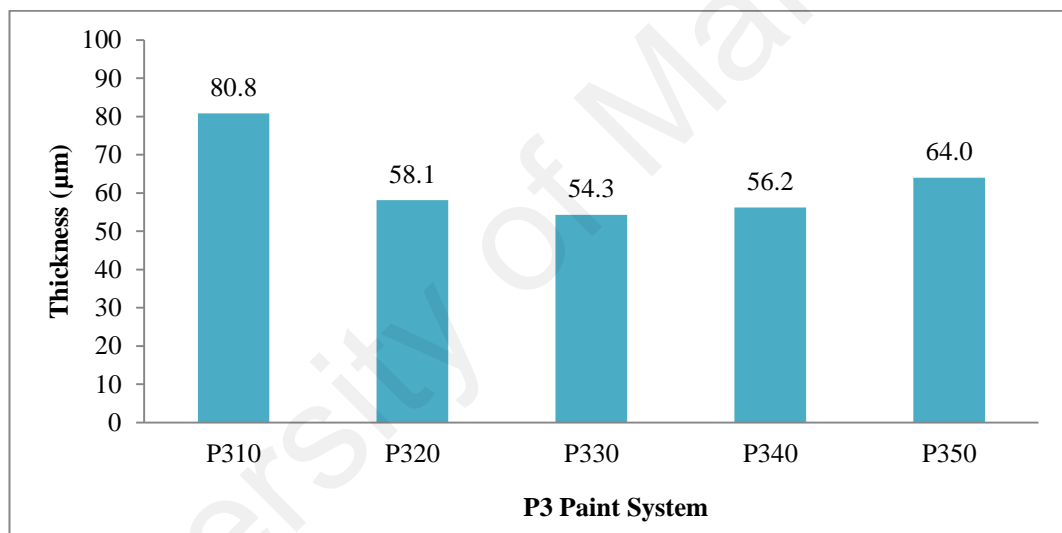


Figure 5.3: Thickness Variation of P3 paint system (Aktisil AM)

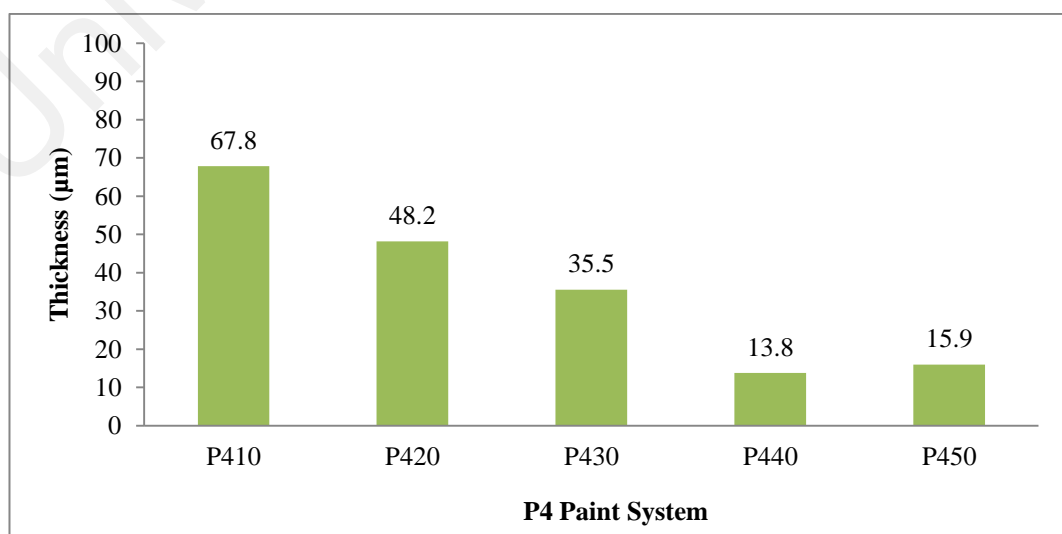


Figure 5.4: Thickness Variation of P4 paint system (Aktisil PF 777)

5.3 Adhesion (Cross-Hatch Method)

Adhesion is an interfacial phenomenon, where physical and chemical forces always operate when surfaces are in contact of each other to form an interface. The ability to adhere to the substrate throughout the desired life of the coating is one of the basic requirements of a surface coating. In this study, testing the adhesion of the developed paint systems on the cold rolled mild steel substrates was carried out by the using of Cross-Hatch Method. A Sheen 750, cross-hatch cutter was used in that regard of the cutter. All reported tests were performed according to the ASTM D3359 method B standard. This test method specifies a procedure for assessing the resistance of the paint system to separation from metal substrates when a right angle lattice pattern is cut into the paint, penetrating through the substrate. The sample area was given a stiff brushing and the pattern inscribed was examined in order to define the classification of test results. The results of these studies were recorded as images of the crossed samples by utilizing a digital polarized microscope (Dino-Lite, AM413ZT). All tested samples were compared with the standard damage schemes of the standards for the cross hatch test (Rau et al., 2012).

Organic coating adhesion to the metal substrate could be considered one of the main factors that must be considered during the development of highly intact paint systems. The hybrid binder system consist of 10 wt% E in 90 wt% A (90A10E) showed the best adhesion performance and was chosen to be the base binder matrix of the paint systems as reported in the 2012 work by Rau et al.

In this study, blending ratio of 90A10E was used as the base binder for the development of the all paint system. Continues studies has been done to investigate the influence of different used inorganic pigments, namely Titanium Dioxide, TiO_2 (P1 system), Silitin Z 86 (P2 system), Aktisil AM (P3 system) and Aktisil PF 777 (P4

system) on the adhesion behavior of the polymeric matrix over the pre-treated cold rolled mild steel substrate. However, there were no significant changes observed after the addition of the inorganic pigments on the adhesion properties of the paint film. This can be attributed to the fact that the coating consists of just the binder system itself demonstrated an excellent adhesion to the substrate and due to the good distribution of the pigments (Clerici et al., 2009) within the polymeric matrix after the successful curing process without any cracks and plastic deformation (Perera, 2004).

Figure 5.5 shows the images of P1 paint system with TiO₂ pigment which were captured in order to present the results of cross-hatch test. It was clearly observed from the results of P1 paint system for all pigment volume concentration (PVC) exhibits good adhesion to the substrate without any sign peel-off spot over entire area under analysis.

The similar trend has been observed in all other prepared paint systems namely P2, P3 and P4. The respective cross-hatch test results were illustrated in Figure 5.6, 5.7 and 5.8 respectively. It can be concluded that all the four types of the inorganic pigments which have been added to the acrylic-epoxy polymeric matrix (90A10E) have shown the same good adhesion properties of the reinforced binder with class 5B ranking according to ASTM D3359 standards.

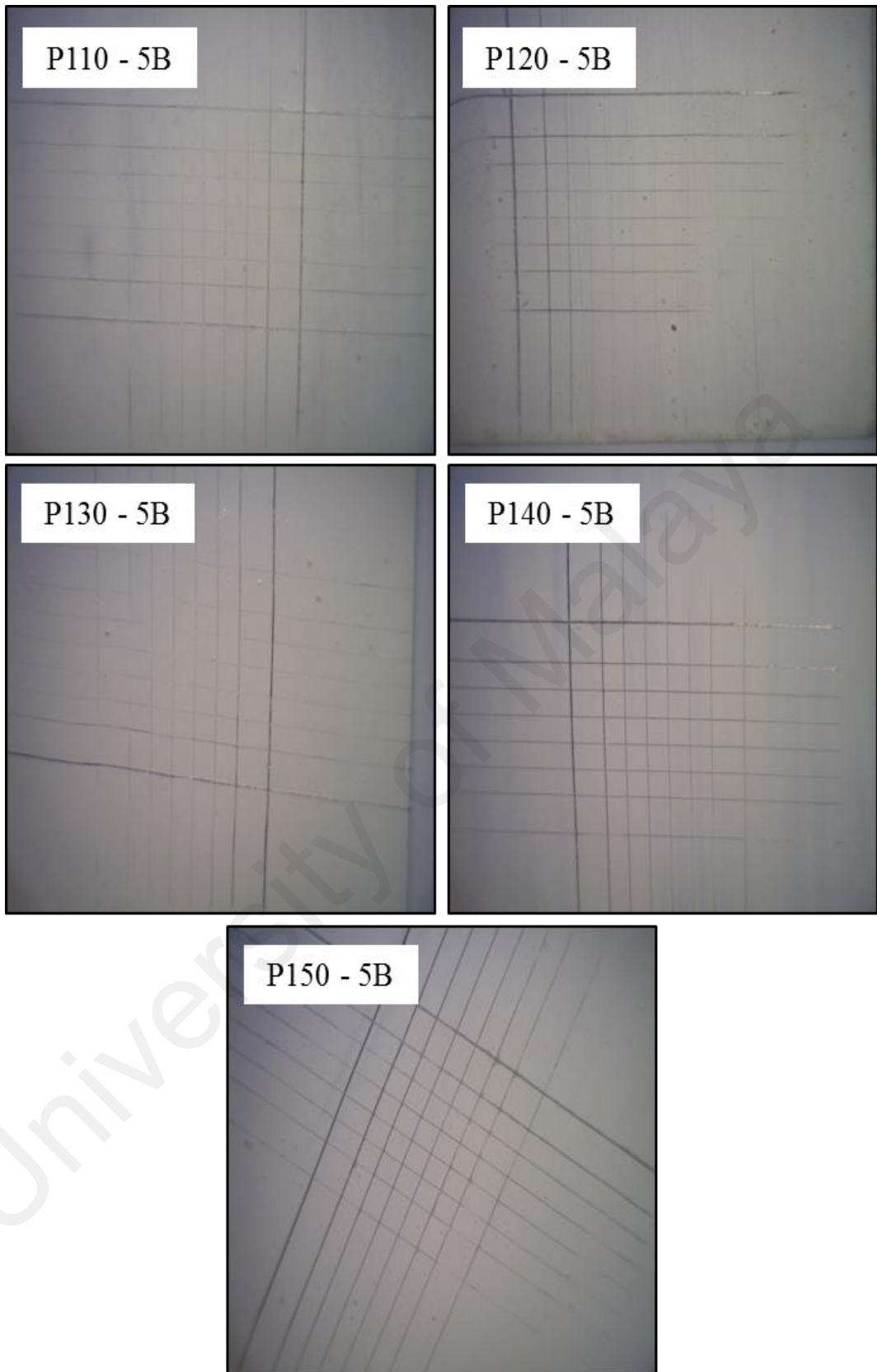


Figure 5.5: Cross Cut Images of P1 paint system

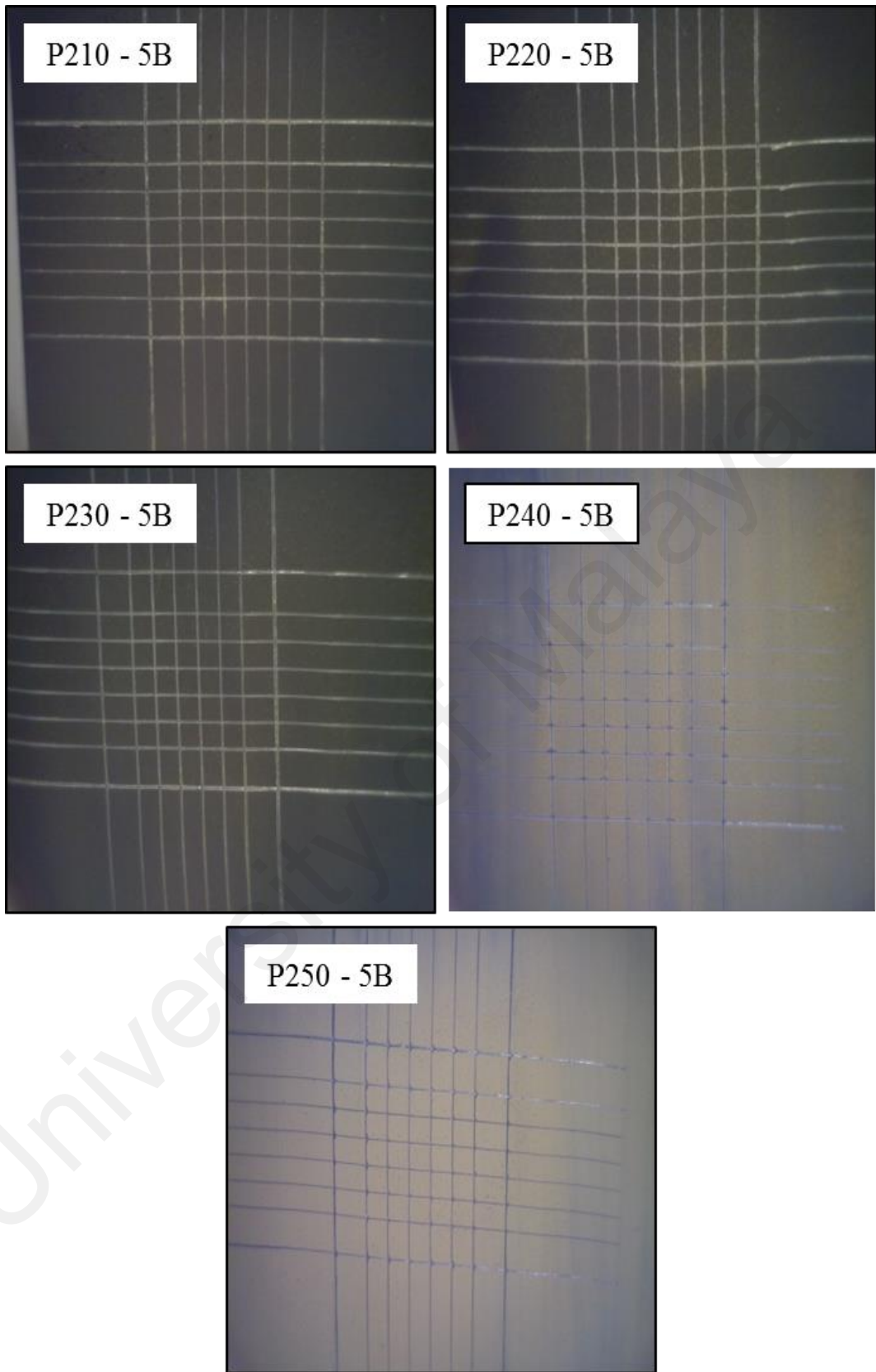


Figure 5.6: Cross Cut Images of P2 paint system

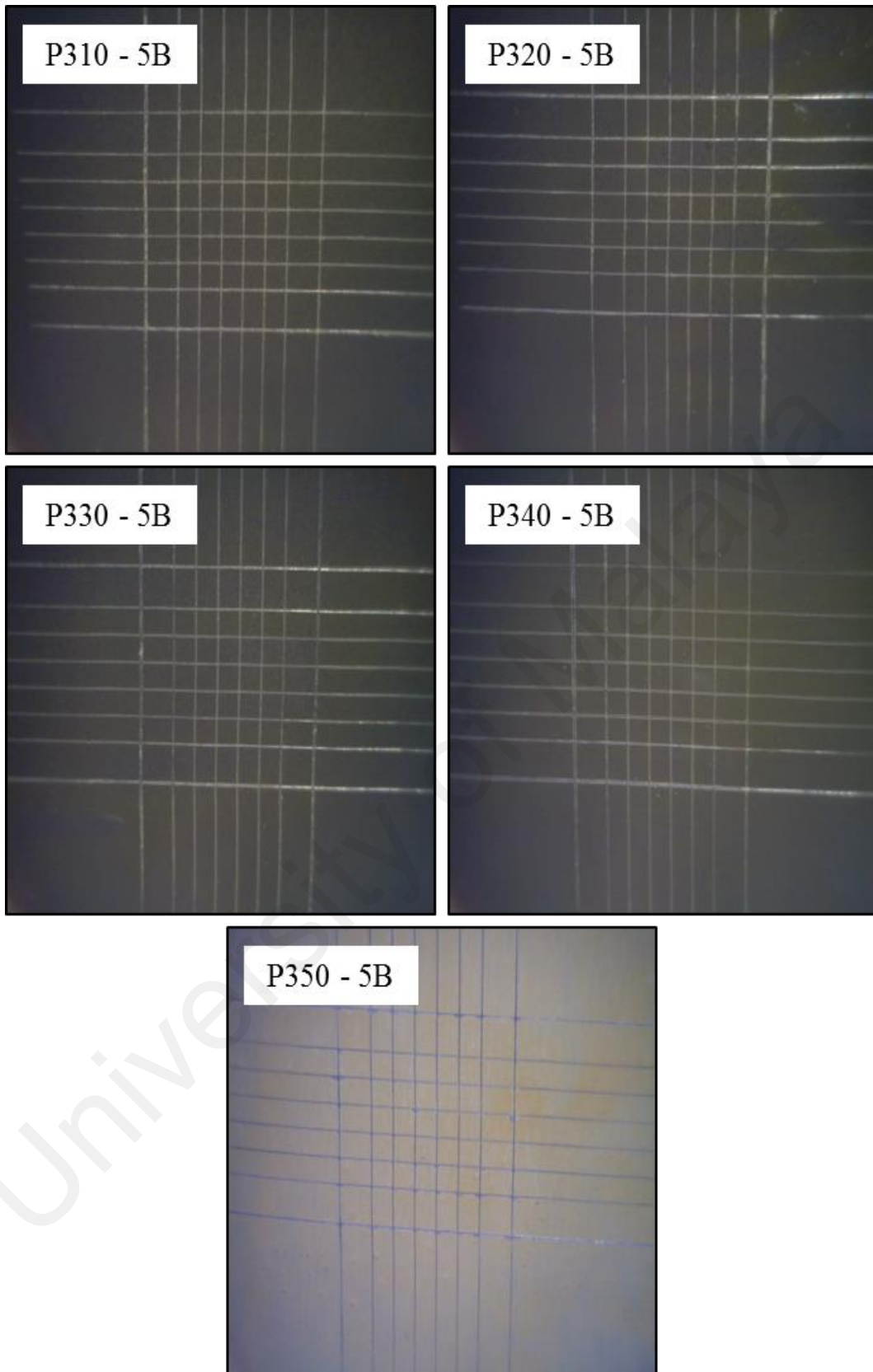


Figure 5.7: Cross Cut Images of P3 paint system

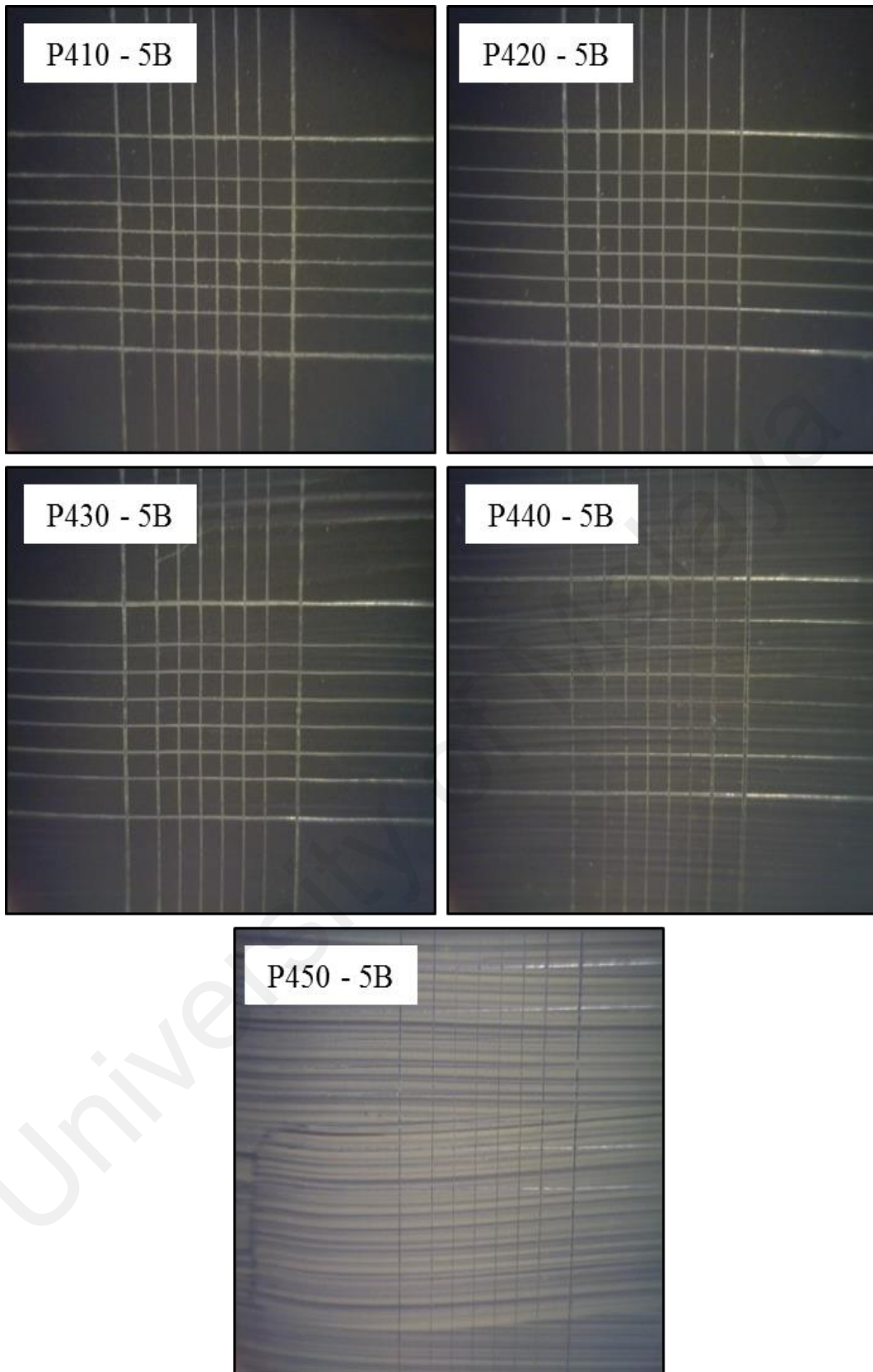


Figure 5.8: Cross Cut Images of P4 paint system

5.4 Glossiness and Accelerated UV Weathering Test

In this investigation, paint glossiness for P1, P2, P3 and P4 before and after exposure to accelerated UV weathering test was analyzed for both at 0 hour (0 h) and 720 hours (720 h) exposure. The experiment is subjected to ASTM D4587 standard with cycle No.4 for general metal coating. The cycle used was 8 hours UV exposure at (60.0 ± 2.5) °C followed by 4 hours condensation at (50.0 ± 2.5) °C at dark period repeatedly for 720 h. The overall performance of the coating system and its appearance were investigated.

Figures 5.9 - 5.13 shows the surface appearance of the samples that have been coated with all P1 paint system at 0 h and 720 h of the exposure under accelerated UV weathering chamber. While, Figure 5.14 shows the attached glossiness results of the P1 paint system for the same duration of exposure. From the weathering results of the P110 and P120 paint system that illustrated in Figure 5.9 and 5.10 respectively show the degradation due to the UV weathering cycle for 720 h. A lower degree of the degradation was observed for pigment volume concentration (PVC) equal to 30 % and 40 %. However, this durability of the paint system did not record to the P150 paint system.

On the other hand, Figure 5.14 shows the glossiness results of all prepared P1 paint system at 0 h and after 720 h of UV weathering exposure. There is no significant change were recorded to the glossiness values after 720 h of exposure when 30-40 % PVC of TiO₂ pigment was used. This could be attributed to the vital role of the critical pigment volume concentration (CPVC) value in enhancing the barrier properties via fill the pores and zigzagging the diffusion pathways against the penetrating of the water and oxygen molecules as well as the corrosive agents and the corrosion products toward the metal-paint interface (Matin et al., 2015; Shi et al., 2009). When the PVC of TiO₂

increased to 40 %, the coating maintained high glossiness value equal to 92 GU at 0 h and 80 GU after the exposure respectively.

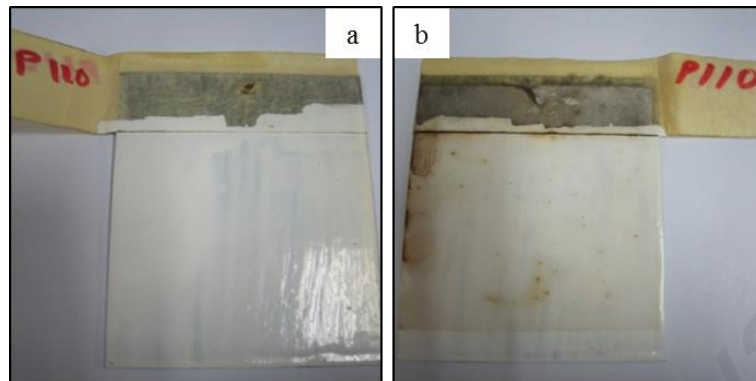


Figure 5.9: Image of P110 paint system a) 0 h and b) 720 h after exposure to accelerated UV weathering test

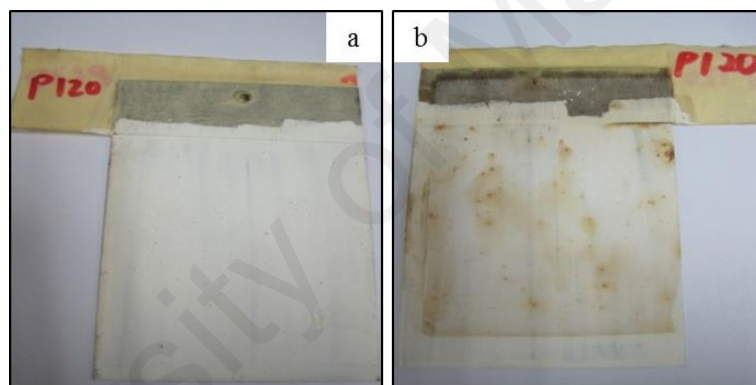


Figure 5.10: Image of P120 paint system a) 0 h and b) 720 h after exposure to accelerated UV weathering test

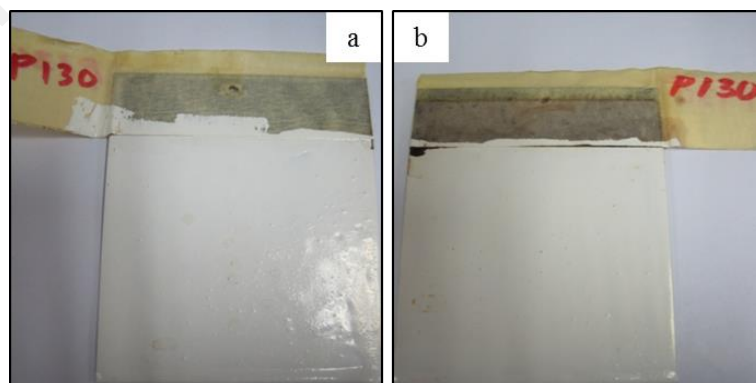


Figure 5.11: Image of P130 paint system a) 0 h and b) 720 h after exposure to accelerated UV weathering test

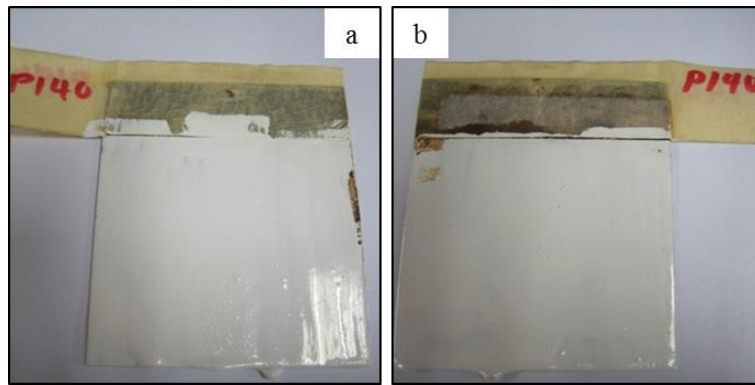


Figure 5.12: Image of P140 paint system a) 0 h and b) 720 h after exposure to accelerated UV weathering test

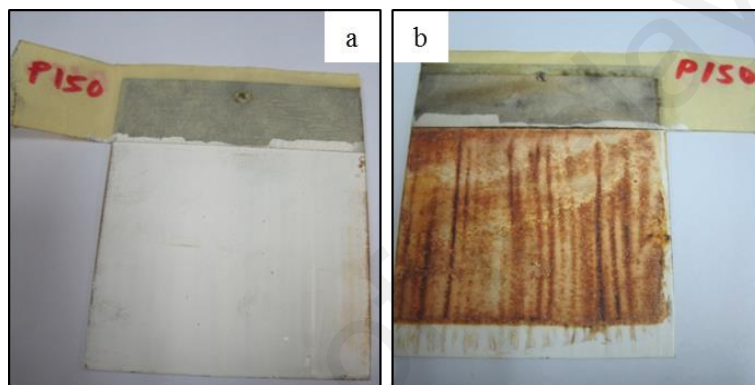


Figure 5.13: Image of P150 paint system a) 0 h and b) 720 h after exposure to accelerated UV weathering test

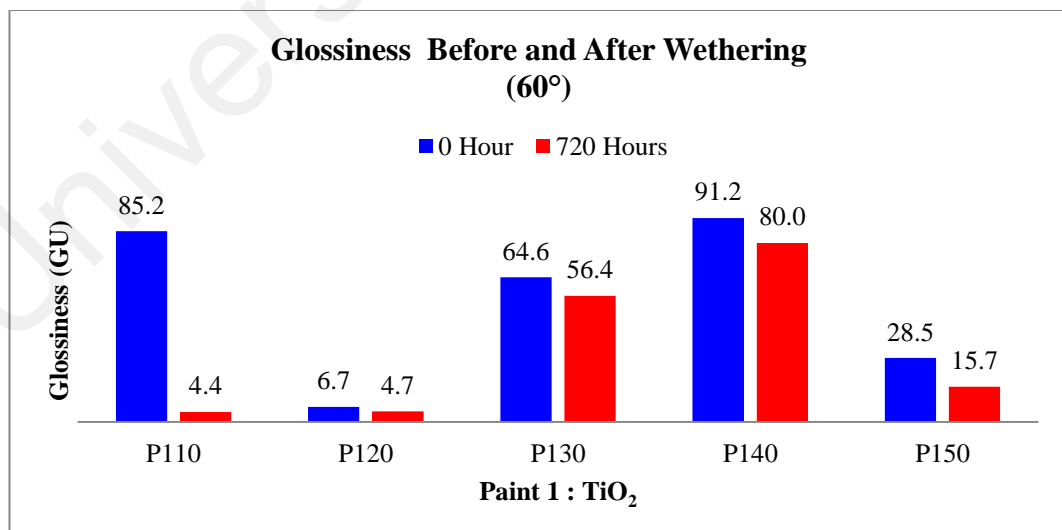


Figure 5.14: Glossiness test results of P1 paint system at 0 h and 720 h after exposure to accelerated UV weathering test

Substrates coated with all P2 paint system containing Silitin Z 86 were subjected to accelerated UV weathering test was illustrated in Figures 5.15 - 5.19. The glossiness reading of these respective surfaces was revealed in Figure 5.20. The surfaces of the coated panels demonstrated a poor resistance against the weathering conditions where blisters appeared on the paint surface after 720 h of degradation. The 2002 work of X.F. Yang et al., explained the effect of the wet and dry cyclic weathering chamber, producing blisters with dimensional in the range of micrometre on the coating surface. X.F. Yang et al., also reported that as the temperature becomes high and the exposure to the wet medium becomes longer, the developed blisters would be larger. Meanwhile, Figure 5.20 shows that all the surfaces with P2 paint system depicts a decreasing in the glossiness value after the 720 h of exposure. Such observation is due to the effect of the weathering conditions in forming blisters which in turn lead to increasing the surface roughness. This idea could be supported by the work that has been carried out by M. Yonehara et al., (2004) where the relation between the surface roughness and the glossiness have been studied and came out with the result that increasing the surface roughness leads to decreasing in the surface glossiness.

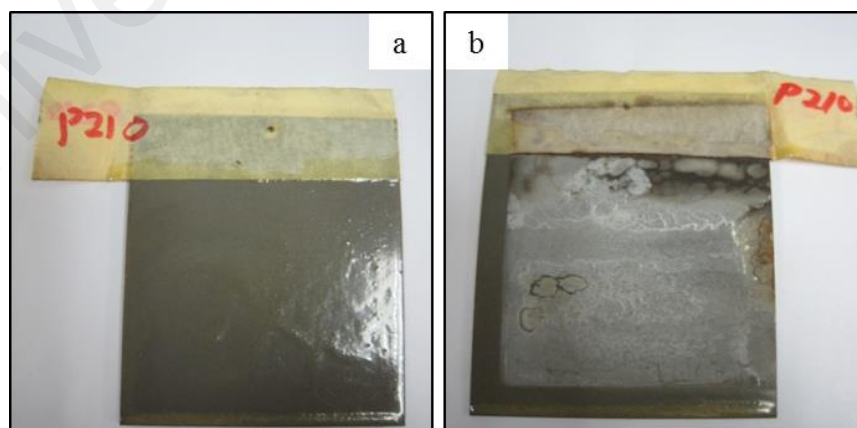


Figure 5.15: Image of P210 paint system a) 0 h and b) 720 h after exposure to accelerated UV weathering test

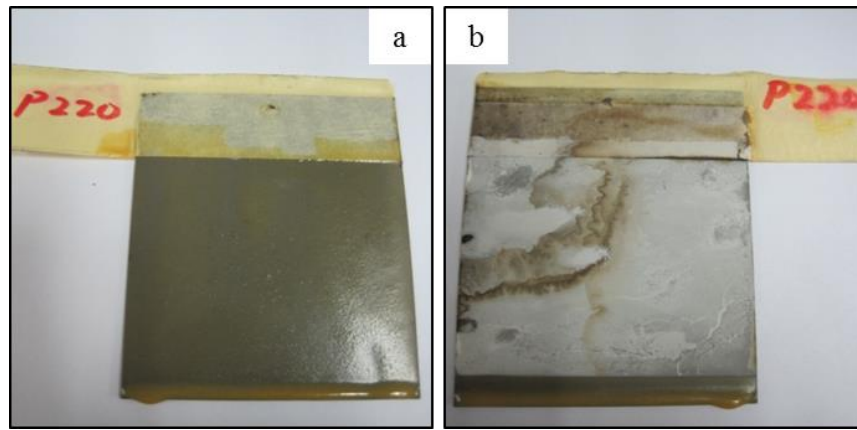


Figure 5.16: Image of P220 paint system a) 0 h and b) 720 h after exposure to accelerated UV weathering test

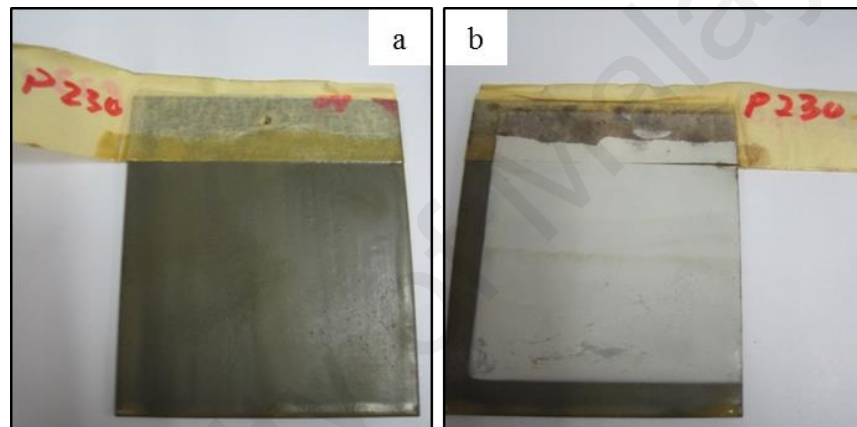


Figure 5.17: Image of P230 paint system a) 0 h and b) 720 h after exposure to accelerated UV weathering test

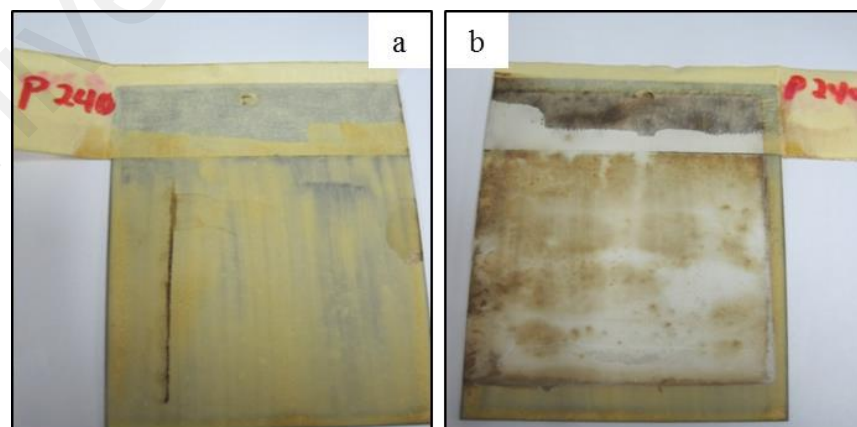


Figure 5.18: Image of P240 paint system a) 0 h and b) 720 h after exposure to accelerated UV weathering test

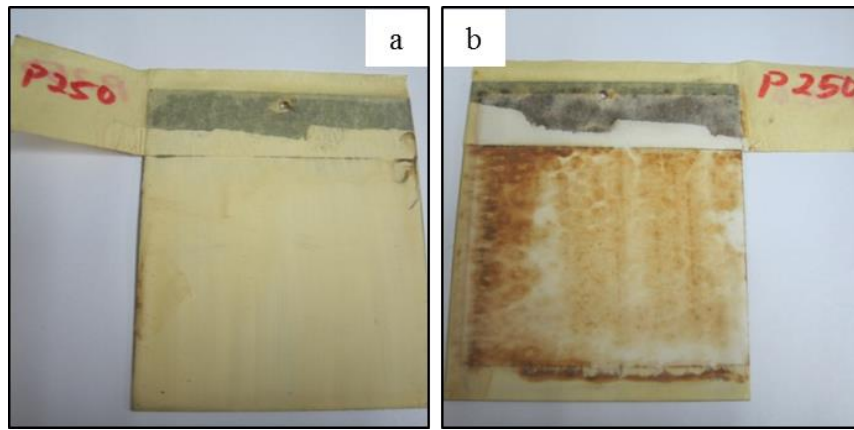


Figure 5.19: Image of P250 paint system a) 0 h and b) 720 h after exposure to accelerated UV weathering test

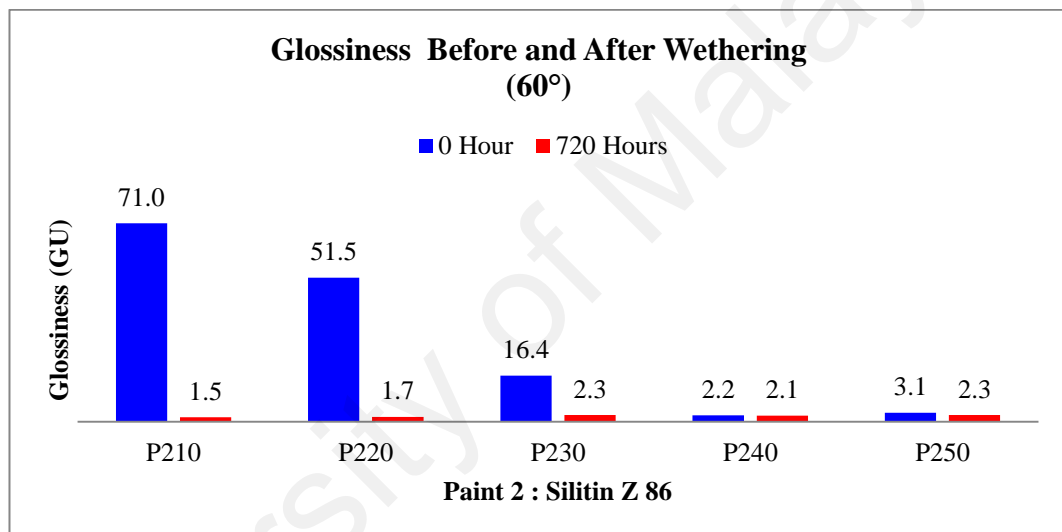


Figure 5.20: Glossiness test results of P2 paint system at 0 h and 720 h after exposure to accelerated UV weathering test

P3 paint systems with various PVC content subjected to accelerated UV weathering test were shown Figures 5.21 - 5.25. While Figure 5.26 shows the attached glossiness results of P3 paint system. P320 observed to have slight gloss improvement at PVC 20 %. In general P3 paint system has a good glossiness up to PVC 30 %. Meanwhile P340 and P350 shows poor performances in both weathering and glossiness test.

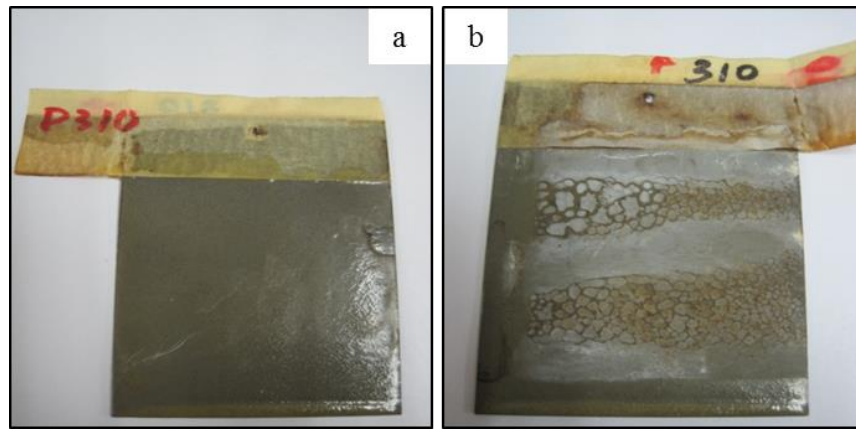


Figure 5.21: Image of P310 paint system a) 0 h and b) 720 h after exposure to accelerated UV weathering test

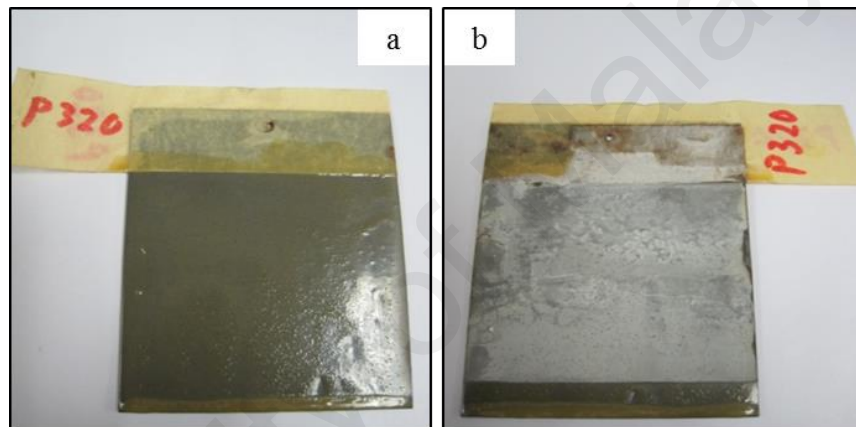


Figure 5.22: Image of P320 paint system a) 0 h and b) 720 h after exposure to accelerated UV weathering test

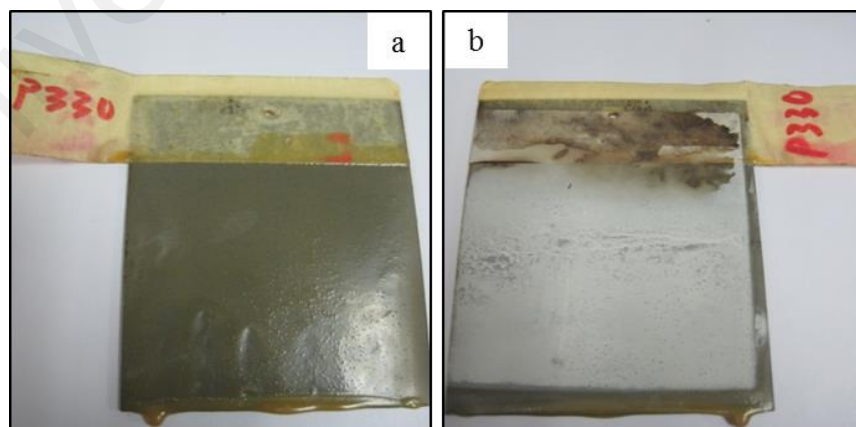


Figure 5.23: Image of P330 paint system a) 0 h and b) 720 h after exposure to accelerated UV weathering test

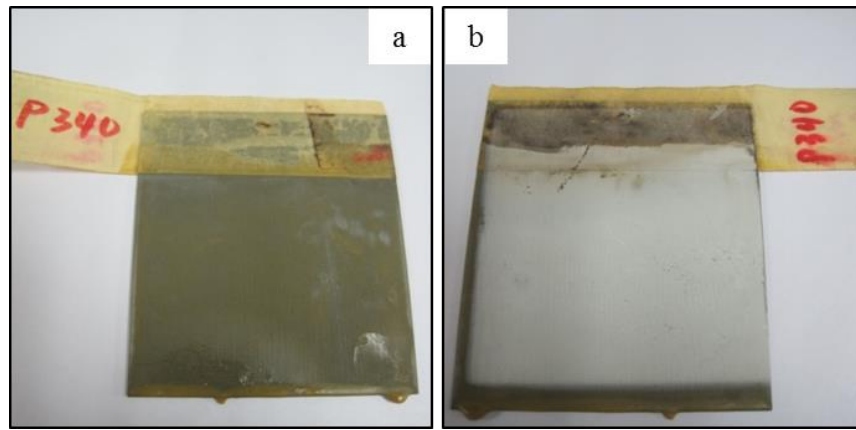


Figure 5.24: Image of P340 paint system a) 0 h and b) 720 h after exposure to accelerated UV weathering test

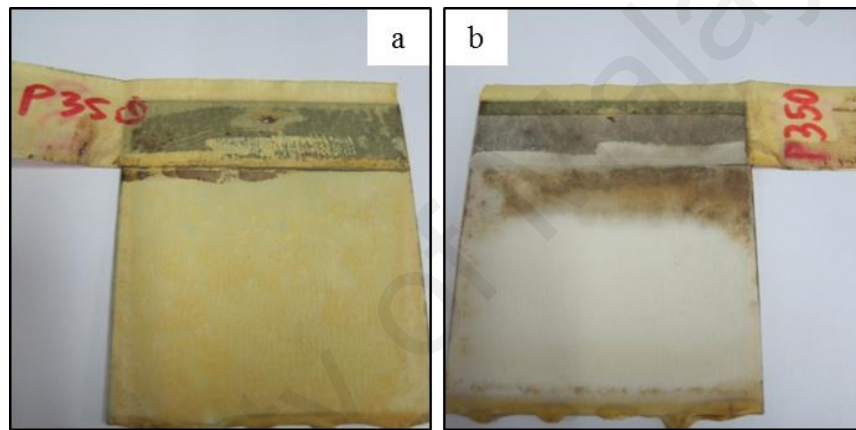


Figure 5.25: Image of P350 paint system a) 0 h and b) 720 h after exposure to accelerated UV weathering test

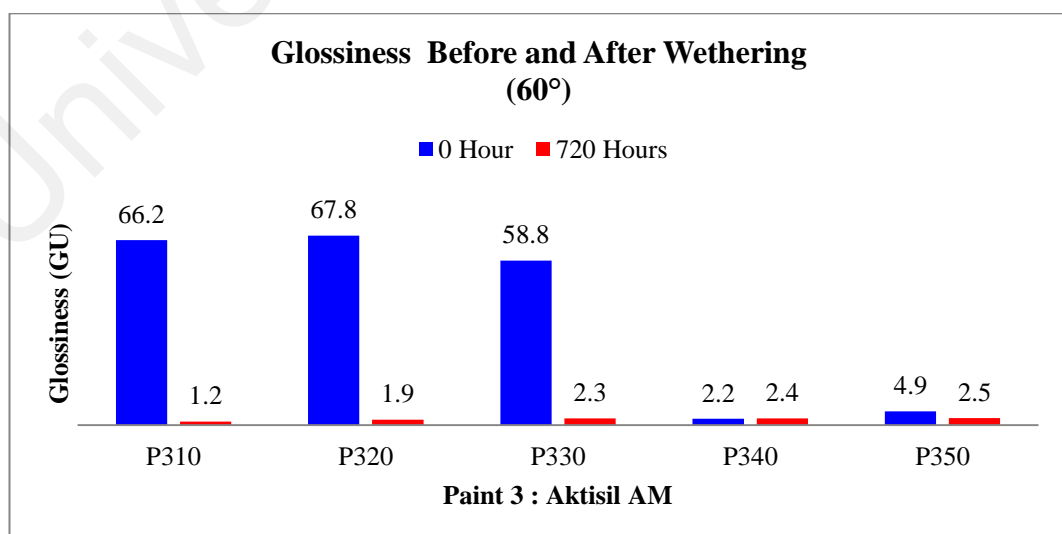


Figure 5.26: Glossiness test results of P3 paint system at 0 h and 720 h after exposure to accelerated UV weathering test

Figures 5.27 - 5.31 represent the accelerated UV weathering test results of P4 paint system and Figure 5.32 illustrates the glossiness results of P4 paint systems. P4 paint system observed to have average glossiness at PVC 10 % and 20 %. Meanwhile when PVC is above 20 %, shows poor performances in both weathering and glossiness test. Therefore, only P410 paint system may have good anti-corrosion properties based on general observation on both properties. The results of P2, P3 and P4 paint systems reflect the similar performance. These paint systems degraded badly PVC 30 % and above, after been subjected to 720 h of UV weathering conditions and the corresponding glossiness demonstrated a significant decrease after the exposure. This correlates the inorganic pigments used to prepare P2, P3 and P4 have similar contents of modified SiO₂ mixture.

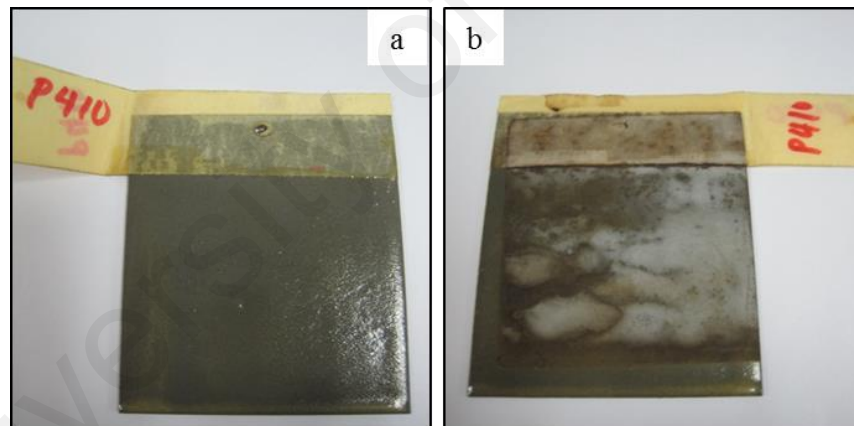


Figure 5.27: Image of P410 paint system a) 0 h and b) 720 h after exposure to accelerated UV weathering test

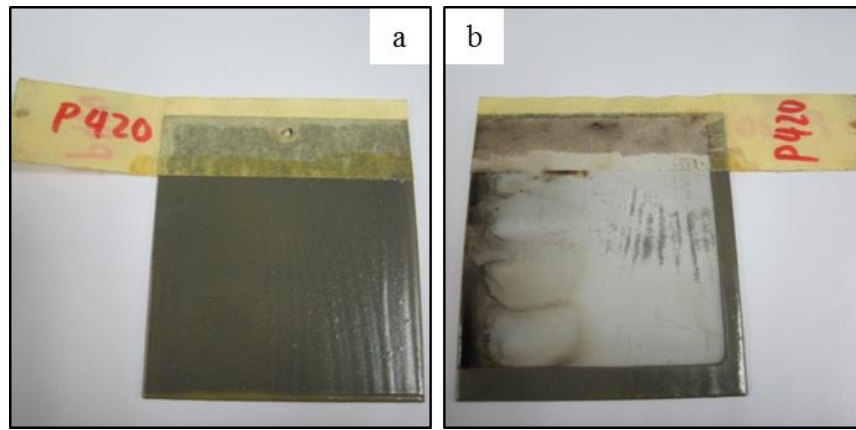


Figure 5.28: Image of P420 paint system a) 0 h and b) 720 h after exposure to accelerated UV weathering test

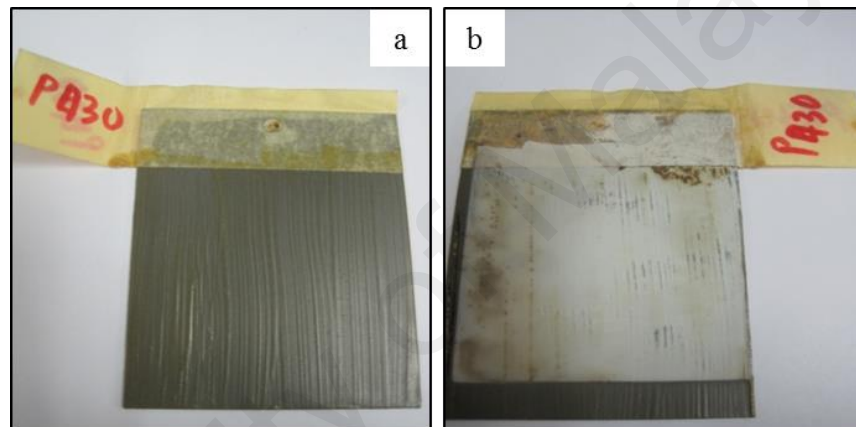


Figure 5.29: Image of P430 paint system a) 0 h and b) 720 h after exposure to accelerated UV weathering test

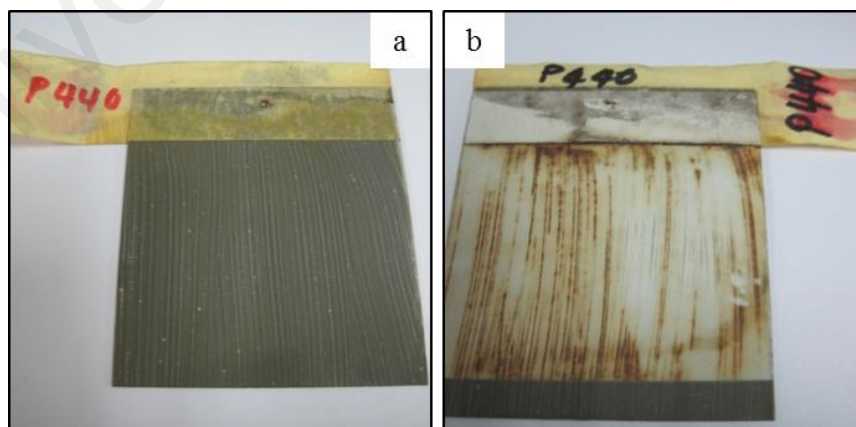


Figure 5.30: Image of P440 paint system a) 0 h and b) 720 h after exposure to accelerated UV weathering test

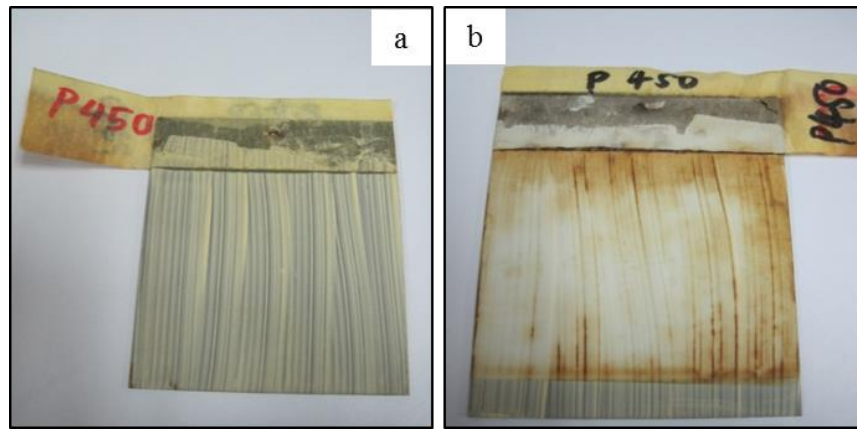


Figure 5.31: Image of P450 paint system a) 0 h and b) 720 h after exposure to accelerated UV weathering test

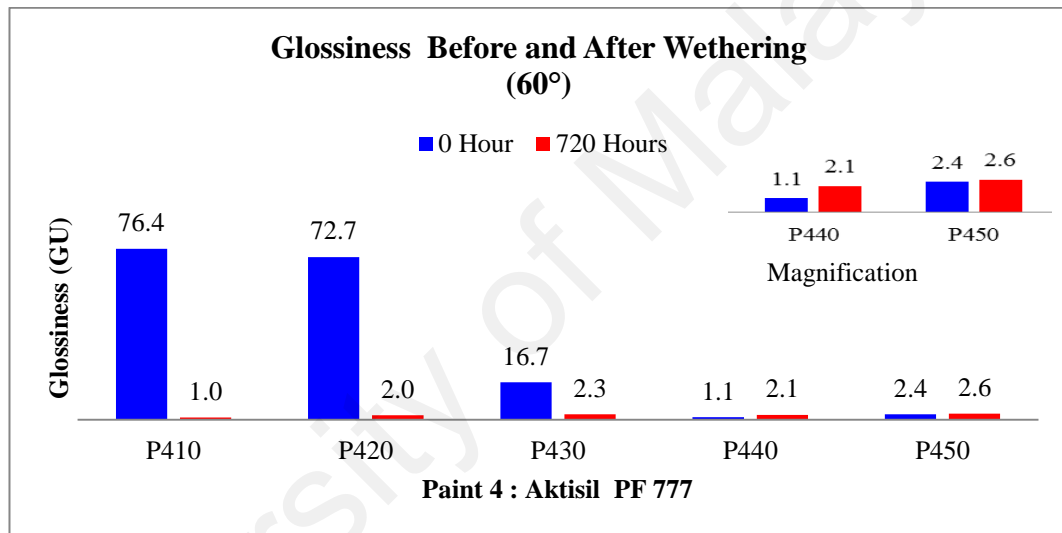


Figure 5.32: Glossiness test results of P4 paint system at 0 h and 720 h after exposure to accelerated UV weathering test

5.5 Summary

This chapter presents the results from physical and mechanical studies of the Acrylic-Epoxy four paint systems formulated using the best performing blending ratio consisting of 10 wt% Epoxy in 90 wt% Acrylic resin (90A10E). The effect of the pigment volume concentration (PVC) ratio to the critical pigment volume concentration (CPVC) on the corrosion resistance properties of P1, P2, P3 and P4 paint system has been investigated. The dry film thickness of the paint systems was found to be in the average range of 40-80 μm . It was observed from the P1, P2 and P3 paint system PVC plots, that these paint systems had good dry film thickness as 90A10E binder system. Cross hatch images reveal that there were no significant changes observed after the addition of the inorganic pigments on the adhesion properties of the paint film. All paint system has shown the same good adhesion properties of the reinforced binder with class 5B ranking.

From the accelerated weathering test results of the paint systems, it was observed that the surfaces of panels were subjected to the major degradation due to the UV weathering exposure. However, P130, P140, P310, P320 and P330 paint systems demonstrated the highest UV weathering resistance and good glossiness results. It is may be a sign on the durability of these systems to withstand the various aggressive environmental conditions. The results of P2, P3 and P4 paint systems reflect the overall similar performance. These paint systems degraded badly at 30 % and above PVC content after subjected to 720 h of accelerated UV weathering conditions and the corresponding glossiness demonstrated a significant decrease after the exposure. This correlates the usage of similar contents of modified SiO_2 mixture inorganic pigments in P2, P3 and P4 paint systems.

CHAPTER 6: RESULTS AND DISCUSSION ON PAINT SYSTEM

THERMAL AND STRUCTURAL

6.1 Introduction

In this investigation, the thermal and structural properties of the developed paint systems as well as determining the changes that took place due to presents of pigments in the prepared paint samples was obtained by using TGA, DSC, FTIR AND SEM-EDAX techniques. AE binder hybrid system (90A10E) that performed well used as a guide in understanding thermal stability and degradation, level of cross-linking and surface morphology of developed paint systems (Rau et al., 2013). With pigment volume concentration (PVC) ranging from 10 % to 50 % used with four types of the inorganic pigments, the corresponding developed paint systems namely P1 with TiO₂, P2 with Silitin Z 86, P3 with Aktisil AM and P4 with Aktisil PF 777 were investigated.

6.2 Thermogravimetric Analysis

Thermogravimetric analysis (TGA) has been used in this study in order to investigate the effect of temperature changes in the mass of the samples made of hybrid binder and paint systems. With a temperature range from the ambient up to 800 °C, reliable information about the polymer degradation temperature, residual solvent levels, decomposition temperature as well as the residue value for all prepared samples have been obtained. Chew et al., (2000), Zhu et al., (2001) and so many other researchers have used the TGA technique to determine the thermal stability and the thermal degradation of the coating and paint systems that mainly consist of a polymeric matrix with one or more of organic and inorganic components.

In this study, the obtained thermographs from developed P1, P2, P3 and P4 paint systems were used to study the best thermal stability of the inorganic pigment and its effect on PVC concentration within the hybrid acrylic-epoxy polymeric matrix. TGA were carried out using a standard hardware and software integration options with TA Instruments Q500 thermal gravimetric analyzer and results were evaluated with TA Universal Analysis V4.7A software package. Standard Test Method for Compositional Analysis by Thermogravimetry (ASTM E1131) was used as guide. The measurements were carried out from 30 °C to 800 °C at a rate of heating equal to 20 °C/min under nitrogen gas flow rate of 60 ml/min and balance nitrogen gas flow rate of 40 mL/min. Samples with a mass range between 1 mg to 2 mg were used for TGA measurement.

Figure 6.1(a-e) shows thermographs of P1 paint systems with all PVC ranging from 10 % to 50 % of TiO₂ pigments. By comparing the TGA graphs of the hybrid binder coating systems as stipulated in Chapter 4, the TGA graphs of P1 systems clearly show that there is no new mass loss were observed after embedding the inorganic TiO₂ pigment within the acrylic-epoxy polymeric matrix. The result shows that the presence of TiO₂ leads the paint system to require a higher temperature and thermal energies for performing the same mass loss comparing with the 90A10E hybrid binder system (Figure 4.9h). Armelin et al., reported the same observation about the effect of the inorganic pigments on the thermal properties of the polymeric coatings and had attributed that enhancement in the thermal stability due to the present of high content of inorganic pigment (Armelin et al., 2007).

The left over thermally stable materials in the AE binder system was recorded approximately 2 % residue of the total weight (Rau et al., 2013). However when TiO₂ pigments was incorporated in the AE binder system, the left over thermal stable materials has been increased approximately up to 85 % residue in P150 system due to specific high thermal stability of TiO₂ pigment (Diebold, 2014).

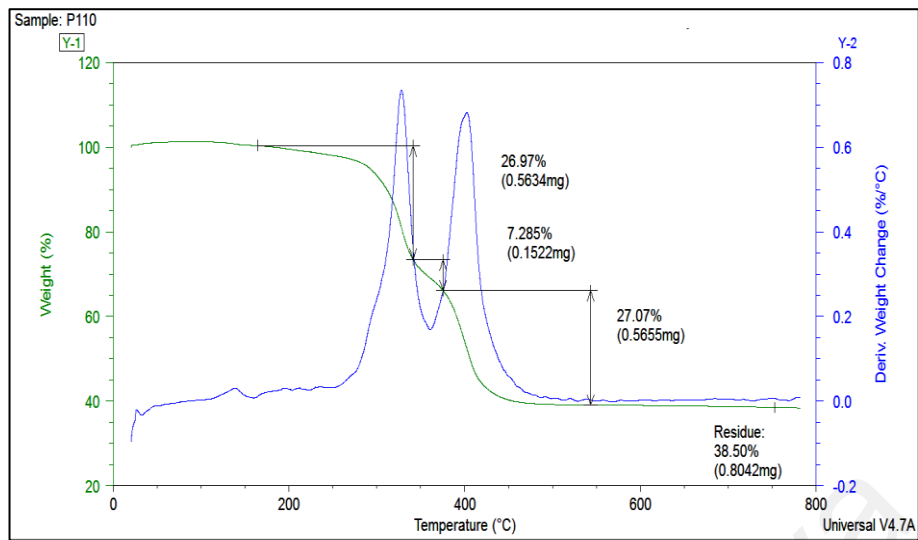


Figure 6.1a: TGA Thermogram of P110 paint system

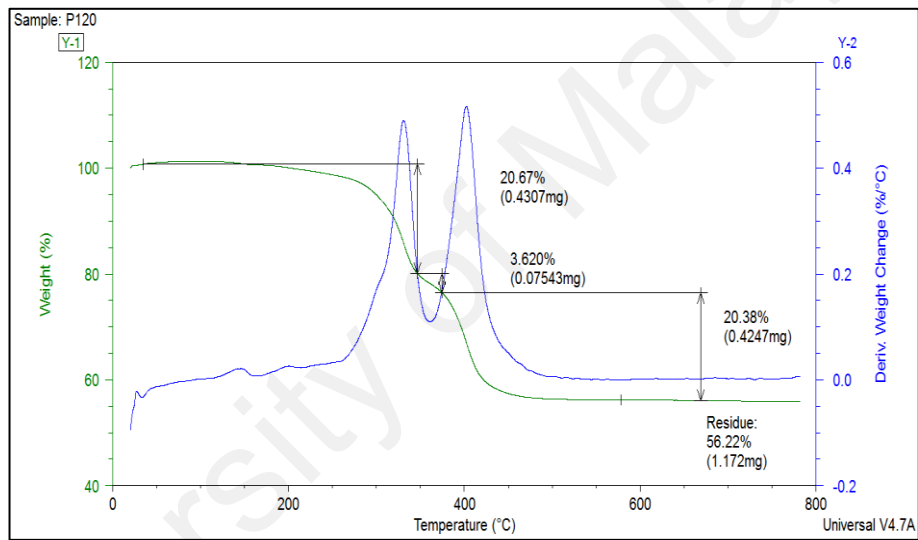


Figure 6.1b: TGA Thermogram of P120 paint system

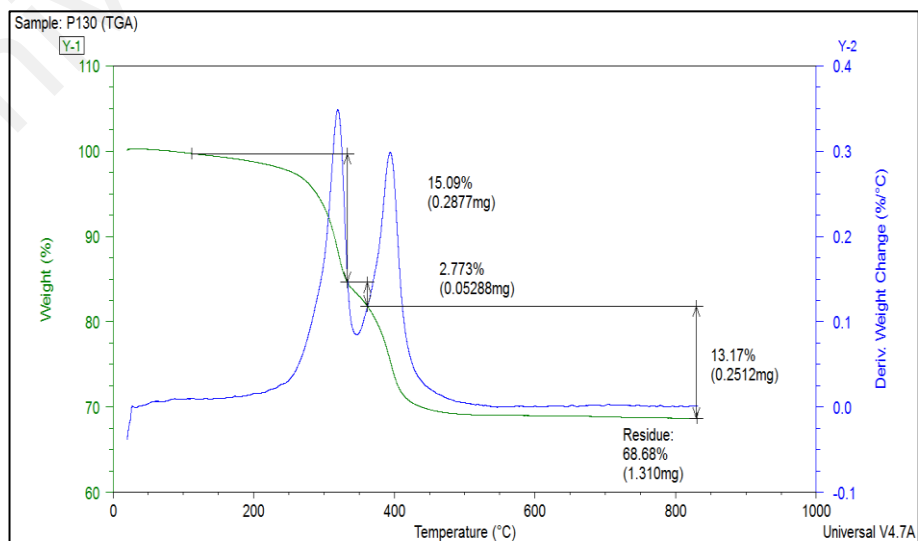


Figure 6.1c: TGA Thermogram of P130 paint system

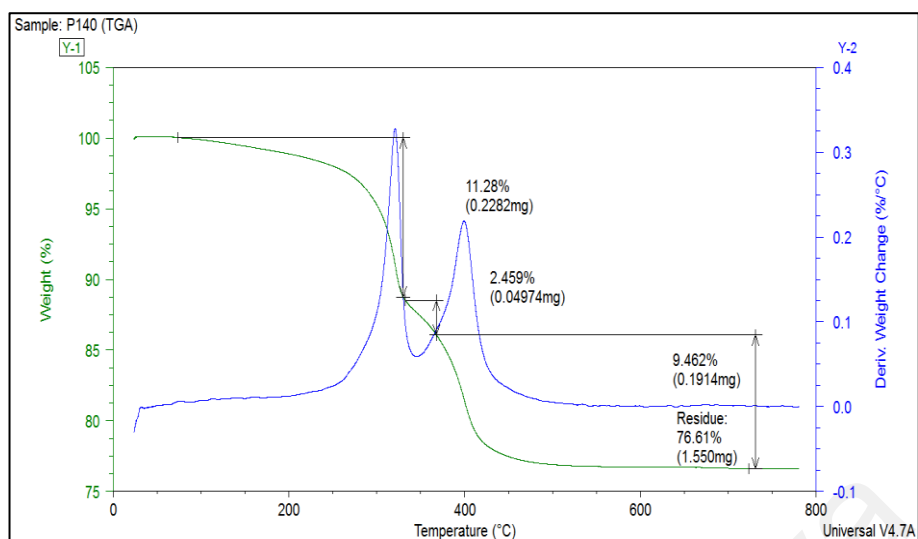


Figure 6.1d: TGA Thermogram of P140 paint system

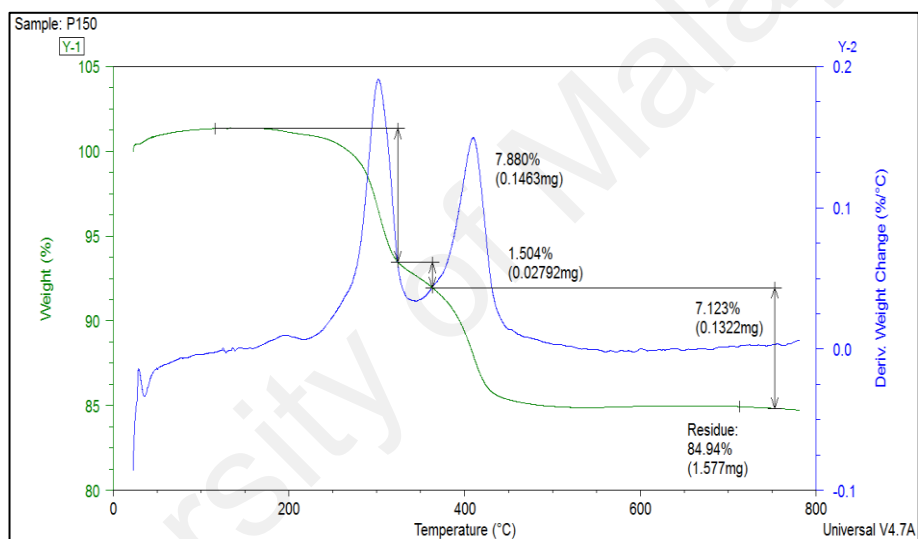


Figure 6.1e: TGA Thermogram of P150 paint system

In the regard of investigating the thermal stability of the P2 paint systems, the respective thermograph of all P2 prepared samples were illustrated in Figure 6.2(a-e). Meanwhile, the P2 systems demonstrated the same steps of mass loss process with slight shifting right toward more thermal stability.

However, there were no significant changes between the incorporation of TiO₂ pigments and Silitin Z 86 pigments. The most prominent change between P1 and P2 paint systems were recorded in the residue percentage value at all PVCs. Residue percentage of P1 system is observed always higher than P2 system. The reason of the

high residue value could be related to the thermal stability of the inorganic TiO₂ pigments withstanding higher temperatures (Diebold, 2014). The differences became greater as the PVC percentage become higher. Residue of 84.9 % was recorded to P150 system against 69.7 % using P250 system. This comparison can be seen in Table 6.1 and Table 6.2.

Table 6.1: The residue values of P1 paint system

Paint System	Residue (%)
P 110	38.5
P 120	56.2
P 130	68.7
P 140	76.6
P 150	84.9

Table 6.2: The residue values of P2 paint system

Paint System	Residue (%)
P 210	28.0
P 220	49.8
P 230	43.7
P 240	66.3
P 250	69.7

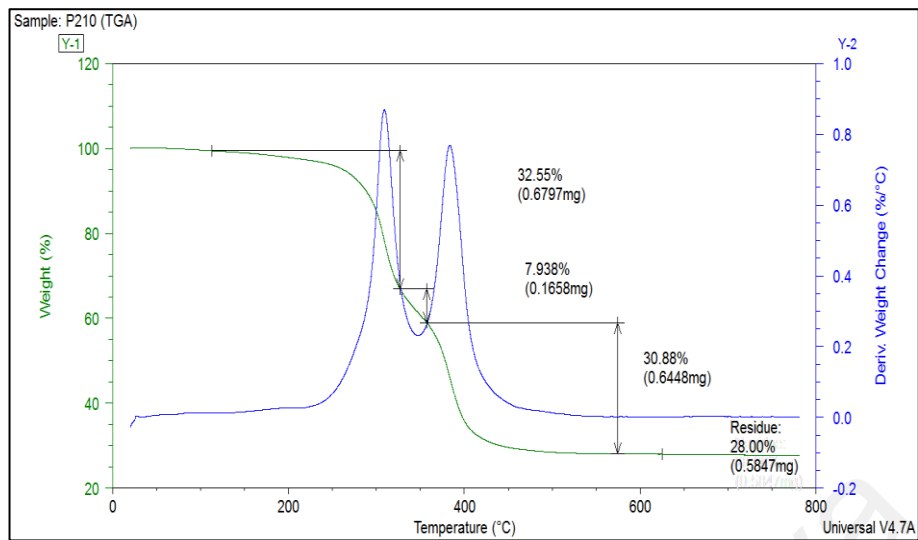


Figure 6.2a: TGA Thermogram of P210 paint system

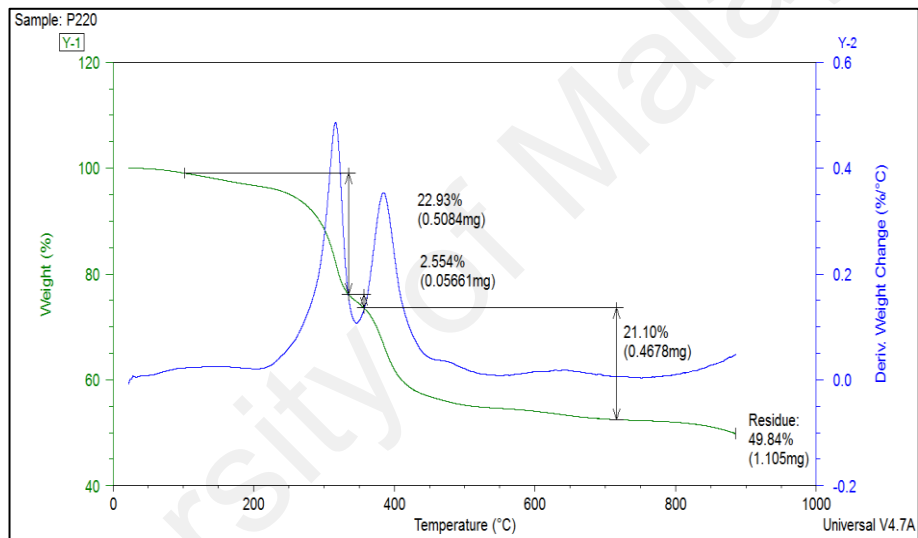


Figure 6.2b: TGA Thermogram of P220 paint system

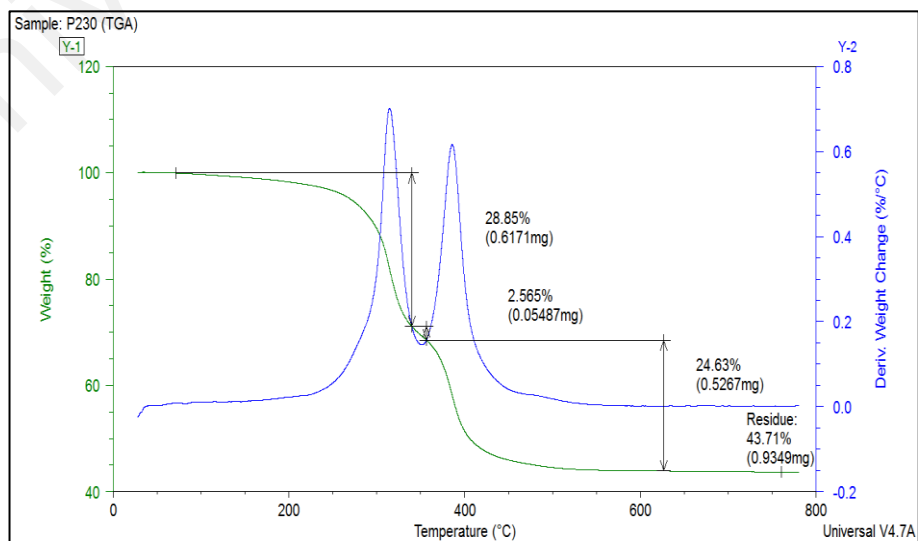


Figure 6.2c: TGA Thermogram of P230 paint system

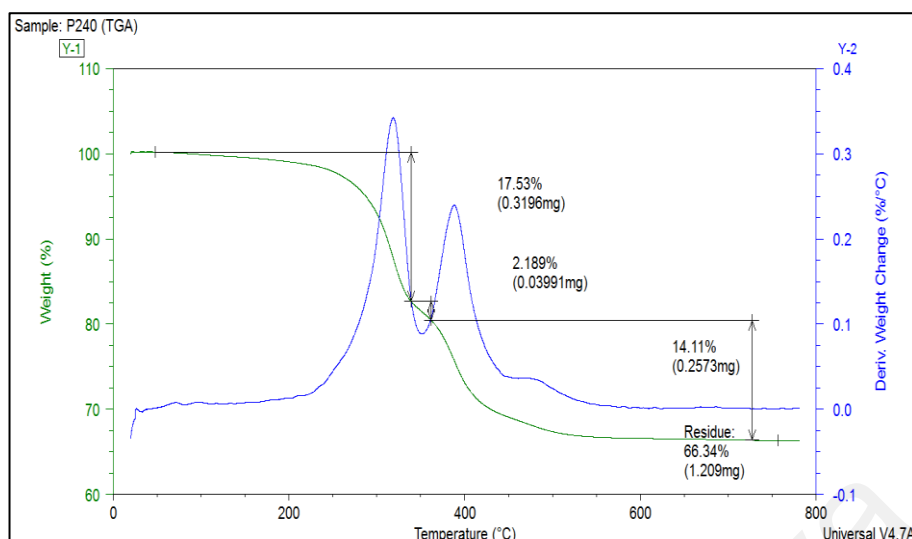


Figure 6.2d: TGA Thermogram of P240 paint system

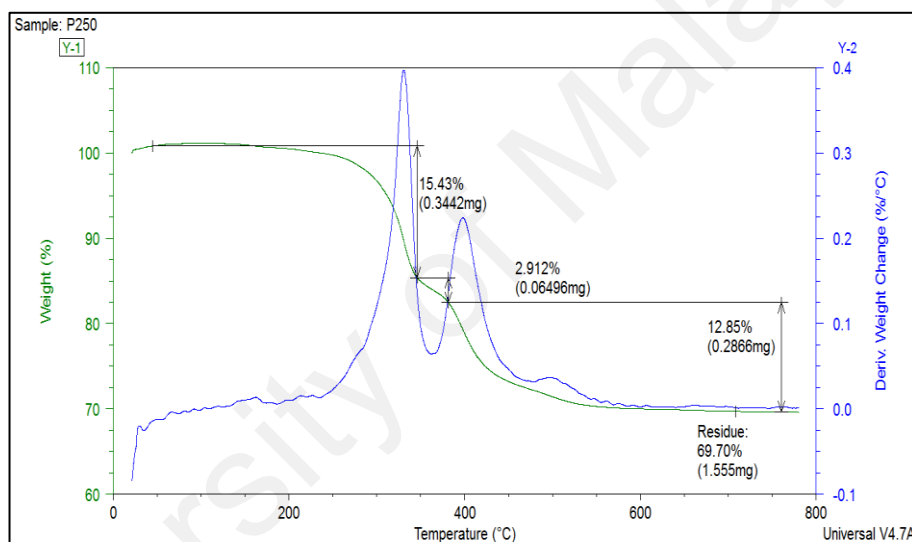


Figure 6.2e: TGA Thermogram of P250 paint system

The Figures 6.3(a-e) and 6.4(a-e) illustrates the thermogravimetric analysis results of P3 and P4 paint systems respectively. As mentioned above analyzing the TGA results of P1 and P2 systems, almost similar pattern seen in P3 and P4 system. It was observed that the addition of the inorganic pigments, namely Aktisil AM and Aktisil PF 777, paint systems did not show any significant changes in the thermal stability of the final dry paint films. Moreover, the degradation steps that were recorded for all P1, P2, P3 and P4 samples were matched with the steps that existed in the thermograph of the hybrid binder coating (90A10E).

This indicates that the best blending ratio for hybrid system was 90 wt% acrylic polyol resin with 10 wt% epoxy resin without any reinforcing pigments, which consider as an evidence of the ability of the paint system in facing high temperature up to 250 °C before showing any intention of the decomposition process. Ramesh et al., have reported the efficiency of the thermogravimetric analysis (TGA) to examine the dependency of the thermal degradation in terms of weight change which can be used to indicate the intact behavior of the developed paint system with high thermal stability (Ramesh et al., 2006).

At the end, one can conclude that the incorporation of inorganic pigments into the polymeric matrix is able to reduce the average total weight loss with residue values ranging from 23 % up to 85 % as the pigment volume concentration varied from 10 % to 50 %. The Tables 6.3 and Table 6.4 shows the corresponding residue values of P3 and P4 paint systems respectively. It is clear that all paint systems show an increase in residue when PVC concentration increased. These left over mass of thermal stable materials will be the pigments such as TiO₂ in P1 and SiO₂ modified mixture pigments in other paint systems. The P2, P3 and P4 have approximately matching residue percentage of 65 %. Where else P1 has 85 % residue due to 100 % of pigments were TiO₂. This enhances a higher temperatures with increased stability was recorded for the base polymeric binder system.

Table 6.3: The residue values of P3 paint system

Paint System	Residue (%)
P 310	23.7
P 320	38.6
P 330	51.2
P 340	63.1
P 350	69.4

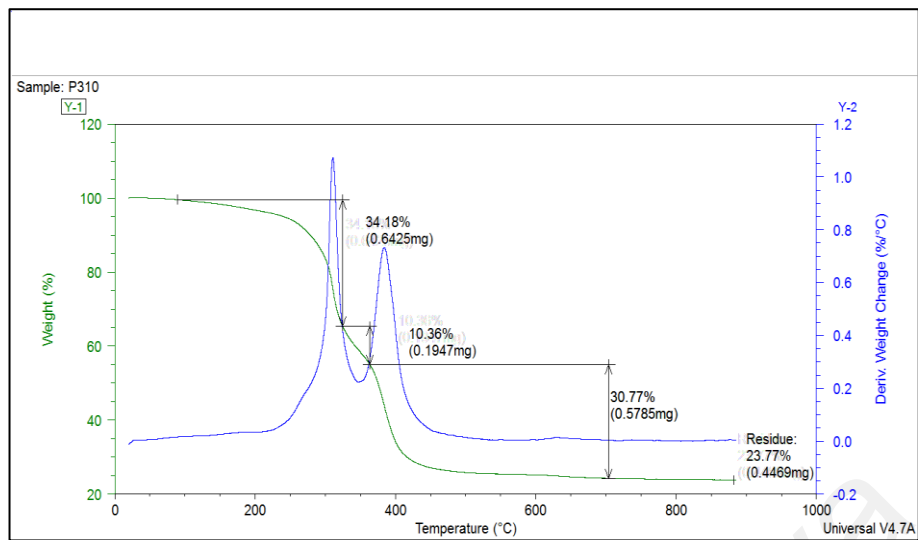


Figure 6.3a: TGA Thermogram of P310 paint system

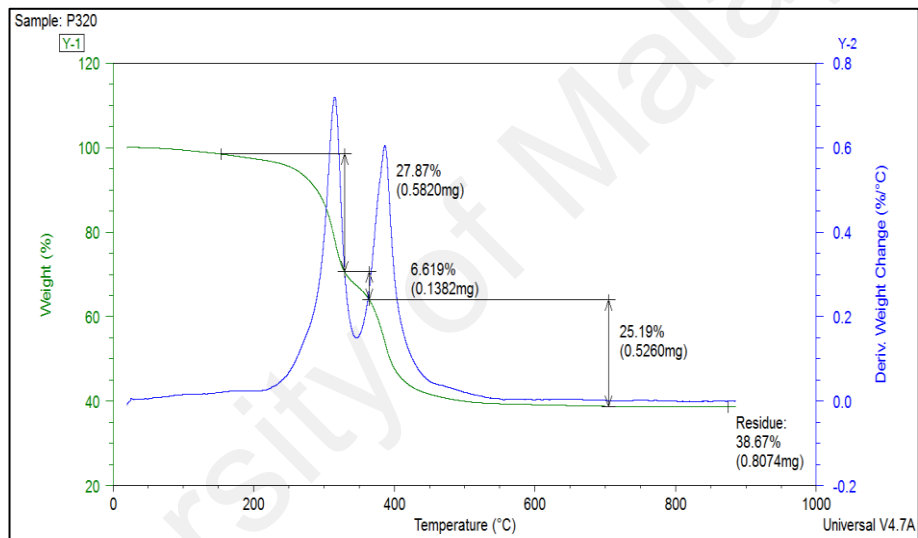


Figure 6.3b: TGA Thermogram of P320 paint system

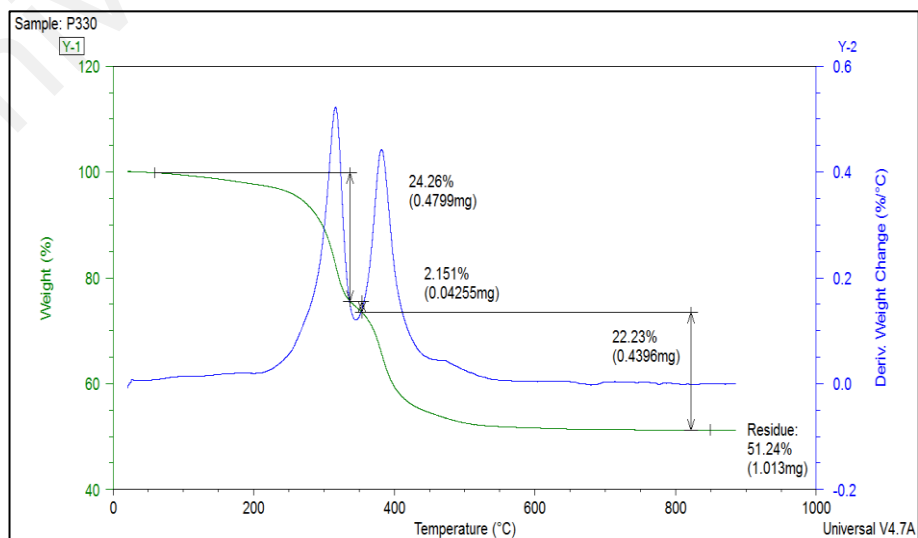


Figure 6.3c: TGA Thermogram of P330 paint system

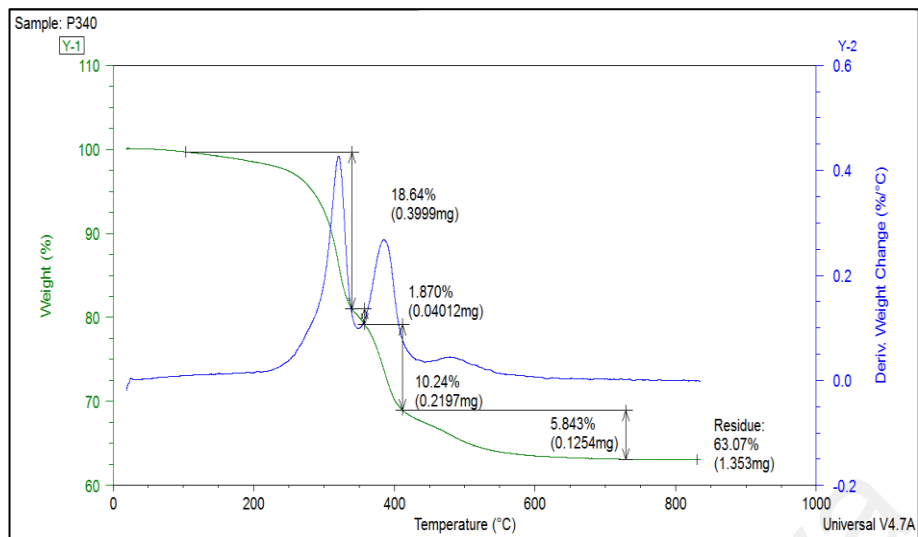


Figure 6.3d: TGA Thermogram of P340 paint system

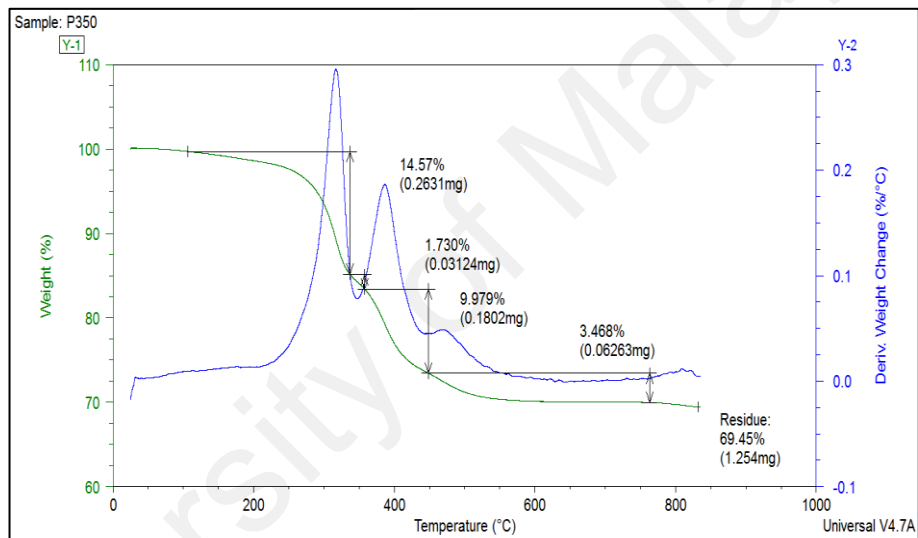


Figure 6.3e: TGA Thermogram of P350 paint system

Table 6.4: The residue values of P4 paint system

Paint System	Residue (%)
P 410	25.6
P 420	40.3
P 430	53.1
P 440	66.6
P 450	65.3

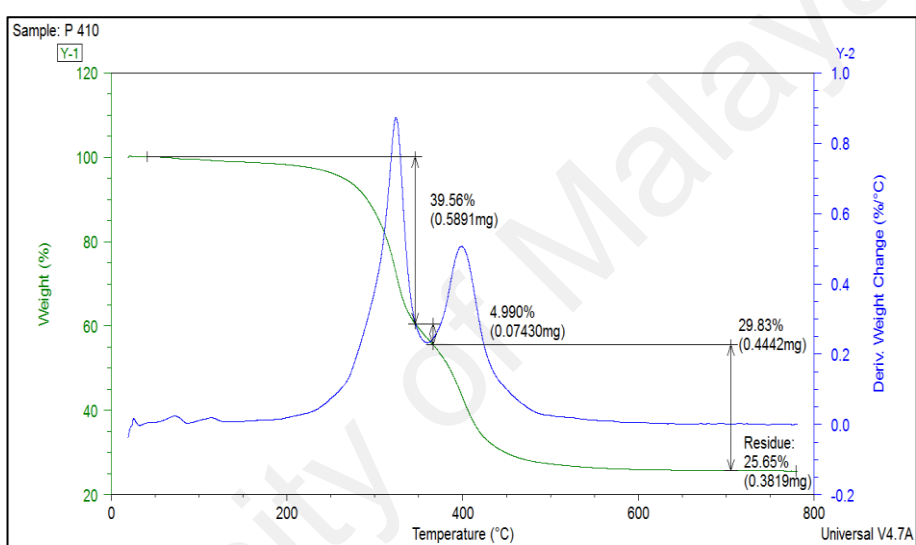


Figure 6.4a: TGA Thermogram of P410 paint system

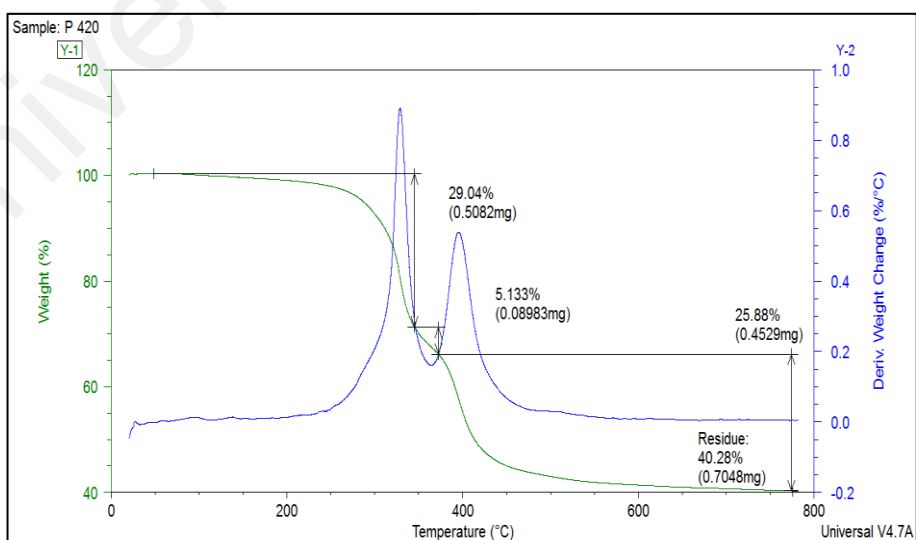


Figure 6.4b: TGA Thermogram of P420 paint system

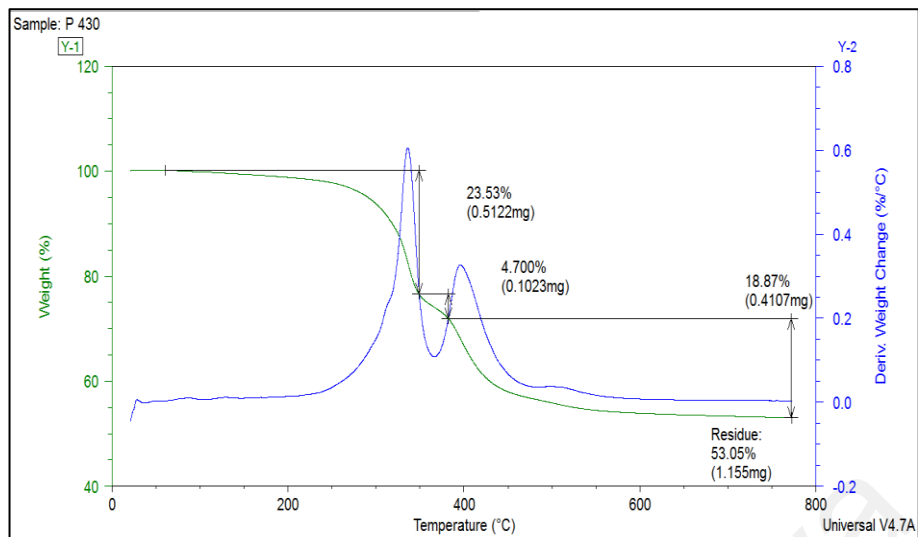


Figure 6.4c: TGA Thermogram of P430 paint system

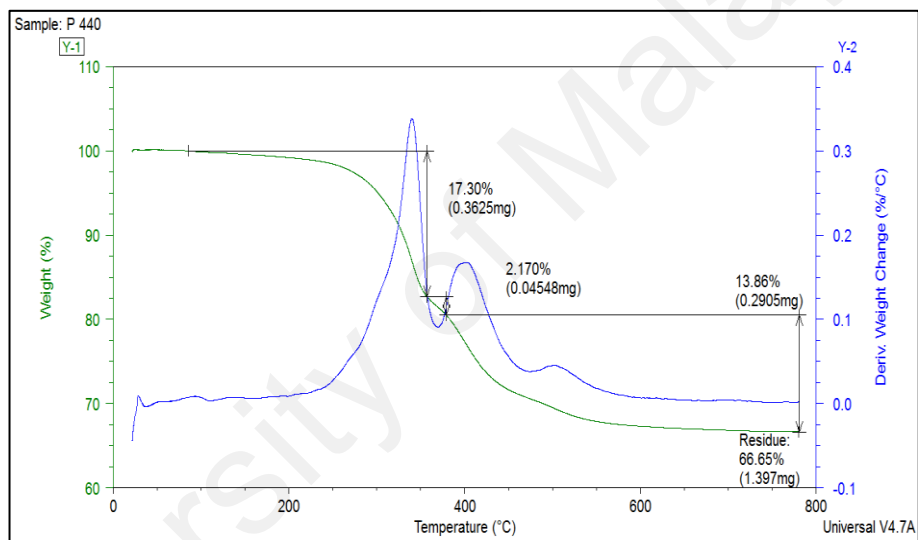


Figure 6.4d: TGA Thermogram of P440 paint system

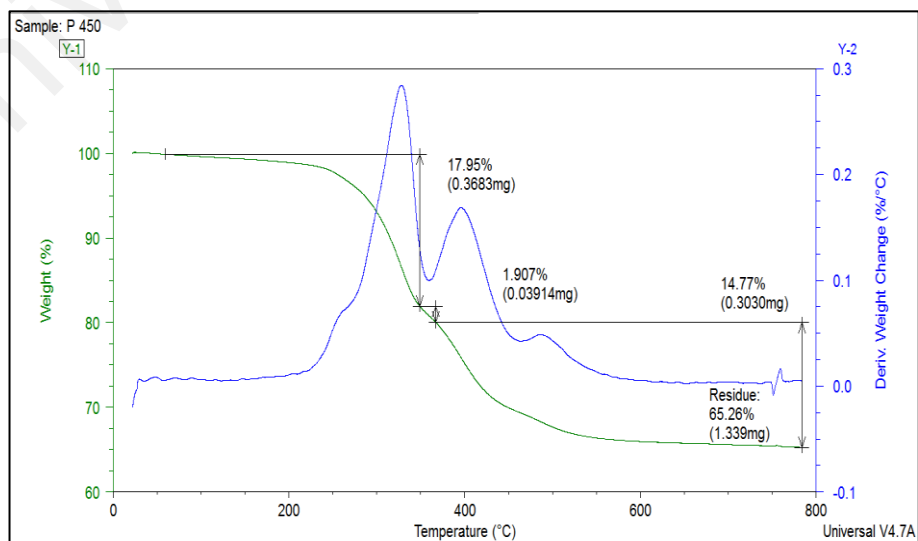


Figure 6.4e: TGA Thermogram of P450 paint system

6.3 Differential Scanning Calorimetry

DSC is a powerful tool for the characterization of polymer coatings given its high sensitivity and ease of use. Glass transition temperature (T_g) provides very important information in coating industries (Sharmin et al., 2004; Weldon, 2009). Therefore, T_g is widely accepted as a predominant factor in determining the physical and mechanical properties of a coating system and was adopted by many research in the last few decades in order to point out the state of the materials under investigation and its thermal behavior (Ramesh et al., 2006; Shen et al., 2015). T_g is defined as the temperature where the polymer changed from a hard, often brittle glass-like material into soft, rubber-like properties. It is useful as a guideline for low temperature flexibility and ambient temperature hard and soft points. T_g for thermoplastic copolymers and the plasticized system can be affected by the molecular interaction between components. The level of cross-linking in thermoset affects the magnitude of accompanying physical changes and the temperature range of the T_g .

Studying the thermal properties of the developed paint systems as well as determining the changes that took place due to absorbing heat energy by the prepared paint samples were obtained by using DSC technique. With pigment volume concentration (PVC) ranging from 10 % to 50 %, inorganic pigments combined paint systems were developed. Paint P1 with TiO_2 , P2 with Silitin Z 86, P3 with Aktisil AM and P4 with Aktisil PF 777 were tested by DSC analysis.

DSC studies were carried out for all P1 paint systems to determine the changes that occurred on the glass transition temperature (T_g) after the incorporation with TiO_2 pigments. The effect of TiO_2 pigments on the T_g of P1 paint systems was illustrated in Figure 6.5 while the values of the T_g of A100 (100 wt% acrylic), P100 (90A10E = 90

wt% acrylic and 10 wt% epoxy) and all P1 paint systems were tabulated in Table 6.5. In addition, the corresponding DSC thermograms were shown in Figure 6.6(a-e).

Table 6.5: The glass transition temperature of acrylic system, acrylic-epoxy binder system and P1 paint system

System	Glass transition temperature T_g (°C)
A 100	38
P 100	46
P 110	44
P 120	41
P 130	33
P 140	26
P 150	15

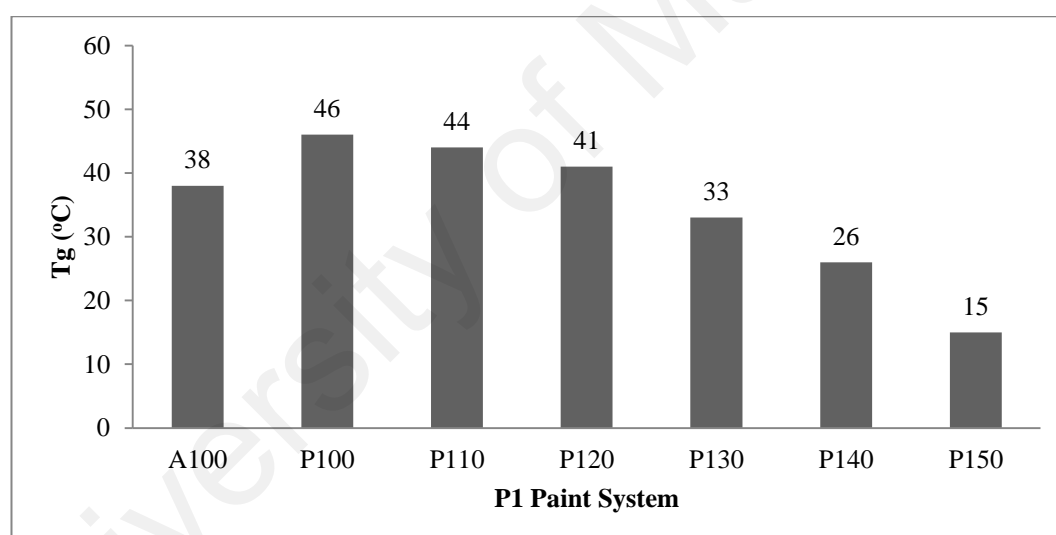


Figure 6.5: The influence of TiO_2 pigment on T_g value of P1 paint system

Rau et al., have reported in detail the reason of the increase of T_g value from 38 °C to 46 °C of the hybrid acrylic-epoxy system (Rau et al., 2013). This increase was attributed due to the homogeneous DGEBA crosslinking with the acrylic resin which in turn reduces the flexibility of the final product after the addition of the hardener. The DSC results of P1 paint systems (Figure 6.5) show decreasing trend in the T_g values as the pigment volume concentration increased. Embedding TiO_2 pigments within the hybrid polymeric matrix result in decreasing T_g values which can be attributed to the

increment in the free volume caused by the present of the inorganic pigments (Ramezanzadeh & Attar, 2011).

The weak interactions among the inorganic pigments and resin chains can be considered as one of the reasons behind the decrease of the T_g when reinforcing the hybrid polymeric matrix with TiO_2 pigment. This weakness in the mentioned interactions, may be due to the poor ability of the agglomerated pigments with increasing the PVC concentration to provide strong interactions within the coating matrix (Ramezanzadeh et al., 2011).

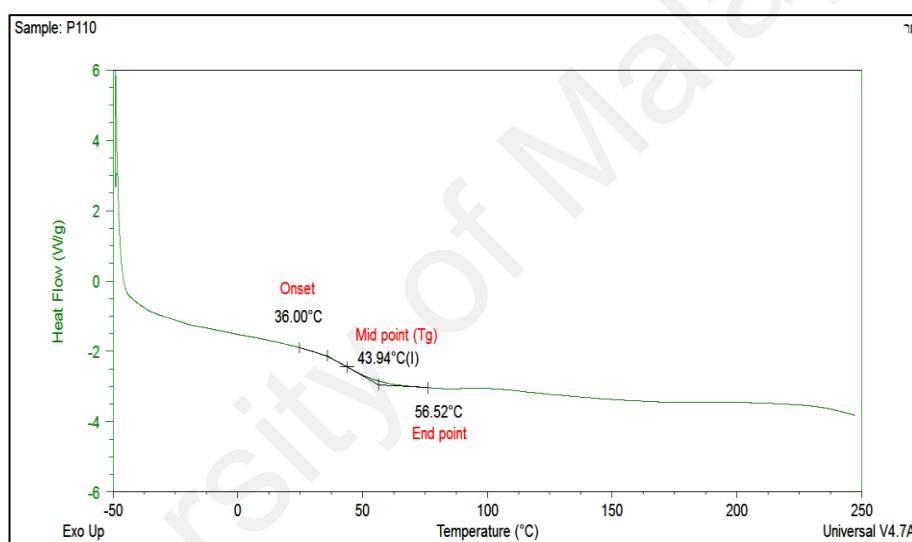


Figure 6.6a: DSC Thermogram of P110 paint system

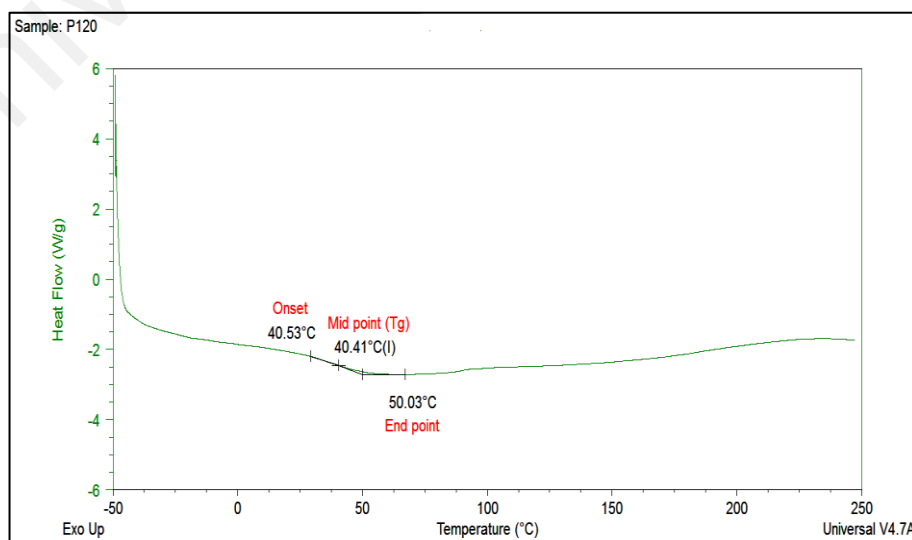


Figure 6.6b: DSC Thermogram of P120 paint system

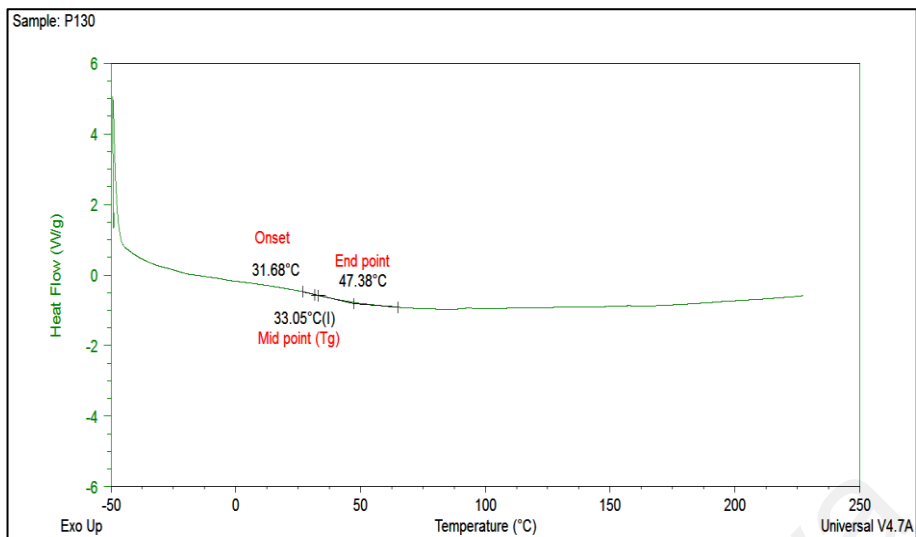


Figure 6.6c: DSC Thermogram of P130 paint system

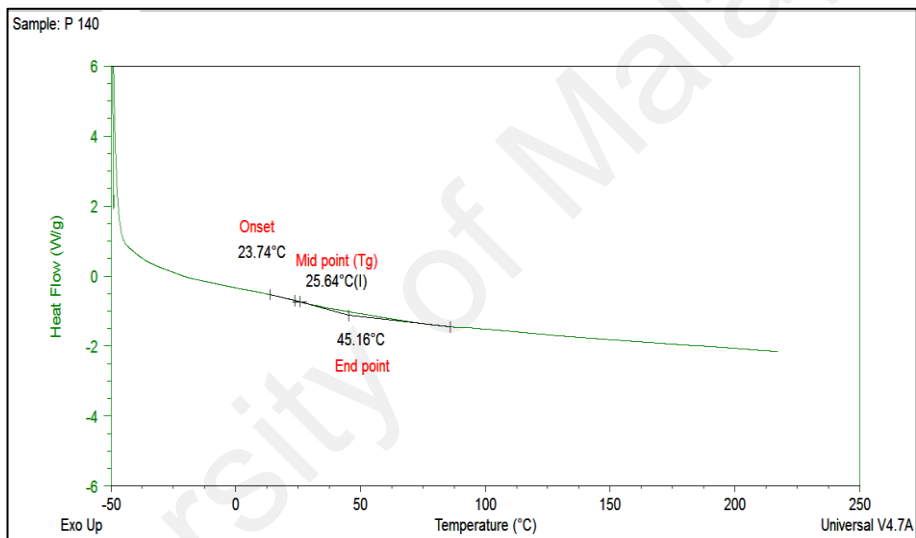


Figure 6.6d: DSC Thermogram of P140 paint system

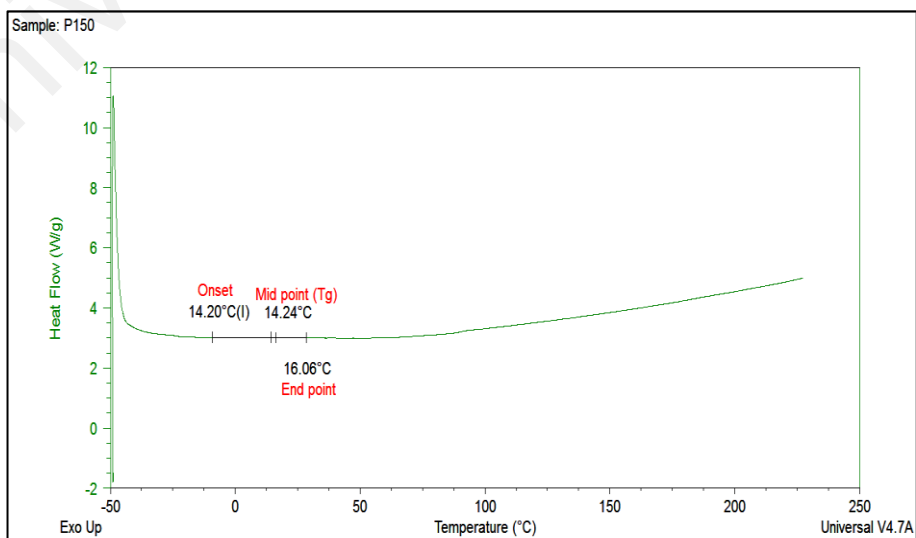


Figure 6.6e: DSC Thermogram of P150 paint system

On the other hand, investigating the influence of another type of pigments on the T_g value extent to all P2 paint systems as shown in Figure 6.7. Whereas, the values of the T_g of A100, P100 and all P2 paint systems were tabulated in Table 6.6. Furthermore, the DSC thermograms of the P2 paint system were illustrated in Figure 6.8(a-e).

Table 6.6: The glass transition temperature of acrylic system, acrylic-epoxy binder system and P2 paint system

System	Glass transition temperature T_g (°C)
A 100	38
P 100	46
P 210	43
P 220	42
P 230	40
P 240	36
P 250	36

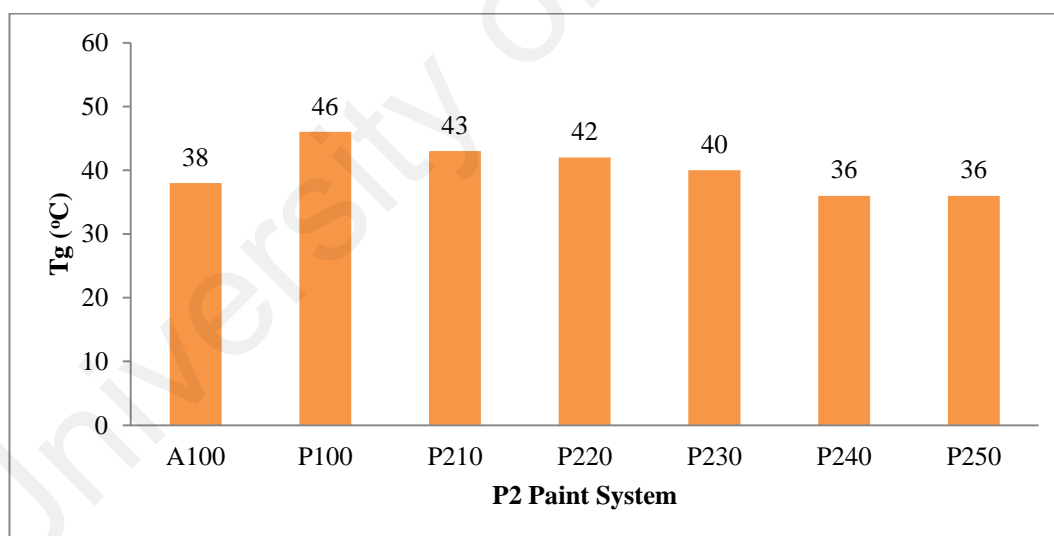


Figure 6.7: The influence of Silitin Z 86 pigment on T_g value of P2 paint system

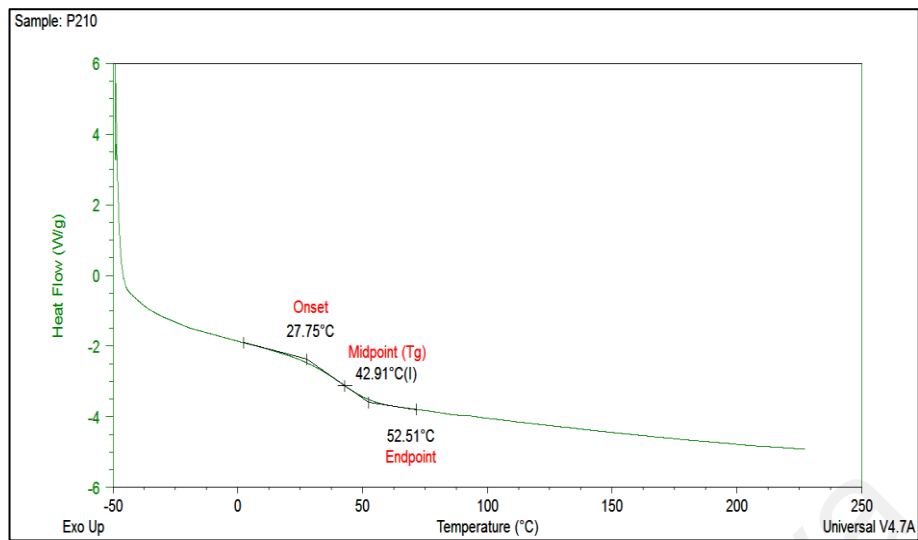


Figure 6.8a: DSC Thermogram of P210 paint system

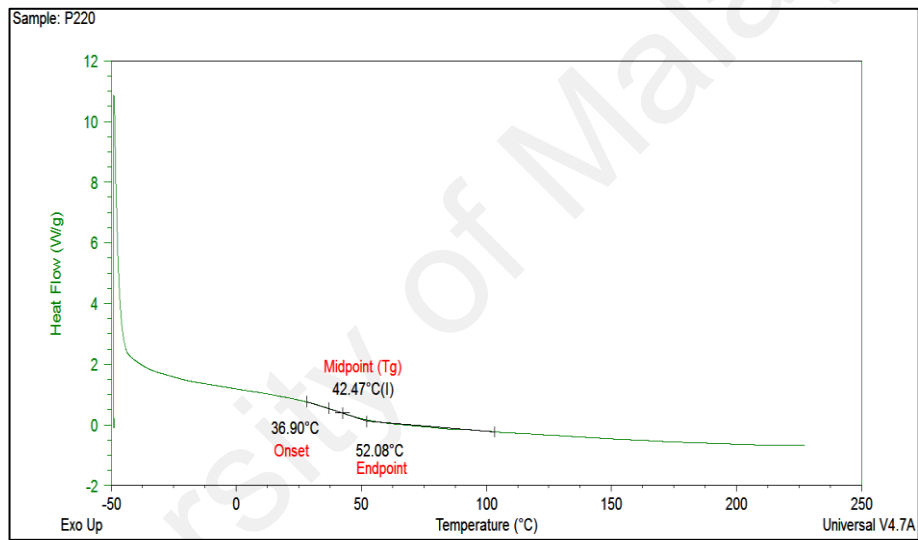


Figure 6.8b: DSC Thermogram of P220 paint system

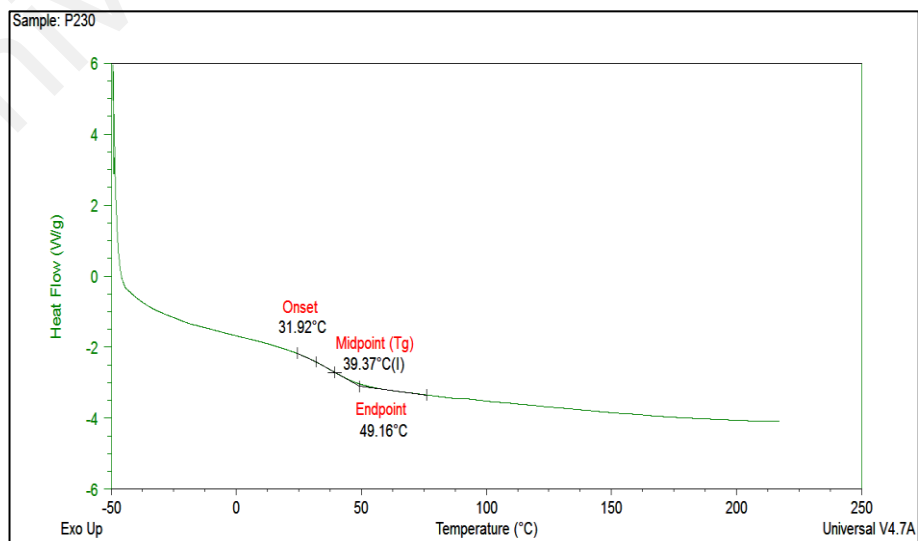


Figure 6.8c: DSC Thermogram of P230 paint system

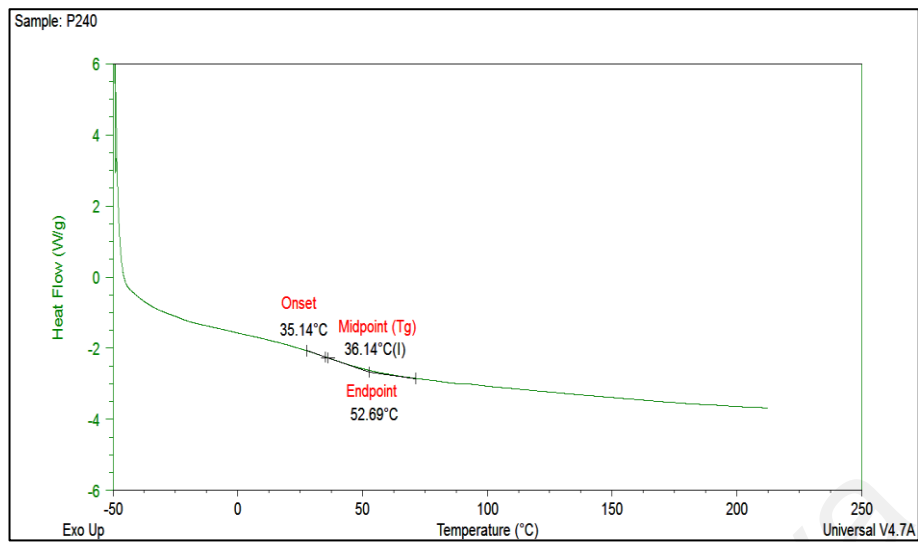


Figure 6.8d: DSC Thermogram of P240 paint system

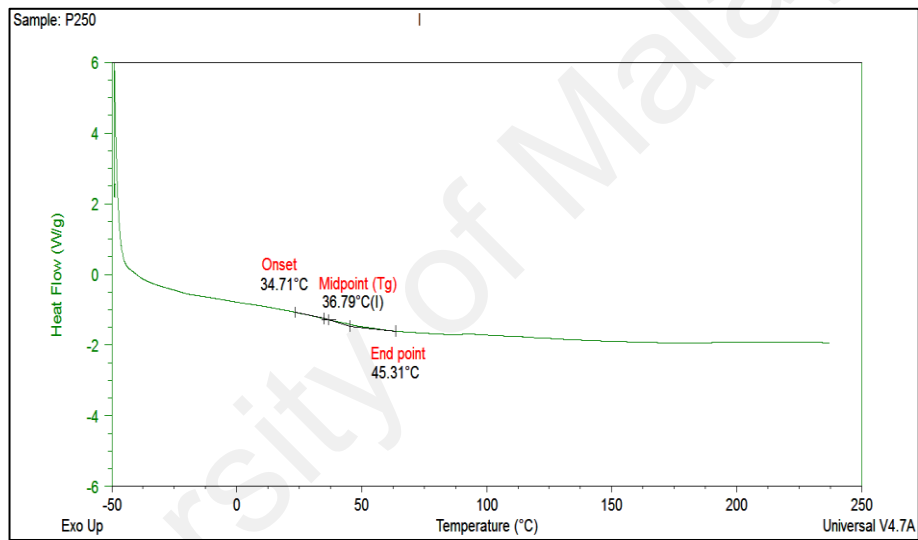


Figure 6.8e: DSC Thermogram of P250 paint system

Figure 6.9 illustrates the T_g values and Figure 6.10(a-e), DSC thermograms which show the influence of Aktisil AM pigments on P3 paint systems. Table 6.7 tabulates the T_g values of P3 in order to show a clear pattern. When Aktisil AM inorganic pigments concentration increases in polymer matrix, the flexibility of the polymer increases. Same performance of the inorganic pigments were reported by many researchers who have pointed out that lower T_g value after the addition of the pigments could be attributed to the role of the pigments in promoting the mobility of adjacent binder segments (Bajaj et al., 1995 Perera, 2004).

Table 6.7: The glass transition temperature of acrylic system, acrylic-epoxy binder system and P3 paint system

System	Glass transition temperature T_g (°C)
A 100	38
P 100	46
P 310	40
P 320	37
P 330	33
P 340	34
P 350	27

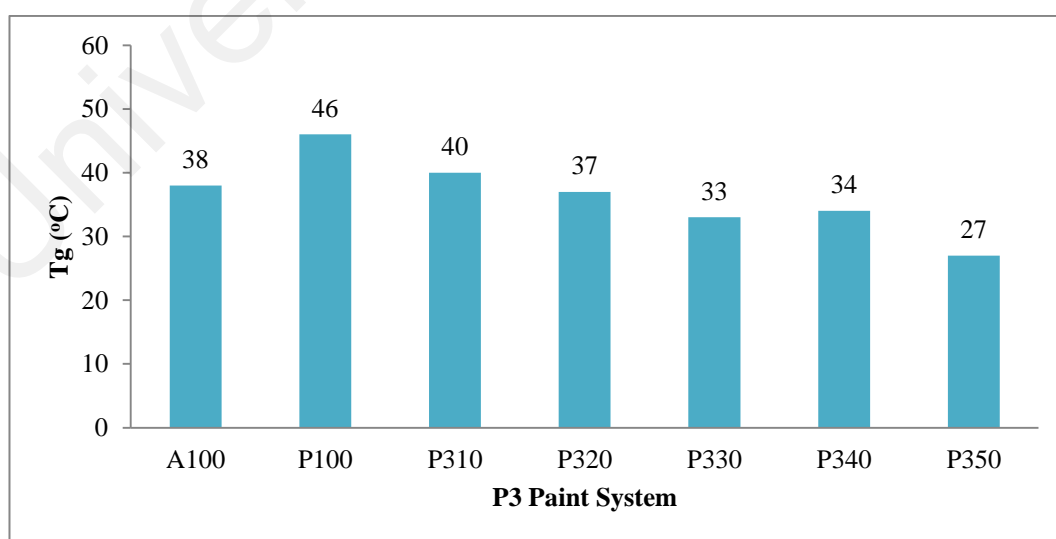


Figure 6.9: The influence of Aktisil AM pigment on T_g value of P3 paint system

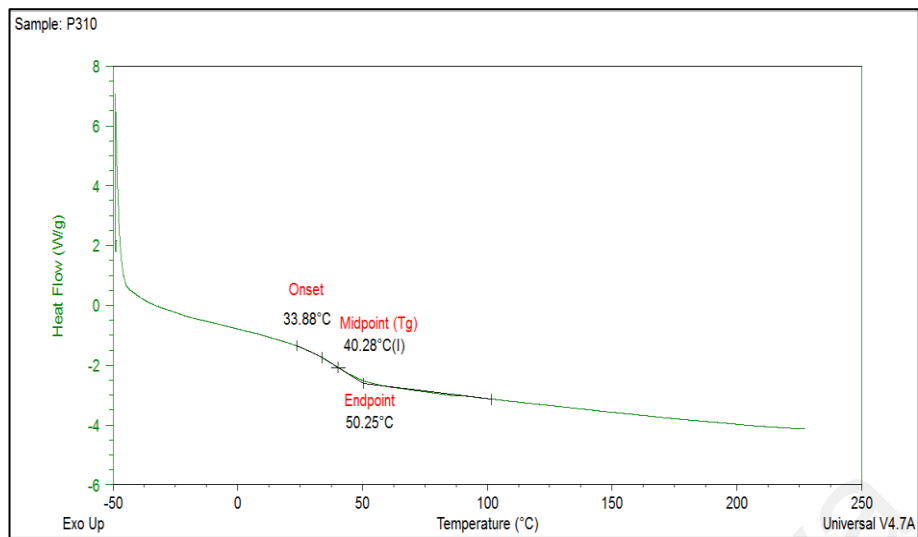


Figure 6.10a: DSC Thermogram of P310 paint system

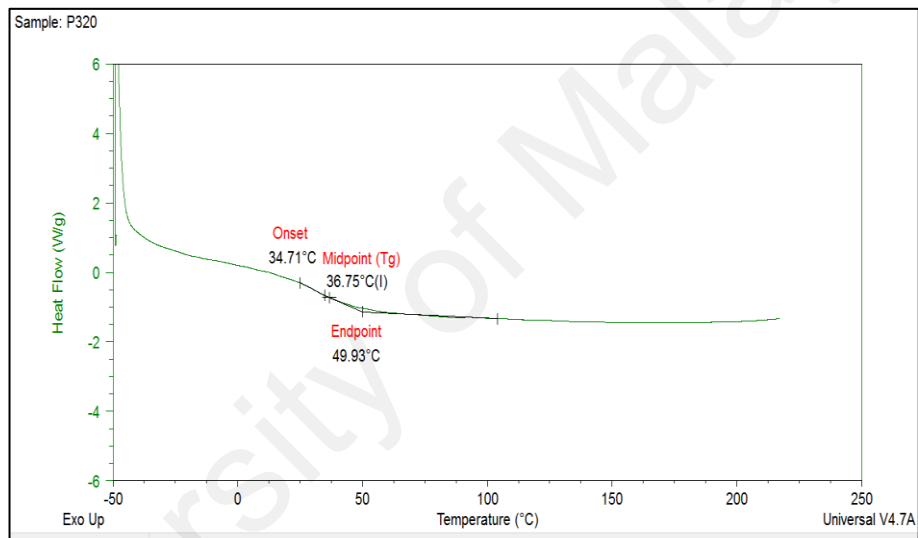


Figure 6.10b: DSC Thermogram of P320 paint system

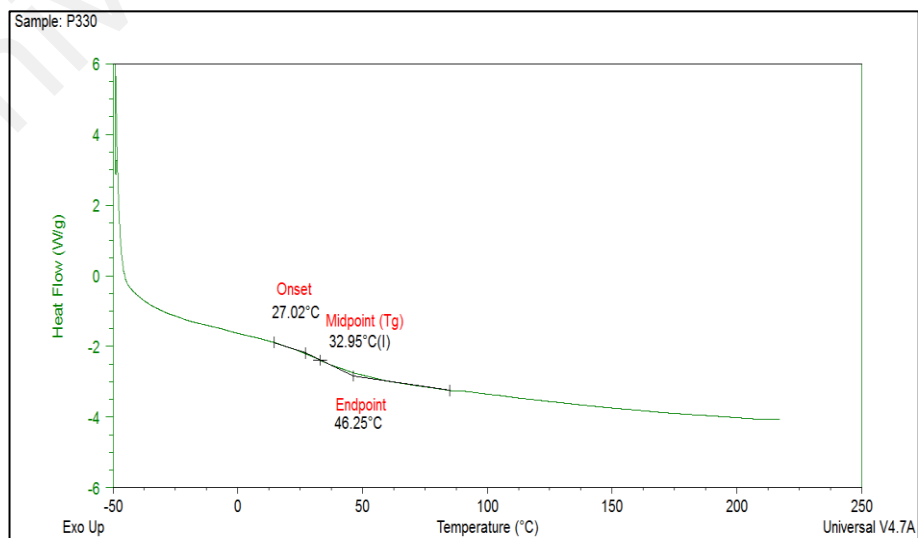


Figure 6.10c: DSC Thermogram of P330 paint system

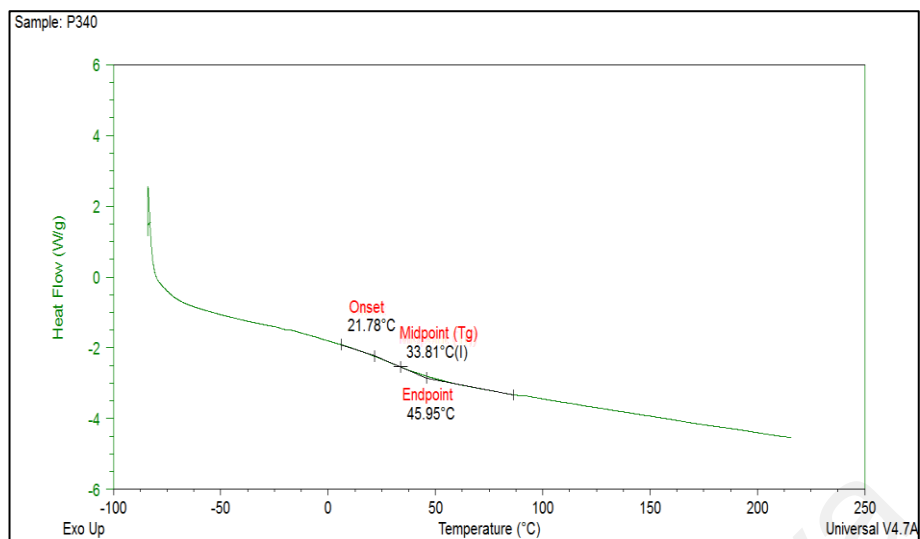


Figure 6.10d: DSC Thermogram of P340 paint system

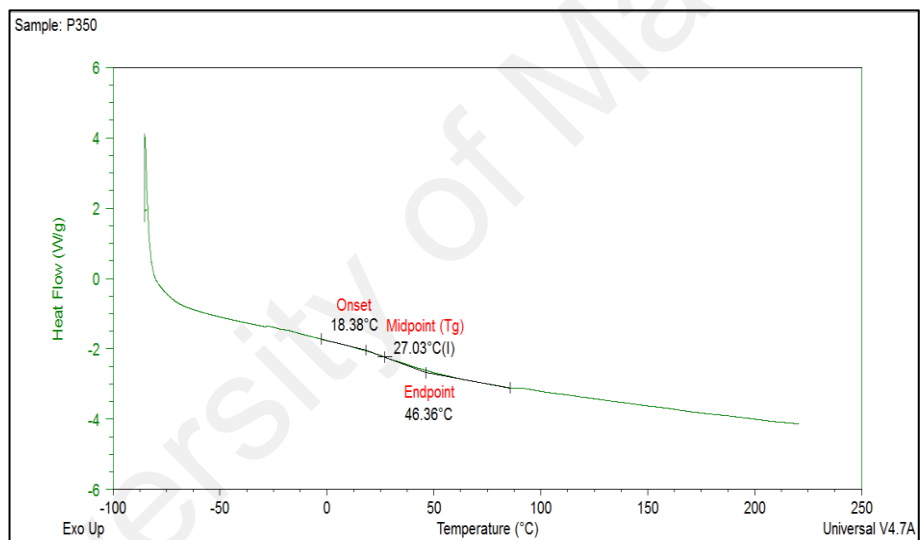


Figure 6.10e: DSC Thermogram of P350 paint system

The P4 paint system (in Table 6.8, Figure 6.11 and Figure 6.12(a-e)) also shows a very similar T_g behavior as the above mentioned paint systems. However, incorporation of inorganic pigments that contain a mixture of SiO_2 at PVC 10 % increase the glass transition temperature up to 54°C and this phenomenon has been elaborated by Perera and Ramezanzadeh et al. The effect of the pigments in restraining the mobility within the binder and obtain a broad distribution of relaxation times as well as the strong physical interactions of the inorganic pigments within the coating matrix could increase T_g value (Perera, 2004; Ramezanzadeh et al., 2011). However, this specifically related to the lowest loading ratio of Aktisil PF 777 pigments only.

Table 6.8: The glass transition temperature of acrylic system, acrylic-epoxy binder system and P4 paint system

System	Glass transition temperature T_g ($^\circ\text{C}$)
A 100	38
P 100	46
P 410	54
P 420	45
P 430	40
P 440	33
P 450	27

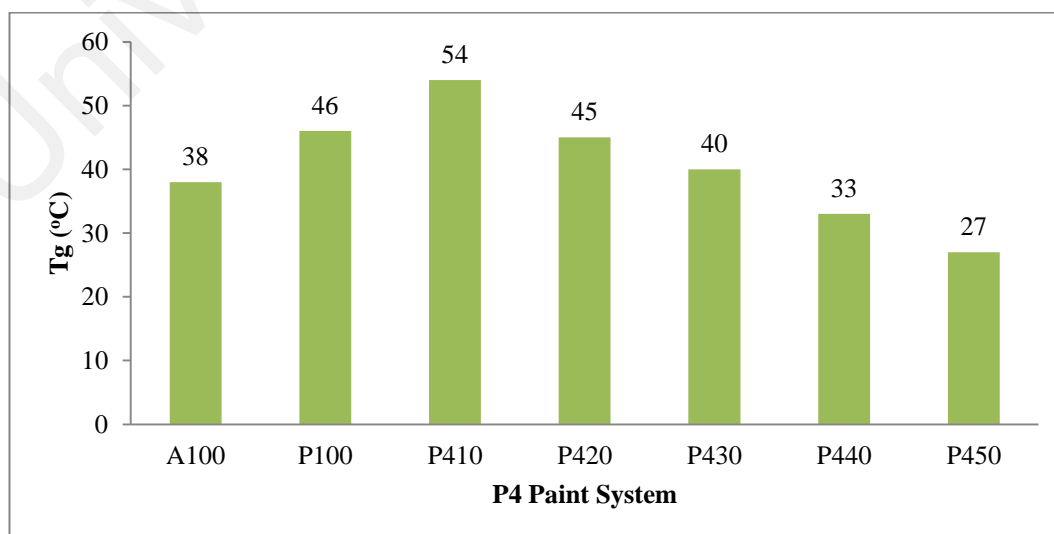


Figure 6.11: The influence of Aktisil PF777 pigment on T_g value of P4 paint system

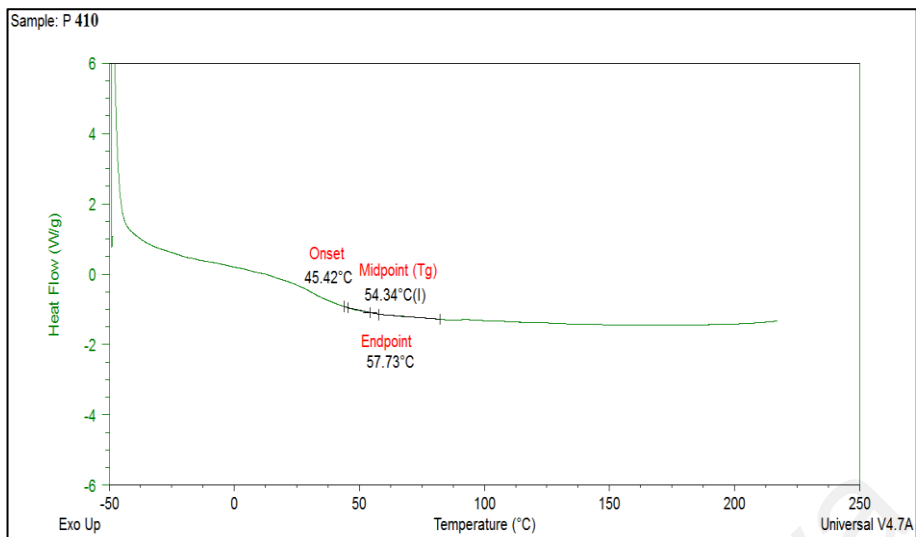


Figure 6.12a: DSC Thermogram of P410 paint system

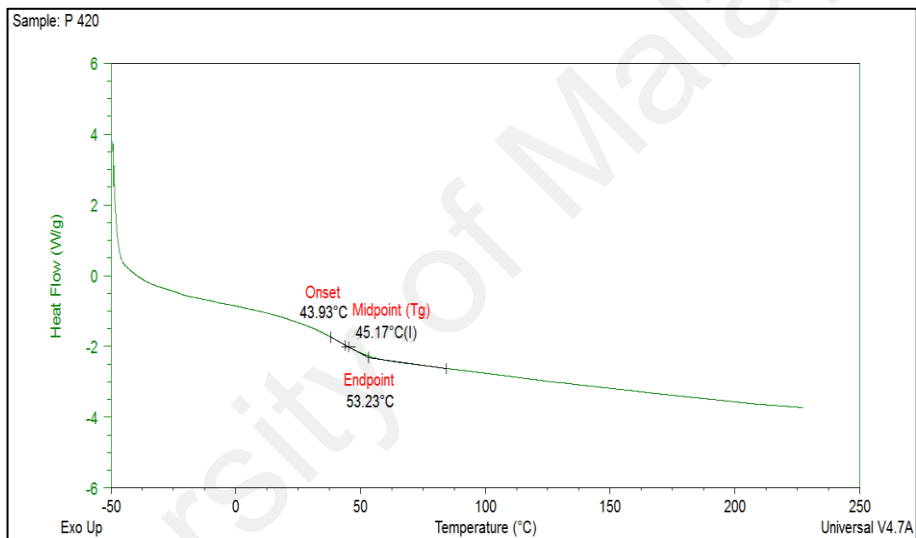


Figure 6.12b: DSC Thermogram of P420 paint system

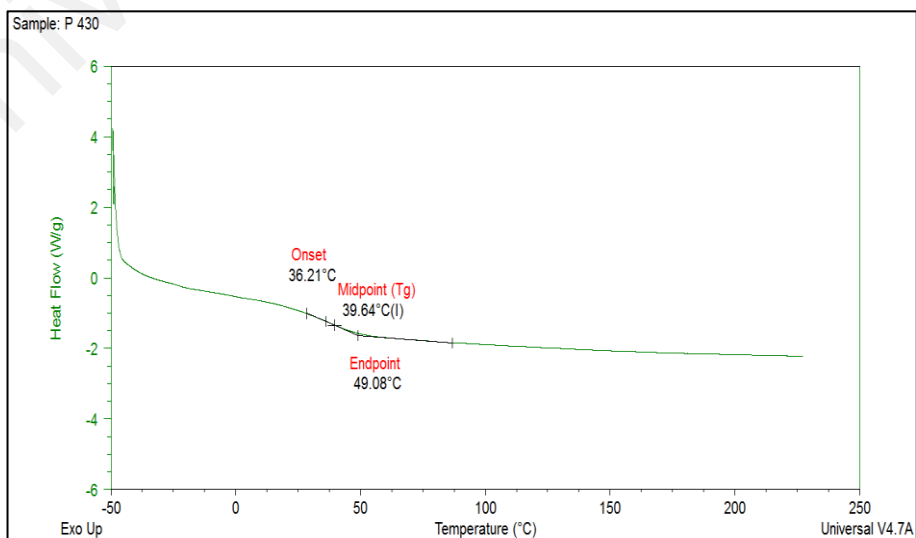


Figure 6.12c: DSC Thermogram of P430 paint system

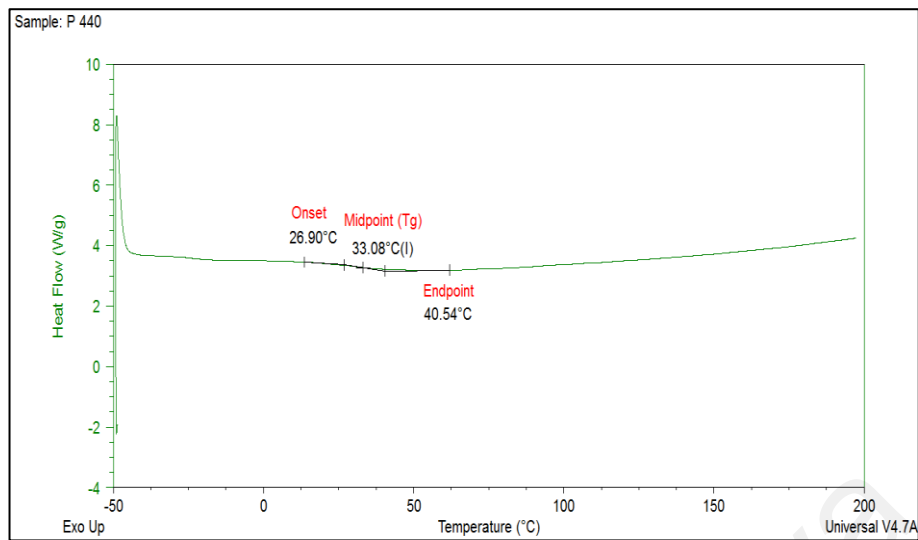


Figure 6.12d: DSC Thermogram of P440 paint system

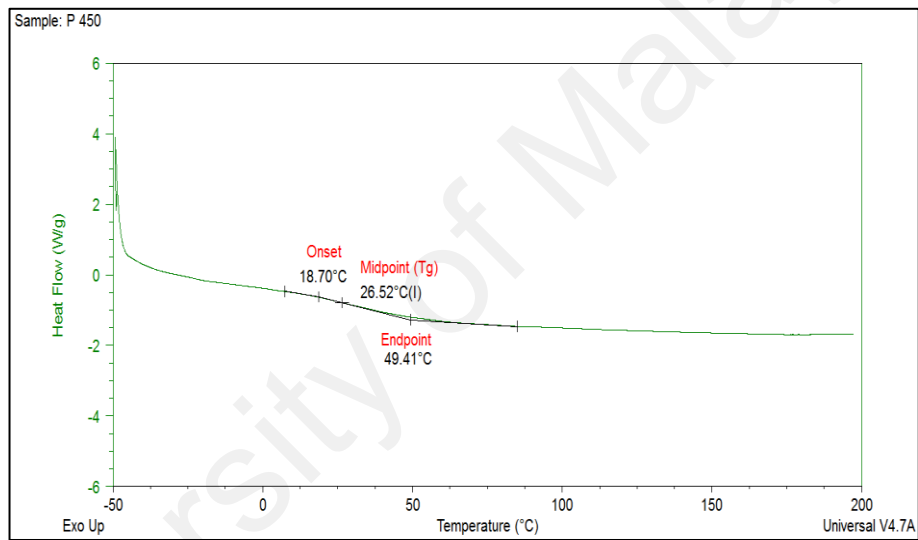


Figure 6.12e: DSC Thermogram of P450 paint system

6.4 Fourier Transform Infrared Spectroscopy

FTIR is a powerful technique that usually used to analyze the chemical structure and complexation appearance in the study of organic coating materials. The advantages could be given by the employment of FTIR technique can be described in giving clear understanding about the cross-linking process among the organic functional groups of the coating system. Moreover, the information that was given by analyzing the recorded spectrum, gives the ability to identify the chemical bond composition and determine the sites containing H-bonded hydroxyls, carboxyl groups and other organic functional groups. The fundamental concepts of FTIR studies based on analyze the spectrums of all developed systems and determine the appearance or absence of some peaks. The observation or absence of some peaks can be considered as an evidence of complete curing or achievement of well cross-linking within the blending system.

FTIR spectra was utilized in order to determine and investigate the changes in the chemical bond structure that may occur from blending acrylic polyol resin with epoxy polyol resin (Rau et al., 2011) as it was well reported in Chapter 4. Furthermore, FTIR studies were carried out on the developed paint systems in order to figure out the effect of the added inorganic pigments and its pigment volume concentration (PVC) amount on the final chemical structure of the developed hybrid paint systems P1 (TiO₂), P2 (Silitin Z 86), P3 (Aktisil AM) and P4 (Aktisil PF 777) Testing for Chemical Properties of Polymers FT-IR Analysis (ASTM E1252) was used as guide. FTIR spectrum was reordered in the transmittance mode using an Attenuated Total Reflectance (ATR-Nicolet iS10) spectrophotometer with OMNIC spectra software from Thermo Scientific. Deuterated Triglycine Sulfate Potassium Bromide (DTGS KBr) method with velocity 0.6329 ms⁻¹ was used for the measurements. For all spectra recorded, a 32 scan data accumulation in a range 400-4000 cm⁻¹ was carried out at a resolution of 4.0 cm⁻¹.

In the regard of extending the FTIR studies that took place on the different mixing ratio of acrylic and epoxy resins (90A10E), the paint systems corresponding FTIR spectra of P1, P2, P3 and P4 were recorded. These spectrums were analyzed in term of the inorganic pigments effect of the chemical structure of the host polymeric matrix binder system. FTIR spectra for binder system and the developed P1 paint systems with different PVC ranging from 10 % to 50 % were illustrated in Figure 6.13.

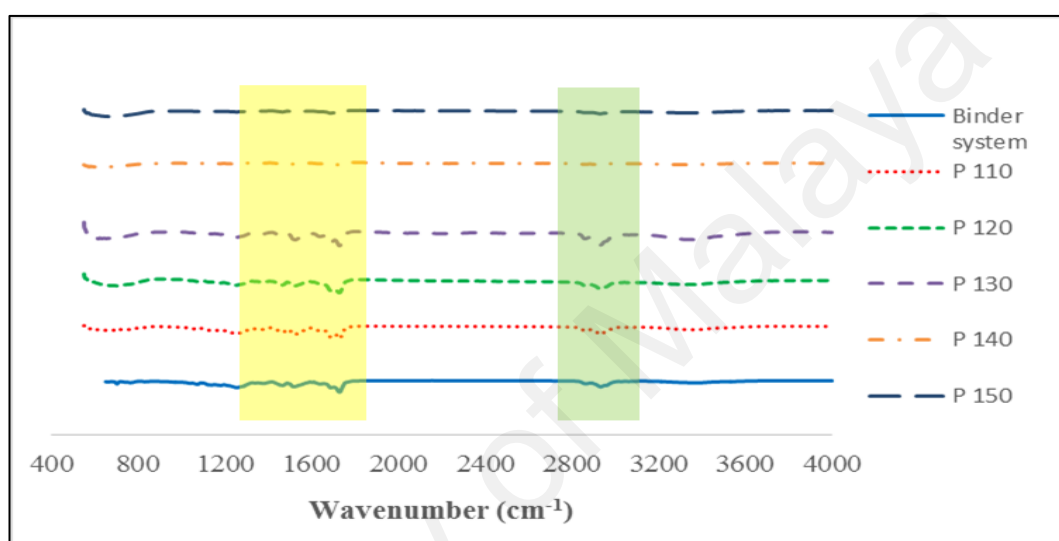


Figure 6.13: FTIR transmission spectrum of binder system and all P1 paint system

It was observed that the presents of TiO_2 pigment did not lead to any peak displacement in positions comparing to the binder system's peaks. This observation can be explained as the used pigments have been dispersed within the polymeric binder matrix without any interaction within the chemical structure of the acrylic-epoxy matrix (Merouani & Amardjia-Adnani, 2008). In addition, embedding Silitin Z 86, Aktisil AM, and Aktisil PF777 pigments, in order to develop P2, P3, and P4 paint systems respectively, have demonstrated the same behavior of TiO_2 pigment.

As the purpose of our FTIR studies of the developed paint systems was to indicate the effect of the inorganic pigments on the hybrid organic matrix, therefore Figures 6.14, 6.15 and 6.16 were illustrated to show the FTIR spectra of P2, P3 and P4

respectively. It was observed that there were no significant changes occurred to the peaks of the binder system after the addition of any inorganic pigments. There is an additional peak for P2, P3 and P4 system in the range of 950-1200 cm^{-1} due to same modified SiO_2 content in the pigments. The important peaks of silicone resins such as C-O-C, Si-C, Si-O, Si- CH_3 and Si-O-Si exist in 950-1200 cm^{-1} range (Kahraman et al., 2006; Ramesh et al., 2008 ; Vengadaesvaran et al., 2010). Since, all the peak values are very closer, there could not get individual peaks. An overlapping of the peaks was observed in this range (Ji et al., 2007; Ramesh et al., 2013).

However, it is worth to be mentioned that the intensity of the peaks at all respective wavenumber was found to be getting smaller as the PVC getting higher from 10 % up to 50 %. These observations were related to all prepared paint systems namely, P1, P2, P3 and P4, and could be attributed to the inorganic properties of the used pigments which are hard to detect by the FTIR technique which mainly used to analyses the organic materials and their functional groups.

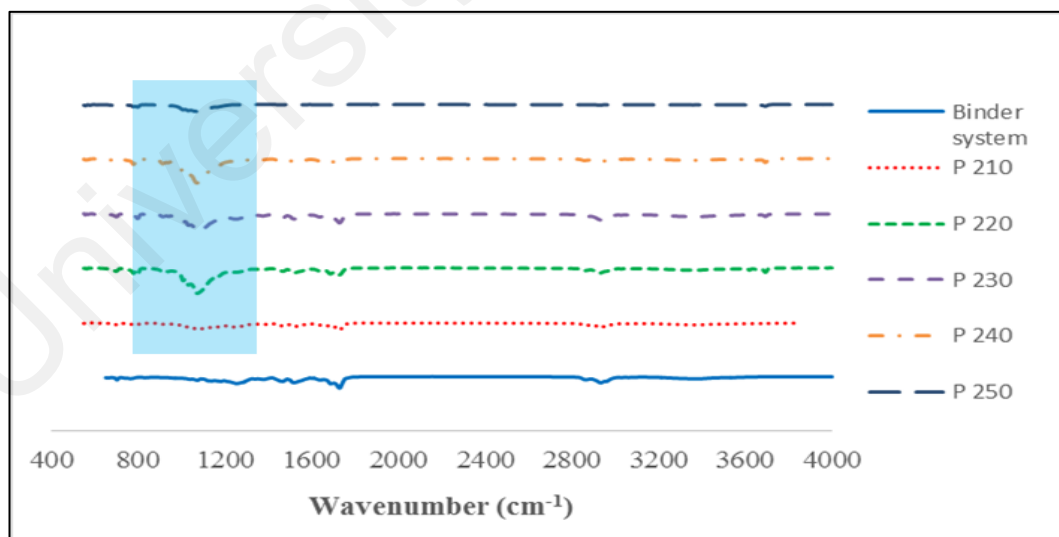


Figure 6.14: FTIR transmission spectrum of binder system and all P2 paint system

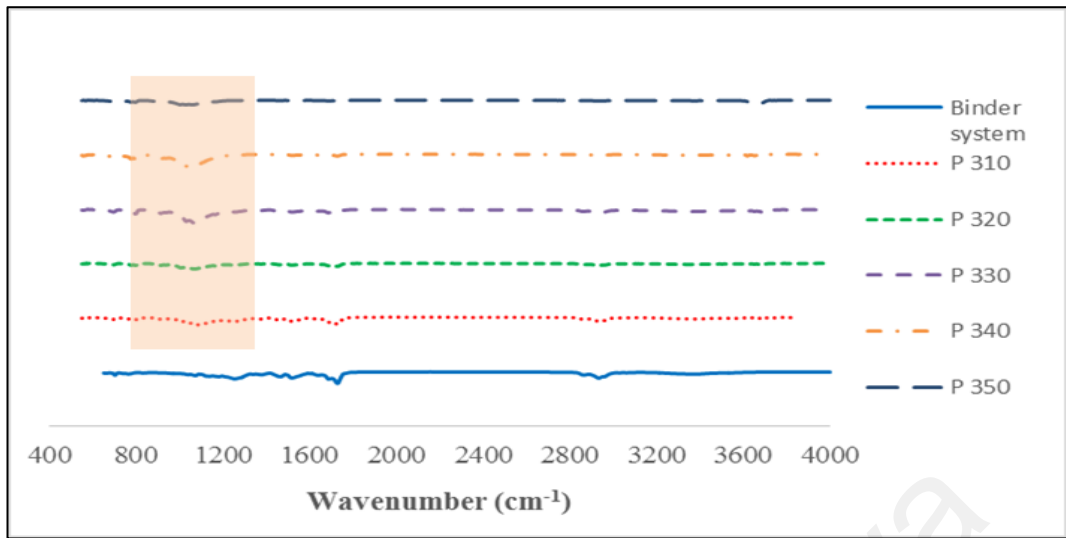


Figure 6.15: FTIR transmission spectrum of binder system and all P3 paint system

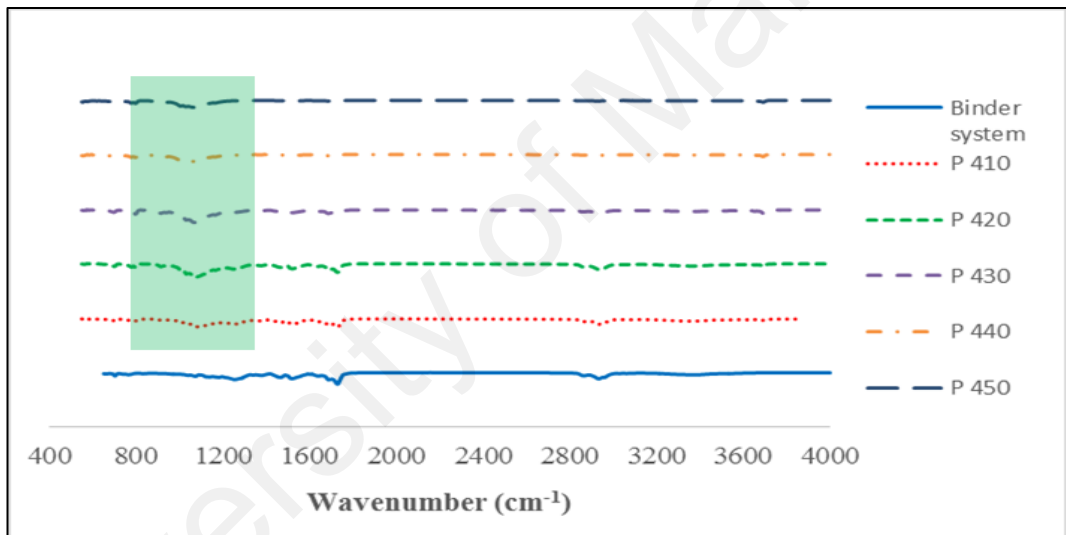


Figure 6.16: FTIR transmission spectrum of binder system and all P4 paint system

6.5 Scanning Electron Microscope and Energy Dispersive Analysis of X-ray

The morphology studies include the investigation of the shape, size, phase distribution within the respective structure. Basic visualization was found not enough to observe and monitor the proper dispersion of the used inorganic pigments within the polymeric hybrid matrix. In this study, SEM was used in order to demonstrate a good understanding about the surface morphology of the paint systems. Apart from this, it is also help to obtain reliable evidence on the successful achievement of cured paint films without cracking or separation phase resulting from the addition as well as dispersion of the utilized pigments. Moreover, EDAX was similarly used and attached with the SEM micrographs in order to determine the composition of the paint films and study the influence of the pigment volume concentration (PVC) value on the dispersion of the different elements within the polymer hybrid matrix.

This analysis can help to identify the uniformness of the coating, composition of pigment, as well as characterization of the defect itself (Ahmed & Selim, 2010). Uniform dispersion of TiO₂ pigments within the homogenous hybrid acrylic-epoxy binder matrix was observed. Characterization of pigments using SEM-EDAX analysis technique was used to assure the presence of TiO₂ (Ferreira et al., 2001). As many researchers reported analyzing SEM images, the absent of the cracks in the cured paint films could be related to the good barrier properties and anti-corrosion performance (Debnath, 2013). The presents of such cracks within the surface after the curing process even in micro-size is considered as one of the main reasons behind the rapid degradation of the substrate as it has been exposed to the surrounding corrosive environment via this cracks (Ahmad et al., 2005; Jiang et al., 2015; Ramesh et al., 2008). The surface morphology and attached EDAX results of P1 paint systems with PVC from 10 % to 50 % is illustrated in Figure 6.17.

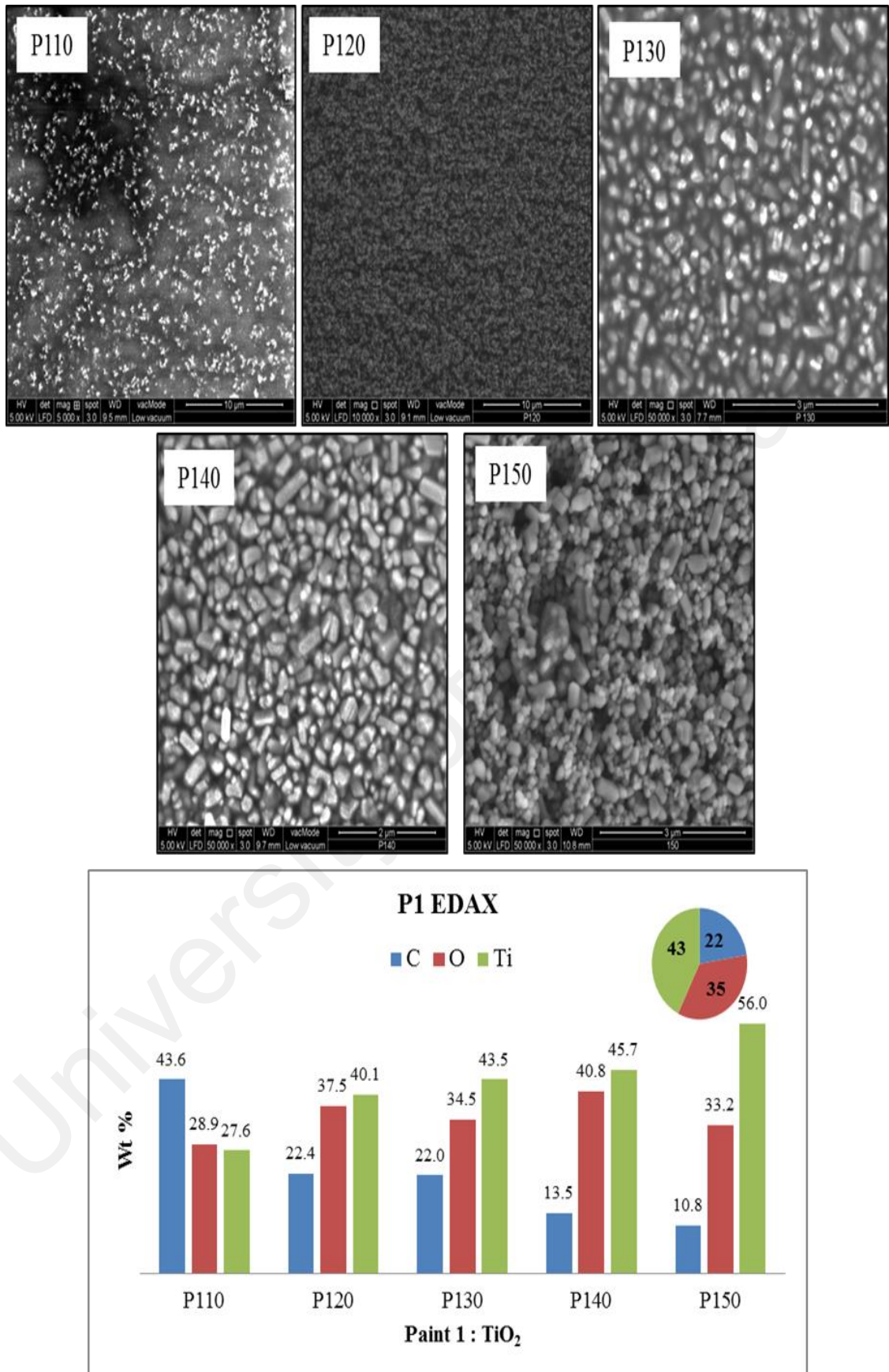


Figure 6.17: SEM micrograph and the corresponding EDAX results of P1 paint system

It is observed that the SEM images support the idea of enhancing the barrier performance of the polymeric matrix by embedding micro-size particles with good dispersion within the paint film. The SEM micrographs illustrated in Figure 6.17 show that, as the PVC increases above 40 %, the pigments are randomly embedded in the matrix of AE binder and the heterogeneity with the surface increases (Ferreira et al., 2001). In addition, Figure 6.17 also shows the EDAX results of the P1 paint systems which point out the present of Titanium which is related to the added pigment. Furthermore, the EDAX results were found in strong agreement with the supplier data sheets that matched with the presence of PVC values from 10 % to 50 %.

In Figure 6.18, Silitin Z 86 pigments were found to be uniformly dispersed and tightly bound to the acrylic-epoxy matrix. These SEM images could be considered as an evidence of the successful dispersion of the pigments. This development of the paint system shows that after the curing process where there were no separation phases or cracks observes on the surfaces. As the PVC of the Silitin Z 86 increase, the tendency of forming agglomeration increased which consider normal as the number of the particles increase in the size unit (Kalendova, 2003; Kalendova et al., 2008). Moreover, the EDAX results, Figure 6.18, were found in complete agreement with the information that given by the data sheet of the inorganic pigments and also were acceptable in the corporation of the PVC values from 10% up to 50 %.

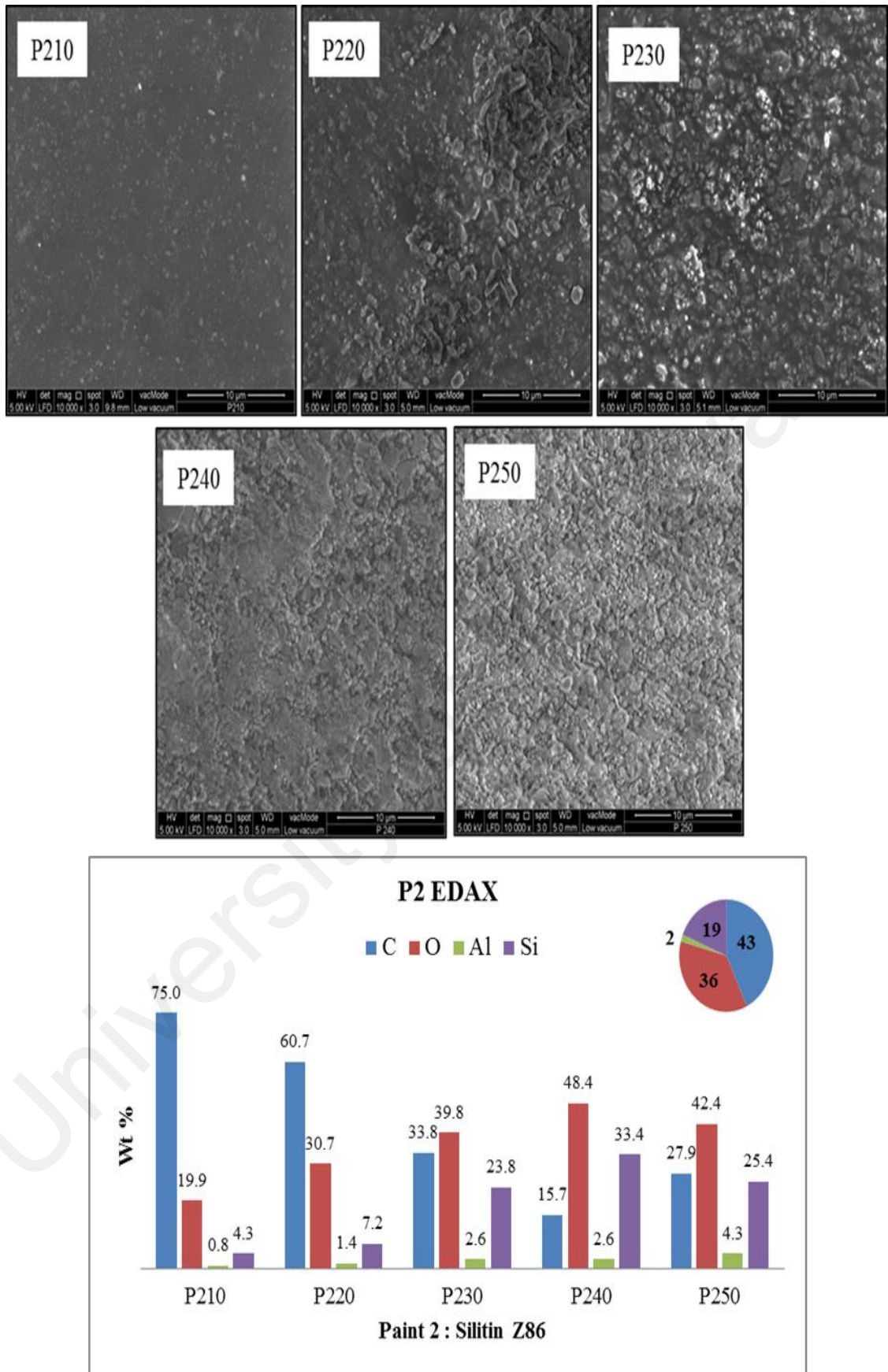


Figure 6.18: SEM micrograph and the corresponding EDAX results of P2 paint system

The SEM micrographs of all prepared P3 paint systems are shown in Figure 6.19. All P3 paint system showed formation of a uniform, homogeneous, crack free, continuous close packed structures. Furthermore, Figure 6.19 also show the attached EDAX results that recorded for P3 paint systems which corresponded to the manufacturer datasheet of Aktisil AM pigments and also EDAX results demonstrated the influence of increasing the PVC values on the combination of the paint film.

The same performance was recorded in the case of the addition of Aktisil PF 777. P4 paint systems SEM images as shown in Figure 6.20 were found crack free with well dispersion of the added particles within the polymeric matrix (Ahmed & Abdel-Fatah, 2012). Also, EDAX results were shown in Figure 6.20 and confirm the presence of all the elements of both the organic polymeric matrix and the inorganic pigments. Paint system P2, P3 and P4 indicates confirmation of same base pigment combination of amorphous silica and lamellar kaolinite with little extra modification using amino silane and alkyl silane as provided in data sheet.

In the end, one can conclude that the morphology studies that were carried out via SEM and EDAX showed that all paint systems had a good morphology structure with the good dispersion of the respective pigments. In addition, the SEM micrographs were used as supporting evidence to the adhesion results with good barrier performance of the paint systems which in turn may result in good corrosion protection capabilities.

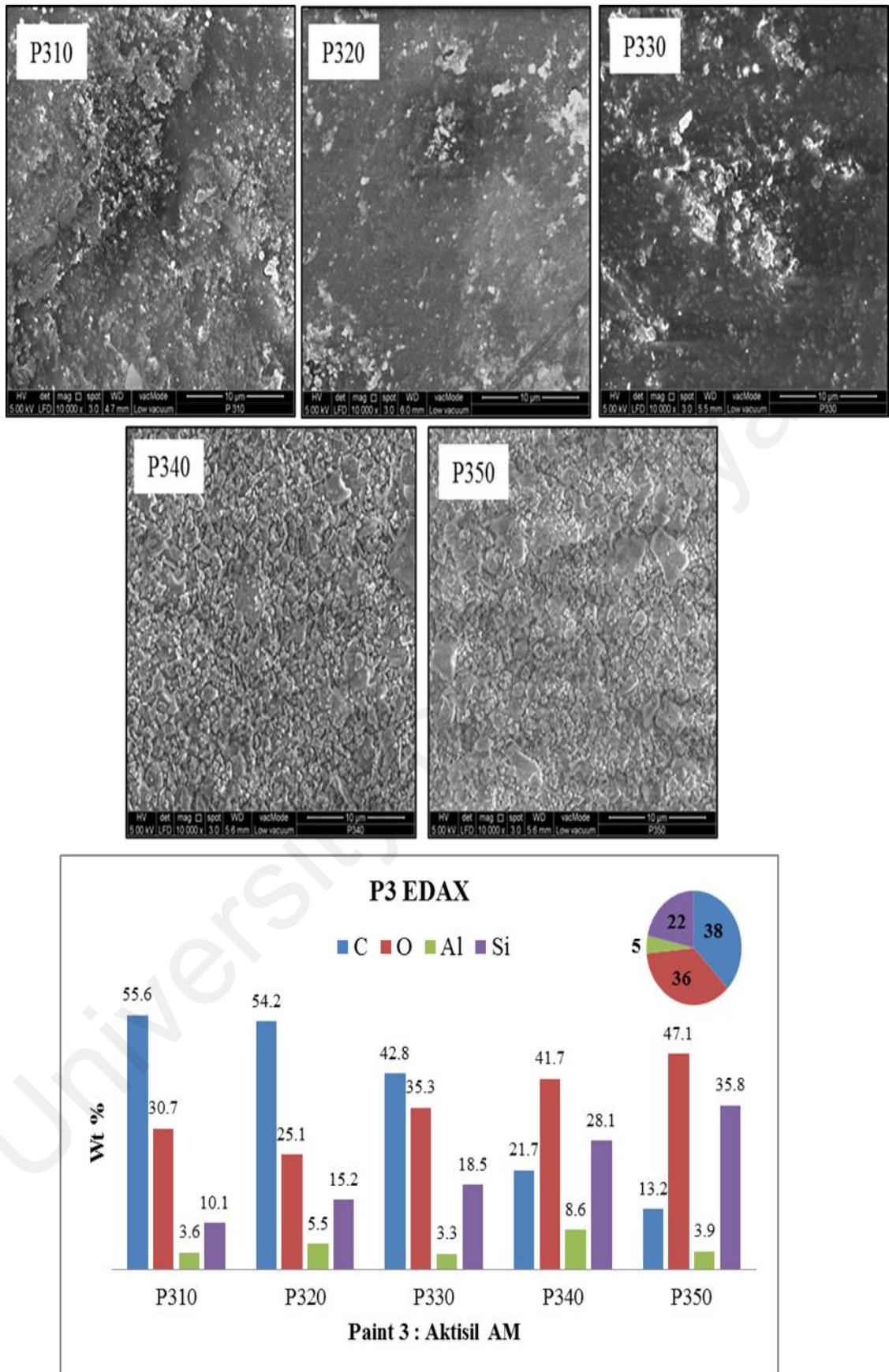


Figure 6.19: SEM micrograph and the corresponding EDAX results of P3 paint system

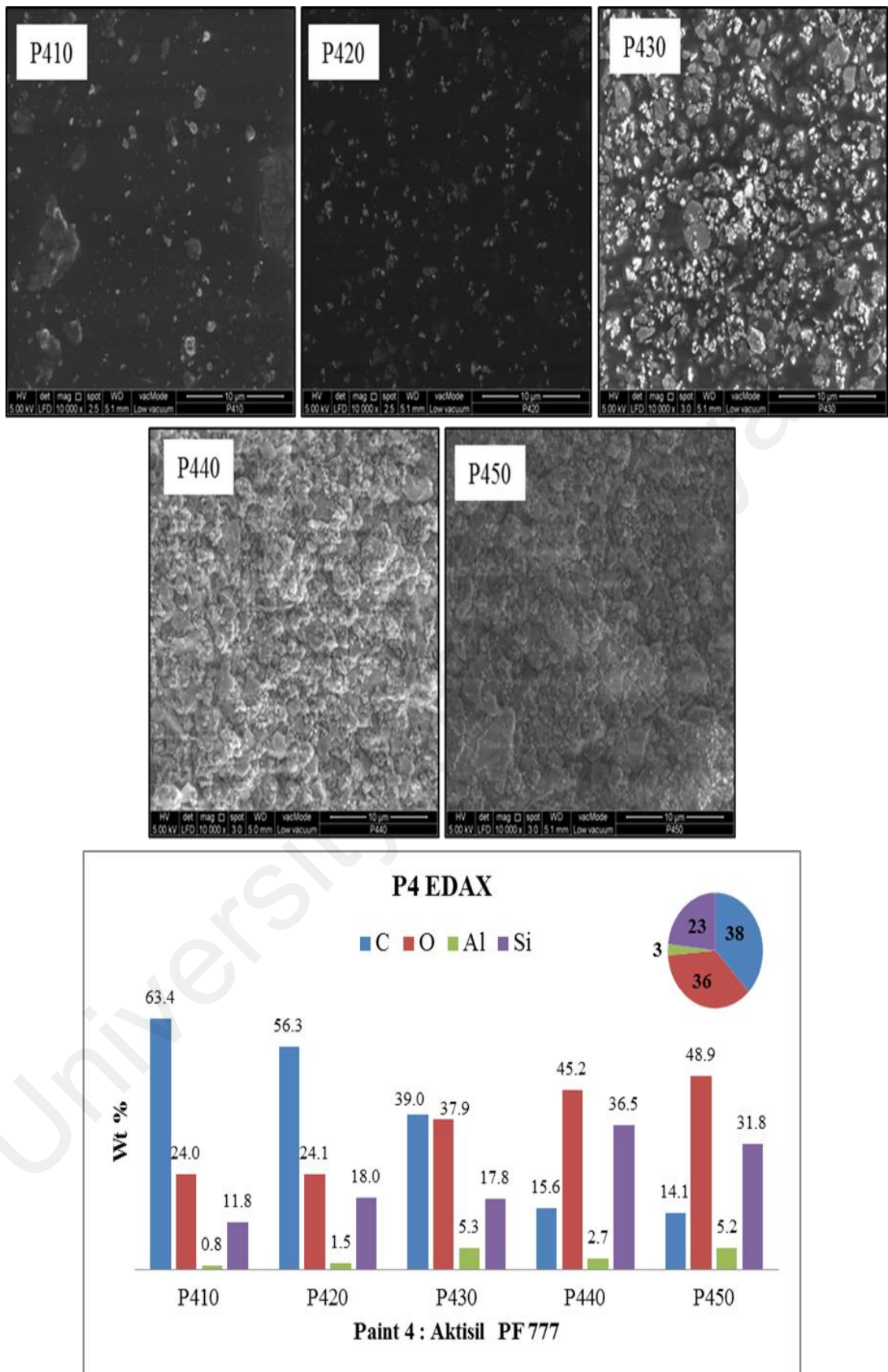


Figure 6.20: SEM micrograph and the corresponding EDAX results of P4 paint system

6.6 Summary

By comparing the TGA thermograms of the hybrid binder system 90A10E as well reported in the 2013 work of Rau. et al., the P1, P2, P3 and P4 paint systems thermograms clearly show that there is no new decomposition steps after combination of inorganic TiO_2 or Hoffmann Minerals within AE polymeric matrix. These pigments improve thermal stability and lead the paint system to require a higher temperature above $250\text{ }^\circ\text{C}$ and thermal energies for performing the same decomposition steps as the base system 90A10E. TGA has shown that the pure AE hybrid binder system undergoes more mass loss compared to all developed pigmented paint system. The reason of higher residue could be related to the thermal stability of the inorganic pigments. Residue percentage of P1 is higher than P2, P3 and P4 with greater differences ranging from 23-85 % as the PVC increases from 10-50 %. These show that TiO_2 has more thermal stability. Similar residue percentage for P2, P3 and P4 indicates confirmation of same base pigment combination of amorphous silica and lamellar kaolinite with little extra modification using amino silane and alkyl silane.

DSC results show an increase of T_g value from $38\text{ }^\circ\text{C}$ to $46\text{ }^\circ\text{C}$ for A100 to P100 system. This explained by relating that homogenous crosslinking rises as the epoxy content increases in acrylic matrix by the addition of polyisocyanate as the hardener. T_g value decreases when PVC content for all paint system increase. Combination of pigment within the AE matrix increases in the free volume that improves flexibility. This is exceptional for P410 which shows an increase in T_g value. This P410 paint system's T_g increase can be attributed to the effect of the pigment in restraining the mobility within the binder and strong physical interactions with polymeric matrix.

These FTIR spectra were analyzed in term of the inorganic pigments effect on the chemical structure of the host polymeric matrix binder system. It was observed that the P1, P2, P3 and P4 paint system did not lead to any peak displacement in positions

comparing to the binder system. This observation was due to the used pigment has been dispersed within the polymeric matrix without any interaction within the chemical structure of the acrylic-epoxy binder matrix. However, there was an additional peak for P2, P3 and P4 system in the range of $950\text{-}1200\text{ cm}^{-1}$ due to same modified SiO_2 content in the pigments. However, it is worth to be mentioned that the intensity of the peaks at all respective wavenumber was found to be decreasing as the PVC content increases from 10 % up to 50 %.

SEM images and EDAX results of all paint system support the idea of enhancing the adhesion and barrier performance of the polymeric matrix by embedding micro-size particles with well dispersion within the paint film. All paint system showed formation of a uniform, homogeneous, crack free, continuous close packed structures. Also, EDAX results confirms the present of the elements for both the organic polymeric matrix and the inorganic pigments.

CHAPTER 7: RESULTS AND DISCUSSION ON PAINT SYSTEM

CORROSION AND ELECTROCHEMICAL

7.1 Introduction

In this chapter tests was carried out in order to evaluate the corrosion resistance of the developed paint systems. Acid resistance test and electrochemical impedance was used to investigate the effect of the addition of various inorganic pigments, namely Titanium Dioxide (P1 system), Silitin Z 86 (P2 system), Aktisil AM (P3 system) and Aktisil PF 777 (P4 system), in enhancing the corrosion resistance of the AE polymeric matrix. These investigations have been conducted in order to evaluate the anti-corrosion performance and the barrier performance of developed paint systems (Bahrami et al., 2010). Painted mild steel panels were subjected to diluted H_2SO_4 10 % in immersion test for 40 days and 3.5 % NaCl in EIS studies up to 30 days. Images and readings were taken from time to time in order to determine the exact degradation time of each individual system and its reasons.

7.2 Acid Immersion Test

The simple principle of this test is based on the visual observation of the immersed cross-scribed side edge protected panels. Visual observation is conducted after immersion. The experimental procedure was accordance with ISO 2812-1. Evaluation is based on blistering and degradation of coated panels. The response of all developed paint systems was recorded after 0, 4, 8, 15, 22 and 40 days of immersion in H_2SO_4 10 % solution as shown in Figure 7.1 to Figure 7.4.

7.2.1 Paint System with TiO₂ – P1

Figure 7.1(a-f) illustrates the response of all prepared samples of P1 systems after different periods of immersion in H₂SO₄ 10 % solution. The initial state of the samples before the exposure start is showed in Figure 7.1a. After 4 days of immersion, as shown in Figure 7.1b, panels coated with P140 and P150 system started loss of adhesion at the centre of the cross-scribed line. However, P110, P120, and P130 systems show excellent adhesion properties and significant barrier stability against the aggressive chemical molecules.

Similar observations were recorded at the 8th day of immersion (Figure 7.1c). As days progresses, P110 and P130 paint systems still demonstrate their durability against the penetration of aggressive chemical molecules toward the metal-coating interface. While P120 start subjected to some adhesion failure just near the scribed lines. P140 paint system, as illustrated in Figure 7.1d, was found partially peeled off from the surface interface. Total failure was recorded for the P150 system after 15 days of immersion. Only the paint system, P110 with 10 % PVC and P130 with 30 % PVC of TiO₂ succeeded to withstand against the acid penetration and show massive barrier ability after 22 days of immersion as shown in Figure 7.1e.

While Figure 7.1f, shows no longer protection by paint systems at the 40th day of immersion. Nevertheless, it is worth to be mentioned that, good adhesion without obvious damage was recorded on some areas of the surface far from the scratches. That in turns could be consider as evidence on the superior barrier performance (Clerici et al., 2009) of the polymeric paint system reinforced with TiO₂ particles up to PVC equal to 30 %.

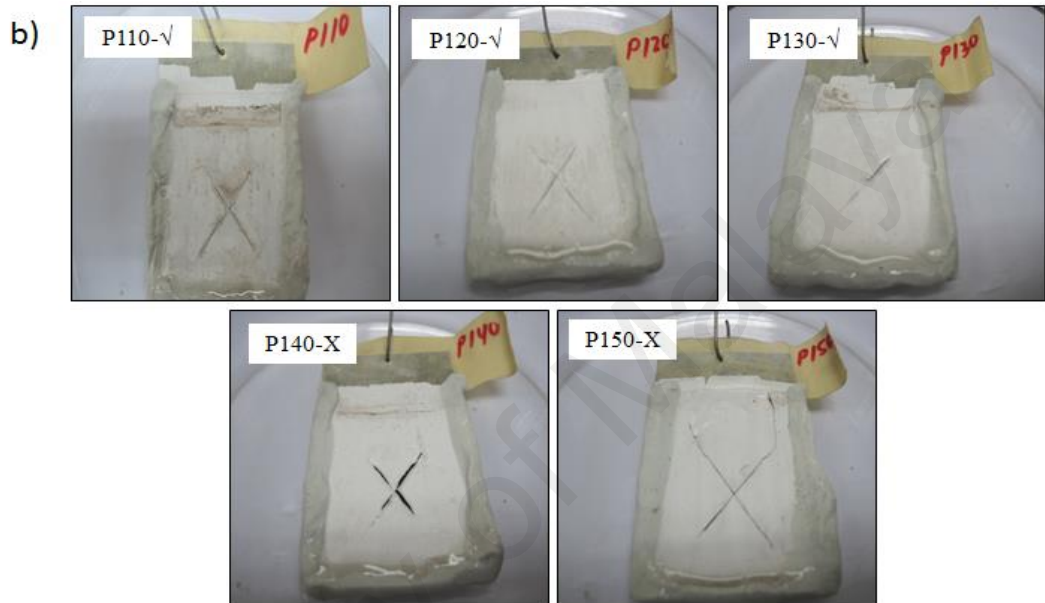


Figure 7.1: Acid resistance response for P1 system after a) 0, b) 4, c) 8, d) 15, e) 22 and f) 40 days of immersion in H_2SO_4 10 % solution



Figure 7.1: continued

7.2.2 Paint System with Silitin Z 86 – P2

All observations that were used to determine the response of the samples coated with Silitin Z 86 (P2) paint systems are illustrated in Figure 7.2(a-f). These figures showed the ability of the prepared samples to withstand immersion in a highly corrosive medium H_2SO_4 10 % solution after 0, 4, 8, 15, 22 and 40 days of immersion. Figure 7.2a show the initial state of P2 samples.

However, the Figures 7.2b and 7.2c showed the samples conditions after 4 and 8 immersion days respectively. It is clear by observing the images at the first 8 days of immersion, P210 and P220 paint systems were found to be with superior barrier performance even near the centre of the cross. Meanwhile, the samples of P230, P240 and P250 systems start indicating loss of adhesion and a partially failure near the centre of the cross after just 4 days of immersion. After 15 days of immersion the P220 paint system showed excellent barrier and corrosion protection properties due to addition of silica based pigments (Ji et al., 2007).

Results recorded of all P2 samples at 22nd and 40th day showed complete loss of adhesion near the cross-scribed line and paint peeling off at the centre of the cross. This observation can be attributed due to the effect of aggressive chemical molecules penetrating and reaching the metal-coating interfaces and break the bonds between the polymeric matrix and the metallic surface (Hosseini et al., 2010).

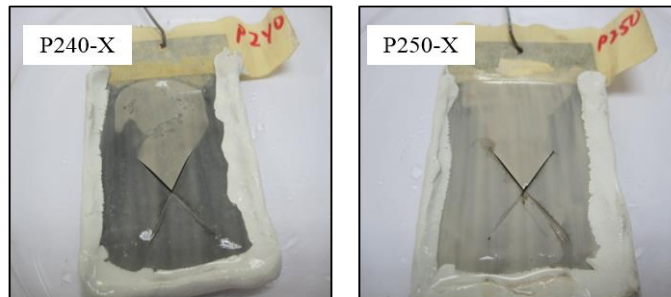
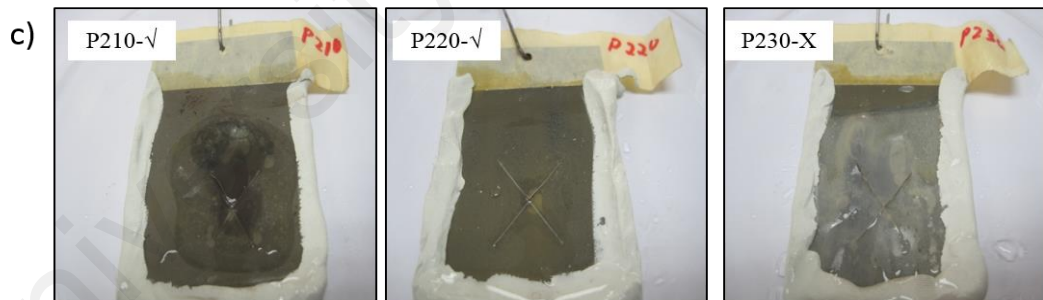
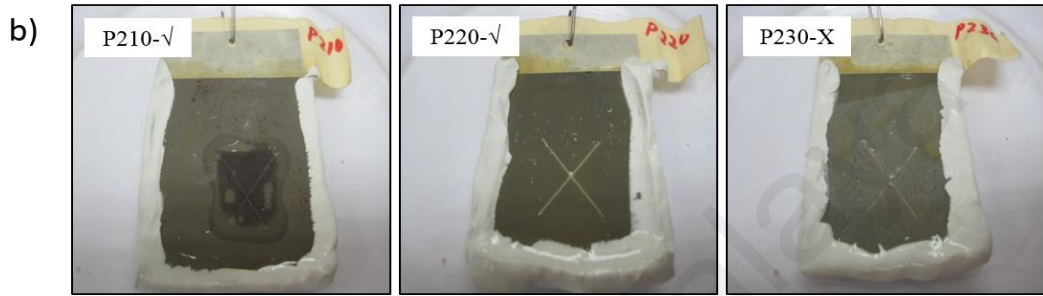
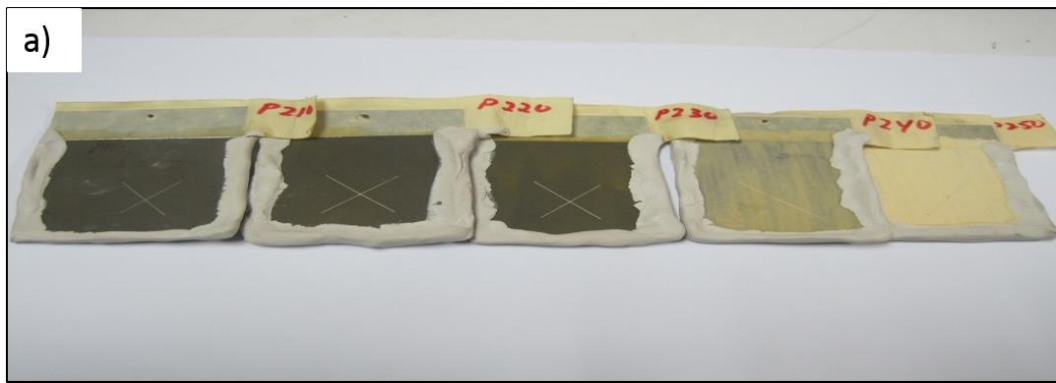


Figure 7.2: Acid resistance response for P2 system after a) 0, b) 4, c) 8, d) 15, e) 22 and f) 40 days of immersion in H_2SO_4 10 % solution



Figure 7.2: continued

7.2.3 Paint System with Aktisil AM – P3

In order to evaluate the chemical resistance of Aktisil AM (P3) paint systems, Figure 7.3a was pointed out to show the initial state of the samples before immersion. All prepared P3 paint samples revealed an excellent barrier performance after 4 days of immersion without any significant changes on the surface or even near the cross-scribed lines, as seen in Figure 7.3b.

At the 8th day of immersion, illustrated in Figure 7.3c, the first sign of degradation was observed in the image of P350 sample which is due to the corrosive chemical penetration. In contrary, the samples P310, P320, P330 and P340, with less loading ratio of Aktisil AM pigments performed well with higher barrier and act as an impermeable layer against the diffusion of the water, oxygen and other corrosive chemical ions.

From Figure 7.3d, after 15 days of immersion, all prepared P3 paint systems show loss of adhesion with slight peeling off near the centre of the cross. However, Figure 7.3d also indicates that the surface modified silane pigment P340 paint systems could be considered the best to stand up for 15 days of immersion.

Figure 7.3e and 7.3f represent the response of the remaining of P3 samples after 22 and 40 days of immersion respectively. There is no longer protection behavior was observed for any of the samples beyond 22 days. This usually is attributed to the failure and complete loss of adhesion of the coatings.



Figure 7.3: Acid resistance response for P3 system after a) 0, b) 4, c) 8, d) 15, e) 22 and f) 40 days of immersion in H_2SO_4 10 % solution



Figure 7.3: continued

7.2.4 Paint System with Aktisil PF 777 – P4

Figure 7.4(a-f) reveal the responses of the P4 paint systems which are reinforced with Aktisil PF 777 inorganic pigments. On the 4th day of immersion P450 paint system which yield under the highly acidic solution, showed a peel off in the coating significantly failing in its protection nature. The images of the immersed samples from only 4 samples out of 5 PVC systems namely P410, P420, P430 and P440 were used after 8 days of immersion.

These 4 paint systems demonstrated high resistance against penetration of the corrosive chemical molecules up to 8 days of immersion without any significant effects from the sulphuric acid as shown in Figures 7.4b and 7.4c.

At the 15th day of the immersion, just P410 paint system was survived with good barrier performance, as shown in Figure 7.4d. Meanwhile, signs of degradation near the centre of the cross-scribed line were observed for PVC content above 10 % in P4 paint systems. Beyond these days, these P4 paint system do not provide any barrier protection against the corrosive medium due to high PVC content. These images were detailed for prepared P4 paint system as shown in Figure 7.4e and 7.4f.



Figure 7.4: Acid resistance response for P4 system after a) 0, b) 4, c) 8, d) 15, e) 22 and f) 40 days of immersion in H_2SO_4 10 % solution



Figure 7.4: continued

7.3 Electrochemical Impedance Spectroscopy

In the present work, Electrochemical Impedance Spectroscopy (EIS) has been used in order to evaluate the anti-corrosion performance and the barrier performance of paint systems (P1, P2, P3 and P4). All experimental activities were carried out by using the three electrodes cell consisting of working electrode (WE), counter electrode (CE) and reference electrode (RE). The uncoated part of all the paint system samples were exposed to the artificial seawater (3.5 % NaCl) in a plastic tube subjected to the EIS studies up to 30 days of immersion and readings were recorded periodically. The response of all developed paint systems were shown in Figure 7.5 to Figure 7.20 and in Table 7.1 to Table 7.8 respectively.

7.3.1 Paint System with TiO₂ – P1

The electrochemical studies that carried out on the P1 paint systems are shown in Figure 7.5 to Figure 7.8. The coating resistance (R_c) values of all prepared P1 systems with different PVC, were recorded and plotted against the time of immersion (Figure 7.5) in order to investigate the effective role of TiO₂ pigments in enhancing the anticorrosion behavior of the acrylic-epoxy polymeric binder system. The performance of all prepared samples was divided according to the R_c value after 30 immersion days into three categories which is good, fair and poor coating. The classification procedures were based on the fact that R_c values above $10^9 \Omega\text{cm}^{-2}$ represent that the coating is very intact and has been described as good coating. Whereas, R_c values in the range between $10^9 - 10^8 \Omega\text{cm}^{-2}$ could be related to the diffusion barrier of electrolyte via coating pores. Coatings with R_c in this range were reported as fair coatings. However, $R_c < 10^6 \Omega\text{cm}^{-2}$ represents that the coating is undergoing a large area of delamination where blister formation and corrosion starts (Bierwagen et al., 2000; Loveday et al., 2004).

As illustrated in Figure 7.5, the first 5 days of immersion were enough to show that P110, P130 and P140 paint systems demonstrated a fair anti-corrosion performance while P120 and P150 paint systems could not sustain even for such short period. As the days progress, P130 paint system showed a stable corrosion resistance with R_c value in the range of $10^9 \Omega\text{cm}^{-2}$ up to 30 days of immersion in artificial sea water. This observation could be considered good evidence on the vital role of TiO_2 pigments (Radhakrishnan et al., 2009) in giving a good corrosion protection performance to the acrylic-epoxy binder. All other prepared P1 paint systems showed a lower R_c value during all the study time. The R_c values were found in complete agreement with coating capacitance results that shown in Figure 7.6. It is clear to notice that the highest R_c value of P130 paint system was corresponded to the lowest value of C_c . This C_c values continuously increasing with the immersion time were recorded for other P1 paint systems. It is worth to be mentioned that the increase in C_c values during the immersion in the electrolyte was attributed to gradual increase in sodium and chloride ions at the coating-metal interface. This leads to swelling of the coating and loss of its ideal dielectric behaviour (Amirudin & Thierry, 1995).

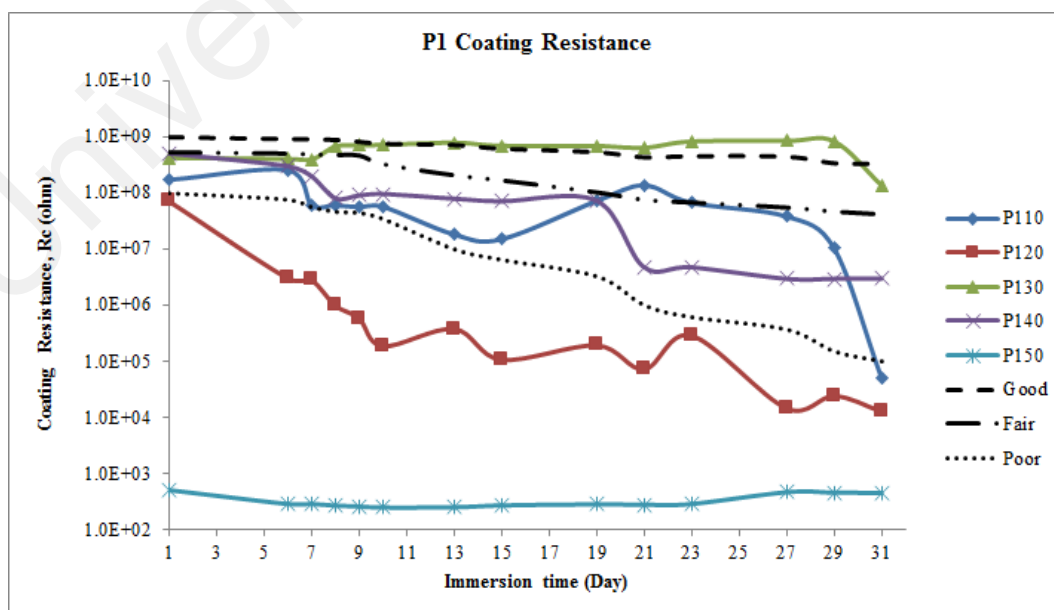


Figure 7.5: Coating Resistance (R_c) vs Time of immersion of P1 paint system

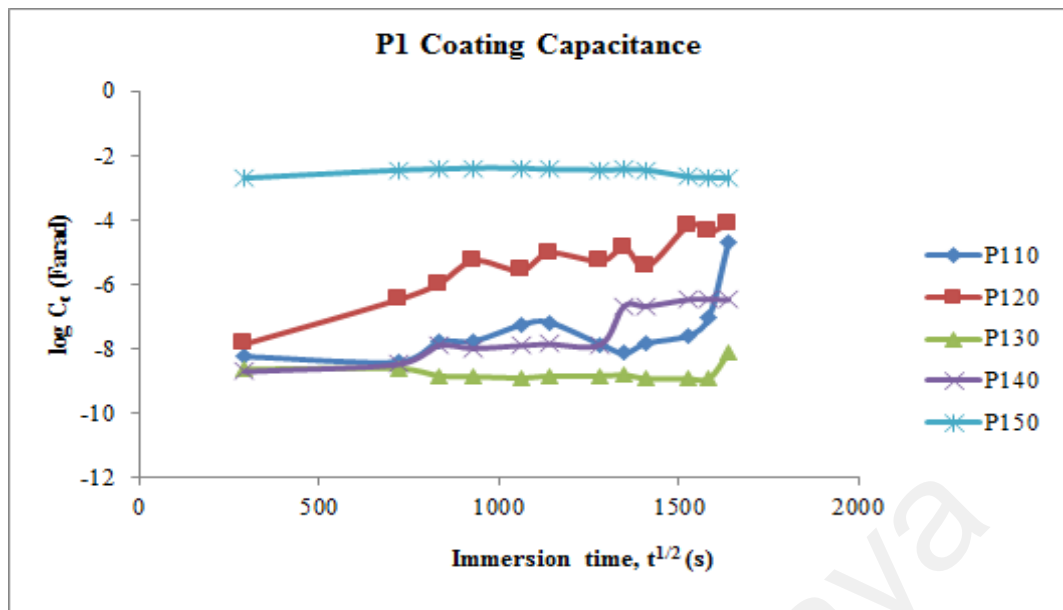


Figure 7.6: Coating Capacitance (C_c) vs Time of immersion of P1 paint system

Furthermore, these capacitance measurements were used to determine the dielectric constant (ϵ) by the employment of the equation mentioned in 2003 work of Castela and Simoes indicated that the uptake of the electrolyte by the paint film will lead to an increase of the dielectric constant and a higher coating capacitance (Castela & Simoes, 2003). Figure 7.7 illustrate the ϵ values of all P1 paint systems. As P130 system demonstrated the highest R_c and the lowest C_c values, so it was expected that P130 system has the lowest ϵ , approximately equal to 10, which was almost constant for 30 days of immersion time. This implies that the P130 paint system exhibits small porosity and possesses good barrier properties. Samples coated with other P1 paint systems showed dielectric constant values higher than 10 as shown in Figure 7.7. These observations in turn indicate the presence of pores and voids which may lead to electrolyte uptake and transport of ions (Na^+ and Cl^-) at the coating-metal interface (Moreno et al., 2012).

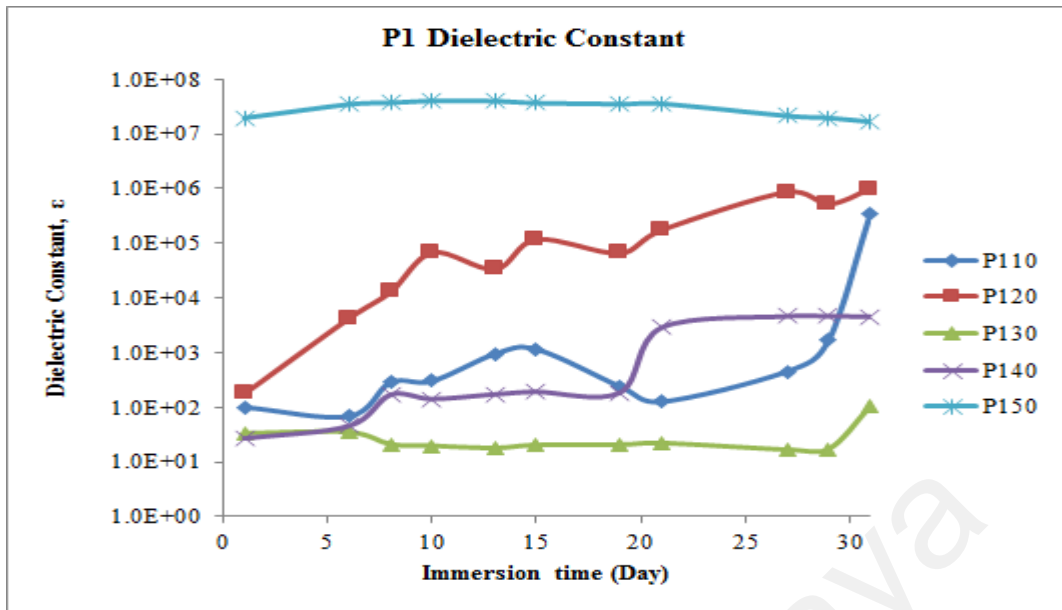


Figure 7.7: Dielectric Constant (ϵ) vs Time of immersion of P1 paint system

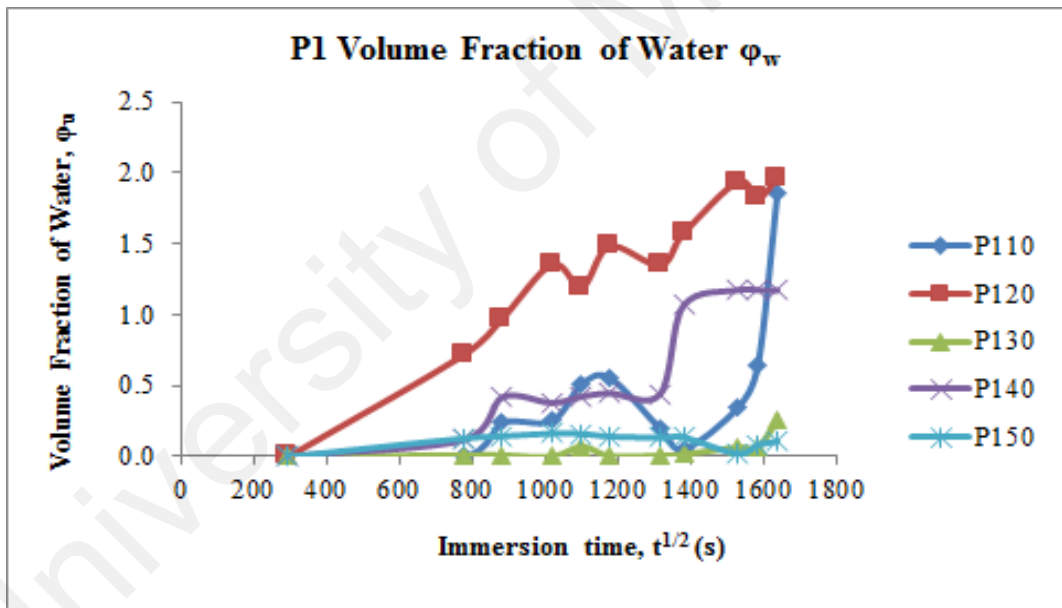


Figure 7.8: Volume Fraction of Water (ϕ_w) vs Time of immersion of P1 paint system

The greater performance of P130 paint system extended to be observed in the water uptake results that shown in Figure 7.8 with high barrier behavior up to 30 days of immersion time. This system has volume fraction of water (ϕ_w) in the range of 0.3 or lesser after 30 days of immersion. TiO_2 pigments at PVC content of 30 % showed the ability to enhance the barrier performance of the polymeric matrix with no significant absorption of the electrolyte. On the other hand, P150 paint system demonstrated water

uptake results incompatible with coating capacitance and dielectric constant for once. This observation could be attributed to the effect of the geochemical changes in the electrolyte, due to the corrosion reaction and its products. In turn, resulting in filling up the pores and the diffusion pathways over the time by the precipitates, thus reducing the permeability and the water uptake (Roh et al., 2000).

All the results recorded for P1 paint system, coating resistance (R_c), coating capacitance (C_c), dielectric constant (ϵ) and the volume fraction of water (ϕ_w) are tabulated in Tables 7.1 and 7.2.

Table 7.1: Coating Resistance and Coating Capacitance values after 1, 15 and 30 days of immersion in 3.5 % NaCl of P1 paint system

System Day	Coating Resistance, R_c (Ωcm^{-2})			Coating Capacitance, C_c (Farad)		
	1	15	30	1	15	30
P 110	1.7×10^8	1.5×10^8	5.0×10^4	5.9×10^{-9}	6.8×10^{-8}	2.0×10^{-5}
P 120	7.0×10^8	1.1×10^5	1.3×10^6	1.4×10^{-8}	9.5×10^{-6}	8.8×10^{-5}
P 130	4.2×10^8	1.9×10^8	1.4×10^8	2.4×10^{-9}	1.5×10^{-9}	3.4×10^{-7}
P 140	5.0×10^8	7.0×10^7	2.9×10^6	2.0×10^{-9}	1.4×10^{-8}	3.4×10^{-7}
P 150	2.0×10^2	2.7×10^2	2.9×10^2	2.0×10^{-3}	3.0×10^{-3}	2.0×10^{-3}

Table 7.2: Dielectric Constant and Water uptake values after 1, 15 and 30 days of immersion in 3.5 % NaCl of P1 paint system

System Day	Dielectric Constant, ϵ			Water uptake, ϕ_w		
	1	15	30	0	15	30
P 110	1.0×10^2	1.1×10^3	3.4×10^5	0	0.56	1.90
P 120	1.7×10^2	1.2×10^5	9.9×10^5	0	1.50	2.00
P 130	3.3×10^1	2.0×10^1	1.0×10^1	0	0.006	0.26
P 140	2.7×10^1	1.9×10^2	4.6×10^3	0	0.45	1.20
P 150	2.0×10^7	3.7×10^7	1.7×10^7	0	0.14	0.11

7.3.2 Paint System with Silitin Z 86 – P2

Figure 7.9 of P2 paint systems shows the changes in the coating resistance over immersion time for 30 days in 3.5 % NaCl solution. It was found that P2 paint systems with 10 % and 20 % PVC could withstand the penetration of the electrolyte and demonstrate good barrier performance with fair corrosion protection. R_c value in the range of $10^9 \Omega\text{cm}^{-2}$ after 15 days of immersion time. A sharp decrease in the coating resistance, R_c was observed with the other systems using PVC of P230, P240 and P250 paint systems with poor anti-corrosion properties. Good R_c value was recorded for P220 paint systems which perform the best protection capability over all the period of immersion. That can be explained as the Silitin Z 86 pigments have given a good contribution in enhancing the barrier performance of the P2 paint systems against the corrosive electrolyte diffusion up to 30 days of immersion.

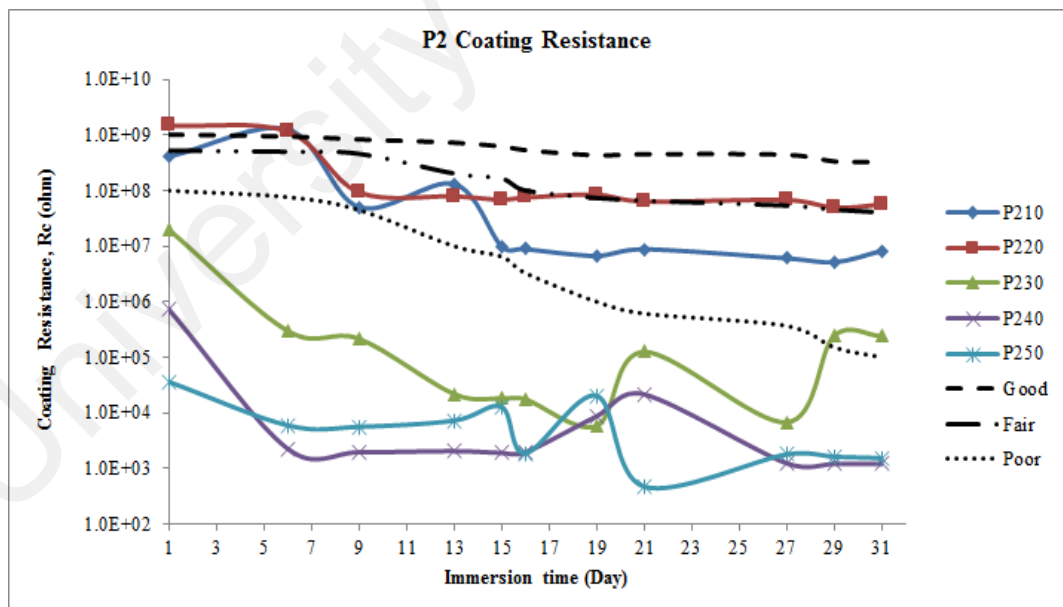


Figure 7.9: Coating Resistance (R_c) vs Time of immersion of P2 paint system

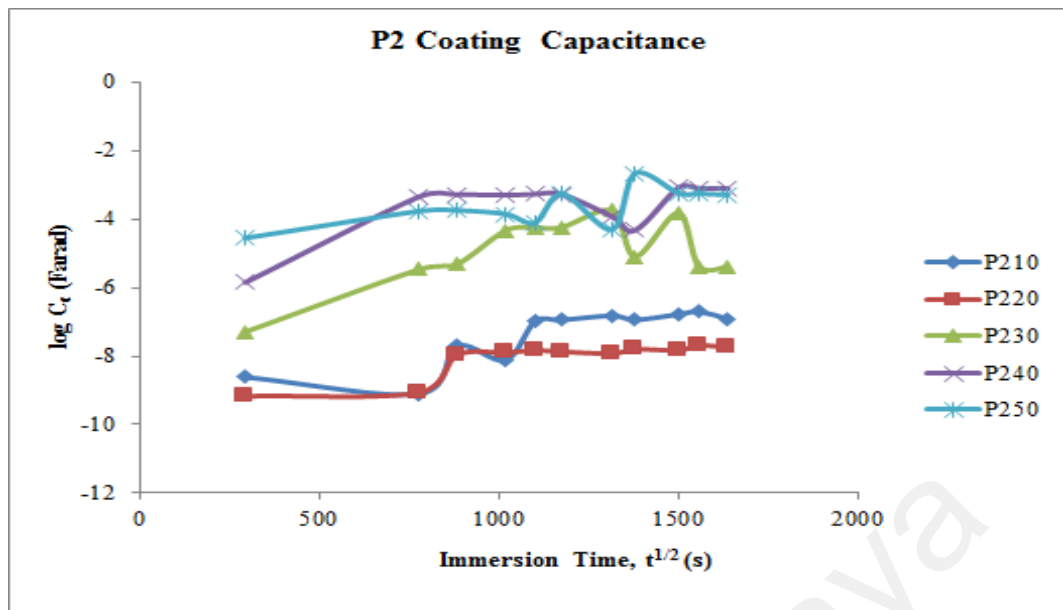


Figure 7.10: Coating Capacitance (C_c) vs Time of immersion of P2 paint system

Amirudin and Thierry (1995) have reported that using C_c to evaluate the coating behavior has the advantage as it can be determined during the whole immersion period as it depends on the deterioration on a microscopic scale along many points of the paint system. C_c values of all prepared P2 paint system were plotted against immersion time as shown in Figure 7.10. By analyzing the capacitance plots, one can conclude that the result of both R_c and C_c were in complete agreement and indicate the superiority of P220 paint system and the degradation over the time for other systems. Further studies were extended to the evaluation of the ϵ over the different periods of the immersion time as illustrated in Figure 7.11. P220 paint system remains demonstrating the lowest dielectric constant within the range of an inert coating system (8-10) which was stable until the 30th day of immersion. While other P2 paint systems showed a continuous increase in the ϵ value over the immersion time which was attributed by Castela and Simoes due to the presence of pores and voids in the paint (Castela & Simoes, 2003).

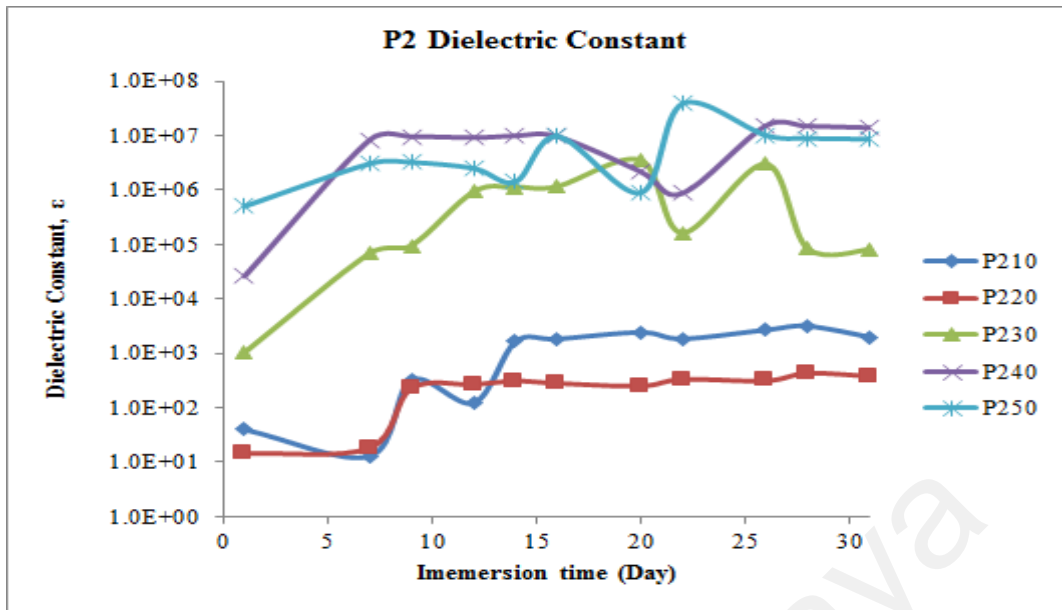


Figure 7.11: Dielectric Constant (ϵ) vs Time of immersion of P2 paint system

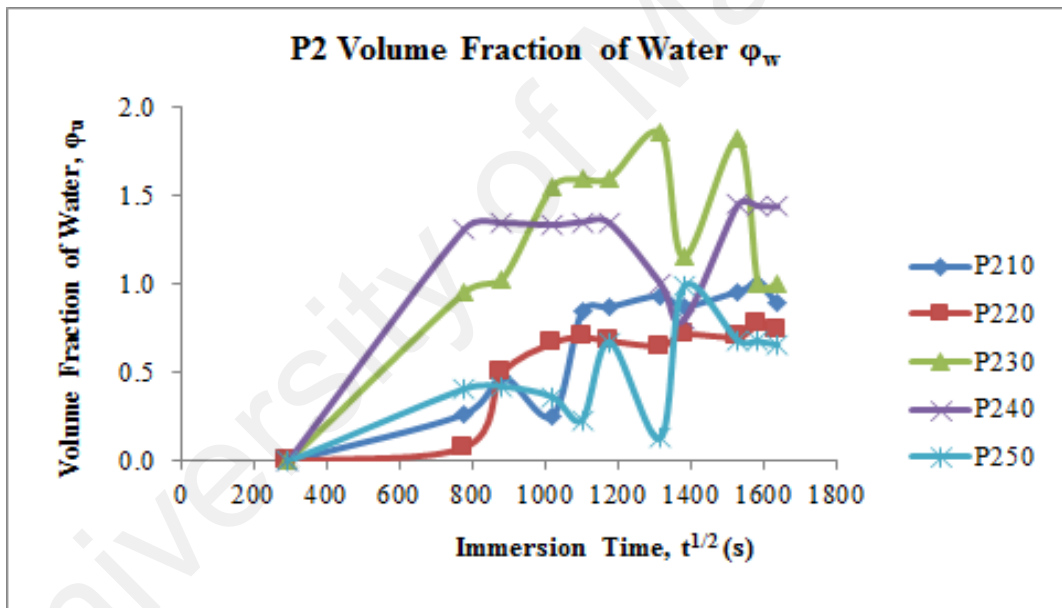


Figure 7.12: Volume Fraction of Water (ϕ_w) vs Time of immersion of P2 paint system

Ramesh et al., (2013) have used the water uptake factor results from EIS studies, in evaluating the barrier performance of the epoxy-polyester hybrid coating system. In the same way, the volume fraction of water (ϕ_w), that shown in Figure 7.12, was used in this study in order to investigate the barrier performance of the developed P2 paint systems. As the other studies revealed the superiority of P220 system, also same trend was observed in Figure 7.12 that the sample with P220 paint system contributed to the

lowest water uptake from the beginning and retain constant until the end of immersion, indicating it has the best barrier behavior. It is worth to mention that, the same observation of the previous P150 paint system with regard to the low value of the ϕ_w , were recorded for P250 paint system which also can be explained due to the same reason as the corrosion products and the precipitates participated in reducing the permeability and the water uptake (Roh et al., 2000).

Tables 7.3 and 7.4 have all the results of P2 paint systems including coating resistance (R_c), coating capacitance (C_c), dielectric constant (ϵ) and the volume fraction of water (ϕ_w).

Table 7.3: Coating Resistance and Coating Capacitance values after 1, 15 and 30 days of immersion in 3.5 % NaCl of P2 paint system

System Day	Coating Resistance, R_c (Ωcm^{-2})			Coating Capacitance, C_c (Farad)		
	1	15	30	1	15	30
P 210	4.1×10^8	9.9×10^6	8.2×10^6	2.4×10^{-9}	1.1×10^{-7}	1.2×10^{-7}
P 220	1.5×10^9	6.8×10^7	5.6×10^7	6.8×10^{-10}	1.3×10^{-8}	1.8×10^{-8}
P 230	2.0×10^7	1.8×10^4	2.4×10^5	5.1×10^{-8}	5.7×10^{-5}	4.1×10^{-6}
P 240	7.2×10^5	1.9×10^3	1.2×10^3	1.4×10^{-6}	5.2×10^{-4}	7.7×10^{-4}
P 250	3.6×10^4	1.3×10^4	1.5×10^3	2.8×10^{-5}	5.4×10^{-4}	5.1×10^{-4}

Table 7.4: Dielectric Constant and Water uptake values after 1, 15 and 30 days of immersion in 3.5 % NaCl of P2 paint system

System Day	Dielectric Constant, ϵ			Water uptake, ϕ_w		
	1	15	30	0	15	30
P 210	3.9×10^1	1.8×10^3	2.0×10^3	0	0.80	0.90
P 220	1.4×10^1	2.8×10^2	3.7×10^2	0	0.60	0.70
P 230	1.0×10^3	1.1×10^6	8.1×10^4	0	1.60	1.00
P 240	2.6×10^4	9.6×10^6	1.4×10^7	0	1.30	1.40
P 250	5.0×10^5	9.7×10^6	8.6×10^6	0	0.60	0.60

7.3.3 Paint System with Aktisil AM – P3

Figure 7.13 and 7.14 display the corrosion resistance (R_c) and coating capacitance (C_c) of P3 paint systems with Aktisil AM against immersion time respectively. The R_c values were utilized to evaluate the corrosion protection ability of the developed P3 paint systems. The results over different immersion periods evidence that the P320 has the highest coating resistance. However, P310, P330 and P340 also showed a good corrosion resistance with R_c in the range of $10^8 \Omega\text{cm}^{-2}$ at the day 30th of immersion. Only the paint system with 50 % PVC demonstrated a poor coating resistance overall during the study period.

The lower R_c of the paint systems reinforced with high value of PVC can be explained as follows: as the amount of the pigments increase within the polymeric matrix, the cross-linking density decrease. Furthermore, the high tendency of the reinforcing particles to form aggregations at high loadings, especially at PVC equals to 50 % can lead to a reducing in the barrier performance of a paint systems (Ramezanzadeh et al., 2011).

The C_c that illustrated in the Figure 7.14, result in the same conclusion where P320 demonstrates the best corrosion resistance as it had the lowest C_c value without significant change during all immersion time. The degradation of the P350 paint system was also confirmed by the continuous increase in the C_c value throughout the time of exposure. It is worth to be mentioned also that the both R_c and C_c results indicate the acceptable durability of P310, P330 and P340 with the observation of the good barrier performance against the penetrating of the electrolyte up to 30 days of immersion.

The 2013 work of Ramesh et al., pointed out that the process which leads to degradation of a polymer usually occur in several ways may initiated with the penetrating of the water molecules and ions into the coating. However, the electrolyte

3.5 % NaCl solution, have a preference to penetrate via the areas with lower cross-linking density. This process will be followed by the ion exchange processes. In this process, the ions carried by the electrolyte turn to be attached to the polymeric coating (Ramesh et al., 2013).

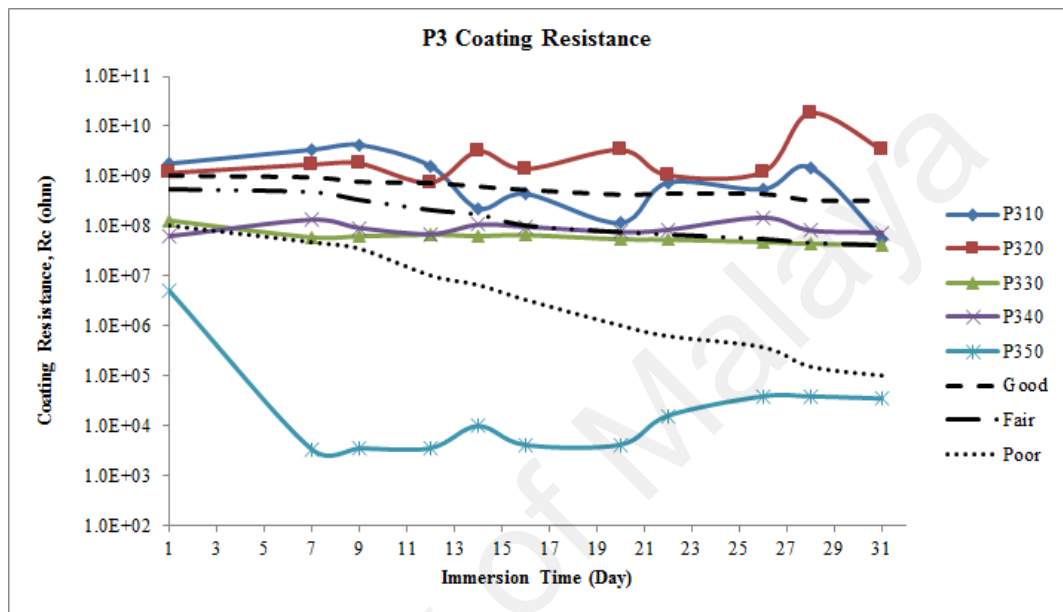


Figure 7.13: Coating Resistance (R_c) vs Time of immersion of P3 paint system

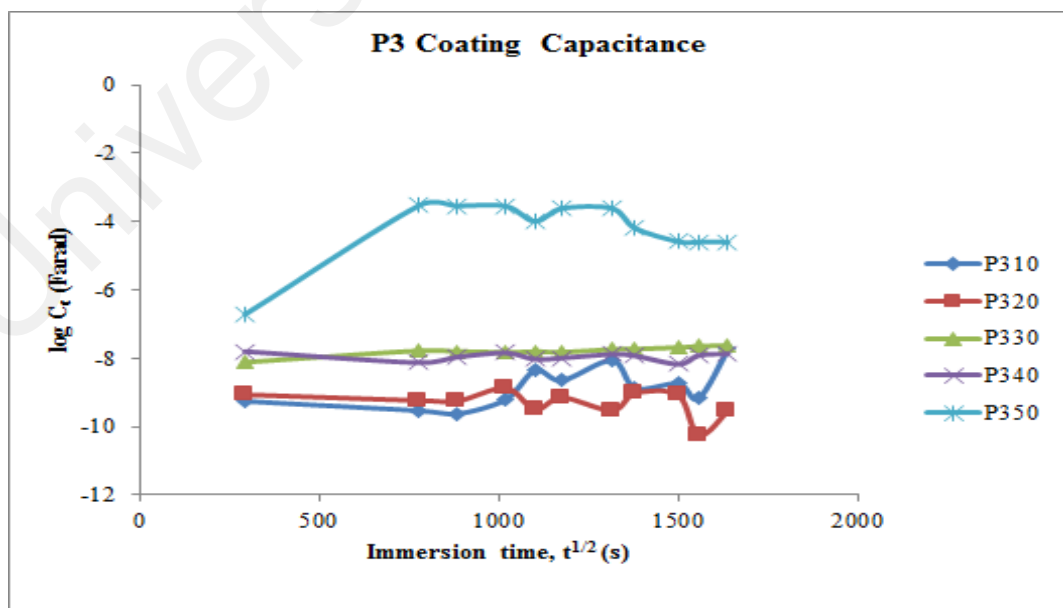


Figure 7.14: Coating Capacitance (C_c) vs Time of immersion of P3 paint system

It is necessary to determine the dielectric constant (ϵ) and the volume fraction of water (ϕ_w) as illustrated in Figures 7.15 and 7.16 respectively, in order to form a full image and a well understanding about the analyzed paint systems. Full matched results among all studied parameters were observed for all P3 paint systems. For instance, the high R_c results in low C_c which in turn leads to the small ϵ and ϕ_w . P320 and P340 has very close and consistent ϕ_w value. This could be related to PVC very close to CPVC.

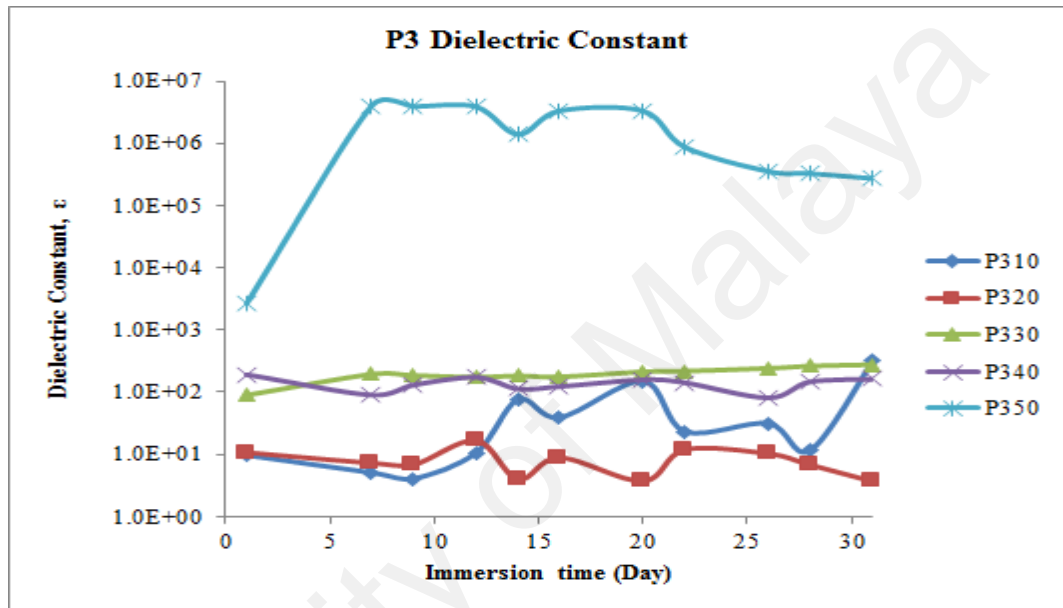


Figure 7.15: Dielectric Constant (ϵ) vs Time of immersion of P3 paint system

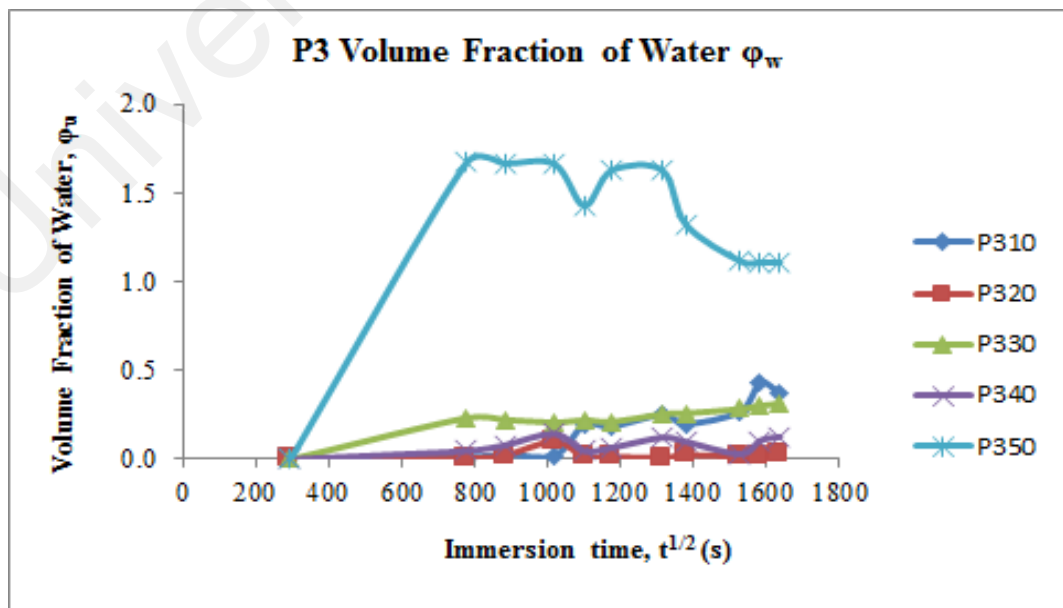


Figure 7.16: Volume Fraction of Water (ϕ_w) vs Time of immersion of P3 paint system

All the results of P3 paint system which include the coating resistance (R_c), the coating capacitance (C_c), the dielectric constant (ϵ) and the volume fraction of water (ϕ_w) after 1, 15 ad 30 days of immersion in 3.5 % NaCl solution are tabulated in Tables 7.5 and 7.6.

Table 7.5: Coating Resistance and Coating Capacitance values after 1, 15 and 30 days of immersion in 3.5 % NaCl of P3 paint system

System Day	Coating Resistance, R_c (Ωcm^{-2})			Coating Capacitance, C_c (Farad)		
	1	15	30	1	15	30
P 310	1.8×10^9	4.4×10^8	5.5×10^7	5.6×10^{-10}	2.3×10^{-9}	1.8×10^{-8}
P 320	1.2×10^9	1.4×10^9	3.4×10^9	8.6×10^{-10}	7.2×10^{-10}	3.0×10^{-10}
P 330	1.3×10^8	6.6×10^7	4.2×10^7	7.7×10^{-9}	1.5×10^{-8}	2.4×10^{-8}
P 340	6.3×10^7	9.7×10^7	7.4×10^7	1.6×10^{-8}	1.0×10^{-8}	1.3×10^{-8}
P 350	5.1×10^6	4.1×10^3	4.5×10^4	1.9×10^{-7}	2.4×10^{-4}	2.5×10^{-5}

Table 7.6: Dielectric Constant and Water uptake values after 1, 15 and 30 days of immersion in 3.5 % NaCl of P3 paint system

System Day	Dielectric Constant, ϵ			Water uptake, ϕ_w		
	1	15	30	0	15	30
P 310	0.9×10^1	3.9×10^1	3.1×10^2	0	0.20	0.30
P 320	1.1×10^1	0.9×10^1	0.9×10^1	0	0.01	0.03
P 330	8.9×10^1	1.8×10^2	2.7×10^2	0	0.20	0.30
P 340	1.9×10^2	1.2×10^2	1.6×10^2	0	0.06	0.10
P 350	2.7×10^3	3.3×10^6	2.7×10^5	0	1.63	1.10

7.3.4 Paint System with Aktisil PF 777 – P4

The Figures 7.17 to Figure 7.20 illustrate all electrochemical studies that took place in order to investigate the properties of P4 paint systems that consist of acrylic-epoxy polymeric matrix as a host and Aktisil PF 777 as inorganic reinforcing pigments. The corresponding coating resistance (R_c) values of all prepared P4 systems over the 30 days of immersion in 3.5 % NaCl solution were recorded and plotted against the time of immersion as shown in Figure 7.17.

The results of R_c indicate that Aktisil PF 777 pigments had a significant influence in enhancing the corrosion resistance at 10 % PVC value up to 30 days of immersion. However, increasing the PVC above 10 % did not show any further improvement in the corrosion protection properties. Despite that, paint system P420 and P430 also showed fair performance over the 30th days of immersion. Noticeable failure was recorded for both P440 and P450 paint systems from the beginning of the immersion process with a major drop in R_c within 7 days of immersion. The initial penetration of electrolyte into the interface of the coating and substrate would have caused the formation of corrosion product and this would have extended to other areas and reduce the adhesion of the coating with the substrate and hence the resistance values decreased further (Deflorian & Rossi, 2006).

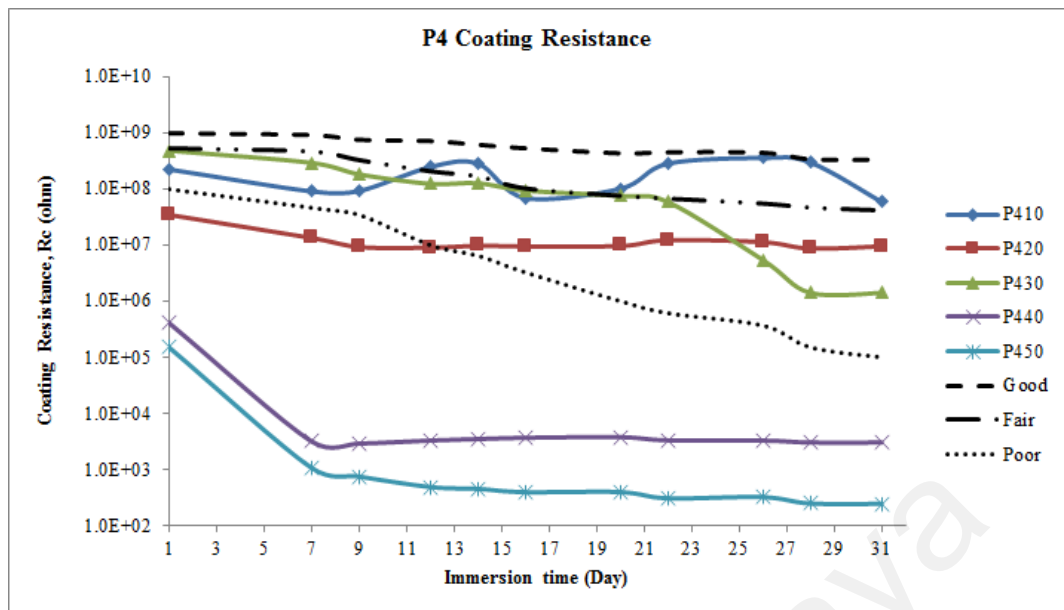


Figure 7.17: Coating Resistance (R_c) vs Time of immersion of P4 paint system

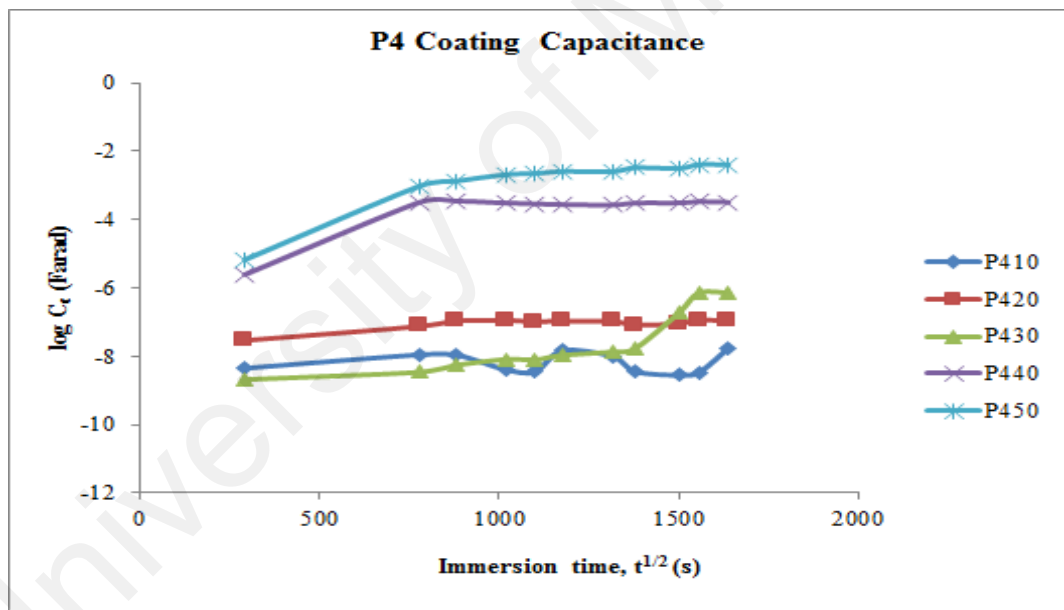


Figure 7.18: Coating Capacitance (C_c) vs Time of immersion of P4 paint system

The C_c behavior of all the mild steel panels coated with P4 paint systems was shown in 7.18. These calculated C_c value designate the superiority of the low PVC content observing a stable low C_c value for P410 paint systems over the 30 days of immersion in this study. Moreover, all C_c values were found in a reasonable match with the R_c values.

All these observations were further supported with the ϵ and ϕ_w which in turn is illustrated in Figures 7.19 and 7.20 respectively. It was found that the increase of the PVC in paint systems leads to the loss of the desirable properties in the P4 paint systems. In other words, high R_c , low C_c , ϵ and ϕ_w were recorded in the case of using the lowest PVC value (10 %). In the meantime, higher PVC values show obvious decrease in R_c and increase on C_c , ϵ and ϕ_w .

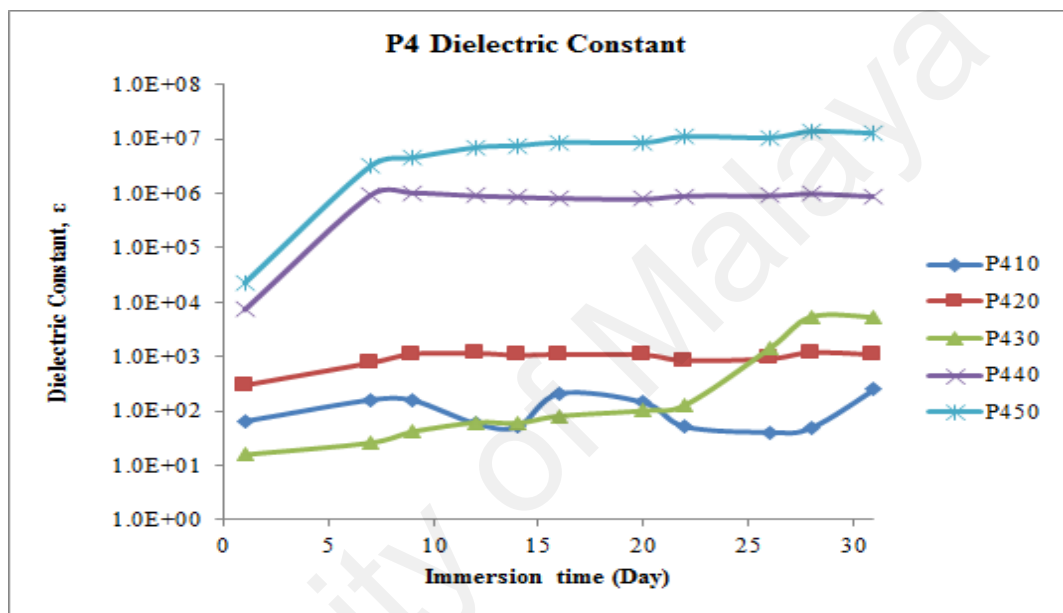


Figure 7.19: Dielectric Constant (ϵ) vs Time of immersion of P4 paint system

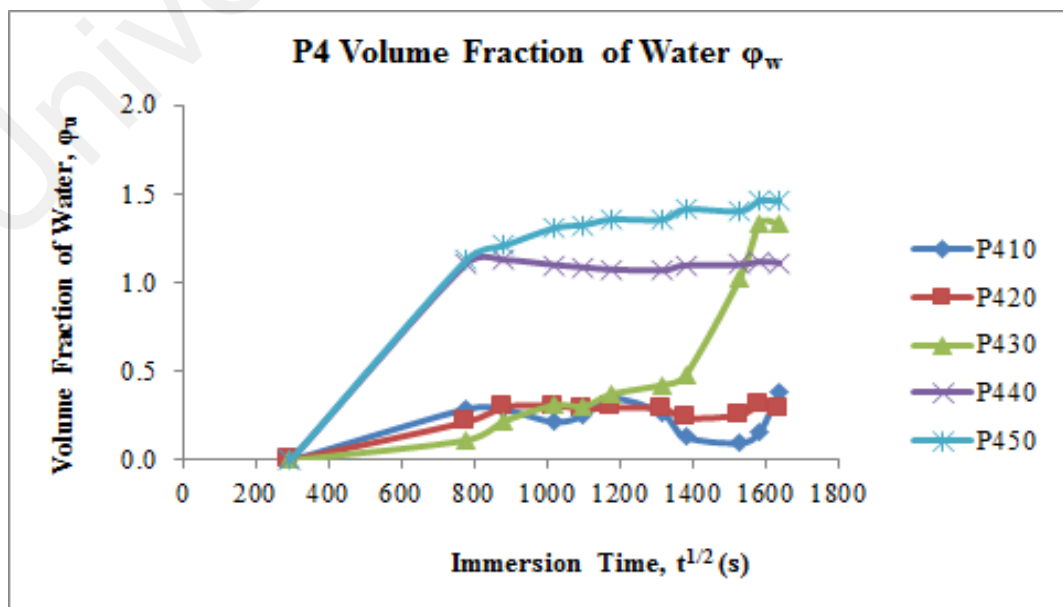


Figure 7.20: Volume Fraction of Water (ϕ_w) vs Time of immersion of P4 paint system

Tables 7.7 and 7.8 have all the results of P4 paint systems including coating resistance (R_c), coating capacitance (C_c), dielectric constant (ϵ) and the volume fraction of water (ϕ_w).

Table 7.7: Coating Resistance and Coating Capacitance values after 1, 15 and 30 days of immersion in 3.5 % NaCl of P4 paint system

System Day	Coating Resistance, R_c (Ωcm^{-2})			Coating Capacitance, C_c (Farad)		
	1	15	30	1	15	30
P 410	2.2×10^8	6.8×10^7	5.8×10^7	4.5×10^{-9}	1.5×10^{-8}	1.7×10^{-8}
P 420	3.4×10^7	9.3×10^6	8.9×10^6	2.9×10^{-8}	1.1×10^{-7}	1.1×10^{-7}
P 430	4.8×10^8	9.3×10^7	1.4×10^6	2.1×10^{-9}	1.1×10^{-8}	7.2×10^{-7}
P 440	4.0×10^5	3.6×10^3	3.0×10^3	2.5×10^{-6}	2.8×10^{-4}	3.2×10^{-4}
P 450	1.5×10^5	3.9×10^2	2.4×10^2	6.8×10^{-6}	2.6×10^{-3}	4.0×10^{-3}

Table 7.8: Dielectric Constant and Water uptake values after 1, 15 and 30 days of immersion in 3.5 % NaCl of P4 paint system

System Day	Dielectric Constant, ϵ			Water uptake, ϕ_w		
	1	15	30	0	15	30
P 410	6.5×10^1	2.1×10^2	2.5×10^2	0	0.30	0.40
P 420	3.0×10^2	1.1×10^3	1.1×10^3	0	0.90	0.30
P 430	1.6×10^1	8.1×10^1	5.3×10^3	0	0.30	1.30
P 440	7.3×10^3	8.1×10^5	8.8×10^5	0	1.00	1.10
P 450	2.3×10^4	8.7×10^6	1.3×10^7	0	1.30	1.40

7.4 Summary

The acid resistance and EIS techniques were used to evaluate the performance and critical properties of AE paint system under laboratory corrosive environments. Interfacial integrity is essential in the barrier performance and overcome the penetrating of the corrosive agents toward the painted panels. Comparing performance from Table 7.9, paint system for P110, P130, P220, P340 and P410 have good acid resistance at least up to 15th day of direct cross-scribed immersion in H₂SO₄ 10 % solution.

Table 7.9: Acid Resistance Test and EIS Performance Comparison

Acid Resistance Test																	Best				
PVC	10%				20%				30%				40%					50%			
DAY	4	8	15	22	4	8	15	22	4	8	15	22	4	8	15	22		4	8	15	22
P1	P110						X	X	P130				X	X	X	X	X	X	X	X	P110 / P130
P2			X	X	P220				X	X	X	X	X	X	X	X	X	X	X	X	P220
P3			X	X			X	X			X	X	P340				X	X	X	X	P340
P4	P410						X	X			X	X			X	X	X	X	X	X	P410
X = Fail																					
Electrochemical Impedance Spectroscopy $R_c, C_c, \epsilon, \phi_w$																	Best				
PVC	10%				20%				30%				40%					50%			
DAY	30				30				30				30					30			
P1	X				X				P130				X				X				P130
P2	X				P220				X				X				X				P220
P3	X				P320				X				X				X				P320
P4	P410				X				X				X				X				P410

EIS is well-suited for quantitative evaluation using equivalent circuit elements that enable to one follow the mechanism of paint protective properties in terms of water uptake, diffusion and electrical conduction through the paint. The paint systems P130, P220, P320 and P410 has performed well by having all the requirements of good coating based on values obtained from Table 7.1 to Table 7.8. A relationship can be seen from these two studies for best performing development of anti-corrosion coating using organic resins hybrid system. The best among all paint systems were the P320, a sample with 10 wt% E in 90 wt% A and PVC 20 % of pigment Aktisil AM. This P320 has better overall performance compared to base binder system (90A10E).

CHAPTER 8: RESULTS AND DISCUSSION ON PAINT SYSTEM

CRITICAL PIGMENT VOLUME CONCENTRATION

8.1 Introduction

When coatings are formulated, one important characteristic value is the pigment volume concentration (PVC), which strongly affects their properties. The volume percentage of pigment in a dry paint has been defined as PVC. Furthermore, there is a critical pigment volume concentration (CPVC) in many coating formulation containing pigments or dyes (Lobnig et al., 2006). Below the CPVC, the pigment can uniformly distribute in the binder matrix without harming its integrity and compactness. While above the CPVC, the excessive pigment cannot be fully packed by the binder, thus pores and voids occur in the coating matrix (Liu et al., 2012).

Various methods can be used to determine this CPVC percentage with one of them is via EIS method. EIS is a suitable method to determine the CPVC of coatings, especially for inorganic pigment based organic coatings (Liu et al., 2010). Acrylic-Epoxy hybrid binder system with best blending ratio (90A10E) that has performed well in physical, mechanical, thermal, structural and corrosion studies were used to formulate paint systems. With four types of the inorganic pigments, PVC ranging from 10 % to 50 % used with the corresponding developed paint systems namely P1 with TiO₂, P2 with Silitin Z 86, P3 with Aktisil AM and P4 with Aktisil PF 777 were investigated. As the PVC increased in a series of coating made with the same pigments and binders, the density, adhesion and mechanical strength increases to a maximum. When PVC equals CPVC, the overall performance of coating system is usually at its best at this point (Kalendova et al., 2008; Sorensen et al., 2009a).

8.2 Critical Pigment Volume Concentration

The CPVC of a solvent based hybrid AE with various PVC was analyzed. It was shown that EIS is suitable method to detect CPVC of paint systems. The CPVC is a transition point with respect to moisture transport in a coating system. Most additives seriously enlarge solubility and equilibrium absorption values of water in the coating, thereby increasing permeability (Van der Wel & Adan, 1999). The parameters such coating resistance (R_c), coating capacitance (C_c), dielectric constant (ϵ) and volume fraction of water (ϕ_w) from previous P1, P2, P3 and P4 EIS studies were used to determine diffusion rate (D). EIS give an accurate measurement to determine diffusion coefficient of water because of the separation of interfacial and diffusion process on the frequency scale (Bierwagen et al., 2008; Hinderliter et al., 2006).

In the present work, EIS results of AE and paint system have been used in order to evaluate the best PVC ratio for anti-corrosion and the barrier performance of paint systems (P1, P2, P3 and P4). The painted samples were exposed to the artificial seawater (3.5 % NaCl) in a plastic tube subjected to the EIS studies up to 30 days of immersion and readings were recorded periodically.

CPVC is determined using R_c and diffusion rate plotted towards PVC values for all paint system. From the results, the coating resistance, R_c response of all developed paint systems were shown in Figure 8.1, Figure 8.2 and Table 8.1. The diffusion coefficient rate, D is shown in Figure 8.3 and Table 8.2 respectively. Correlation of high R_c value and low diffusion rate would indicate the CPVC position for the respective paint systems.

During the 30 days of immersion, the values of coating resistance will be in the range of $10^9 - 10^7 \Omega\text{cm}^{-2}$ for good performing coating system. From the Figure 8.1a and Table 8.1, it is observed that the R_c value of $8.35 \times 10^8 \Omega\text{cm}^{-2}$ for the P1 system solely containing TiO_2 with PVC 30 % were the highest resistance recorded among all other PVCs.

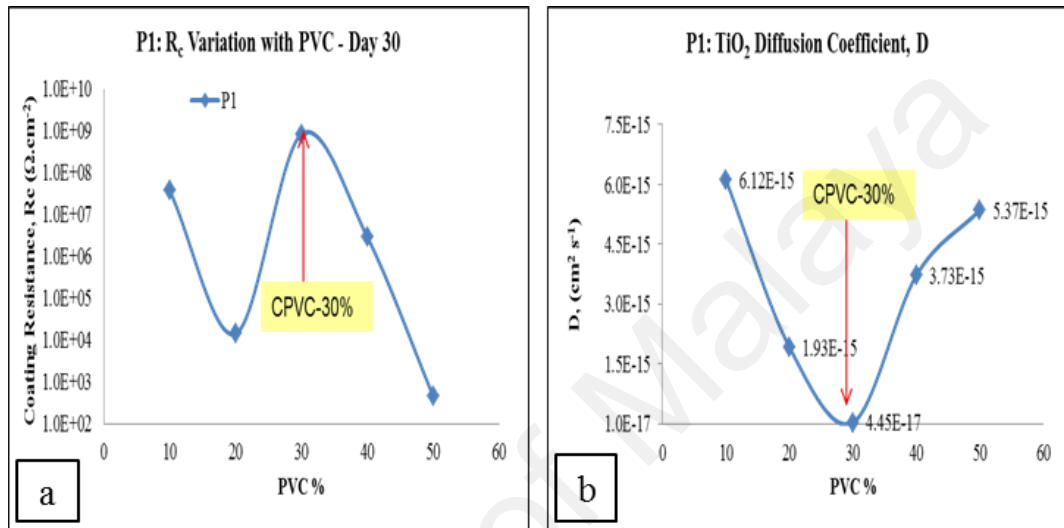


Figure 8.1: a) Coating Resistance, R_c b) Diffusion coefficient, D

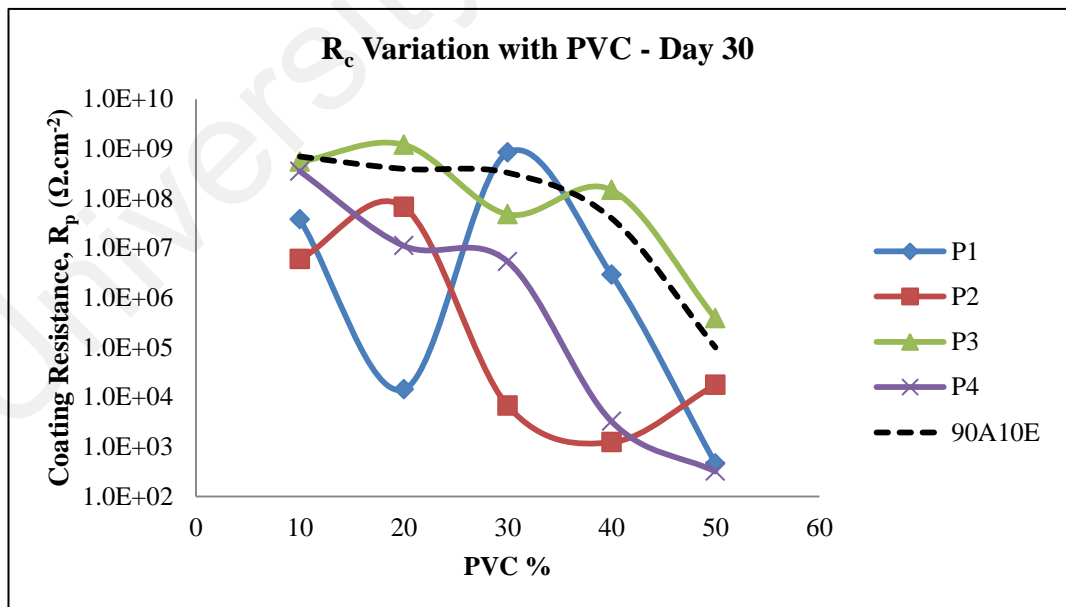


Figure 8.2: Coating Resistance, R_c vs PVC % of AE binder and paint system

Table 8.1: Paint Coating Resistance values at 30 days of immersion in 3.5 % NaCl

PVC %	P1-TiO ₂	P2-Silitin Z 86	P3-Aktisil AM	P4-Aktisil 777	90A10E
10	3.8 x 10 ⁷	6.0 x 10 ⁶	5.5 x 10 ⁸	3.5 x 10 ⁸	7.0 x 10 ⁸
20	1.4 x 10 ⁴	6.8 x 10 ⁷	1.2 x 10 ⁹	1.1 x 10 ⁷	3.9 x 10 ⁸
30	8.4 x 10 ⁸	6.7 x 10 ³	4.8 x 10 ⁷	5.4 x 10 ⁶	3.3 x 10 ⁸
40	2.9 x 10 ⁶	1.2 x 10 ³	1.5 x 10 ⁸	3.2 x 10 ³	4.0 x 10 ⁷
50	4.6 x 10 ²	1.8 x 10 ⁴	3.8 x 10 ⁵	3.4 x 10 ²	1.0 x 10 ⁵

While, comparing diffusion rate from Figure 8.1b and Table 8.2, D for P1 paint system has the lowest value of $4.4 \times 10^{-17} \text{ cm}^2\text{s}^{-1}$ at PVC 30 %. This confirms that CPVC for paint system P1 with inorganic pigment TiO₂ will be at 30 % of PVC. P1 system containing PVC below CPVC shows an increasing trend in R_c. The R_c of P1 system decreases when PVC value is greater than CPVC. Opposite trend are observed in diffusion graphs where D value decreases to a minimum point and there after it shows an increasing trend.

This indicates that for P1 paint system, CPVC 30 % of TiO₂ addition in the polymeric binder matrix will yield best overall properties. Below this CPVC values, the pigment are uniformly distributed in the binder matrix without harming its integrity and compactness. While above the CPVC, the excessive pigment cannot be fully packed by the binder, and pore and voids occur in the coating matrix (Liu et al., 2012).

Comparing performance from Figure 8.2, Figure 8.3, Table 8.1 and Table 8.2, paint system for P2 has CPVC at 20 % of Silitin Z 86 and 20 % of Aktisil AM for P3. Meanwhile P4 has CPVC at 10 % of Aktisil PF 777. Therefore paint system P130, P220, P320 and P410 have CPVC at different PVC concentration due to different inorganic pigments were used in the development of anti-corrosion coating using organic resins hybrid system.

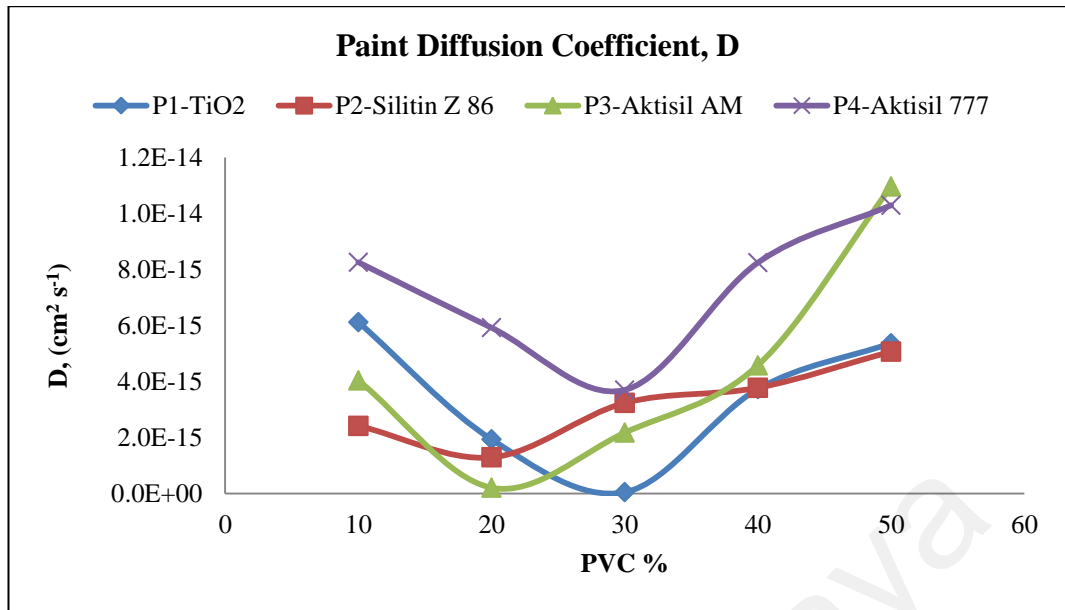


Figure 8.3: Paint Diffusion Coefficient Rate, D vs PVC % of paint system

Table 8.2: Paint Diffusion Rate values at 30 days of immersion in 3.5 % NaCl

PVC %	P1-TiO ₂	P2-Silitin Z 86	P3-Aktisil AM	P4-Aktisil 777
10	6.1 x 10 ⁻¹⁵	2.4 x 10 ⁻¹⁵	4.0 x 10 ⁻¹⁵	8.3 x 10 ⁻¹⁵
20	1.9 x 10 ⁻¹⁵	1.3 x 10 ⁻¹⁵	2.1 x 10 ⁻¹⁶	5.9 x 10 ⁻¹⁵
30	4.4 x 10 ⁻¹⁷	3.2 x 10 ⁻¹⁵	2.2 x 10 ⁻¹⁵	3.7 x 10 ⁻¹⁵
40	3.7 x 10 ⁻¹⁵	3.8 x 10 ⁻¹⁵	4.6 x 10 ⁻¹⁵	8.2 x 10 ⁻¹⁵
50	5.4 x 10 ⁻¹⁵	5.1 x 10 ⁻¹⁵	1.1 x 10 ⁻¹⁴	1.0 x 10 ⁻¹⁴

In this study, R_c value of AE hybrid binder system was also plotted along with all paint systems. From Figure 8.2, P130, P320 and P340 has improved its anti-corrosion properties compared to its own binder system during long exposure in aggressive corrosion medium. The acid resistance and EIS techniques were used to evaluate the performance and critical properties of AE paint system that confirming correlation in findings. Paint system for P130, P220, P340 and P410 have good acid resistance at least up to 15th day of direct cross-scribed immersion in H₂SO₄ 10 % solution. Meanwhile paint system for P130, P220, P320 and P410 performed well, having all the requirements of good corrosion resistance properties as stipulated in EIS

studies. Interfacial integrity is essential in the barrier performance and overcome the penetrating of the corrosive agents toward the painted panels (Roh et al., 2000). Critical permeability profiles such as these can reasonably be controlled by balancing the PVC and CPVC ratio of the primer in the initial formulating process so that sufficient moisture reaches the pigment to dissolve enough inhibitor to maintain the passive film for as long as possible and without its being so permeable as to allow depassivating ions access from the exterior of the film to the substrate (Gowri & Balakrishnan, 1994; Rodriguez et al., 2004).

8.3 Summary

EIS is well-suited for quantitative evaluation using equivalent circuit elements that enable to one follow the mechanism of paint protective properties in terms of coating resistance, coating capacitance, water uptake, diffusion rate and electrical conduction through the paint film. CPVC is determined using R_c and diffusion rate plotted towards PVC values for all paint system. A relationship with CPVC confirmation can be seen from these two studies for best performing development of anti-corrosion coating using organic resins hybrid system. P3 system has performed well in all the analytical tests. A sample with 10 wt% Epoxy in 90 wt% Acrylic and PVC 20 % of pigment Aktisil AM was a good stand out paint system.

CHAPTER 9: DISCUSSION

As the development of the protective coatings industry moves into the 21st century, the need to develop high-performance and cost effective coating is a must. Coating materials with superior properties to suit the stringent environmental conditions is pressing. This has shifted the manufacturers to emphasize onto laboratory research for new coating materials, particularly in accelerated anti-corrosion coatings.

Corrosion control can be achieved with proper material selection, environmental modifications, alloying, anodizing, cathodic protection and protective coatings. Coatings may possibly be organic (polymer), inorganic (ceramics or glass) or metallic (electroplating or galvanizing metals) and hybrid coatings (Rau et al., 2011; Xing et al., 2011). Although corrosion control techniques are much diversified, in principle coating prevents contact between the corrosion agent and the material surface (Bierwagen, 1996). The main function of a coating is to isolate, separate and protect the metal from any aggressive medium.

Organic coatings are the most popular form of corrosion protection compared to other means because of the low cost, ease of application and suitability to various environments. Organic protective coatings, such as paint must have good flexibility, high resistance against impact, chemical and environment attack, resistance to permeation of moisture, good adhesion and cohesion. Paints are used for protection purpose as well as for decoration. The main constituents of paints are binders, solvents, pigments and extenders. Binders are basically organic resins. They provide the backbone of the coating system.

Coating formulation involves a combination of performance and costing. Applications for excellent resistance to extreme environments require resins that are more costly, such as epoxies and polyurethanes. Most decorative finishes contain lower cost acrylic resin that is perfectly suitable for general settings. Different resins can be combined into a hybrid mixture designed to deliver specific performance capabilities.

In this first part of study, a hybrid system which forms compatible blends with epoxy resin was developed. The developed hybrid system can be used as a flexibilizer and toughener for the low priced acrylic polyol resin. The properties of the developed hybrid coating system (AE) have been methodically investigated using different analytical methods covering physical, mechanical, thermal, structural and electrochemical performances in order to satisfy corrosion protection.

For the development of good performing hybrid binder system AE, two different resins have been utilized. Acrylic Polyol resin (A) with 2.9 % of OH value and Bisphenol-A Epoxy (E) resin were used in the binder formulations. Polyisocyanate (NCO) was also used as a cross-linking agent. These resins have been taken in different compositions from 20-80 wt% and vice versa. The mixtures were thoroughly blended and applied using decorative brush on the pretreated mild steel panels. The panels were allowed to dry for 1 week before proceeding to perform the characteristic analyzes.

In view of the increasing use of modern coating systems, rheological characterization is becoming more important to guarantee constant product quality in terms of pot life and application preference (Dulux, 2010). In the investigation, the viscosity measurement has been taken as a measure of resistance to flow and as the shear stress divided by shear rate (Ocampo et al., 2005). When shear flow is driven by gravity, kinematics viscosity is measured and analyzed using viscosity master software.

If the shear rate is high then the viscosity is low and vice versa. Viscosities for 20-50 wt% of acrylic resin (A) are lower due to higher percentage of epoxy resin (E) and less chemical reaction between the resins. This is caused by incompatible ratio in blending system. Conversely hybrid systems with 60-90 wt% of A have a higher viscosity with shear thickening compared to 100 wt% A. The coating developed to be highly protective, tend to have higher viscosities. To achieve good application characteristics, good paints have to be non-Newtonian liquids, which are highly shear rate dependent (Ocampo et al., 2005). It is possible that the available hydroxyl group in acrylic resin to form bonding in order to increase network density, thereby increasing viscosity of the blending systems as reported by Ocampo et al., 2005 and Rau et al., 2011.

It is observed that the average drying time was directly proportional with epoxy resin blending ratio. As expected, the binder system consisting 10 wt% acrylic resin and 90 wt% epoxy resin (10A90E) was not cured permanently. Polyisocyanate resin was the only hardener used in binder mixture and epoxy resin was prepared by dissolving a known amount of commercial grade xylene as solvent. From the results, high viscosity of the coating system consisting 80A20E and 90A10E takes about 3 hours to cure perfectly. As the percentage of epoxy resin increases above 40 wt%, the coating system takes an average of 30 h to cure completely. This is due to the absence of polyamide resin as a curing agent (Rau et al., 2013).

The dry film thickness of the coatings was found to be in the average range of 40-80 μm . Good film thickness observed in the coating system consisting 80A20E and 90A10E is expected to improve mechanical and electrochemical properties. As the percentage of epoxy resin increases above 50 wt%, the coating system gives lower values of thickness and may have lower adhesive strength and flexibility towards impact resistant test (Selvaraj et al., 2009).

The adhesion of the coating is generally considered to be good indicator of its longevity and measured by using Cross-Hatch method. This method specifies a procedure for assessing the resistance of the coating system separation from substrates when a right angle lattice pattern is cut into the coating, penetrating through the substrate. The crossed samples were checked for damages using a digital polarized microscope, Dino-Lite. These images were compared with the standard damage schemes following ASTM D3359 method B. Wet adhesion is an important factor in ability of the coating to resist corrosion of the substrate.

It is observed that coatings 80A20E and 90A10E have good adhesion to the substrate compared to the coating 100A, pure acrylic polyol resin (Rau et al., 2012). The epoxy resin contributes additional carboxylic and hydroxyl functional groups that together with the functional groups in the acrylic polyol resin form hydrogen bonding with the oxides and hydroxides on the metal substrate. This increases crosslinking and network density resulting in improved adhesion to the substrate (Ramesh et al., 2008). For other compositions 40-70 wt% A, the degree of adhesiveness is slightly lower (4B). Coating with 3B adhesiveness for sample 30A70E and 2B for 20A80E, can be easily peeled off from the substrate. It may be inferred that upon increasing above 20 wt% epoxy resin in the acrylic matrix, the cross link density produces strain in the coating membrane and lowers the resistance to scratch and introduces brittleness (Sharmin et al., 2004).

Impact resistance is another important mechanical property for surface coatings. ASTM D2794 standard was followed to carry out the experiments. An intender weight was raised to a set of heights and released onto the panels. The height was increased by known manipulated intervals until the coating failed. Each impact with different height was tested with new panels. The impact resistance is explained in terms of impact energy and sufficiently strong to withstand external attacks (Radhakrishnan et al.,

2009). The maximum impact energy was obtained using 80A20E and 90A10E blending ratios in the acrylic polymer matrix. The coating were observed further from images taken using digital polarized microscope and counter checked with pinhole detector. Images of intrusion and extrusion were used to study the impact flexibility on the hybrid systems. It is observed that the coating 80A20E and 90A10E have excellent flexibility and attraction between molecules as well as with the substrate. Increase in the concentration of epoxy resin above 20 wt% in the acrylic matrix leads to moderate and poor impact resistance.

When the indenter strikes the coating, a shock wave is generated that induces stress to the coating causing the molecules in the coating membrane to vibrate (Rau et al., 2011). These stress wave vibrations will generate cracks that propagate along the surface of the coating. The intensity of the crack depends on coating flexibility, which is composition dependent. High concentration of epoxy resin increases inner tension which can weaken cohesive forces between the molecules in the blend (Kader et al., 2002).

FTIR has been used to locate the positions of functional groups in AE hybrid systems. Crosslinking between acrylic, epoxy resin and polyisocyanate as hardener were identified here. Evidence confirming crosslinking between A and E is the existence of stretching asymmetrical C-C band and contraction of the C-O band (Rau et al., 2011). This band was not observed in the pure acrylic sample (100A), but observed in all samples containing epoxy resin. In 100A, the C-N band is observed at 1258 cm^{-1} . As the epoxy concentration increases in the acrylic matrix, a prominent band shift observed at 1249 cm^{-1} related to the asymmetrical -C-O-C- stretching of aryl alkyl ether of DGEBA-epoxy (Sharmin et al., 2004) is observed. Sharmin et al. also reported a sharp peak in the spectrum of epoxy resins at 1182 cm^{-1} and attributed it to ether linkages. The band corresponding to C-O which was observed at 1174 cm^{-1} shows a shift to 1182

cm^{-1} , further confirming the formation of polymer network between AE hybrid systems. The identical peak for the NCO group has been reported at 2280 cm^{-1} (Rau et al., 2011). From the spectra analysis, NCO band at 2280 cm^{-1} is not observed; as such the NH stretching band is expected to appear in the range of $1518\text{-}1581 \text{ cm}^{-1}$. This indicates that the crosslinking between acrylic and polyisocyanate resin has occurred and completed.

TGA is an important tool to investigate the thermal stability and thermal degradation of the polymer blends (Huang et al., 2009). From the thermogravimetric analysis graphs, there are different stages available. These are obtained due to the various stages of degradation of the xylene, polyisocyanate, acrylic resin and epoxy resin in the hybrid system mixture. Every stage reduction is related to the degradation of an individual or group of compounds presence in the system. According to data sheet, boiling point of Xylene is $135\text{-}145 \text{ }^\circ\text{C}$, polyisocyanate is $280 \text{ }^\circ\text{C}$, epoxy resin is $300 \text{ }^\circ\text{C}$ and acrylic resin is $370 \text{ }^\circ\text{C}$. These TGA thermograms of AE hybrid system also show the percentage of the residue left at the end of the degradation for all sample ratios.

These thermograms reveal that the blends have thermal degradation patterns of four steps. The first step mass loss occurs at temperature range $90\text{-}120 \text{ }^\circ\text{C}$, which is due to loss of solvent and moisture in resins. The second stage of loss is due to the degradation of polyisocyanate which started degrading after this stage that ended around $320 \text{ }^\circ\text{C}$. A further slight mass loss at about $275\text{-}320 \text{ }^\circ\text{C}$ can be explained by the degradation of the secondary hydroxyl group of the propyl chain in epoxy resin. The major mass loss occurs in the range of $365\text{-}420 \text{ }^\circ\text{C}$, which corresponds to the loss of bisphenol-A group (Rau et al., 2013).

The third step of the degradation takes place at a temperature before $380 \text{ }^\circ\text{C}$ and this can be attributed to epoxy degradation. Finally the point of inflexion at $320 \text{ }^\circ\text{C}$ until $380 \text{ }^\circ\text{C}$, the decrease in mass occurs at a slower rate. This could be due to the smaller

loss in acrylic resin percentage. Above 380-450 °C, the loss in mass again occurs at a higher rate and at 450 °C the mass remain almost constant until 480 °C. The final percentage of residue of all binder system can be seen and understood that the higher amount of epoxy resin in the mixture, the higher the percentage of residue left at the end of the combustion. This is due to the properties of the epoxy resin itself that can withstand high heat (Yew & Ramli Sulong, 2011). The thermograms show clearly that the rate of degradation of acrylic resin is largely reduced following epoxy resin combination and furthermore the beginning of polymer decomposition improves as a greater amount of mixture component is incorporated into the epoxy network (Cardiano et al., 2003).

DSC is used to study the thermal behavior of thermosetting and thermoplastic polymers by determining the glass-transition temperature (T_g) of the samples according to ASTM D7426. T_g of the hybrid system shows an decreasing trend. This behavior can be explained by relating that the homogenous cross-linking increases as the epoxy concentration increases in the acrylic matrix. The cross-linking network might be highly achieved by the addition of the hardener, aliphatic polyisocyanate resin (Ramesh et al., 2006). The decrease in T_g has improved mechanical properties up to 20 wt% epoxy resin in AE matrix. It was observed that the coatings were becoming brittle as the epoxy resin content exceeds 30 wt%. A brittle coating leads to higher inner tension and thus lowers the cohesive strength (Rau et al., 2011). Therefore it can be concluded here that the increasing T_g for samples with epoxy content greater than 30 wt% causes a reduction in the mechanical properties and adhesion power of the coating (Rau et al., 2013).

Electrochemical studies provide detailed anti-corrosion properties of all samples. EIS reveals the properties of the coating adhesion in terms of pore resistance (R_p), coating capacitance (C_c), dielectric constant (ϵ) and volume fraction of water (ϕ_w). The

sample with 10 wt% E in 90 wt% A (90A10E) shows that the R_p value is in the order of $10^9 \Omega\text{cm}^{-2}$ and a very low C_c ($<10^{-7}$ Farad) that is almost constant for 30 days of immersion time in the 3.5 % NaCl electrolyte (Rau et al., 2012). A small increase in ϵ , but within the range of an inert coating system (8-10) and ϕ_w with low water absorption at the saturation stage indicates that the 90A10E sample exhibits small porosity and possesses good barrier properties (Rau et al., 2012). In this EIS study incorporation of 10 wt% of epoxy resin in acrylic polyol resin in the developed hybrid systems gave the best performing binder for the anti-corrosion development of the paint systems.



In the second part of investigation for the development of anti-corrosion coating using organic resins hybrid system, blending ratio of 90A10E was used as the base binder for the improvement of all paint system. The formulation and the investigation of the anti-corrosion paint system using different inorganic pigments, namely Titanium Dioxide, TiO_2 (P1 system), Silitin Z 86 (P2 system), Aktisil AM (P3 system) and Aktisil PF 777 (P4 system) were finalized. The physical, mechanical, thermal, structural and electrochemical properties of the developed paint systems have been analyzed extensively. The effect of the pigment volume concentration (PVC) ratio to the critical pigment volume concentration (CPVC) on the corrosion resistance properties of paint system has been investigated in four paint systems namely P1, P2, P3 and P4. The study has established on the variation of pigment composition to prepare single hybrid paint

coat on mild steel panel. The panels were allowed to dry for 1 week before carried out the characteristic analysis.

Dry film thickness was determined using at least 50 readings taken within same paint system sample and the average thickness was calculated. The hybrid paint system mixtures were thoroughly blended using a paint mixer. The 90A10E base without NCO hardener was mixed with additives of inorganic pigment to achieve a complete dispersion in the paint container for the right thickness improving the mechanical properties (Rodriguez et al., 2004). The coating system must flow well over the panels to have a good intermolecular contact. This was achieved by adding known amount of xylene as solvent in the mixture. The dry film thickness of all paint system was found to be in the average range of 40-80 μm .

From the 90A10E binder system results, good film thickness observed in the coating system (Rau et al., 2013). It was clearly observed from the P1, P2 and P3 paint systems plot with all PVC percentages, that these paint systems have good dry film thickness. Meanwhile, the film thickness decreased for P4 system at higher PVC. Lower coating thickness will have disadvantages in mechanical, electrochemical and corrosion studies (Hu et al., 2012). This result will contribute an early prediction on adhesion, acid resistance and EIS investigations. It is worth to mention that all paint system with PVC below 40 % would observe better performance. However, the P4 samples with PVC \geq 40 % might fail in accelerated investigations.

The ability to adhere to the substrate throughout the desired life of the coating is one of the basic requirements of a surface coating. In this adhesion study, testing the adhesion of the developed paint systems on the cold rolled mild steel substrates was carried out by the using of Cross-Hatch method and all reported tests were performed according to the ASTM D3359 method B standard. The sample area was given a stiff

brushing and the pattern inscribed was examined in order to define the classification of test results. The results of these studies were recorded as images of the crossed samples by utilizing a digital polarized microscope. All tested samples were compared with the standard damage schemes of the standards for the cross hatch test (Rau et al., 2012).

These images reveal that there were no significant changes observed after the addition of the inorganic pigments on the adhesion properties of the paint film. This can be attributed to the fact that the binder system itself demonstrated an excellent adhesion to the substrate and due to the good distribution of the pigments (Clerici et al., 2009) within the polymeric matrix after the successful curing process without any cracks and plastic deformation (Perera, 2004). It was clearly observed from the results of TiO₂ pigmented, P1 paint system for all PVC exhibits good adhesion to the substrate without any peel-off spot. Similar trend has been observed in other prepared paint systems namely P2, P3 and P4. All the four types of the inorganic pigments which have been added to the acrylic-epoxy polymeric matrix (90A10E) have shown the same good adhesion property of the reinforced binder with class 5B ranking. This observation also in agreement with SEM images of the paint systems. The absence of the cracks in the cured paint films could be related to the adhesion of coating to have good barrier properties and anti-corrosion performance (Debnath, 2013).

Paint glossiness for P1, P2, P3 and P4 after exposure to accelerated UV weathering test was studied at 0 hour (0 h) and at 720 hours (720 h). The results of the glossiness tests were attached with the weathering surface images of the paint samples. ASTM D4587 standard with cycle No.4 for general metal coating was followed to carry out the experiments. The cycle used was 8 hours UV exposure at (60.0 ± 2.5) °C followed by 4 hours condensation at (50.0 ± 2.5) °C at dark period repeatedly for 720 h. The glossiness results of P1 paint system show there was no significant change recorded

to the glossiness values after 720 h of exposure with 30-40 % PVC of TiO₂ pigments was used. TiO₂ addition at 40 % PVC gives highest glossiness value equal to 92 GU at 0 h and 80 GU after 720 h exposure respectively. This could be attributed to the vital role of the critical pigment volume concentration (CPVC) value in enhancing the barrier properties via fill the pores and zigzagging the diffusion pathways against the penetrating of the water and oxygen molecules as well as the corrosive agents and the corrosion products toward the metal-paint interface (Matin et al., 2015; Shi et al., 2009).

P2 paint system containing Silitin Z 86 coated panels demonstrated a poor resistance against the weathering conditions where blisters appeared on the paint surface after 720 h of exposure. The 2002 work of X.F. Yang et al., explained the effect of the wet and dry cyclic weathering chamber, producing blisters with dimensional in the range of micrometre on the coating surface. X.F. Yang et al also reported that as the temperature becomes high and the exposure to the wet medium becomes longer, the developed blisters would become larger. Meanwhile, P2 paint system show a decreasing trend in the glossiness value after the 720 h of exposure. Such observation could be attributed to the effect of the weathering conditions in forming blisters which in turn lead to increasing the surface roughness. This idea could be supported by the work that has been carried out by M. Yonehara et al., (2004) where the relation between the surface roughness and the glossiness have been studied and came out with the result that increasing the surface roughness leads to decreasing in the surface glossiness.

The P3 and P4 paint systems shows similar trend with P2 paint system. Exceptionally, P320 observed to have slight gloss improvement at PVC 20 %. In general P3 paint system has a good glossiness up to PVC 30 %. Meanwhile P340 and P350 shows poor performances in both accelerated UV weathering and glossiness test. As for P4 paint system, only P410 paint system may have good anti-corrosion properties based on general observation on both properties. The results of P2, P3 and P4

paint systems reflect the similar performance due to similar pigment content of modified SiO₂ mixture. These SiO₂ based paint systems degraded badly at PVC 30 % and above, after have been subjected to 720 h of weathering conditions and the corresponding glossiness demonstrated a significant decrease after the exposure.

By comparing the TGA thermograms of the hybrid binder system 90A10E as reported in the 2013 work of Rau. et al., the P1, P2, P3 and P4 paint system thermograms clearly show that there is no new decomposition steps after combination of inorganic TiO₂ or Hoffmann Minerals within AE polymeric matrix. However, these pigments improve thermal stability and lead the paint system to require a higher degradation temperature above 250 °C and thermal energies for performing the same decomposition steps as the base system 90A10E (Rau et al., 2013). TGA has shown that the pure AE hybrid binder system undergoes more mass loss compared to all the developed pigmented paint systems. The reason of higher residue could be related to the thermal stability of the inorganic pigments.

Residue percentage of P1 is higher than P2, P3 and P4 with greater differences ranging from 23-85 % as the PVC increases from 10-50 %. These show that TiO₂ has more thermal stability (Diebold, 2014). Similar residue percentage for P2, P3 and P4 indicates confirmation of same base pigment combination of amorphous silica and lamellar kaolinite with little extra modification using amino silane and alkyl silane as provided in data sheet. Armelin reported the same observation about the effect of the inorganic pigments on the thermal properties of the polymeric coatings and had attributed that enhancement in the thermal stability due to the present of high content of inorganic pigment (Armelin et al., 2007). These left over mass of thermal stable materials will be the pigments such as TiO₂ in P1 and SiO₂ modified mixture pigments in other paint systems. The P2, P3 and P4 have approximate matching residue percentage of 65 %, whereas P1 has 85 % of residue due to 100 % of pigments being

TiO₂. This enhances a higher temperature with increased stability recorded for the base polymeric binder system.

T_g is widely accepted as a predominant factor in determining the physical and mechanical properties of a coating system and was adopted by many research in the last few decades in order to point out the state of the materials under investigation and its thermal behaviour (Sharmin et al., 2004; Shen et al., 2015). The effect of TiO₂ pigment on the T_g of P1 paint system was compared with T_g of A100 (100 wt% acrylic) and P100 (90A10E). DSC results show an increase of T_g value from 38 °C to 46 °C for A100 to P100 system (Rau et al., 2013). This is explained by relating homogenous crosslinking rises as the epoxy content increases in acrylic matrix by the addition of polyisocyanate as the hardener (Rau et al., 2013).

P1 paint system show decreasing trend in the T_g values as the pigment volume concentration increased. Addition of TiO₂ pigment within the hybrid polymeric matrix result in decreasing T_g values which can be attributed to the increment in the free volume caused by the present of the inorganic pigments (Ramezanzadeh & Attar, 2011). Furthermore T_g value of all paint system clearly decreases when PVC content increases. Combination of pigments within the AE matrix increases in the free volume that improves flexibility. This is exceptional for P410 which show an increase in T_g value can be attributed to the effect of the pigment Aktisil PF 777 in restraining the mobility within the binder and strong physical interactions with polymeric matrix (Perera, 2004; Ramezanzadeh et al., 2011).

These FTIR spectrums were analyzed in term of the effect of pigment addition on the chemical structure of the host polymeric matrix binder system. It was observed that P1, P2, P3 and P4 paint system did not lead to any peak displacement in positions comparing to the binder system peaks. This observation can be explained as the used

pigments have been dispersed within the polymeric matrix without any interaction within the chemical structure of the acrylic-epoxy matrix. There was an additional peak for P2, P3 and P4 system in the range of 950-1200 cm^{-1} due to same modified SiO_2 content in the pigments and supported by EDAX results. However, it is worth to be mentioned that the intensity of the peaks at all respective wavenumber was found to be decreasing as the PVC getting higher from 10 % up to 50 %.

SEM images and EDAX results of all paint system confirms the idea of enhancing the barrier and anti-corrosion performance of the polymeric matrix by embedding micro-size pigment particles within the paint film. All paint system showed formation of a uniform, homogeneous, crack free, continuous close packed structures up to PVC 30 %. Also, EDAX results confirm the presence of all the elements of both the organic polymeric matrix and the inorganic pigments.

Acid resistance test and EIS was used to investigate the effect of various inorganic pigments under laboratory corrosive environments. These investigations have been conducted in order to evaluate the anti-corrosion and the barrier performance of developed paint systems (Bahrami et al., 2010). Painted mild steel panels were subjected to diluted H_2SO_4 10 % in immersion test for 40 days and 3.5 % NaCl in EIS studies up to 30 days. Images and readings were taken from time to time in order to determine the exact degradation time of each individual system.

The simple principle of acid resistance test is based on the visual observation of the immersed cross-scribed side edge protected panels. The experimental procedure was in accordance with ISO 2812-1 standards. Paint system for P110, P130, P220, P340 and P410 have good acid resistance at least up to 15th day of direct cross-scribed immersion.

EIS is well-suited for quantitative evaluation using equivalent circuit elements that enable to one follow the mechanism of paint protective properties in terms of

coating resistance, coating capacitance, water uptake, diffusion rate and electrical conduction through the paint film. The paint systems P130, P220, P320 and P410 have performed well by having all the requirements of good coating. Accelerated UV weathering test also was found to be in complete agreement with the EIS result. P130, P140, P320 and P410 paint systems demonstrated the highest coating resistance which is considered as an evidence of anti-corrosion performance and good barrier properties. It is a sign on the durability of these systems to withstand the various aggressive environmental conditions. In addition, the SEM micrographs were used as supporting evidence to the EIS results with high barrier performance of the paint systems which in turn result in good corrosion protection ability (Zhu et al., 2010).

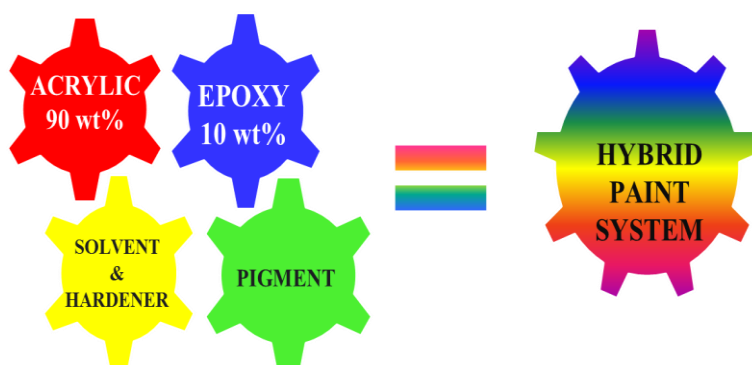
Generally when coatings are formulated, one important characteristic value is pigment volume concentration (PVC), which strongly affects coating performance properties. The volume percentage of pigment in a dry paint has been defined as PVC. Furthermore, there is a critical pigment volume concentration (CPVC) to consider in many coating formulation containing pigments or dyes (Lobnig et al., 2006). Below the CPVC value, the pigment can uniformly distribute in the binder matrix without harming its integrity and compactness. While above the CPVC value, the excessive pigment cannot be fully packed by the binder, thus pores and voids occur in the coating matrix (Liu et al., 2012).

Various methods can be used to determine this CPVC percentage, with one of them being EIS method. EIS is a suitable method to determine the CPVC of coatings, especially for inorganic pigment based organic coatings (Liu et al., 2010). When PVC equals CPVC, the overall performance of coating system is usually at its best point (Kalendova et al., 2008; Sorensen et al., 2009a).

The CPVC of a solvent based AE hybrid system with various PVC was analyzed with respect to moisture transport. Most additives truly increase solubility and equilibrium absorption values of water in the coating, thereby increasing permeability (Van der Wel & Adan, 1999). EIS give an accurate measurement to determine diffusion coefficient rate of water because of the separation of interfacial and diffusion process on the frequency scale (Bierwagen et al., 2008; Hinderliter et al., 2006).

CPVC is determined using R_c and diffusion coefficient rate plotted towards PVC values for all paint system. From the results, the response of all developed paint system were shown for coating resistance, R_c and diffusion coefficient rate, D . Correlation of high R_c value and low diffusion rate would indicate CPVC for the respective paint system. Results show that for P1 paint system, CPVC 30 % of TiO_2 addition in the polymeric binder matrix will yield best overall properties. P2 has CPVC at 20 % of Silitin Z 86 and 20 % of Aktisil AM for P3. Meanwhile P4 has CPVC at 10 % of Aktisil PF 777.

Paint systems P130, P220, P320 and P410 have CPVC at different PVC concentration owing to different inorganic pigments. A relationship with CPVC confirmation can be seen from these two studies for best performing development of anti-corrosion coating using organic resins hybrid system. P3 system has performed well in all the analytical tests. A sample with 10 wt% Epoxy resin in 90 wt% Acrylic polyol resin and PVC 20 % of pigment Aktisil AM was a good stand out paint system.



CHAPTER 10: CONCLUSION



Dating from colorful prehistory, paint or coating developed slowly to meet every day needs well past the Renaissance. Coatings were used in human civilization to meet individual preferences. Today, coating has become a subject of scientific investigation and is applied universally for various functions. Organic coatings, along with proper surface pre-treatment, are the most common and cost effective mode of corrosion protection for metallic objects and structures. From automobiles to jet aircraft, from chemical factories to dishwashers, exterior surfaces of corrodible metals such as steel and other metalloid are effectively protected from their environment by a coating system. The role for development of anti-corrosion coating using organic resins hybrid system is a key issue for coating science and is the main initiating idea of this research.

The first part of the research, involves formulation of organic hybrid binder system and investigation of its properties. This demonstrates an interesting correlation between viscosity, adhesion, impact resistance, FTIR, TGA, DSC and EIS. High viscosity of the coating system consisting 80A20E and 90A10E provides a uniform dry film thickness and takes about 3 hours to cure. Blending ratio of Acrylic resin 40 wt% represents a minimum degree of good adhesion for the various AE blends. It was observed that coatings 80A20E and 90A10E have the best adhesion onto the mild steel panels. These two sample ratios also performed well in impact resistance test conforming to have excellent attraction between molecules as well as with the interface.

FTIR revealed cross linking between the components of the binders were successful and has the maximum thermal stability. Thermal studies confirms that the T_g

of these binders range between 35-75 °C making coating samples sufficiently flexible with strong adhesion and best in withstanding impact test. Both 80A20E and 90A10E has similar characteristics in terms of physical, mechanical and thermal performances. Electrochemical studies provide detailed anti-corrosion properties of all samples. The sample with 10 wt% E in 90 wt% A shows that the pore resistance, R_p of $10^9 \Omega\text{cm}^{-2}$ and a very low coating capacitance, C_c ($<10^{-7}$ Farad) value. A small increase in dielectric constant, ϵ but within the range of an inert coating system (8-10) and low volume fraction of water, ϕ_w at the saturation stage indicates that the 90A10E sample exhibits small porosity, possesses good barrier and anti-corrosion properties. In this hybrid binder study, incorporation of 10 wt% of epoxy resin in acrylic polyol resin gave the greatest performing binder for the development of the paint systems for the second part of this study.

The second part of the research, involves formulation of paint systems incorporated with inorganic pigments using the best blending ratio of 90A10E binder. Four types of pigments were used to formulate four paint systems namely P1, P2, P3 and P4. The effects of PVC were investigated using physical, mechanical, thermal, structural and electrochemical studies. CPVC is determined using R_c and diffusion rate plotted towards PVC values for all paint system.

The dry film thickness of the all paint system was found to be in the average range of 40-80 μm . It was clearly observed from the P1, P2 and P3 paint systems plot with all PVC percentages, that these paint system had good dry film thickness. Meanwhile, the film thickness is decreasing for P4 system at higher PVC content. Cross hatch cut images reveal best class 5B for all paint system. There were no significant changes observed after the addition of inorganic pigments on the adhesion properties of the paint film comparing to 90A10E.

From the accelerated UV weathering test results of the paint system, it was observed clearly that the surfaces of panels were subjected to major degradation due to the weathering chamber conditions, UV light and temperature. However, P130, P140, P310, P320 and P330 paint systems demonstrated the highest UV weathering resistance and good glossiness results which is considered as an evidence of the good barrier properties with PVC content. It is a sign on the durability of these systems to withstand the various aggressive environmental conditions. The results of P2, P3 and P4 paint systems reflect overall similar performance. These paint systems degraded badly at PVC 30 % and above after subjected to 720 h of UV weathering conditions and the corresponding glossiness demonstrated a significant decrease after the exposure. This correlates the inorganic pigments used to prepare P2, P3 and P4 have similar contents of modified SiO₂ mixture.

The paint system TGA thermograms clearly show that there were no new decomposition steps after combination of pigments. But these pigments improve thermal stability to a higher degradation temperature above 250 °C with a lower mass loss. Residue percentage of P1 is higher than P2, P3 and P4 with greater differences ranging from 23-85 % as the PVC increases. The P2, P3 and P4 have approximate matching residue percentage of 65 % of SiO₂ mixture pigments. Where else P1 has 85 % of residue due to 100 % of pigments was TiO₂. Furthermore T_g value of all paint system clearly decreases when PVC content increases. Combination of pigments within the AE matrix increases in the free volume that improves flexibility. This is exceptional for P410 which show an increase in T_g value can be attributed to the effect of the pigment Aktisil PF 777 in restraining the mobility within the binder and strong physical interactions with binder polymeric matrix.

SEM images and EDAX results of all paint system confirms the idea of enhancing the barrier and anti-corrosion performance of the polymeric matrix by

embedding micro-size pigment particles within the paint film. All paint system showed formation of a uniform, homogeneous, crack free, continuous close packed structures up to PVC 30 %. Also, EDAX results confirm the presence of all the elements of both the organic polymeric matrix and the inorganic pigments.

The simple principle of acid resistance test is based on the visual observation of the immersed cross-scribed side edge protected panels. Paint system for P110, P130, P220, P340 and P410 have good acid resistance at least up to 15th day of direct cross-scribed immersion. EIS is well-suited for quantitative evaluation using equivalent circuit elements that enable to one follow the mechanism of paint protective properties in terms of coating resistance, coating capacitance, water uptake, diffusion rate and electrical conduction through the paint film. The paint systems P130, P220, P320 and P410 have performed well by having all the requirements of good coating.

From the EIS results, the response of all developed paint system were shown for coating resistance, R_c and diffusion coefficient rate, D . Correlation of high R_c value and low diffusion rate would indicate CPVC for the respective paint system. Results show that for P1 paint system, CPVC 30 % of TiO_2 addition in the polymeric binder matrix will yield best overall properties. P2 has CPVC at 20 % of Silitin Z 86 and 20 % of Aktisil AM for P3. Meanwhile P4 has CPVC at 10 % of Aktisil PF 777.

A relationship with CPVC confirmation can be seen from these two studies for best performing development of anti-corrosion coating using organic resins hybrid system. The best among all paint system were the P320, a sample with 10 wt% Epoxy resin in 90 wt% Acrylic polyol resin and PVC 20 % of pigment Aktisil AM was a good stand out paint system.

This P320 paint system has better overall performance compared to base binder (90A10E) as summarized in next page. The current research has resulted in an

improvement to the currently used acrylic based coating. This work reveals the blending complexity is very important for the selective resins. Therefore the complexity is beneficial for the practical performance which is by controlling the different hybrid systems with organic, inorganic and functional fillers. This may give the key roles of the best and cost effective anti-corrosion coatings. Continued research will result in a better understanding of how and why organic coatings fail in corrosion protection.

Paint Studies	P1		P2		P3		P4	
Dry Film Thickness (μm)	63		88		63		36	
Adhesion (B)	5B		5B		5B		5B	
Glossiness GU (0 h)	P130	P140	P210	P220	P320	P330	P410	P420
UV Weathering (720 h)	P130	P140	P210	X	P320	P330	P410	P420
Glossiness GU (720 h)	P130	P140	X	X	P320	X	X	X
TGA Stability ($^{\circ}\text{C}$)	> 250		> 250		> 250		> 250	
TGA Residue at PVC 50 % (%)	85		70		69		65	
Tg comparing 90A10E	↓		↓		↓		↑↓	
FTIR comparing 90A10E	similar		similar		similar		similar	
Acid Resistance	P110	P130	P220		P340		P410	
EIS	P130		P220		P320		P410	
CPVC (PVC %)	30		20		20		10	
Best	P320							

Suggestions for Further Research

- Faster curing system; the paint developed in this study was found to be a good coating for mild steel panels. It cures at room temperature and requires an average 7 days of curing before putting into use. However, on this substrate, a faster curing at elevated temperature is normally required and hybrid systems can be modified to suit those applications.
- More versatile and high-performance pigment systems; instead of being a single pigment, Silitin and Aktisil pigment systems are more likely to be combinations of synergistic pigments can be intensively investigated.
- Superbinder; hybrid of acrylic-epoxy resins were demonstrated in this study. For most of these coatings, a proper surface treatment is required. Among the large quantity of applications of polymer coatings, the idea of superbinder can certainly find its use, especially in the applications where the pretreatment cannot be easily accommodated.
- Nanotechnology; the properties of coating can be enhanced by using nanotechnology for specific usage like fire retardant and dust free coating for everyday applications.
- Eco-friendly; apart from solvent-based resin, further work should consolidate with organic pigments and natural pigments from plants for water-based resins. Waterborne coatings could be used to replace the more environmentally hazardous coatings currently. The present increase in the use of waterborne coating will provide better or more scope for future research and development.

In the infinite knowledge, like everyone I'm still learning.

REFERENCES

- Ahmad, Sharif, Gupta, AP, Sharmin, Eram, Alam, Manawwer, & Pandey, SK. (2005). Synthesis, characterization and development of high performance siloxane-modified epoxy paints. *Progress in organic coatings*, 54(3), 248-255.
- Ahmed, Nivin M, & Abdel-Fatah, Hesham Tawfik M. (2012). *The role of silica fume pigments in corrosion protection of steel surfaces*: INTECH Open Access Publisher.
- Ahmed, Nivin M, & Selim, Mohamed M. (2010). Anticorrosive performance of titanium dioxide-talc hybrid pigments in alkyd paint formulations for protection of steel structures. *Anti-Corrosion Methods and Materials*, 57(3), 133-141.
- AM, NSE Aktisil. (2008). *Aktisil AM*.
- Amirudin, A, & Thierry, D. (1995). Application of electrochemical impedance spectroscopy to study the degradation of polymer-coated metals. *Progress in organic coatings*, 26(1), 1-28.
- Armelin, Elaine, Oliver, Ramón, Liesa, Francisco, Iribarren, José I, Estrany, Francesc, & Alemán, Carlos. (2007). Marine paint formulations: Conducting polymers as anticorrosive additives. *Progress in Organic Coatings*, 59(1), 46-52.
- Aznar, AC, Pardini, OR, & Amalvy, JI. (2006). Glossy topcoat exterior paint formulations using water-based polyurethane/acrylic hybrid binders. *Progress in organic coatings*, 55(1), 43-49.
- Bahrami, MJ, Hosseini, SMA, & Pilvar, P. (2010). Experimental and theoretical investigation of organic compounds as inhibitors for mild steel corrosion in sulfuric acid medium. *Corrosion Science*, 52(9), 2793-2803.
- Bajaj, Pushpa, Jha, NK, & Kumar, Anand. (1995). Effect of coupling agents on thermal and electrical properties of mica/epoxy composites. *Journal of applied polymer science*, 56(10), 1339-1347.
- Baukh, Viktor, Huinink, Hendrik P, Adan, Olaf CG, Erich, Sebastiaan JF, & Van Der Ven, Leendert GJ. (2012). Predicting water transport in multilayer coatings. *Polymer*, 53(15), 3304-3312.
- Behzadnasab, M, Mirabedini, SM, Kabiri, K, & Jamali, S. (2011). Corrosion performance of epoxy coatings containing silane treated ZrO₂ nanoparticles on mild steel in 3.5% NaCl solution. *Corrosion Science*, 53(1), 89-98.

- Bentiss, F, Traisnel, M, Chaibi, N, Mernari, B, Vezin, H, & Lagrenee, M. (2002). 2, 5-Bis (n-methoxyphenyl)-1, 3, 4-oxadiazoles used as corrosion inhibitors in acidic media: correlation between inhibition efficiency and chemical structure. *Corrosion science*, 44(10), 2271-2289.
- Bierwagen, Gordon, Allahar, Kerry, Hinderliter, Brian, Simões, Alda MP, Tallman, Dennis, & Croll, Stuart. (2008). Ionic liquid enhanced electrochemical characterization of organic coatings. *Progress in Organic Coatings*, 63(3), 250-259.
- Bierwagen, Gordon P. (1996). Reflections on corrosion control by organic coatings. *Progress in organic coatings*, 28(1), 43-48.
- Bierwagen, Gordon P, He, L, Li, J, Ellingson, L, & Tallman, DE. (2000). Studies of a new accelerated evaluation method for coating corrosion resistance—thermal cycling testing. *Progress in Organic Coatings*, 39(1), 67-78.
- Blustein, G, Romagnoli, R, Jaén, JA, Di Sarli, AR, & Del Amo, B. (2006). Zinc basic benzoate as eco-friendly steel corrosion inhibitor pigment for anticorrosive epoxy-coatings. *Colloids and Surfaces A: Physicochemical and Engineering Aspects*, 290(1), 7-18.
- Cardiano, P, Mineo, P, Sergi, S, Ponterio, RC, Triscari, M, & Piraino, P. (2003). Epoxy-silica polymers as restoration materials. Part II. *Polymer*, 44(16), 4435-4441.
- Castela, AS, & Simoes, AM. (2003). Assessment of water uptake in coil coatings by capacitance measurements. *Progress in Organic Coatings*, 46(1), 55-61.
- Chawla, Vikas. (2013). Corrosion Behavior of Nanostructured TiAlN and AlCrN Thin Coatings on ASTM-SA213-T-11 Boiler Steel in Simulated Salt Fog Conditions. *Materials Science and Metallurgy Engineering*, 1(2), 31-36.
- Chew, KW, Yahaya, AH, & Arof, AK. (2000). Studies on the properties of silicone resin films on mild steel. *Pigment & resin technology*, 29(6), 364-368.
- Chruściel, Jerzy J, & Leśniak, Elżbieta. (2015). Modification of epoxy resins with functional silanes, polysiloxanes, silsesquioxanes, silica and silicates. *Progress in Polymer Science*, 41, 67-121.
- Clerici, Cyril, Gu, Xiaohong, Sung, Li-Piin, Forster, Aaron M, Ho, Derek L, Stutzman, Paul, . . . Martin, Jonathan W. (2009). Effect of pigment dispersion on durability of a TiO₂ pigmented epoxy coating during outdoor exposure *Service Life Prediction of Polymeric Materials* (pp. 475-492): Springer.

- D4587, ASTM. (2011). *Standard Practice for Fluorescent UV-Condensation Exposures of Paint and Related Coatings*.
- Dashtizadeh, Ahmad, Abdouss, Majid, Mahdavi, Hossein, & Khorassani, Manuchehr. (2011). Acrylic coatings exhibiting improved hardness, solvent resistance and glossiness by using silica nano-composites. *Applied Surface Science*, 257(6), 2118-2125.
- Davis, J. R. (2000). *Corrosion: Understanding the basics*: ASM International.
- Debnath, Narayan Chandra. (2013). Importance of surface preparation for corrosion protection of automobiles. *Journal of Surface Engineered Materials and Advanced Technology*, 3(01), 94.
- Deflorian, Flavio, & Rossi, Stefano. (2006). An EIS study of ion diffusion through organic coatings. *Electrochimica Acta*, 51(8), 1736-1744.
- DHS. (2008). Hazard Evaluation System and Information Service (pp. 1-6).
- Diebold, Michael P. (2014). TiO₂ Pigments in Liquid Paints *Application of Light Scattering to Coatings* (pp. 83-109): Springer.
- Dulux. (2009). PC Tech Notes Protective Coating Mild Steel *Mild Steel* (pp. 1-3).
- Dulux. (2010). PC Tech Notes 5.6 Pot Life *Pot Life* (pp. 1-3).
- Dulux. (2014). PC Tech Notes 2.2 Solvent *Solvent* (pp. 1-2).
- Dupont. (2007). Polymers, Light and Science *Titanium Dioxide* (pp. 1-6).
- Dušek, K, & Dušková-Smrčková, M. (2000). Network structure formation during crosslinking of organic coating systems. *Progress in Polymer Science*, 25(9), 1215-1260.
- El Rayes, Magdy M, Abdo, Hany S, & Khalil, Khalil Abdelrazek. (2013). Erosion-corrosion of cermet coating. *Int. J. Electrochem. Sci*, 8, 1117-1137.
- Essen, Bodo. (2005). Protecting the surface. *European coatings journal*, 7(08), 18-24.
- Ferreira, CA, Domenech, SC, & Lacaze, PC. (2001). Synthesis and characterization of polypyrrole/TiO₂ composites on mild steel. *Journal of applied electrochemistry*, 31(1), 49-56.

- Foix, D, Serra, A, Amparore, L, & Sangermano, Marco. (2012). Impact resistance enhancement by adding epoxy ended hyperbranched polyester to DGEBA photocured thermosets. *Polymer*, 53(15), 3084-3088.
- Forsgren, Amy. (2006). *Corrosion control through organic coatings*: CRC Press.
- Freitag, Werner, & Stoye, Dieter. (2008). *Paints, coatings and solvents*: John Wiley & Sons.
- Gangloff, Richard P. (2005). Environmental cracking corrosion fatigue. *ASTM International, West Conshohocken*, 302-321.
- Gowri, S, & Balakrishnan, K. (1994). The effect of the PVC/CPVC ratio on the corrosion resistance properties of organic coatings. *Progress in Organic Coatings*, 23(4), 363-377.
- Gu, Xiaohong, Nguyen, Tinh, Oudina, Mounira, Martin, David, Kidah, Bouchra, Jasmin, Joan, . . . Martin, Jonathan W. (2005). Microstructure and morphology of amine-cured epoxy coatings before and after outdoor exposures—an AFM study. *JCT research*, 2(7), 547-556.
- Gui, F, & Kelly, RG. (2006). A study of performance of corrosion prevention compounds on AA2024-T3 with electrochemical impedance spectroscopy. *Electrochimica acta*, 51(8), 1797-1805.
- Hao, Yongsheng, Liu, Fuchun, Han, En-Hou, Anjum, Saima, & Xu, Guobao. (2013). The mechanism of inhibition by zinc phosphate in an epoxy coating. *Corrosion Science*, 69, 77-86.
- Heidarian, M, Shishesaz, MR, Kassiriha, SM, & Nematollahi, M. (2010). Characterization of structure and corrosion resistivity of polyurethane/organoclay nanocomposite coatings prepared through an ultrasonication assisted process. *Progress in Organic Coatings*, 68(3), 180-188.
- Hinderliter, BR, Croll, SG, Tallman, DE, Su, Q, & Bierwagen, GP. (2006). Interpretation of EIS data from accelerated exposure of coated metals based on modeling of coating physical properties. *Electrochimica acta*, 51(21), 4505-4515.
- Hirose, Masakazu, Zhou, Jianhui, & Nagai, Katsutoshi. (2000). The structure and properties of acrylic-polyurethane hybrid emulsions. *Progress in Organic Coatings*, 38(1), 27-34.

- Hosseini, SMA, Salari, M, Jamalizadeh, E, Khezripor, S, & Seifi, M. (2010). Inhibition of mild steel corrosion in sulfuric acid by some newly synthesized organic compounds. *Materials Chemistry and Physics*, 119(1), 100-105.
- Hu, Rong-Gang, Zhang, Su, Bu, Jun-Fu, Lin, Chang-Jian, & Song, Guang-Ling. (2012). Recent progress in corrosion protection of magnesium alloys by organic coatings. *Progress in Organic Coatings*, 73(2), 129-141.
- Huang, Kuan-Yeh, Weng, Chang-Jian, Lin, Su-Yin, Yu, Yuan-Hsiang, & Yeh, Jui-Ming. (2009). Preparation and anticorrosive properties of hybrid coatings based on epoxy-silica hybrid materials. *Journal of applied polymer science*, 112(4), 1933-1942.
- Ji, Wei-Gang, Hu, Ji-Ming, Liu, Liang, Zhang, Jian-Qing, & Cao, Chu-Nan. (2007). Improving the corrosion performance of epoxy coatings by chemical modification with silane monomers. *Surface and coatings technology*, 201(8), 4789-4795.
- Jiang, JY, Xu, JL, Liu, ZH, Deng, L, Sun, B, Liu, SD, . . . Liu, HY. (2015). Preparation, corrosion resistance and hemocompatibility of the superhydrophobic TiO₂ coatings on biomedical Ti-6Al-4V alloys. *Applied Surface Science*, 347, 591-595.
- Jiang, Xu-Bao, Zhu, Xiao-Li, Zhang, Zhi-Guo, Kong, Xiang-Zheng, & Tan, Ye-Bang. (2011). Determination of crosslinking and grafting in polyurethane-acrylic hybrid material and their theoretical calculations. *Chem. Res. Chinese Universities*, 27(1), 154-157.
- Jones, Denny A. (1995). *Principles and Prevention of Corrosion* (2nd Edition ed.): Prentice Hall.
- Kader, M Abdul, Bhowmick, AK, Inoue, T, & Chiba, T. (2002). Morphology, mechanical and thermal behavior of acrylate rubber/fluorocarbon elastomer/polyacrylate blends. *Journal of Materials Science*, 37(8), 1503-1513.
- Kahraman, M Vezir, Kuğu, Murat, Menceloğlu, Yusuf, Kayaman-Apohan, Nilhan, & Güngör, Atilla. (2006). The novel use of organo alkoxy silane for the synthesis of organic-inorganic hybrid coatings. *Journal of non-crystalline solids*, 352(21), 2143-2151.
- Kalendová, Andréa. (2003). Effects of particle sizes and shapes of zinc metal on the properties of anticorrosive coatings. *Progress in Organic Coatings*, 46(4), 324-332.

- Kalendová, Andrea, Sapurina, Irina, Stejskal, Jaroslav, & Veselý, David. (2008). Anticorrosion properties of polyaniline-coated pigments in organic coatings. *Corrosion Science*, 50(12), 3549-3560.
- Kalendová, Andrea, Veselý, David, & Stejskal, Jaroslav. (2008). Organic coatings containing polyaniline and inorganic pigments as corrosion inhibitors. *Progress in Organic Coatings*, 62(1), 105-116.
- Kardar, Pooneh, Ebrahimi, Morteza, & Bastani, Saeed. (2014). Curing behaviour and mechanical properties of pigmented UV-curable epoxy acrylate coatings. *Pigment & Resin Technology*, 43(4), 177-184.
- Lacnjevac, CM, Zlatkovic, S, Cakic, S, Stamenkovic, J, Rajkovic, MB, Nikolic, G, & Jelic, S. (2010). New Organic Solvent Free Three-Component Waterproof Epoxy-Polyamine Systems. *Sensors & Transducers*, 119(8), 91.
- Lang, Erich. (2012). *The role of active elements in the oxidation behaviour of high temperature metals and alloys*: Springer Science & Business Media.
- Leloup, Frédéric B, Pointer, Michael R, Dutré, Philip, & Hanselaer, Peter. (2010). Geometry of illumination, luminance contrast, and gloss perception. *JOSA A*, 27(9), 2046-2054.
- Lewis, OD, Critchlow, GW, Wilcox, GD, & Sander, J. (2012). A study of the corrosion resistance of a waterborne acrylic coating modified with nano-sized titanium dioxide. *Progress in Organic Coatings*, 73(1), 88-94.
- Liu, Fuchun, Yang, Lihong, & Han, Enhou. (2010). Effect of particle sizes and pigment volume concentrations on the barrier properties of polyurethane coatings. *Journal of Coatings Technology and Research*, 7(3), 301-313.
- Liu, Jian-hua, Zhan, Zhong-wei, Li, Song-mei, & Yu, Mei. (2012). Corrosion resistance of waterborne epoxy coating pigmented by nano-sized aluminium powder on steel. *Journal of Central South University*, 19, 46-54.
- Lobnig, RE, Villalba, W, Goll, K, Vogelsang, J, Winkels, I, Schmidt, R, . . . Soetemann, J. (2006). Development of a new experimental method to determine critical pigment–volume–concentrations using impedance spectroscopy. *Progress in organic coatings*, 55(4), 363-374.
- Loveday, David, Peterson, Pete, & Rodgers, Bob. (2004). Evaluation of organic coatings with electrochemical impedance spectroscopy. *JCT coatings tech*, 8, 46-52.

- Mahdavian A, M, & Attar, MM. (2005). Investigation on zinc phosphate effectiveness at different pigment volume concentrations via electrochemical impedance spectroscopy. *Electrochimica Acta*, 50(24), 4645-4648.
- Malshe, VC, & Waghoo, Gulzar. (2004). Weathering study of epoxy paints. *Progress in organic coatings*, 51(4), 267-272.
- Marcus, Philippe. (2011). *Corrosion mechanisms in theory and practice*: CRC Press.
- Mathivanan, L, & Arof, AK. (1998). The degradation of silicone coatings in high temperature atmospheres. *Anti-Corrosion Methods and Materials*, 45(6), 403-412.
- Matin, E, Attar, MM, & Ramezanzadeh, B. (2015). Investigation of corrosion protection properties of an epoxy nanocomposite loaded with polysiloxane surface modified nanosilica particles on the steel substrate. *Progress in Organic Coatings*, 78, 395-403.
- McCreight, Kevin W, Stockl, Rebecca, Testa, Carlo, & Seo, Kab Sik. (2011). Development of low VOC additives to extend the wet edge and open time of aqueous coatings. *Progress in Organic Coatings*, 72(1), 102-108.
- McMurray, HN, Holder, A, Williams, G, Scamans, GM, & Coleman, AJ. (2010). The kinetics and mechanisms of filiform corrosion on aluminium alloy AA6111. *Electrochimica Acta*, 55(27), 7843-7852.
- Merouani, A, & Amardjia-Adnani, H. (2008). Spectroscopic FT-IR study of TiO₂ films prepared by sol-gel method. *International Scientific Journal for Alternative Energy and Ecology*, 6(62), 151-154.
- Moreno, C, Hernández, S, Santana, JJ, González-Guzmán, J, Souto, RM, & González, S. (2012). Characterization of water uptake by organic coatings used for the corrosion protection of steel as determined from capacitance measurements. *Int. J. Electrochem. Sci*, 7, 8444-8457.
- NACE. (2013). Corrosion Cost and Preventive Strategies in the United States. Retrieved from <http://www.nace.org/Publications/Cost-of-Corrosion-Study/> website:
- Nematollahi, M, Heidarian, M, Peikari, M, Kassiriha, SM, Arianpouya, N, & Esmaeilpour, M. (2010). Comparison between the effect of nanoglass flake and montmorillonite organoclay on corrosion performance of epoxy coating. *Corrosion Science*, 52(5), 1809-1817.

- Ocampo, Cintia, Armelin, Elaine, Liesa, Francisco, Alemán, Carlos, Ramis, Xavier, & Iribarren, José Ignacio. (2005). Application of a polythiophene derivative as anticorrosive additive for paints. *Progress in organic coatings*, 53(3), 217-224.
- Pang, Yongyan, Watson, Stephanie S, & Sung, Li-Piin. (2014). Surface degradation process affected by heterogeneity in nano-titanium dioxide filled acrylic urethane coatings under accelerated UV exposure. *Polymer*, 55(25), 6594-6603.
- Perera, Dan Y. (2004). Effect of pigmentation on organic coating characteristics. *Progress in organic coatings*, 50(4), 247-262.
- Pérez-Quiroz, JT, Alonso-Guzmán, EM, Martínez-Molina, W, Rendón-Belmonte, HL Chávez-García M, & Martínez-Madrid, M. (2014). Electrochemical Behavior of the Welded Joint Between Carbon Steel and Stainless Steel by Means of Electrochemical Noise. *Int. J. Electrochem. Sci*, 9, 6734-6750.
- Peruzzo, Pablo J, Anbinder, Pablo S, Pardini, Oscar R, Vega, Jorge, Costa, Carlos A, Galembeck, Fernando, & Amalvy, Javier I. (2011). Waterborne polyurethane/acrylate: Comparison of hybrid and blend systems. *Progress in Organic Coatings*, 72(3), 429-437.
- Petzow, Günter. (1999). *Metallographic etching: techniques for metallography, ceramography, plastography*: ASM international.
- PF, NSE Aktisil PF 777. (2008). *Aktisil PF 777*.
- Popov, Branko N, Alwohaibi, Mohammed A, & White, Ralph E. (1993). Using electrochemical impedance spectroscopy as a tool for organic coating solute saturation monitoring. *Journal of the Electrochemical Society*, 140(4), 947-951.
- Puteh, R, Vengadaesvaran, B, & Rau, S Ramis. (2009). *The Physical, Mechanical and Thermal Analysis on Methoxy Functional Silicone Intermediate Resin Blending with Acrylic Polyol Resin*. Paper presented at the Proceedings of Asian Physics Symposium.
- Radhakrishnan, S, Siju, CR, Mahanta, Debajyoti, Patil, Satish, & Madras, Giridhar. (2009). Conducting polyaniline–nano-TiO₂ composites for smart corrosion resistant coatings. *Electrochimica Acta*, 54(4), 1249-1254.
- Rajgopalan, N, & Khanna, AS. (2013). Effect of nano-ZnO in lowering yellowing of aliphatic amine cured DGEBA-based epoxy coatings on UV exposure. *International Journal of Scientific and Research*, 3(4).

- Ramesh, Duraisamy, & Vasudevan, Thiagarajan. (2012). Evaluation of Corrosion Stability of Water Soluble Epoxy-Ester Primer through Electrochemical Studies. *Materials Sciences and Applications*, 3, 333-347.
- Ramesh, K, Abidin, ZHZ, Osman, Zurina, Basirun, Wan Jeffrey, & Arof, AK. (2006). *Development of a coating system for high temperature corrosion protection*. Paper presented at the Materials science forum.
- Ramesh, K, Nor, NA, Ramesh, S, Vengadaesvaran, B, & Arof, AK. (2013a). Studies on Electrochemical Properties and FTIR analysis of Epoxy Polyester Hybrid Coating System. *Int. J. Electrochem. Sci*, 8, 8422-8432.
- Ramesh, K, Nor, NA, Ramesh, S, Vengadaesvaran, B, & Arof, AK. (2013b). Studies on Electrochemical Properties and FTIR analysis of Epoxy Polyester Hybrid Coating System. *International Journal of Electrochemical Science*, 8(6), 8422-8432.
- Ramesh, K, Osman, Z, & Arof, AK. (2007). Studies on the properties of silicone resin blend materials for corrosion protection. *Anti-Corrosion Methods and Materials*, 54(2), 99-102.
- Ramesh, K, Osman, Z, Arof, AK, Vengadaeswaran, B, & Basirun, WJ. (2008). Structural and corrosion protection analyses of coatings containing silicone-polyester resins. *Pigment & Resin Technology*, 37(1), 37-41.
- Ramesh, K, Vengadaesvaran, B, Rau, SR, Ramesh, TS, & Arof, AK. (2013). Preparation and characteristic analyses of polymer coatings developed by different organic resins. *Pigment & Resin Technology*, 42(2), 123-127.
- Ramezanzadeh, B, & Attar, MM. (2011). Characterization of the fracture behavior and viscoelastic properties of epoxy-polyamide coating reinforced with nanometer and micrometer sized ZnO particles. *Progress in Organic Coatings*, 71(3), 242-249.
- Ramezanzadeh, B, Attar, MM, & Farzam, M. (2011). A study on the anticorrosion performance of the epoxy-polyamide nanocomposites containing ZnO nanoparticles. *Progress in Organic Coatings*, 72(3), 410-422.
- Raps, D, Hack, T, Wehr, J, Zheludkevich, ML, Bastos, AC, Ferreira, MGS, & Nuyken, O. (2009). Electrochemical study of inhibitor-containing organic-inorganic hybrid coatings on AA2024. *Corrosion Science*, 51(5), 1012-1021.

- Rashidi, Navid, Alavi-Soltani, Seyed R, & Asmatulu, Ramazan. (2007). *Crevice corrosion theory, mechanisms and prevention methods*. Paper presented at the Proceedings of the 3rd Annual GRASP Symposium, Wichita State University, 2007.
- Rau, S Ramis, Vengadaesvaran, B, Naziron, NN, & Arof, AK. (2013). Strength and adhesion properties of acrylic polyol-epoxy polyol resin protective coating on mild steel substrate. *Pigment & Resin Technology*, 42(2), 111-116.
- Rau, S Ramis, Vengadaesvaran, B, Puteh, R, & Arof, AK. (2009). *Development of Organic Resins Hybrid System Using Epoxy Resin*. Paper presented at the Proceedings of Asian Physics Symposium.
- Rau, S Ramis, Vengadaesvaran, B, Ramesh, K, & Arof, AK. (2012). Studies on the Adhesion and Corrosion Performance of an Acrylic-Epoxy Hybrid Coating. *The Journal of Adhesion*, 88(4-6), 282-293.
- Rau, SR, Vengadaesvaran, B, Puteh, R, & Arof, AK. (2011). Development of organic resin hybrid systems using epoxy polyol resin for mild steel protective coating. *The Journal of Adhesion*, 87(7-8), 755-765.
- Revie, R Winston. (2008). *Corrosion and corrosion control*: John Wiley & Sons.
- Rodriguez, MT, Gracenea, JJ, Saura, JJ, & Suay, JJ. (2004). The influence of the critical pigment volume concentration (CPVC) on the properties of an epoxy coating: Part II. Anticorrosion and economic properties. *Progress in Organic Coatings*, 50(1), 68-74.
- Roh, Y, Lee, SY, & Elless, MP. (2000). Characterization of corrosion products in the permeable reactive barriers. *Environmental Geology*, 40(1-2), 184-194.
- Sangaj, Nivedita S, & Malshe, VC. (2004). Permeability of polymers in protective organic coatings. *Progress in Organic coatings*, 50(1), 28-39.
- Schneider, O, Ilevbare, GO, Kelly, RG, & Scully, JR. (2007). In Situ Confocal Laser Scanning Microscopy of AA2024-T3 Corrosion Metrology III. Underfilm Corrosion of Epoxy-Coated AA2024-T3. *Journal of The Electrochemical Society*, 154(8), C397-C410.
- Scopelliti, David P. (2013). The Pain of Fretting Corrosion. 1-8. Retrieved from www.samtec.com website: <http://suddendocs.samtec.com/productspecs/fretting-corrosion.pdf>

- Selvaraj, R, Selvaraj, M, & Iyer, SVK. (2009). Studies on the evaluation of the performance of organic coatings used for the prevention of corrosion of steel rebars in concrete structures. *Progress in organic coatings*, 64(4), 454-459.
- Sharmin, Eram, Imo, L, Ashraf, SM, & Ahmad, Sharif. (2004). Acrylic-melamine modified DGEBA-epoxy coatings and their anticorrosive behavior. *Progress in Organic Coatings*, 50(1), 47-54.
- Shen, Lu, Li, Yinwen, Zheng, Jian, Lu, Mangeng, & Wu, Kun. (2015). Modified epoxy acrylate resin for photocurable temporary protective coatings. *Progress in Organic Coatings*, 89, 17-25.
- Shi, Xianming, Nguyen, Tuan Anh, Suo, Zhiyong, Liu, Yajun, & Avcı, Recep. (2009). Effect of nanoparticles on the anticorrosion and mechanical properties of epoxy coating. *Surface and Coatings Technology*, 204(3), 237-245.
- Sigma. (2014). Paintings and Coatings Solvent (pp. 1-4).
- Socrates, George. (2004). *Infrared and Raman characteristic group frequencies: tables and charts*: John Wiley & Sons.
- Sørensen, Per Aggerholm, Kiil, Søren, Dam-Johansen, Kim, & Weinell, CE. (2009a). Anticorrosive coatings: a review. *Journal of Coatings Technology and Research*, 6(2), 135-176.
- Sørensen, Per Aggerholm, Kiil, Søren, Dam-Johansen, Kim, & Weinell, CE. (2009b). Influence of substrate topography on cathodic delamination of anticorrosive coatings. *Progress in Organic Coatings*, 64(2), 142-149.
- Talbert, Rodger. (2007). *Paint technology handbook*: CRC Press.
- Van der Wel, GK, & Adan, OCG. (1999). Moisture in organic coatings—a review. *Progress in organic coatings*, 37(1), 1-14.
- Vengadaesvaran, B, Rau, S Ramis, Kasi, Ramesh, & Arof, AK. (2013). Evaluation of heat resistant properties of silicone-acrylic polyol coating by electrochemical methods. *Pigment & Resin Technology*, 42(2), 117-122.
- Vengadaesvaran, B, Rau, S Ramis, Puteh, R, & Arof, AK. (2009). *Investigation on the Effect of Hydroxyl Functional Solid Phenyl Silicone Intermediate Resin blending with Acrylic Polyol Resin*. Paper presented at the Proceedings of Asian Physics Symposium.

- Vengadaesvaran, B, Rau, SR, Ramesh, K, Puteh, R, & Arof, AK. (2010). Preparation and characterisation of phenyl silicone-acrylic polyol coatings. *Pigment & Resin Technology*, 39(5), 283-287.
- Weldon, Dwight G. (2009). *Failure analysis of paints and coatings*: John Wiley & Sons.
- Wicks Jr, Zeno W, Jones, Frank N, Pappas, S Peter, & Wicks, Douglas A. (2007). *Organic coatings: science and technology*: John Wiley & Sons.
- Wika, Sandra Finsås. (2012). Pitting and Crevice Corrosion of Stainless Steel under Offshore Conditions.
- Winkler, Jochen. (2013). *Titanium dioxide: production, properties and effective usage*: Vincentz Network.
- Xing, Weiyi, Jie, Ganxin, Song, Lei, Wang, Xin, Lv, Xiaoqi, & Hu, Yuan. (2011). Flame retardancy and thermal properties of epoxy acrylate resin/alpha-zirconium phosphate nanocomposites used for UV-curing flame retardant films. *Materials Chemistry and Physics*, 125(1), 196-201.
- Xu, Jin, Sun, Cheng, Yan, MC, & Wang, FH. (2012). Effects of sulfate reducing bacteria on corrosion of carbon steel Q235 in soil-extract solution. *Int. J. Electrochem. Sci*, 7, 11281-11296.
- Yang, Xiong F, Tallman, DE, Bierwagen, GP, Croll, SG, & Rohlik, S. (2002). Blistering and degradation of polyurethane coatings under different accelerated weathering tests. *Polymer degradation and stability*, 77(1), 103-109.
- Yew, Ming Chian, & Ramli Sulong, Nor Hafizah. (2011). *Effect of epoxy binder on fire protection and bonding strength of intumescent fire protective coatings for steel*. Paper presented at the Advanced Materials Research.
- Yonehara, Makiko, Matsui, Tsutomu, Kihara, Koichiro, Isono, Hiroaki, Kijima, Akira, & Sugibayashi, Toshio. (2004). Experimental relationships between surface roughness, glossiness and color of chromatic colored metals. *Materials Transactions*, 45(4), 1027-1032.
- Z86, NSE Sillitin. (2008). *Sillitin Z 86*.
- Zhang, QB, & Hua, YX. (2009). Corrosion inhibition of mild steel by alkyimidazolium ionic liquids in hydrochloric acid. *Electrochimica Acta*, 54(6), 1881-1887.

Zhu, Jin, Uhl, Fawn M, Morgan, Alexander B, & Wilkie, Charles A. (2001). Studies on the mechanism by which the formation of nanocomposites enhances thermal stability. *Chemistry of Materials*, 13(12), 4649-4654.

Zhu, Yanfang, Xiong, Jinping, Tang, Yuming, & Zuo, Yu. (2010). EIS study on failure process of two polyurethane composite coatings. *Progress in Organic Coatings*, 69(1), 7-11.

Ziegler, A, McNaney, JM, Hoffmann, MJ, & Ritchie, RO. (2005). On the Effect of Local Grain-Boundary Chemistry on the Macroscopic Mechanical Properties of a High-Purity Y₂O₃-Al₂O₃-Containing Silicon Nitride Ceramic: Role of Oxygen. *Journal of the American Ceramic Society*, 88(7), 1900-1908.

University of Malaya

LIST OF PUBLICATIONS AND PAPERS PRESENTED

- Rau, S Ramis**, Vengadaesvaran, B, Naziron, NN, & Arof, AK. (2013). Strength and adhesion properties of acrylic polyol-epoxy polyol resin protective coating on mild steel substrate. *Pigment & Resin Technology*, 42(2), 111-116.
- Rau, S Ramis**, Vengadaesvaran, B, Ramesh, K, & Arof, AK. (2012). Studies on the Adhesion and Corrosion Performance of an Acrylic-Epoxy Hybrid Coating. *The Journal of Adhesion*, 88(4-6), 282-293.
- Rau, S Ramis**, Vengadaesvaran, B, Puteh, R, & Arof, AK. (2011). Development of organic resin hybrid systems using epoxy polyol resin for mild steel protective coating. *The Journal of Adhesion*, 87(7-8), 755-765.
- Vengadaesvaran, B, **Rau, S Ramis**, Ramesh, K, & Arof, AK. (2013). Evaluation of heat resistant properties of silicone-acrylic polyol coating by electrochemical methods. *Pigment & Resin Technology*, 42(2), 117-122.
- Vengadaesvaran, B, **Rau, S Ramis**, Ramesh, K, Puteh, R, & Arof, AK. (2010). Preparation and characterisation of phenyl silicone-acrylic polyol coatings. *Pigment & Resin Technology*, 39(5), 283-287.
- Ramesh, K, Vengadaesvaran, B, **Rau, S Ramis**, Ramesh, TS, & Arof, AK. (2013). Preparation and characteristic analyses of polymer coatings developed by different organic resins. *Pigment & Resin Technology*, 42(2), 123-127.

CONFERENCES

Rau S.R., Vengadaesvaran B, Ramesh K, Ramesh T.S, Arof A.K. *Investigation on Correlation between Adhesion and Electrochemical Impedance Spectroscopy for Hybrid Paint System*,

9th International Materials Technology Conference and Exhibition (IMTCE-2014), Kuala Lumpur, Malaysia, 13-16 May 2014: – **Oral Presentation**.

Rau S.R., Ramesh T.S, Arof A.K. *Investigation on Correlation between Adhesion and Electrochemical Impedance Spectroscopy for Acrylate-Epoxy Paint System*,

4th International Conference of Functional Material and Devices (ICFMD-2013), Penang, Malaysia, 08-11 April 2013: – **Poster Presentation. Gold**

Rau S.R., Ramesh T.S, Arof A.K. *Investigation on Correlation between Adhesion and Electrochemical Impedance Spectroscopy for Acrylate-Epoxy Paint System*,

4th International Conference of Functional Material and Devices (ICFMD-2013), Penang, Malaysia, 08-11 April 2013: – **1 minute Presentation. Gold**

Rau S.R., Vengadaesvaran B, Jamari S.K.M, Ramesh K, Ramesh T.S, Arof A.K. *Strength and adhesion properties of novel silicone – acrylate hybrid system*,

6th International Conference on Advanced Computational Engineering and Experimenting (ACE-X 2012)

Istanbul, Turkey, 01-04 July 2012:– **Oral Presentation**

Rau, S.R., Arof A.K. *Strength and adhesion properties of acrylic polyol-epoxy polyol resin protective coating on mild steel substrate*,

3rd International Conference of Functional Material and Devices (ICFMD-2010), Kuala Terengganu, Malaysia, 14-17 June 2010: – **Oral Presentation**

Rau, S.R., Vengadaesvaran, B, Puteh, R, & Arof, AK. *Development of organic resin hybrid system using epoxy resin*,

The 3rd Asian Physics Symposium (APS-2009),

Bandung, Indonesia, 22-23 July 2009: – **Oral Presentation**

WORKSHOP

Rau, S.R. *Interpretation of FTIR Spectra, A Practical Approach in Protective Coating*
Workshop on FTIR; Application in Polymer Electrolytes, Department of Physics,
Faculty of Science, University of Malaya, 17-19 January 2012:– **Oral Presentation**

EXPO

Rau, S.R., Abidin Z.H.Z, Arof A.K. *Electrochemical and Mechanical Studies of Chlorophyll-Polymer Resin,*
Malaysia Technology Expo 2009
Kuala Lumpur, Malaysia, 19-21 February 2009:– **Poster Presentation. Bronze**

University of Malaya